INFORMATION TO USERS

This manuscript has been reproduced from the microfilm master. UMI films the text directly from the original or copy submitted. Thus, some thesis and dissertation copies are in typewriter face, while others may be from any type of computer printer.

The quality of this reproduction is dependent upon the quality of the copy submitted. Broken or indistinct print, colored or poor quality illustrations and photographs, print bleedthrough, substandard margins, and improper alignment can adversely affect reproduction.

In the unlikely event that the author did not send UMI a complete manuscript and there are missing pages, these will be noted. Also, if unauthorized copyright material had to be removed, a note will indicate the deletion.

Oversize materials (e.g., maps, drawings, charts) are reproduced by sectioning the original, beginning at the upper left-hand corner and continuing from left to right in equal sections with small overlaps.

ProQuest Information and Learning
300 North Zeeb Road, Ann Arbor, MI 48106-1346 USA
800-521-0600

EVALUATION OF LOAD TRANSFER IN AXIALLY LOADED REPAIRED CONCRETE COLUMNS

BY

MOHAMMED HAMEEDUDDIN

A Thesis Presented to the

DEANSHIP OF GRADUATE STUDIES

KING FAHD UNIVERSITY OF PETROLEUM & MINERALS

DHAHRAN, SAUDI ARABIA

In Partial Fulfillment of the
Requirements for the Degree of

MASTER OF SCIENCE

In

CIVIL ENGINEERING

MAY 2002

ProQuest Information and Learning Company
300 North Zeeb Road
P.O. Box 1346
Ann Arbor, MI 48106-1346

KING FAHD UNIVERSITY OF PETROLEUM AND MINERALS
DHAHRAN 31261, SAUDI ARABIA

DEANSHIP OF GRADUATE STUDIES

This thesis, written by **Mohammed Hameeduddin** under the direction of his Thesis Advisor and approved by his Thesis Committee, has been presented to and accepted by the Dean of Graduate Studies, in partial fulfillment of the requirements for the degree of **MASTER OF SCIENCE IN CIVIL ENGINEERING.**

Thesis Committee

Dr. Ahmad S. Al-Gahtani (Advisor)

Prof. Mohammad H. Baluch (Member)

Prof. Alfarabi M. Sharif (Member)

Dr. Abdullah A. Al-Musallam (Member)

Dr. Muhammad Kalimur Rahman (Member)

Prof. Hamad I. Al-Abdul Wahhab
Department Chairman

Prof. Osama A. Jannadi
Dean of Graduate Studies

Date

Dedicated To My
Beloved Parents
And
My Brothers & Sister

ACKNOWLEDGEMENTS

I thank Allah (subhana wa taala) for bestowing me with health, knowledge and patience to complete this work. Thereafter, acknowledgement is due to KFUPM for the support given to this research through its tremendous facilities and for granting me the opportunity to pursue graduate studies with financial support.

I acknowledge, with deep gratitude and appreciation, the inspiration, encouragement, valuable time and guidance given to me by my Committee Chairman, Dr. Ahmad S. Al-Gahtani. I press my profound gratitude to Committee Member, Dr. Mohammad Kalimur Rahman, for his extensive guidance, support, stimulation and personal involvement in all phases of this research. I am grateful to my Committee members, Dr. Mohammad H. Baluch, Dr. Alfarabi M. Sharif and Dr. Abdullah A. Al-Musallam for their constructive guidance and technical support.

I also acknowledge the sincere and untiring efforts of Mr. Hassan Zakaria, Mr. Nahash, Mr. Abdullah and Mr. Mohammad who assisted me in the experimental work. Thanks are also due to the laboratory personnel Mr. Omer and Mr. Mukarram for their substantial assistance. I am indebted to Mr. Younus at Research workshop for the fabrication of equipment for the research.

I am grateful to the local repair product suppliers FOSAM and SIKA for generous material donations. In particular, Mr. Des Smith and Mr. Monjid Yaseen were of great help.

Special thanks are due to my colleagues and friends at the University, Aurif, Anwar, Imran, Khasim, Salman, Ali, Baseer, Majid, Abdullah, Faheem and Jalal who were always there to help me in my work. I would also like to thank my friends Aijaz, Mubeen, Faisal, and Sarfaraz who provided wonderful company and some memories that will last a lifetime.

Finally, thanks are due to my mother and father for their emotional and moral support throughout my academic career and also for their love, patience, encouragement and prayers.

TABLE OF CONTENTS

CHAPTER 3

LIST OF TABLES

LIST OF FIGURES

THESIS ABSTRACT

Full Name **MOHAMMED HAMEEDUDDIN**

Title of Study **EVALUATION OF LOAD TRANSFER IN AXIALLY LOADED REPAIRED COLUMNS**

Major Field **CIVILL ENGINEERING (Structures)**

Date of Degree **MAY, 2002**

The harsh and highly corrosive environment in the Eastern Province of Saudi Arabia results in corrosion of reinforcement and subsequent cracking and spalling of concrete. Corrosion of reinforcing steel is also prevalent in columns at ground level, due to the presence of groundwater by capillary action. The deterioration in primary load carrying members poses a potential threat to overall structural integrity. When a patch repair of deteriorated column is carried out, its effectiveness in restoring the original stress pattern is not known. Repair material properties and the effect of carrying out repairs in columns in loaded or unloaded state is believed to play an important role in magnitude of stresses developed in repair layer and concrete core.

An experimental investigation was carried out to assess the behavior and performance of a patch repair in an axially loaded column. It is found that the key repair material parameters, which play a central role in the distribution of loads in a patch repaired column and its long-term behavior includes the compressive modulus of elasticity E, free compressive creep strain ε_{cr}, free shrinkage strain ε_{sh}, and tensile strength f_t.

The magnitude of stress and load distribution between the repair and concrete in columns repaired in unloaded state depends upon the relative modulus of elasticity of the repair and concrete at the age of loading. In the repair layer, the stress is significantly affected due to the time dependent phenomenon of creep and shrinkage. The stress in repair relaxes with time depending upon the magnitude of elastic strains due to restrained shrinkage and creep developed in repair. The concrete core also looses some stress with time due to creep in the concrete. The loss of stress in repair and concrete is accompanied with a substantial increase in stress in steel. The repair layer however, functions as an integral part of the column in resisting loads.

In columns, which are repaired in loaded state, it is found that the patch repair does not play an effective role in resisting the loads coming on the column. The restraint provided to the time dependent phenomenon of shrinkage in the repair layer results in tensile stresses in the repair which may lead to cracking if it exceeds the tensile strength capacity of repair layer. For performing effective patch repair in deteriorated columns, it is highly recommended to relieve the structure from loads, at least partially, and then proceed for patch repair.

MASTER OF SCIENCE
KING FAHD UNIVERSITY OF PETROLEUM AND MINERALS
Dhahran, Saudi Arabia
May 2002

ملخص البحث

اسم الطالب: **محمد حميد الدين**

عنوان الرسالة: **تقييم تحول الاحمال في الاعمدة المرممة ذات الحمل المحوري**

حقل التخصص: **هندسة مدنية (انشاءات)**

تاريخ منح الدرجة : **مايو ٢٠٠٢**

تتسبب البيئة القاسية و شديدة التآكل بالمنطقة الشرقية في المملكة العربية السعودية، في تآكل حديد التسليح مؤدية الي تشقق وتكسر الخرسانة. يغلب حدوث تآكل حديد التلسيح في الأعمدة علي مستوى السطح، بسبب وجود المياه الجوفية بفعل الخاصية الشعرية. ان التدهور في أعضاء التحميل الأساسية يخلق وضعية تهديدية لسلامة كامل المنشآة. عند عمل ترميم لعمود متدهور، فان فاعلية ارجاع صيغة الاجهاد الاولية تكون غير معلومة. ان خواص مواد الترميم و تاثير عمل الترميم في اعضاء في حالة تحميل أو عدم تحميل قد تلعب دروا مهما في شدة الاجهادات المتولدة في طبقة الترميم ولب الخرسانة.

اجريت اختبارات معملية لتحديد سلوك واداء رقعة ترميم في عمود محمل تحميل محوري. وجد ان المؤشرات الاساسية و التي تلعب دورا مركزيا في توزيع الاحمال في رقعة من عمود مرممة وسلوكها على المدى البعيد، تشمل معامل المرونة للضغط، انفعال الزحف الضاغط الحر، انفعال الانكماش الحر ومقاومة الشد.

تعتمد شدة الاجهادات و توزيع الاحمال بين اجزاء الترميم و الخرسانة في الاعمدة المرممة في حالة عدم التحميل، على معامل المرونة النسبي لمادة الترميم والحرسانة في عمر التحميل. في طبقات الترميم، يتأثر الاجهاد بصورة ملحوظة بظاهرتي الزحف والانكماش ذوات الارتباط الزمني. يرتخي الاجهاد في الترميم بمرور الوقت اعتمادا على شدة الانفعال المرن نتيجة للانكماش والزحف المثبت المتولد في الترميم. يفقد اللب الحرساني جزء من الاجهاد ايضا بمرور الوقت نتيجة للزحف في الخرسانة. يصاحب الفقد في الاجهاد في الترميم و الخرسانة زيادة ملحوظة في الاجهاد في الحديد. تلعب طبقة الترميم دورا تكامليا في مقاومة العمود للاحمال.

في الاعمدة المرممة في حالة التحميل، وجد ان رقعة الترميم لا تلعب دورا فعالا في مقاومة الاحمال الواصلة للعمود. يتسبب التثبيت الموفر لظاهرتي الزحف والانكماش ذوات الارتباط الزمني في طبقة الترميم، في اجهادات شدية في الترميم قد تؤدي الى تشققات اذا زادت عن سعة طبقة الترميم للمقاومة الشدية. لاداء فعال لرقعة الترميم في الاعمدة المتدهورة، يوصى بشدة بتفريغ المنشأ من الاحمال، جزئيا على الاقل، قبل البدء في عمل رقعة الترميم.

ماجستير في العلوم

جامعة الملك فهد للبترول والمعادن

الظهران، المملكة العربية السعودية

مايو ٢٠٠٢

CHAPTER 1

INTRODUCTION

1.1 BACKGROUND

1.1.1 Deterioration of Concrete

Reinforced concrete has proved to be an efficient and durable construction material for structures over a long period of time. Its low-cost, ecologically favorable profile, and excellent strength and stiffness properties coupled with its ease of manufacture at the construction site are important factors that have established it as a major construction material.

Although concrete is the most widely used construction material, it has its own limitations. It has been observed that concrete deteriorates rapidly in conditions where moisture and temperature are high and more so, in the presence of aggressive ions. The reduction in the useful service-life of reinforced concrete construction, mainly due to reinforcement corrosion, in North America, Europe and the arid and semi-arid regions of

the world is of concern to the construction industry. The damage to concrete structures can be attributed to a wide variety of causes including, but not limited to the following [1].

- Lack of quality control in construction.
- Design defects including insufficient concrete strength, cover, structural depth, and reinforcement.
- A phenomenal increase in loading spectra on infrastructure like bridges associated with impact and vibration, abrasion, wear and fatigue.
- Damage due to concrete under physical and chemical attack from:
    - Air borne chlorides and sulfates,
    - Soil borne chlorides and sulfates,
    - Leaching of salts,
    - Salt crystal expansion,
    - Alkali aggregate reaction,
    - Chemical exposure,
    - Thermal movement,
    - Erosion,
    - Humidity dynamics, and
    - Freeze and thaw reaction.

- Damage to concrete due to reinforcement under attack from
    - Chloride attack on reinforcement, and
    - Carbonation resulting in destruction of steel passivation layer.

The consequences of such a diverse and aggressive warfare on living and breathing concrete is tremendous. The concrete responds to such an attack with a softening behavior associated with extensive cracking, delamination of concrete and dilution of reinforcement. It loses the prime characteristics of being a dense material. The porous concrete consequently becomes vulnerable to more profound attack, which if allowed continuing results in disastrous failures. In the international sphere the deterioration has been attributed to aging and degradation of concrete, carbonation, chloride contamination due to usage of de-icing salt, freeze and thaw action and alkali-aggregate reaction. In the Arabian Gulf region and the Eastern province of Saudi Arabia potentially aggressive environment, has resulted in premature deterioration of numerous structures in a service performance span of a couple of decades or less. The environment in this region characterized by high humidity and temperature and excessive air/soil borne salinity has resulted in corrosion of the reinforcement and subsequent cracking and spalling of concrete. This has been termed as "cancer in concrete."

Deterioration of concrete is attributed mainly to the chloride-induced corrosion of the reinforcing steel in the Arabian Gulf. The environmental conditions in the coastal areas of the Arabian Gulf, where the temperature can vary by as much as 30^0C during a typical summer day, and the relative humidity ranges from 40 to 100% over a period of 24 hours [2], are conducive for the acceleration of corrosion of the reinforcing steel. This corrosion is mainly due to the ingress of chloride ions from environment with excessive ambient salinity. The corrosion of embedded steel is accompanied with considerable expansive force, which results in spalling and cracking of concrete.

1.1.2 Deterioration of Columns

Deterioration of concrete columns on the coastal flats of the Arabian Gulf is mainly attributed to the chloride-induced corrosion of reinforcing steel, which is highly prevalent in columns at ground level of the first floor. The portion above ground level is the most active zone for the corrosion to occur. Due to the groundwater table the moisture rises few feet above the soil by capillary action followed by high evaporation rates due to high temperatures, leaving heavy crest of salt in this zone. Usually, more salt penetrates than is leached out, thereby causing significant concentrations to develop within the concrete over a period of years. Pockets of hygroscopic salts within concrete tend to retain moisture even when the external humidity is temporarily low, thus creating microclimates within the concrete pores that promote corrosive action. Salt on concrete surfaces is also dissolved in surface moisture and enters the pores of concrete by capillary action. This leaves the ground, groundwater, atmosphere, and the aggregates heavily contaminated with chlorides and sulfate salts thus resulting in problems like corrosion and sulfate attack.

The climatic factors like sudden and continuous variations in temperature and humidity initiate ever-present cycles of expansion/contraction and hydration/dehydration, which cause damage due to thermal and mechanical stresses [3]. Expansive cracking and spalling due to the mechanical pressure by the expanding volume of corrosion products has been found to be the commonest factor of concrete cracking, which can be seen in figures 1.1 and 1.2. All the above factors finally lead to heavy deterioration of concrete in this zone. This type of deterioration in primary load carrying members (columns) poses a potential threat to overall structural integrity and may lead to failure if left unattended.

1.1.3 Patch Repair of Deteriorated Columns

It is a common practice to carry out patch repair of deteriorated columns. The portion of column requiring repair is marked and the deteriorated concrete, chloride contaminated concrete and a portion beyond the reinforcing steel is chipped or cut off until sound concrete is reached. The concrete substrate receiving repair material is prepared either by sandblasting or mechanical cleaning. The corroded reinforcement is cleaned and a protective coating is applied. If the reinforcing steel is severely damaged, it is replaced or strengthened. After destressing the column, the damaged sections of the corroded bar are removed and the new reinforcing bar is joined to the old ones by lapping splices, by welding, or by coupling devices. Then the repair material is cast to restore the dimensions of the deteriorated column.

If the statical function of a structure requires the repaired parts to be in compression as in a column, the structure must be relieved of its load before repairs are carried out so that, when reloaded, the new and the old parts act together. Otherwise the repaired parts will not be subjected to the deformations, which are prerequisite to create the necessary stress. It is essential that any such repair must form an integral part of the composite structural member and should be effective in the load distribution over the entire section.

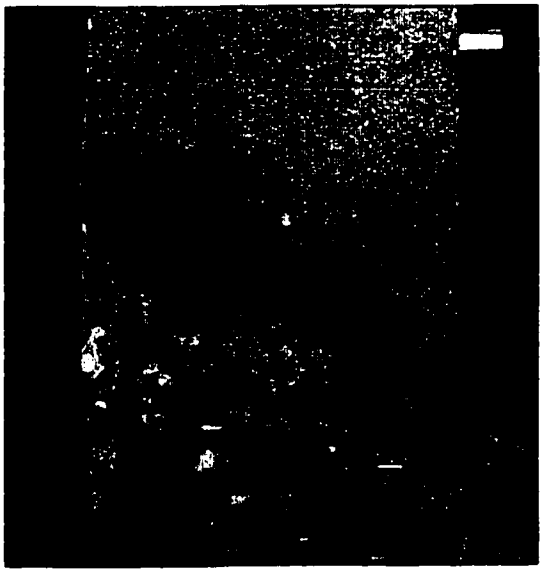

Figure 1.1: Spalling of the Lower Portion of Column [Zoom-in view]

Figure 1.2: Development of Cracks and spalling of concrete in column due to rebar corrosion

1.1.4 Problems Associated with Patch Repair in Columns

In patch repaired columns, repairs are of a scale where structural integrity is significant and is necessary to ensure the transfer of load from concrete substrate into the repair and back. Problems in such repairs may arise fairly quickly because of the difference in properties between the repair and the concrete substrate. The typical differences in some of the important short-term mechanical properties of repair materials can be categorized as follows [4]:

- Curing shrinkage of repair material relative to the concrete substrate,
- Differences in the stiffness [Modulus of Elasticity] and Poisson's ratio causing unequal load sharing and strains resulting in interface, excessive stresses,
- Creep of repair material under sustained load as compared with that of the concrete,
- Relative fatigue performance of the components in the composite system of patch-repaired columns, and
- Differential thermal expansion/contraction between the repair material and concrete substrate.

Such differences in properties may result in either tensile strain induced in the repair, or cracking at or adjacent to the repair-substrate interface. Both of these may reduce long-term performance and structural capacity. Incompatibilities in the form of differing elastic moduli and differential thermal movement between repair and substrate can cause problems. Also, creep of repair material under sustained stress may render the repair less effective with time.

The effects of carrying out repairs while the deteriorated column is under load, and failure to support some of the load during the repair process may result in stresses being transferred to undamaged parts of the column. Little load may be subsequently transmitted through repaired patches making the repair non-structural.

1.2 NEED FOR THIS RESEARCH

As discussed earlier, deterioration of concrete structures is a well-known phenomenon all over the world. Vast resources are directed every year on repair and rehabilitation of structures. The harsh and highly corrosive environment in the Arabian Gulf results in corrosion of reinforcement and subsequent cracking and spalling of concrete. Such corrosion is highly prevalent in columns at ground level of the first floor. This type of deterioration in primary load carrying members poses a potential threat to overall structural integrity and may lead to failure if left unattended. Corrosion induced deterioration in compression members is generally repaired by removing the damaged concrete and replacing it by prepackaged non-shrink cementitious repair materials. If a significant amount of material in compression zone is lost, loads are transferred to the intact core of the compression members. The loss of a significant cross sectional area results in substantially higher stresses in the parent intact concrete. An increase in stresses at prime locations where adequacy of axial and lateral load resisting capacity is warranted is detrimental to the structural integrity and safety.

When a patch repair of a compression member is carried out, it is not known if an effective section is recreated such that the stress distribution in the member prior to corrosion induced damage is restored. There are several factors that play an important role in load redistribution in a repaired compression member. These include the role of shrinkage, elastic modulus and creep in the patch repair, the effect of shoring (load support) of deteriorated compression member prior to the application of repair material and the effect of carrying out repairs in the compression member in a loaded state.

A detailed experimental investigation is required to assess the role of various factors highlighted above in the behavior and performance of a patch repair in a compression member. It is also required to predict with confidence the stress distribution in a repaired column. The principal objective of this thesis is to address the above mentioned problems by carrying out detailed investigation of critical repair material properties and full-scale long-term load testing of columns repaired by patching.

The findings of this research will enable the repair engineers to select repair materials and carryout patch repair of columns ensuring durable performance of the composite system. The results obtained from this study will be beneficial in identifying the role of repair material properties and the effect of load relief on load redistribution between repair and host concrete. The results of this research can be used to formulate guidelines for performing an effective patch repair of deteriorated concrete columns.

1.3 AIMS & OBJECTIVES OF RESEARCH

The primary objectives of this research are to contribute towards a deeper understanding of the load redistribution in columns that are repaired by patching. The research will focus on:

1. Identifying, selecting and testing of locally available non-shrink cementitious repair materials to determine critical material properties,
2. Carrying out full-scale load testing on repaired columns (shored/un-shored),
3. Identifying the variables and examining the factors involved in load redistribution in repaired compression members.

1.4 RESEARCH METHODOLGY

The research comprises of five phases involving principally experimental work on small scale and large-scale specimens.

The **first phase** involves a comprehensive literature review and data collection. The data collection involves a detailed survey of repair materials available in Eastern Province, commercially for carrying out structural repair. Based on this survey, two repair materials were selected for carrying out various tests. The selected materials are representative of two different categories, one with a high modulus of elasticity and the other with a low modulus of elasticity. The literature survey covers the following areas.

- Conventional Method of Repairing Columns damaged by corrosion of reinforcement,
- Effective repair strategies for corrosion damaged structures,
- Types of repair materials,
- Effect of repair material properties on patch repairs,
- Behavior of patch repaired columns,
- Shrinkage, and
- Effect of time dependent deformations on patch repairs (Creep effect).

The **second phase** of the research was devoted to the fabrication of equipment. The equipment fabricated at the KFUPM research workshop includes:

1. Rigs for carrying out tests on patch-repaired columns under sustained compressive loads,
2. Creep rigs for evaluating the compressive creep characteristics of selected repair materials,
3. Loading frame for carrying out destructive tests on repaired/un-repaired columns, and
4. Moulds for various specimens and formwork for columns.

These rigs are designed to apply concentric force to the columns and creep specimens and preclude any moment transfer to the columns.

The **third phase** of this research involved comprehensive laboratory testing of the two selected repair materials. The tests were carried out to evaluate the following properties of repair materials and concrete:

1. Compressive strength,
2. Tensile strength,
3. Bond strength,
4. Compressive Modulus of elasticity and Poisson's ratio,
5. Tensile Modulus,
6. Shrinkage,
7. Compressive creep,
8. Chloride penetrability, and
9. Sulfate attack.

Tests on strength properties were conducted at various ages 1, 3, 7, 28, 60 & 180 days after casting. Shrinkage tests were conducted after the initial setting of the repair material.

The **fourth phase** of this research involved full scale testing of concrete columns (with and without recess) repaired with two repair materials, to ascertain the load distribution and stresses in the column or composite section. An elaborate monitoring of strains in the columns was carried out. The columns tested were 250 x 250 mm in cross section and 1.2 meters in length with reinforcement of 1% high strength steel. A total of ten columns (three full columns, three with recess and four repaired, two for each repair material) were tested for their ultimate strength capacity.

The **fifth phase** of this research involved Full scale testing of repaired/un-repaired concrete columns under constant load to monitor the creep effect in the repaired and un-repaired portions. The columns were loaded to 20% of their Ultimate Load Capacity, and the load was sustained up to a period of 5 months, continuously monitoring the strains in concrete, repair material and steel. A total of 10 columns of size 250 x 250 mm were tested under constant load.

CHAPTER 2

LITERATURE REVIEW

2.1 CONVENTIONAL METHOD FOR REPAIRING COLUMNS DAMAGED BY CORROSION

Repair refers to modification of structure, damaged in its appearance or serviceability, to restore, partly or wholly, the pre-existing characteristics of serviceability, load-bearing capacity and if necessary, to improve its durability [5]. Concrete structures deteriorate due to a number of processes as discussed earlier. These processes lead to cracking and spalling of the concrete. To date, the strategy has been repair and rehabilitation rather than replacement. Replacement may represent a programmed operation if referred to structural elements having a lower intrinsic longevity than the service life of the whole structure [5]. Repairs can range from the elementary, repair of a form-related defect, to the complex, rehabilitation of a load bearing structure.

Repair techniques are used to restore the structural integrity and shape of a concrete element. Repair techniques generally include removal of damaged concrete and placement of new concrete in its place.

Repair entails removing the loose, deteriorated concrete and installing a compatible patch of repair concrete or mortar that dovetails into the existing sound concrete. In order to prevent future crack development after the spall has been patched and to ensure that the patch matches the concrete, great attention must be paid to the treatment of rebars, the preparation of the existing concrete substrate, the selection of compatible patch material, the development of good contact between patch and substrate, and the curing of the patch.

Depending upon the damaged concrete surface, it is first of all necessary to chip off loose concrete. This is usually achieved by using a chisel and hammer. Care has to be taken to ensure that only the loose and damaged portion is removed and that the sound concrete is left untouched. Any use of extra force to chip off sound concrete may only be more harmful to the structure since this can result in micro-cracks in sound concrete. This should be followed by the use of a suitable system or a combination of systems to prepare the surface.

2.1.1 Types of surface preparations

The method of surface preparation to be used depends upon a variety of factors. In all cases where concrete surfaces are repaired, the condition of the existing concrete in the exposed damaged area is of primary importance in the durability of the repair. Given below are the types of surface preparations commonly adopted [5].

a) Mechanical methods

b) Thermal methods

c) Chemical methods.

Mechanical methods

a) Demolition by means of explosions, splitting and impacting,

b) Demolition by means of drilling and separating,

c) Chipping off: If a concrete layer of small thickness has to be removed, chipping off is recommended.

d) Milling: Removal of concrete to a flat surface may be accomplished by means of a milling device.

e) Sand-blasting (Blasting of solid particles with compressed air): It is especially suitable for roughening of the surface, for removal of pollutants, layers of cement grout and loose particles. It may be used for removal of loose particles after milling or chipping operations.

f) Hydraulic water jet: A water jet under 10 to 40 MPa pressure at the jet will remove loose particles, scaled concrete or vegetation coatings. This method is not applicable to roughening concrete surfaces.

g) High-pressure water jet: In this method the pressure at the jet reaches 40 to 120 MPa. The high-pressure water jet is the most efficient for soft areas of concrete surfaces-honeycombs, cracks and loose strata.

h) Hydro-jet method: The water jet with a pressure of 140 to 240 MPa, is capable of a deep penetration into the concrete or even cutting grooves in it.

i) Grit blasting: It is a method whereby small steel balls (shot) are impacted upon the concrete surfaces through a centrifugal device, thus producing an abrasive action on the concrete surface.

j) Steam blasting: This method is used for cleaning of the concrete surfaces. A cleaning material may be added to the water. Concrete removal cannot be achieved with this method.

Thermal methods

During thermal procedures, concrete surface is heated to 1500 ^{0}C with a 3200 ^{0}C oxy-acetylene flame, thus producing a thermal shock. This thermal shock, because of the intense temperature gradient perpendicular to the surface of concrete and the different thermal expansion coefficients of stone aggregates and cement, leads to very high residual stresses causing scaling at the concrete surface. Because of the high temperature of the flame, it cannot be guaranteed that distress will not occur at greater depths of the concrete. Therefore, after concrete removal by a thermal procedure, the last layer should be removed mechanically.

Chemical methods

Acids or alkalines are used for concrete removal. Acid etching is being widely recommended as a means of surface preparation for reinforcement as well as concrete surfaces. Because of a corrosion risk, acids should not be used for reinforced and prestressed concrete. Because of a lack of control procedures, there exists the risk of adverse impacting on the adhesion properties of the concrete. In addition, there is a risk of injury and/or long-term health to the workmen. Therefore, because of these risks, the method is not recommended.

Once the deteriorated concrete in a spalled area has been removed, rust on the exposed rebars must be removed by wire brush or sandblasting. As a general rule, if the rebars are so corroded that a structural engineer determines they should be replaced, new supplemental reinforcing bars will normally be required. Additional bars are added to the existing bars either by welding or splicing. A rebar primer applied immediately over the cleaned rebars will diminish the possibility of further corrosion. There are many types of rebar primers in use today, for example: Cement mortar slurry, Polymer modified cement slurry, Non-passivating epoxy, Passivating epoxy and Zinc rich epoxy.

Proper preparation of the substrate will ensure a good bond between the patch and the existing concrete. The surface of the area to be patched and exposed reinforcing steel is to be thoroughly cleaned of all dirt, dust or other foreign materials by the use of water, air under pressure, or any other method that produces satisfactory results. The surface is to be thoroughly drenched with clean water. Before placing the concrete, the surface shall be allowed to dry to a damp condition. In all cases, the substrate should be kept moist with wet rags, sponges, or running water for at least an hour before placement of the patch. Bonding between the patch and substrate can be encouraged by scrubbing the substrate with cement paste, or by applying a liquid bonding agent to the surface of the substrate. Admixtures such as epoxy resins, latexes, and acrylics in the patch may also be used to increase bonding.

2.1.2 Bonding agents

Bonding agents are recommended to improve the bond between old concrete and the new repair concrete. There are two different types of bond mechanisms: physical bond

through adhesion and cohesion, and chemical adhesion through reaction with the surface. There are several types of bonding agents out of which some are listed below:

Cement paste

This bonding agent consists of a cement paste with a low water/cement ratio, which is brushed into the surface to be repaired.

Cement mortar

This bonding agent can be of high or low viscosity, consisting of equal parts of cement and sand along with water. It can, however, also consist of the repair mortar itself, from which the coarse aggregate has been removed.

Bonding systems of plastic modified cement

Generally in these systems the plastic is mixed into the cement paste or cement mortar via the mixing water. These additives are often used not only to improve the bond strength, but also to improve the workability and water retention capacity.

Resins

There are two basic types of bonding agent made of two component resins: emulsifiable agents and normal agents. The first case consists of a combination of a water-emulsifiable epoxy resin, a polyamide resin hardener and a filling material. The epoxy resin and the hardener are initially mixed together before placement. The filling material is about 50% by weight. If required, the mixture may be diluted with water. In the two-component resin bonding agents, a pure resin-hardener mixture is used, with or without fillers. Resins with filling materials are used in practice for the following reasons:

a) filling materials prevent a deep penetration of resin into the old concrete

b) filling materials prevent a penetration of resin into the new concrete

c) filling materials are less expensive than epoxy resin

d) resins with fillers can be placed in thick layers.

After preparing the substrate by cleaning and applying bonding agent, placement of repair material in the area to be repaired should be accomplished in such a manner as not to impede concrete flow and to avoid the entrapment of air, thus avoiding voids in the concrete. Therefore, the formwork must be sufficiently rigid and tightly fitted to the existing concrete in a manner to minimize leakage of cement paste. The types of repair material which can best suit the member to be repaired has to be decided with great care and engineering judgment. The factors to be considered for selecting repair material are discussed in the next section of this chapter. If the selected repair material is a mortar then it is to be applied using trowel in layers as specified by the manufacturer.

After the removal of formwork the repair has to be properly cured to avoid plastic shrinkage cracking, delamination and matrix friability. The curing period and method has to be decided taking into account the environmental conditions, mechanical properties of material and the feasibility of the method or as specified by the manufacturer of the repair material. Sprayed-on curing membranes can be used after the complete patch has been applied.

2.2 EFFECTIVE REPAIR STRATEGIES FOR CORROSION DAMAGED STRUCTURES

2.2.1 Repair Strategy

The planning, design, implementation and monitoring of a repair and/or strengthening project should basically be directed toward the following objectives [5]:

a) ascertaining the present state of the structure,

b) establishing the repair and/or strengthening requirements,

c) preparation of a repair program,

d) determining the required target condition of the structure after repair and strengthening,

e) determination of the suitability of the proposed repair and/or strengthening systems,

f) site supervision with quality control, and

g) re-checks and inspection controls.

Repair techniques are used to restore the structural integrity and shape of a concrete element. Rehabilitation methods on the other hand, in addition to restoring structural integrity and shape, mitigate or stop the process responsible for the damage. Because rehabilitation includes addressing the cause of the problem itself, the repairs last significantly longer [5]. However, rehabilitation differs from new construction in several important aspects including project scale, accessibility of the area being repaired, and control of ambient conditions during the repair and interactive processes that arise because of the repair.

For individual members, it will be necessary to determine whether the best option is to repair or replace. In making this decision, cost must be considered along with factors such as convenience to the public, longevity of the structure, whether the rehabilitation is long term or short term, and the practicality of either option. Due to the variation in the types of problems encountered, the engineer must perform an in depth inspection of the structure to identify the defects that exist, and develop a solution which is unique to the problems found.

The general procedure for evaluating the condition and correcting the deficiencies of a concrete structure is as follows: The first step is to evaluate the current condition of the concrete. Once the evaluation of a structure has been completed, the visual observations and other supporting data must be related to the mechanism or mechanisms that caused the damage.

It is essential to establish the extent of the damage, and determine if the major portion of the structure is of suitable quality on which to build a sound repair. Based on this information, the type and extent of the repair is to be chosen. This is the most difficult step-one, which requires a thorough knowledge of the subject and mature judgment by the engineer. If damage is the result of moderate exposure of what was an inferior concrete in the first place, then replacement by good quality concrete should assure lasting results. On the other hand, if good quality concrete was destroyed, the problem becomes more complex. In that case, a very superior quality of concrete is required.

The deterioration of concrete due to corrosion of reinforcement requires a more detailed study. Simply replacing the deteriorated concrete and restoring the original cover over the steel will not solve the problem. Also, if the structure is salt-contaminated, the

electrolytic conditions will be changed by the application of new concrete, and the consequences of these changed conditions must be considered before any repairs are undertaken.

2.2.2 Repair material requirements

The next step is the selection of appropriate repair materials and methods. Figure 2.1 lists the factors to be considered in the selection of a repair material. For ease of selecting repair methods and materials, it is helpful to divide the possible approaches into two general categories: those more suited for cracking or those more suited for spalling and disintegration. Cracking is the primary cause of virtually all deterioration in reinforced concrete structures. Due to the wide variety of cracking types, there is no single repair method that will work in all instances. Spalling and disintegration are only symptoms of many types of concrete distress. Again, there is no single repair method that will always apply. A basic understanding of underlying causes of concrete deficiencies is essential to performing meaningful evaluations and successful repairs. The repair material chosen depends on the extent of deterioration that has already occurred, whether a permanent or short-term repair is desired, time to complete, the expected life of the repair, accessibility to the repair location, the need to keep the facility open while repairs are being carried out and lack of control of ambient conditions.

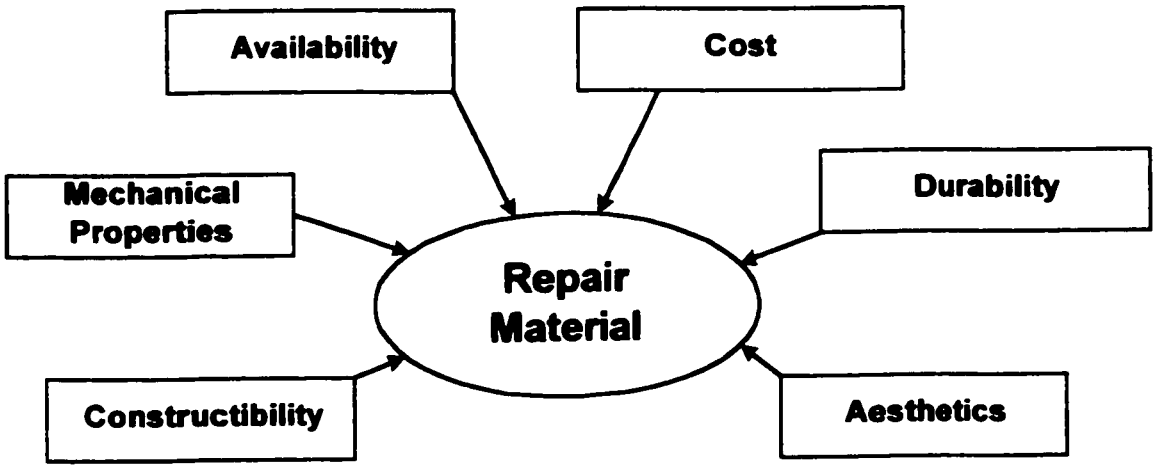

Fig 2.1: Factors to be considered in the selection of Repair Material.

Compatible matching of patch material to the existing concrete is critical for both appearance and durability. In general, repair material should match the composition of the original material as closely as possible so that the properties of the two materials are compatible. Pre-repair considerations are as important as the repairs and consequently proper materials selection and surface preparation are essential to high quality, durable, and functional repair. Materials selected for use in concrete repair must meet specification requirements for the particular application or intended use. Engineers, therefore, need to know the relevant properties of available products and existing substrates before an assessment of compatibility can be made and suitable repair systems chosen [4].

The list of requirements for a patching repair material is given as follows [6]:

- It should be as durable as the surrounding material.
- It should require a minimum of site preparation.
- It must be tolerant of a wide range of temperature and moisture conditions.

- It must be chemically compatible with the substrate.
- It should have a color and surface texture to the surrounding material.

The choice of the right product also depends on the anticipated service conditions and the prevailing conditions at the time of application of the products. The following information relating to application and service conditions is important and pertinent; details should be ascertained to enable proper selection [4].

- The presence of moisture in the substrate will affect some polymer materials, as they will not cure properly in the presence of moisture.
- The temperature of the time of placing will influence the curing rate of polymeric products. High and low temperatures will affect the work life of the materials.
- Location of repair section vertical or horizontal surface: This may require either flowing or non-sag materials.
- Turn-around time: If the repairs are subjected to early loading, rapid strength gain characteristics are essential.
- Chemical exposure: strong solvents may soften polymeric products.
- Exposure to heavy traffic: exposure to heavy traffic will require a material with good abrasion.
- Maximum and minimum service temperatures: Range of service temperature will indicate possible thermal movements and build up stresses.
- Life of repair: life of repair will determine cost and complexity of repair.

Information on the thickness of the repair section is required to determine possible exothermic and consequent thermal stresses, shrinkage, ability to featheredge, or what maximum size aggregate can be used.

Where the repair depth is 3 inches (75 mm) or greater and the surface can be readily formed and concrete placed. This type of patch is the most durable due to its depth and the utilization of reinforcing bars to tie it together. The surfaces to be patched and the exposed reinforcing steel should be abrasively cleaned within 24 hours of application of patching material (or erection of forms if the forms would render the area inaccessible to blasting). Trowelable mortar should generally be specified when the repair depth is less than 1½ inches (40 mm) deep, and the repair area is less than 150 square feet (15 m^2). Trowelable mortar should also be specified for pneumatically placed mortar for the case where the depth of patch is equal to or less than 3 inches (75 mm). 3 inches (75 mm) is the maximum depth of patch that should be attempted with this type of mortar [5].

2.2.3 Reinforcement cleaning requirements

The important step in preparing reinforcement for repair or cleaning is the removal of deteriorated concrete or sound chloride contaminated concrete surrounding the reinforcement. Extreme care should be exercised to ensure that the process of removing concrete does not cause further damage to the reinforcing steel. Once the larger areas of unsound concrete have been removed, a smaller chipping hammer should be used to remove the concrete in the vicinity of the reinforcement. Care should be taken not to vibrate the reinforcement or otherwise cause damage to its bond to concrete adjacent to the repair area.

All weak, damaged and easily removable concrete should be chipped away. If reinforcing steel is exposed and found to have corrosion products, or incorporated in chloride contaminated concrete, or it is not adequately bonded to the surrounding concrete, then

concrete removal around the bar shall continue to provide a minimum 19 mm (3/4 in) clear space between the rebar or surrounding concrete or 6 mm (1/4 in) larger than the maximum size aggregate in the repair material [7]. Steel exposed less than one-half of its perimeter and not affected by corrosion, not surrounded by chloride-contaminated concrete, and with adequate bond to the existing concrete, undercutting of the rebar shall not be required.

Removal of the concrete behind the rebar allows the relatively more accurate cleaning of corrosion products prior to repair placement, and provides conditions for full embedment of the rebar in the repair material. Full embedment offers two important advantages:

- The steel is fully passivated in the highly alkaline cement-rich environment;
- Failure (if corrosion continues) will occur at the higher stress level corresponding to the tensile strength of the repair material rather than at the bond strength level.

Once concrete has been removed, rust on the exposed rebars must be removed by wire brush or sandblasting. Reinforcing steel shall be carefully inspected to determine whether the steel shall be simply cleaned or repaired. The objective of the inspection is to determine whether the reinforcing steel is capable of performing as intended by the design. The need to replace or supplement reinforcement bars which are severely damaged by corrosion and which have lost a significant portion of their area. In this case additional bars may have to be welded or spliced to the existing bars. The potential problems of adding bars are [8]:

1. The new reinforcement will not assist in carrying the dead load unless it has been relieved of load by propping.

2. Welding may increase the stress in the adjacent section of bar as the replacement length cools.
3. Heat from cutting and welding may have an adverse effect on the adjacent concrete.

A rebar primer applied immediately over the cleaned rebars will diminish the possibility of further corrosion. The ideal requirements for a rebar primer are that it must protect the steel, not be subject to undercutting (i.e., progressive rust creep under the primer) and have a good bond to the steel and subsequent repair, have no adverse effect on the adjacent steel and be easy to use. Before priming takes place the substrate must be suitably prepared to remove any surface contamination and provide a mechanical key between the substrate and repair.

2.2.4 Concrete surface requirements

The appropriate preparation of the concrete surface depends on the preceding operations and on the type of repair being undertaken. Some of the concrete removal methods can also be used for surface cleaning. However, an effective method for concrete removal may not be appropriate for required surface cleaning. Micro cracking of the concrete surface is common when impact tools are used which may weaken the bond between the existing concrete and the repair. In this case, a less aggressive method of surface preparation such as abrasive or water blasting is necessary.

Strength

Usually a minimum strength of adhesion 1.5 N/mm^2 is required [5]. If this value is not attainable, the concrete is required to be removed to a further depth. A possible

improvement of the concrete surface may be accomplished by an impregnation of the surface area with a synthetic resin.

Moisture content

The permissible and required moisture content depend on the selected repair method and the applied materials and require a differentiation between cement and plastic bond systems.

a) A cement bond system requires a wetting of the concrete surface, so that the concrete will not absorb water from the repair coating applied. However, excess water content may also be detrimental to adhesion properties. Therefore, the ponding of water on the concrete surface should be avoided. The concrete surface should be moist but not saturated.

b) Some of the plastic bond systems require a dry surface. An approximate requirement is that the moisture content of the concrete should not exceed 6% by weight to a depth of approximately 20 mm [5]. A good adhesion between the repair and the original concrete will be achieved, when the applied liquid material can penetrate into the concrete this penetration is not possible if the pores of the concrete are filled with water, retarding the capillary action. The moisture content of the concrete should also be co-coordinated with the properties of the liquid plastic materials being used. In any case, the system being used should not change its properties coming in contact with the alkaline concrete, for example by saponification.

Bonding between the patch and substrate can be encouraged by applying a liquid bonding agent to the surface of the substrate. Admixtures such as epoxy resins, latexes, and acrylics in the patch are also be used to increase bonding. The requirements for a concrete bonding aid are compatibility with cement, adequate bond, usable working life, tolerance to misuse and ease of use. Many types are available, for example: Water, Slurry coat, Polymer emulsions, Polymer emulsion slurries and Epoxies.

2.2.5 Repair process requirements

Before starting repair process involving the removal of existing concrete, the effect of the removal on the structural integrity should be reviewed. A temporary shoring system should be provided to relieve the loads from the structure or its member being repaired where removal of deteriorated concrete and/or severely corroded reinforcing steel can affect the load carrying capacity of the structure or its elements. In load carrying members it should be ascertained that if the spalled outer concrete is removed to behind the steel, thus destressing this outer layer of steel, that the concrete and the remaining steel should be capable of carrying the load.

After preparing the substrate by cleaning and applying bonding agent, the formwork must be sufficiently rigid and tightly fitted to the existing concrete in a manner to minimize leakage of cement paste. Placement of repair material in the area to be repaired should be accomplished in such a manner as not to impede concrete flow and to avoid the entrapment of air, thus avoiding voids in the concrete. If the selected repair material is a mortar then it is to be applied using trowel in layers as specified by the manufacturer.

After the removal of formwork the repair has to be properly cured to avoid plastic shrinkage cracking. The curing period and method has to be decided taking into account the environmental conditions, mechanical properties of material and the feasibility of the method or as specified by the manufacturer of the repair material. Good quality concrete is made from cement, aggregate and water and so is bad quality concrete. The same can be said about concrete repairs. Even the best methods and materials will not serve their purpose if there is the slightest neglect in construction practices. The placement technique must deliver the repair material to the prepared substrate with specified results. The repair material must achieve satisfactory lasting bond to the substrate, must fill the prepared cavity without segregation, and must fully encapsulate the exposed reinforcing steel. A failure in workmanship means that the repair may not be able to perform its intended structural, protective, and aesthetic functions.

Careful curing is essential to avoid shrinkage cracking, delamination, and matrix friability. Sprayed-on curing membranes can be used after the complete patch has been applied, but they cannot be used between layers of a multiplayer repair because they would prevent bond between layers. For the same reason, they should not be used on a completed repair if a surface coating is to be applied later. Alternate wetting and drying must be prevented because of the alternating stresses that it would cause. If repairs are to be carried out during hot weather, it is advisable to shade the work from direct sunlight in order to prevent drying out of repairs or the rapid stiffening of materials.

2.3 TYPES OF REPAIR MATERIALS

In recent years, the growing need to maintain and repair structures has brought about a definite variation in the expenditure for restoration compared to the investment for new structures. The rapid growth in repair/restoration has undoubtedly greatly influenced the market for the products used in maintenance and repair of deteriorated structures, which has literally been inundated by new products. However, this explosion of new products has not only considerably complicated the selection of the most suitable material for the specific repair work, but has helped the circulation on to the market of products which are unsuitable for repair of reinforced concrete structures. The circulation of these products was possible due to the complete lack of norms indicating performance requirements of repair materials.

In response to the tremendous demand for repairs, a wide array of specialty and conventional repair materials are now commercially available. The repair materials fall into two main categories [9].

(a) Cementitious and modified cementitious repair mortars / concrete.

(b) Resin based repair mortars and pure resins.

The later category is used principally in crack injections and thin repairs. For patch repairs of deteriorated beams, columns, slab and other elements current trend is however towards the usage of cementitious repair mortars [10]. This class of repair products includes:

1) Cementitious products including ordinary portland cement (OPC) and sand, OPC and silica fumes/flyash, high alumina cement and flowing microconcrete.
2) Polymer modified cementitious products, which includes acrylic polymers, styrene butadiene rubber (SBR), polyvinyl acetate, styrene acrylic and magnesium phosphate.
3) A combination of polymers and silica fume with or without fibers has also been introduced recently.

This research focuses on repair and rehabilitation using the first group, which includes the cementitious and modified cementitious repair products and fluid microconcrete. These are commonly used for patch repair of damaged concrete, thin overlays, jacketing of structural elements and several applications. The current trend in the usage of the repair materials is also towards the usage of cement based repair materials [11].

The principal materials used in concrete repair include:

1) Concrete,
2) Sprayed concrete (Shotcrete/Guniting),
3) Sand/cement mortars,
4) Polymer modified cementitious mortars,
5) Resin mortars,
6) Pre-formulated commercial repair systems,

2.3.1 Concrete:

Concrete offers a number of advantages as patching material, thermal movement similar to the existing concrete, similarity in appearance, cost, readily available and familiarity. Casting new concrete to replace defective concrete can be done successfully where the areas/volume of defective concrete are significant. In general, the minimum thickness that should be reinstated with concrete is normally 75 mm but with good mix designs and the incorporation of superplasticizers, thickness to 40mm may be used [12]. Proper curing of repairs with concrete is most important.

2.3.2 Sprayed concrete (Shotcrete/Guniting):

Shotcrete is suitable for the repair of surface damages, concrete replacement and for the strengthening of structural elements. Where relatively large areas (and in some instances relatively small areas) require repairing, particularly on arches, soffits etc. repair by sprayed concrete techniques are probably the most cost effective [12]. In this technique, the sand and cement are pre-blended and blown by air pressure to the nozzle where the gauging water is introduced under pressure. The gauged material is then pressure sprayed on to the work. Gunite is normally applied up to 40mm thick and well-compacted material can be achieved. However, a very skilled operative is needed to ensure that there is good compaction behind the reinforcement.

Shotcreting in multiple layers requires that the preceding layer achieve a sufficient degree of hardness. Minimum reinforcement may be required for thickness larger than 50mm. This reinforcement should be fixed in position in such a manner that it remains stiff and keeps its position during shotcreting operations.

There are two basic shotcrete processes [5]:

a) a dry mix process where, most of the mixing water is added at the nozzle and the cement/sand mixture is carried by compressed air through the delivery hose to a special nozzle.

b) a wet mix process, where all of the ingredients, including water, are mixed before entering the delivery hose.

2.3.3 Sand/Cement mortars:

Mortars can be placed by hand, gravity, or pump, and is generally used in applications where the repairs are too shallow for the coarse aggregate present in concrete and where the fluidity of grout is not required. The use of sand/cement mortars for the repair of surface damage is dependent upon the thickness required. Correctly designed sand/cement mortar mixes often incorporating special waterproofing admixtures based on quality sands carefully placed by skilled operatives are the most cost effective repair materials where the cover on the reinforcement exceeds 25-30mm [12].

2.3.4 Polymer modified cementitious mortars:

This system is one in which a 5% by weight or more of polymer additive (by weight of cement) is mixed with conventional concrete or mortar mixtures [5]. This additive improves the final properties of the concrete or grout mix and provides high early strength. A requirement for the use of such materials is their compatibility to concrete, i.e., a sufficient degree of alkaline resistance to avoid saponification. Furthermore, the use of such materials, from an economic point of view, is only justified, when compared

to pure cement mortars or concretes. They effectively improve properties such as: water retention capacity, workability, especially in case of low water/cement ratios, flexural tensile strength, strength of adhesion, freeze-thaw/salt resistance, and resistance against the penetration of chemicals or other aggressive substances. These have low tendency towards shrinkage cracking, especially for thin layers.

Sand/cement mortars gauged with the polymer latexes have proved very satisfactory materials for concrete repairs. Such mortars afford the same alkaline passivation protection of the steel as conventional cementitious materials and can readily be placed in a single application at 12-15mm thickness which gives adequate cover [12]. The polymer latex acts in several ways:

a) It functions as a water reducing plasticizer producing a mortar with good workability and lower shrinkage at lower water/cement ratios.

b) It improves the bond between the repair mortar and the concrete repaired providing, of course, that they are applied and used properly.

c) It reduces the permeability of the repair mortar to water, carbon dioxide and oils and also increases its resistance to chemicals.

d) It acts, to some extent as an integral curing aid, but in drying conditions very careful curing is still essential.

There are four categories that should be taken into account when considering polymer-based materials for a given repair job [4]:

(i) a true appreciation of polymer characteristics and the significant differences between the repair material and the substrate.

(ii) material properties particularly those critical to its interaction with the concrete in the composite and its durability in the in-service environment.

(iii) installation parameters, which define application conditions.

(iv) test methods used to assess properties published in data sheets.

In the recent years several repair products with combined use of polymer latex, multifunctional chemical admixtures and mineral admixtures have been developed. These includes [1]:

- Micro silica or condensed silica fume (CSF) in polymer modified repair mortars. It enhances the durability and strength of the matrix. It results in the formation of a dense matrix with extremely low permeability.

- Polymer modified mortars, consisting of polymer latex and chemical admixtures such as alkyl alkoxy silanes, calcium nitrite as a corrosion inhibitor and amino alcohol derivative for durability.

- Systems with polymer latex and superplasticizers, polymer latex and flyash or other mineral admixtures, and polymer-modified mortars with fiber reinforcement are commercially available. Polymer addition to fiber reinforced cementitious products results in higher synergistic effect than for ordinary fiber reinforced product.

2.3.5 Resin repair mortars:

These are particularly beneficial when a short curing time, a high early strength and a high resistance to chemical and physical attack is required. They are suitable for repair of surface damage, or edge damage at joints and defects in concrete. Resin systems can be quite expensive.

Unlike cement based repair systems, whose high alkalinity helps prevent steel reinforcement corrosion by passivation, the protection afforded by resin mortars is achieved by encapsulating the steel reinforcement with an impermeable 'macro' coating which exhibits excellent adhesion to both the steel and concrete substrate. Epoxy resin mortars are most widely used in concrete repairs. Polyester resin and acrylic resin based mortars are used for generally for small area repairs where rapid development of strength is required.

2.3.6 Pre-formulated commercial repair systems:

These are repair products, which have been developed for specific repair conditions (surface roughness, minimum and/or maximum thickness of application, etc.) and generally under specific environmental conditions (temperature range, degree of surface wetness, etc.). They generally have specific instructions and procedures for application of the material to the damaged surface.

The pre-formulated commercial repair systems includes but are not limited to the following:

1) Modified cementitious repair materials,
2) Polymer modified cementitious materials,
3) Fiber reinforced cementitious products,
4) Flowing micro concrete,
5) Hybrid cement-epoxy repair materials.

2.4 EFFECT OF REPAIR MATERIAL PROPERTIES ON PATCH REPAIR

The key material parameters which needs to be considered in evaluating a repair material includes the following [1]:

Structural properties

- Compressive strength,
- Tensile strength,
- Flexural strength,
- Elastic modulus in compression, tension and flexure,
- Poisson's ratio,
- Creep,
- Ductility and toughness,
- Strain capacity,
- Abrasion and skid resistance.

Physical properties

- Shrinkage and swelling,
- Coefficient of thermal expansion,
- Adhesion in tension and shear [pull off strength],
- Diffusivity.

Barrier properties

- Resistance to ingress of chloride ions,
- Resistance to carbonation,
- Water absorption,
- Permeability to water, air, gasses and chemicals,
- Resistance to seawater and sulfates.

Many researchers have done extensive work to determine the basic parameters involved in performing successful repair on concrete structures. Research on polymer modified cement mortar and concrete using several types of polymers continued over several decades. However, it is only in the last quarter of 20^{th} century that modified cementitious mortars and concrete is being extensively used in various applications in construction industry and now more commonly referred to as repair materials. The modification is achieved using traditional polymers, new generation polymers, chemical and natural additives like expansive agents, condensed silica fume, fly ash, blast furnace slag and several others [1]. The principle objectives of such modifications has been directed to achieve:

- Increased workability,
- Improved performance in tensile, flexural and compressive strengths,
- Increased flexibility and impact resistance,
- Improved bonding to concrete substrates,
- Decreased permeability,
- Improved resistance to frost action,
- Enhanced resistance to penetration of aggressive species, and
- Enhance resistance to chemicals.

The material characteristics of repair systems likely to be of importance in ensuring satisfactory structural performance have been identified as [1]:

(a) strength in tension and compression,
(b) modulus of elasticity,
(c) coefficient of thermal expansion,
(d) adhesion to substrate concrete,
(e) shrinkage, and
(f) creep.

Repair material characteristics of importance in ensuring satisfactory durability of repair material will include [1]:

(a) the effect of curing temperature and temperature in-service on adhesion to the substrate concrete.

(b) the effect of thermal, moisture and freeze-thaw cycling on adhesion strength

(c) the effect of cyclic loading in-service on adhesion strength

(d) the effect of temperature on modulus of elasticity, tensile strength and development of compressive strength

(e) permeability to water, gases and salt solution.

(f) the reactivity of the patching material to steel reinforcement, aggregate in the concrete or specific sealers or protective coatings applied over the patch

According to Fonteney [13], if a **Structural repair** is needed, and possibly, some of the substrate properties should be duplicated into the repair concrete while the remaining properties should be improved:

Properties to be duplicated

- static and dynamic moduli of elasticity
- coefficient of thermal expansion
- drying shrinkage
- water permeability
- chloride permeability
- water vapor diffusivity

Properties to be improved

- cement type
- bond strength
- flexural strength
- chloride content

- oxygen diffusivity
- carbon dioxide diffusivity

Rizzo and Sobelman, [14] suggest that the properties of repair materials necessary for successful concrete repair are adhesion/bond, shrinkage, thermal movement, permeability, chemical passivation of embedded steel, mechanical strength, and ease of application. Methods for testing these characteristics are also described in the reference.

According to the investigation on shrinkage-compensating mortars by Luigi Coppola [15], the shrinkage-compensating mortars have high compressive strength and elastic modulus, since they are produced with a large amount of cement. Consequently, 3-month unrestrained shrinkage for these mortars is higher than 1200 μm/m. As a result of the high shrinkage and elastic modulus, these mortars experience tensile stress capable of promoting cracking of repair material. Cracks are followed by a loss of bond of the mortar irremediably compromising the success of the repair work. In order to avoid these problems, selection criteria of repair mortar must be based on tensile strength, on elastic modulus, on drying shrinkage, creep in tension and restrained expansion in real structures. Selection criteria based on the strength properties of the mortar ("the higher the compressive strength the better the repair material") is without any technical and scientific basis.

Many new generation repair materials have **time-state oriented** chemical admixtures, which serves as expansive agents. These expansive agents, also called "**Shrincomp**" are added to compensate for shrinkage at various states of the repair layer. The expansive action triggers off at plastic and hardened state of the repair mortar. The gaseous expansion system in plastic states compensates for the shrinkage and settlement in plastic

state and typically takes place up to the initial setting of the repair mortar. A controlled expansion varying from 1-4% takes place in both plastic and hardened states. In hardened state expansion generally occurs during the initial period up to 3-4 days [1].

A repair layer is generally unrestrained at the top surface in out of plane direction. Unrestrained expansion may result in self-destruction of the matrix due to tensile stresses that are set up. Hence, an application of pressure is generally recommended, at the top surface of the repair layer. When the repair mortar is in a nascent state the stiffness of the mortar is very low. Restrained expansion during this state will give rise to only low stresses. However, restrained expansion in the hardened state, with significant stiffness being already developed the beneficial prestress in the repair system will be significant.

According to the investigation on three commercially available generic repair materials carried out by Mangat and Limbachiya [16] the shrinkage of the repair materials is significantly greater than shrinkage of normal concrete. The shrinkage of the specially formulated repair mortars, especially those modified with a polymer admixture, is very sensitive to relative humidity of exposure compared with normal concrete. The permeability of normal concrete is similar to that of both the high performance non-shrinkable repair material and the polymer modified repair material. The other repair material based on a mineral cement binder is more permeable than normal concrete. The inclusion of aggregates improves the mechanical properties and dimensional stability of repair materials.

Several studies have been conducted to evaluate the properties of various generic repair materials. Mays and Wilkinson [17] have given the range of some commonly measured

properties for three major groups of repair materials as shown in Table-2.1. This table shows a wide variation of various properties.

Property	Resin mortar	Polymer-modified cementitious mortar	Plain cementitious mortar
Compressive strength, N/mm^2	50-100	30-60	20-50
Tensile strength, N/mm^2	10-25	5-10	2-5
Modulus of elasticity in compression, kN/mm2	10-20	15-25	20-30
Coefficient of thermal expansion per °C	$25\text{-}30x10^{-6}$	$10\text{-}20x10^{-6}$	$10x10^{-6}$
Water absorption, percent by weight	1-2	0.1-0.5	5-15
Maximum service temperature, °C	40-80	100-300	>300

Table 2.1: Typical mechanical properties of repair materials

Yuan and Marosszeky [18] investigated the restrained shrinkage in repaired reinforced concrete elements and concluded that the properties of repair materials, such as ultimate strain in tension, creep coefficient and free shrinkage, are major factors influencing the performance of structural repairs. Restrained shrinkage is related to the stiffness of a repaired section of known structure. The effect of moment redistribution on restrained shrinkage is significant in elements of indeterminate structures. The stress and strain caused by restrained shrinkage in elements of indeterminate structures are higher than in elements of known structure.

The two volume-change properties that may critically affect dimensional compatibility are drying shrinkage and thermal expansion. When making large thick patches or when

placing an overlay, it is important to closely match the coefficient of thermal expansion of the repair material with the concrete being repaired. The differences in volume change that arise when a composite system of two materials with quite different thermal coefficients undergo a significant temperature change, often cause failure at the bond interface or within the section of lower strength material [4].

Coefficient of thermal expansion and drying shrinkage are of less importance if the moduli of elasticity are very low compared to the substrate [13]. To upgrade the repair concrete to resist a locally more aggressive exposure; in those cases permeability and diffusivity of the repair concrete must be reduced.

When materials with widely differing moduli are in contact with each other, the significant difference in deformability will cause problems under specific loading conditions [4]. For example, when the external load is perpendicular to the bond line as in the case of pavement repair, a difference in modulus of elasticity between the repair material and concrete is usually not a problem. In repairs where the service load is parallel to the bond line however, the deformation of the lower modulus materials transfers the load to the higher modulus material, which may then fracture.

Not all failures of bonded materials with widely differing modulus of elasticity are caused by external loads. Shrinkage or thermal expansion and contraction can cause loss of bond unless the modulus of the repair material is low enough to permit movement without excessive stress at the bond line [4].

2.5 BEHAVIOR OF PATCH REPAIR IN COLUMNS

Patch repair in columns is a structural repair. A structural repair is one in which the reinstated patch of damaged concrete is of critical importance in resisting the applied load or an overlay/patch is implanted to enhance the load resisting capacity of the member. In a structural repair, where load has been relieved from the member or the live load is precluded from the member, stresses are developed at two stages [1].

I. Stresses originating in the patch repair from restrained environmentally induced deformations [no loads]. Such deformations are stress independent deformations such as shrinkage or swelling.

II. The stresses in a patch repair due to application of relieved dead loads and/or excluded live loads.

The stresses in structural repair in stage-I are very significant and alter significantly the stress response when loads are added in stage- II.

Emberson and Mays [19], have calculated the redistribution of stress within an axially loaded reinforced concrete member by assuming elastic behavior and a transformed concrete section and have concluded that, when the modulus of repair material is equal to that of concrete, distortion of the transverse interface is virtually eliminated, and transmission of load through the repair becomes almost uniform.

Shambira and Nounu [27] made an attempt to investigate the time-dependent deformations on the behavior of patch-repaired reinforced concrete short columns. Columns were cast using polystyrene blocks to form cavities of various depths only on

one side to receive repair material later. They used two repair materials, polymeric and polymer-modified concrete for the study. Some columns were loaded before repair to simulate instantaneous elastic behavior before repair and then reloaded after repair to observe time-dependent behavior, while others were monitored under zero load after repair for a period of up to 6 weeks.

From their experimental results and observations they concluded that the effect of loss of concrete from one side of the axially loaded columns is to induce bending which the column may not have been designed to sustain. After repair, both the repair materials considered to contribute in the short term to resist the load applied on the columns. This contribution is higher for the repair material with a higher elastic modulus. The polymer-modified repair mortar suffered higher shrinkage than the polymeric repair mortar. Because of higher repair material time-dependent deformations relative to the substrate, the short-term load-carrying ability of the repair material is reduced such that the structural function of the polymer-modified repair material was completely lost within a few weeks of repairing the columns. The contribution of the polymeric mortar was sustained for the duration of the experimental measurements. They have also suggested that the straight line is a good description of the strain distribution across the patch-repaired cross-section, which implies that conventional methods of structural analysis are applicable.

Deterioration and distress of repaired concrete structures in service are a result of a variety of physico-chemical processes such as the corrosion of embedded reinforcing steel, freezing and thawing, etc. The cracking of the repair material causes the most serious deterioration processes leading to repair failures are caused by the cracking of the

repair material Fig.2.2 [20]. Restrained contraction of repair materials, the restraint being provided through bond to the existing concrete substrate is a major factor leading to cracking and delamination of the repair phase. In simple terms, the repair material cracks when the tensile stress exceeds the tensile strength. While development of tensile cracks may be favorable from the point of view of stress redistribution in the concrete, the situation becomes extremely different when judged from the point of view of concrete's permeability, its capability to resist the penetration of aggressive elements.

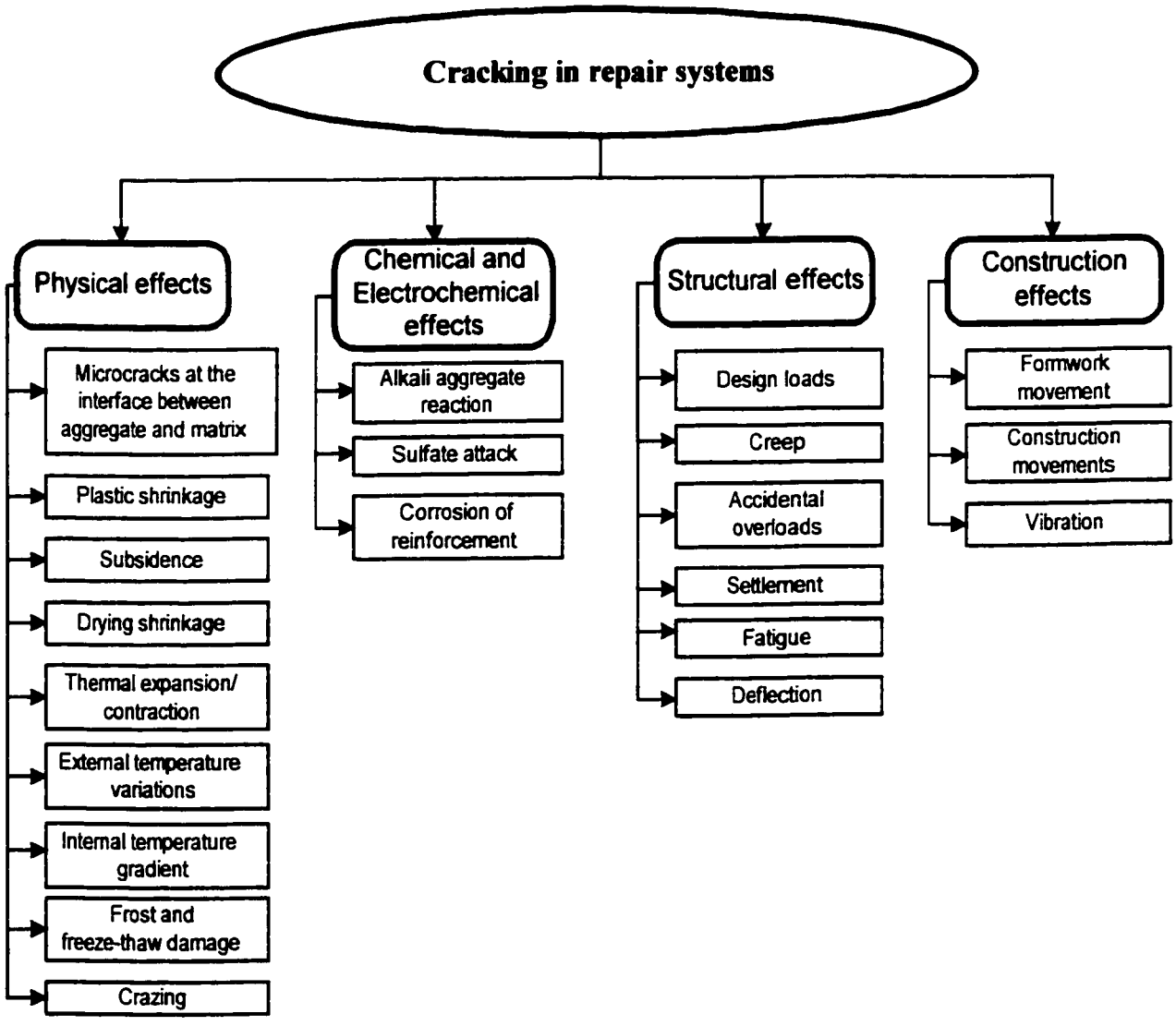

Fig 2.2: Factors affecting cracks in repair systems

For the satisfactory patch repair to a concrete structural element the prevention of reinforcement against further corrosion is an important consideration. Therefore, the performance of a repair material and reinforcement coating in protecting the reinforcement against further corrosion may need to be considered in the selection of a repair system. An experimental investigation carried out by Cleland, Yeoh and Long [21], on five repair materials in preventing corrosion of both coated and uncoated reinforcing bars have concluded that, corrosion of reinforcement is affected by shrinkage, adhesion, cover to reinforcement, permeability at the interface and compaction of the repair material.

Repair mortars applied to hardened concrete substrates have a tendency to shrink on drying. As a result of restraint provided by the substrate at the interface and/or the periphery for an enclosed patch repair, drying shrinkage cannot proceed freely. These results in the development of various stress components, the interaction of which can lead to premature failure of the patch. The potential failure modes include vertical cracking due to direct tension, horizontal cracking due to transverse or peeling tensile stresses and delamination due to interface shear stresses [22].

Luigi Coppola [15] suggests that in order to achieve successful repair of deteriorated concrete structures, using shrinkage-compensating mortars, strain-induced compressive stress from expansion plus tensile strength of the mortar must be higher than the tensile stress induced by restrained drying shrinkage.

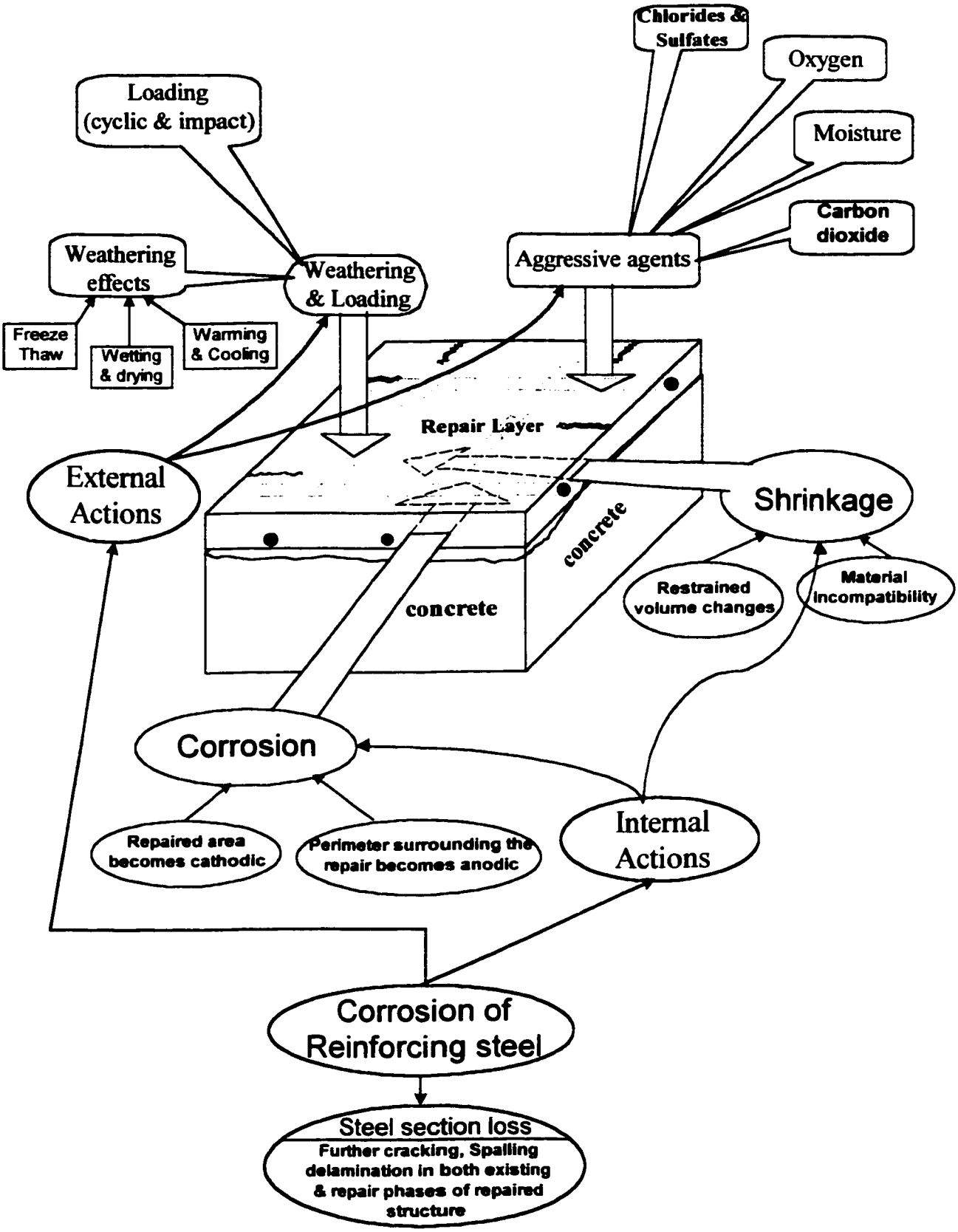

Fig 2.3: Concrete repair failure caused by cracking.

A good bond between the steel and the cement matrix allows for easy supply of OH^- ions to the steel surface due to the buffering action of the lime-rich layer; the movement of destructive Cl^- ions is limited by the dense mortar. But, most importantly, a good bond blocks the accumulation of corrosion products [7].

In concrete and other cement-based materials, micro-cracks already exist at the aggregate-mortar and reinforcement-mortar interfaces. When large, visible cracks become interconnected with micro-cracks, the network of cracks facilitates the transport of aggressive ions and gases to the embedded reinforcement, leading to premature corrosion and deterioration. The external and internal actions responsible for concrete repair failure by cracking are shown in Fig 2.3 [1,20].

Concrete repair is a composite system of materials and in composites the bond between the individual components is most critical for overall viability. The durability of the bond in repair systems can be defined as a lasting interfacial coexistence of repair and existing phases [7]. High initial bond strength is generally not an indication of bond durability. Any improvement of the bond will improve the properties of the composite system. Achieving an adequate lasting bond between repair materials and existing concrete is a critical requirement for durable surface repairs. The bond at the interface between the two constituents, or phases, is likely to be subject to considerable stresses from volume changes, freeze-thaw cycles, the force of gravity, and, sometimes, impact and vibration. The stress conditions that develop at the bond line will vary considerably, depending on the type and use of the structure.

It is essential that the repair material achieves a strong bond to the substrate and that subsequent stresses not be severe enough to cause de-bonding. Repairs that have bond

lines in direct tension have the greatest dependence on bonding. Repairs that are subject to shear stresses at the bond line are capable of stress resistance not only by bonding mechanisms, but also by aggregate interlock mechanisms, which add greatly to shear bond capacity. Factors that influence the formation of a bond and the degree of adhesion include: the properties of the substrate concrete and its surface, the properties of the repair material and adhesive used as bonding agent, absorption, adhesion, the adequacy of the repair material's adherence in cured and uncured states, and environmental conditions, such as temperature, moisture, and radiation. When an additional adhesive is not used the repair material and concrete substrate, like the classic glued connections, can be considered a contact couple where the repair acts as the glue. In this case, the strength of the bond can be seen as the result of the mechanical bond, pure adhesion, cohesion, and the contraction of the repair material. The first three factors increase the bond strength. The contraction decreases it. Another factor in bond strength is the cohesion of the repair material, which itself is determined by the strength of the binder and its mineralogical components, as well as by conditions during the curing.

On the effect of surface moisture condition of substrate concrete Chorinsky [23] reported that, if an unmodified cement mortar is applied to a dry concrete surface, part of the mixing water will be sucked into the concrete before any soluble and reactive components in the cement paste are formed. If, on the other hand, the surface of the substrate concrete is saturated with water before the mortar is applied, the excess water from the capillaries will raise the water-cement ratio in the boundary of the fresh mortar and lower its mechanical properties. For polymer modified cementitious mortars, the effect of moisture conditions is probably dependent on the polymer content.

Austin [24] and others performed tests using different moisture surface conditioning: saturated surface dry (SSD), saturated surface wet (SSW), air surface wet (ASW) and air surface dry (ASD). The results of these tests were inconclusive because of the insufficient differences in bond strength. These results indicate that it is not adequate to consider just the surface moisture condition, because the performance of the bond depends on the way the substrate will affect the direction and rate of water movement between layers of the composite repair system.

Moisture diffusivity is also an important parameter in accessing the performance of concrete patch repair [25]. As moisture evaporates from the repair layer into the surrounding ambiance of known relative humidity, the hardened concrete substrate restrains free shrinkage movement of the repair layer. As a consequence, primary tensile stresses are set up in the repair layer together with shear and peeling stresses at the interface of the repair layer-concrete substrate. The repair layer under non-uniformly increasing tensile shrinkage stresses undergoes restrained creep in tension, which results in the development of secondary stresses in the system. The secondary stresses due to restrained creep being of opposite sign to that of restrained shrinkage serve to relieve the primary shrinkage stress field and the net or combined stress buildup as a result is reduced.

The Electrochemical non-homogeneity of phases in a repair system asserts itself adversely by creating conditions conductive to electrolytic corrosion of embedded reinforcement. The resistivity of the patching material may also affect the durability of the patch and the concrete in the members undergoing repair. Materials that are highly resistive or non-conductive have a tendency to isolate the repaired area from the adjacent

undamaged areas. Consequently, if there is a large permeability or chloride content differential between the patched area and the rest of the concrete, the corrosion current becomes concentrated in a restricted area and the rate of corrosion may then be accelerated, causing premature failure in either the patch or adjoining concrete.

If impermeable materials are used for large patches, overlays or coatings, moisture vapor that passes up through the base concrete can be entrapped between the concrete and the surfacing. Entrapped moisture can saturate the surface layers causing failure by freezing and thawing action either at the bond line or within the weaker of the two materials. For most of the situations, the location of the repair in the repaired structure and moisture transport will determine whether the repair material shall be low or compatible with the substrate permeability.

According to Emmons and Vaysburd [4], a holistic approach to repairs ensures that no part of the system is overlooked and takes into account the concurrent interaction of many factors and the consequent physico-chemical changes occurring simultaneously.

2.6 SHRINKAGE

Shrinkage is defined as the time dependent deformation resulting from reduction in volume of an unloaded specimen made of cementitious material or concrete at constant temperature and relative humidity. The shrinkage is associated with the loss of moisture to the ambient environment or due to chemical processes. The volume change of the colloidal inert system in a cementitious mortar, as its moisture content is changed, due to the diffusion of moisture into ambience is the principal component of shrinkage. It occurs in both plastic and hardened states and are termed as the **plastic shrinkage and**

drying shrinkage, respectively. Autogenous shrinkage, thermal shrinkage and carbonation shrinkage, on the other hand, occur due to direct or related chemical processes. The **autogenous shrinkage or chemical shrinkage** is the volume change associated with the change in the concentration of the cement gel due to the chemical process of hydration. The **carbonation shrinkage** results from the local release of crystallization pressure, due to dissolution of the crystals of calcium hydroxide embedded in the structure of the hydrated cement paste. The volume contraction due to dissipation of heat generated by the hydration of cement is called **thermal shrinkage**.

When the evaporation rate exceeds the rate of bleeding and the free settlement period is ended, a hydrostatic tension begins to develop throughout the mass owing to the formation of menisci at the water surfaces in the capillaries. This results in vertical as well as lateral compressive forces. It is called **plastic shrinkage**. As drying takes place, three mechanisms cause shrinkage [26]:

1. The unstable nature of newly-formed calcium silicate hydrate results in shrinkage as drying occurs; the exact nature of this mechanism is not clearly understood but it is permanent and irreversible;
2. Compressive stresses are set up in the concrete because of the development of menisci in the capillaries as drying progresses;
3. Energy changes occur at the surface of calcium silicate as the water evaporates.

These mechanisms (phenomena) acting separately or in combination cause initial drying shrinkage of the concrete. Part of it, 30 per cent or more, is irreversible.

2.6.1 Significance of drying shrinkage in a repair system

In concrete structures with relatively massive elements, the rate of moisture loss is slow and is spread over several years. The shrinkage-induced stresses are consequently low. Repair and rehabilitation of deteriorated structural concrete elements using patch repair system results in bi-layered systems with a thin top layer. In a repair system, on the other hand, the moisture movement across the exposed domains of the thin repair layer is predominant. The effect of drying shrinkage in a repair system is, therefore, highly pronounced and rapidly manifested. Coupled with rapid moisture loss, the repair layer has a high degree of restraint from the host layer. This results in early age cracking and delamination of the repair layer. The drying shrinkage, therefore, plays a vital role in the long-term integrity of a repair system [1].

2.6.2 Factors affecting drying shrinkage

The drying shrinkage is associated with the moisture movement from the cementitious mortars into the ambience. The driving force for such moisture transport is the potential provided by ambient relative humidity. The evolution of drying shrinkage in a cementitious mortar depends on several factors. The environmental conditions have a pronounced influence on magnitude of drying shrinkage together with the moisture content in the mortar. Several other factors like composition of cementitious material and additives also have significant effect on drying shrinkage. Construction practices also affect drying shrinkage.

The factors affecting drying shrinkage includes:

- Environmental conditions like temperature, relative humidity and wind velocity,

- Pore structure of cementitious mortar,
- Mortar constituents like water-cement ratio and cement content,
- Aggregate type and gradation,
- Admixtures added to the cementitious mortar,
- Geometry of patch, mainly the thickness,
- Type of curing, use of curing compounds,
- Presence of cracks,
- Addition of fibers to the cementitious mortar, and
- Age.

2.6.3 Shrinkage Free and restrained

Free shrinkage is a contraction that an element of cementitious material would undergo due to moisture diffusion (drying), if there were no constraint on its movement, i.e. each infinitesimal element of the specimen was unrestrained. The free shrinkage deformation evolves with time. The shrinkage strain-time curve becomes asymptotic after some time, when the moisture content in the specimen is in equilibrium with the environmental humidity. The free shrinkage strain at this stage is called the **ultimate free shrinkage strain**.

The shrinkage strain measured experimentally in systems with external and/or internal restraints is always less than the free shrinkage strain of the material. This is generally termed as the **restrained shrinkage** or **apparent shrinkage**. The restrained or apparent shrinkage includes not only the free shrinkage strain but the stress-related strain as well.

2.7 EFFECT OF TIME DEPENDENT DEFORMATIONS ON PATCH REPAIRS (Creep Effect)

Creep resulting from the action of a sustained stress is a gradual increase in strain with time. As defined, creep does not include any immediate elastic strains caused by loading or any shrinkage or swelling caused by moisture changes.

If the sustained load is removed, the strain decreases immediately by an amount equal to the elastic strain at the given age; this is generally lower than the elastic strain on loading since the elastic modulus has increased in the intervening period. This instantaneous recovery is followed by a gradual decrease in strain, called creep recovery. This recovery is not complete because creep is not simply a reversible phenomenon.

It is now believed that the major portion of creep is due to removal of water from between the sheets of a calcium silicate crystallite and to a possible rearrangement of bonds between the surfaces of the individual crystallites [26].

2.7.1 Significance of creep in patch repair systems

The time dependent deformations due to creep play an important role in repair systems. For creep in repair material in compression, excessive creep may result in reduced load bearing effectiveness in repair material and diversion of loads into substrate, resulting in higher stresses in it [1]. It therefore renders the repair less effective with time. For repairs in compression, it is therefore desirable to have repair materials with lower creep potential in compression. The compressive creep in structural repair results from the applied external compressive load.

2.7.2 Factors affecting creep

The factors affecting creep can be grouped into two major classes apart from age of loading:

(a) Environmental factors
- ambient temperature,
- relative humidity,
- wind.

(b) Intrinsic factors
- mix proportions,
- degree of hydration,
- moisture content,
- stress/strength ratio,
- age of application of load,
- mineral admixtures,
- aggregate type and gradation,

Concrete that exhibits high shrinkage generally also shows a high creep, but how are these two phenomena connected is still not understood. Evidence suggests that they are closely related. When hydrated cement is completely dried, little or no creep occurs, for a given concrete the lower the relative humidity the higher the creep.

Strength of concrete has a considerable influence on creep and within a wide range creep is inversely proportional to the strength of concrete at the time of application of load. From this it follows that creep is closely related to the water-cement ratio. There is no doubt also that the modulus of elasticity of aggregate controls the amount of creep that

can be realized and concretes made with different aggregates exhibit creep of varying magnitudes.

Experiments have shown that creep continues for a very long time; detectable changes have been found after as long as 30 years [26]. The rate decreases continuously, however, and it is generally assumed that creep tends to a limiting value. It has been estimated that 75 per cent of 20-year creep occurs during the first year.

CHAPTER 3

EXPERIMENTAL PROGRAM FOR THE RESEARCH

3.1 LABORATORY TESTING OF CONCRETE & REPAIR MATERIAL PROPERTIES

The work in this task is testing of concrete and repair materials for their properties, which are required to analyze and predict the performance of repair materials when used for patching of corrosion damaged columns. The laboratory oriented tests for this task on small-scale specimens includes two major categories:

1. Evolution of strength and stiffness, and
    (a) Compressive strength,
    (b) Tensile strength,

(c) Bond Strength,

(d) Compressive modulus of elasticity and poison's ratio,

(e) Tensile modulus of elasticity.

2. Evolution of time dependent properties.

(f) Shrinkage,

(g) Compressive creep,

(h) Chloride penetrability, and

(i) Sulfate attack.

3.1.1 SELECTION OF REPAIR MATERIALS

A detailed survey of repair materials available in Eastern Province commercially, for carrying out structural repair was carried out. Data regarding the field performance of repair materials in structural repairs was collected from contractors and consultants of Eastern Province of Kingdom of Saudi Arabia.

The companies visited includes:

1. FOSAM Co. Ltd, Dammam – Repair material supplier
2. SIKA Ltd - Repair material supplier
3. Master Builders (MBT) - Repair material supplier
4. Modern Arab Construction (MAC), Al-Khobar – Repair contractors
5. Nabil A. Abu Nahaya, Al-khobar – Repair contractors
6. SCECO East
7. Al- Rabiah COWI – Repair Consultants

Based on this survey, two repair materials were selected for carrying out this research. The criteria for the selection of two repair materials was as follows:

1. The stiffness of the repair mortar is an important factor in load distribution in a repaired column. Hence a material with a low and high elastic modulus value needs to be selected.

2. Creep and shrinkage significantly changes the stresses in a structural repair and is an important parameter in selecting the repair material.

Meetings were held with the representatives of repair companies in the Eastern Province and data sheets for the repair materials suggested by these companies for the repair of test columns and its long term testing to assess the load redistribution was obtained and evaluated.

The repair materials selected for the study includes:

1. Fluid Micro Concrete (FMCX). It is a prepackaged, ready to use blend of dry powders and selected aggregates, non-shrink, fluid micro concrete suitable for mass infill to structural repairs in all types of load bearing situations and structural repairs. It has a high modulus of elasticity and low shrinkage. It is recommended for repair to columns suffering from major loss of section.

2. Polymer modified, Fiber reinforced, Silicafume Mortar (PFSM). It is a prepackaged, cementitious, silica fume containing, fiber reinforced, polymer modified, high strength, shrinkage compensating, and one component repair mortar suitable for tropical conditions. It is used for concrete repairs especially for

overhead and vertical applications. It has a lower modulus of elasticity as compared to FMCX.

The major characteristics of the repair material FMCX as stipulated by the manufacturer is as follows:

Test method	Age	Typical result
Drying shrinkage ASTM C157-93	7 days	: < 300 microstrains
	28 days	: < 500 microstrains
Permeability DIN 1048 Part 5		: < 10 mm
Flexural strength BS 6319 part 3	28 days	: > 9 N/mm^2
Tensile Strength BS 6319 Part 7	28 days	: > 5 N/mm^2
Compressive Strength BS 1881 part 116	3 days	: > 39 N/mm^2
	7 days	: > 45 N/mm^2
	28 days	: > 60 N/mm^2
Water absorption BS 1881 Part 121		: < 2%
Modulus of Elasticity	28 days	: > 33 GPa

The major characteristics of the repair material PFSM, as stipulated by the manufacturer is as follows:

Test method	Age	Typical result
Drying shrinkage ASTM C157-93		Not provided
Flexural Strength ASTM C-348	28 days	: > 7-9 N/mm^2
Adhesive tensile strength ACI 503	28 days	: > 1.5-2.5 N/mm^2
Compressive Strength ASTM C-109	28 days	: > 45-55 N/mm^2

Modulus of Elasticity (Static) : > 25 GPa

3.1.2 CONCRETE MIX SPECIFICATIONS

The mix proportion for concrete specimens used in this research is as follows. The same mix design was used for all specimens cast, which include small-scale specimens for testing properties and large-scale columns. The total quantity of concrete used is 2 cubic meters.

Mixture	Quantity	Units
Cement	355	kg/m^3
Microsilica	30	kg/m^3
w/c ratio	0.4	
Fine aggregate	680	kg/m^3
Coarse aggregate 10 mm	485	kg/m^3
Coarse aggregate 20 mm	625	kg/m^3
Superplasticizer	1.4	ltr/m^3
Air content	0	%
Slump	110	mm

3.1.3 TEST SPECIMENS

Various types of prismatic specimens were used in the study. Some of the specimens fall in the category of standard specimen as per ASTM or BS standards. However, in order to

minimize the variation in specimen size some non-standard specimen sizes were also adapted in the study as detailed herein below.

(a) Compressive Strength Tests

Cylinders 75Øx150mm and cubes 50x50x50mm were used for repair materials. Cylinders 75Øx150mm were used for concrete.

(b) Tensile Strength Tests

Standard briquettes as per BS standard were used for the direct tensile test of repair materials.

(c) Bond Strength Tests

Cylinders 75Øx150mm and cores 75mm Ø from slabs 350x350mm were used for testing the bond strength of repair materials with concrete in direct tension.

(d) Compressive modulus of Elasticity & Poison's Ratio

Cylinders 75Øx150mm were used for repair materials and concrete.

(e) Tensile Modulus of Elasticity

Prisms 40x40x160mm were used for testing the tensile modulus.

(f) Shrinkage Tests

Shrinkage tests were conducted on three sets of specimen.

(a) Prisms 25x25x285mm as per ASTM standard C-157,

(b) Prisms 40x40x160mm.

(c) Prismatic slabs 300x250x75mm, which are the same size of patch repair on columns used in this research.

(g) Compressive Creep Tests

Cylinders 150Øx300mm were used for repair materials and concrete, and prismatic slabs 300x250x75mm.

(h) Chloride Penetrability Tests

Cylindrical slices 75Øx50mm were used for repair materials and concrete

(i) Sulfate Attack

Cubes 50x50x50mm were used for repair materials and concrete

3.1.4 MOULDS FOR SPECIMEN

All specimens for this study were cast in moulds. Metallic and Plexiglass molds were used for this purpose. Six moulds of Plexiglass for casting 40x40x160mm size prisms were made in the research workshop to cast three specimens in each mould. Cylindrical moulds of size 75Øx50mm, 150Øx300mm and moulds for briquettes were available in the concrete laboratory.

3.1.5 MANUFACTURE OF SPECIMENS

The manufacture of all small scale specimens for measuring strength and stiffness evolution and time dependent properties was programmed to meet the restrictions on using portion of bag contents by the manufacturer of the repair products. A sufficient number of moulds were prepared for casting specimens using entire bag for each of the selected repair materials.

Mixing Procedure

The mixing of the repair mortar was carried out using a forced action mixer. The forced action mixer was enacted using a spiral paddle attached to a heavy-duty drill machine of speed up to 500 rpm. The amount of clean water specified by the manufacturer was placed in a suitable sized drum, which was cleaned thoroughly. A full bag of repair mortar was added slowly or rapidly and continuously as per manufacturer's recommendations to the drum while the spiral paddle was set in motion. The mixing was carried out for 2-5 minutes depending upon manufacturer's instructions, until a smooth and even consistency is obtained and the mortar is homogeneous and lump free, wherever applicable. Restrictions by the manufacturer on mixing longer time, reworking of the mortar and adding additional water to get workability after some elapsed time was strictly adhered to.

Placing of Repair Mortars

The repair mortar was placed in the moulds immediately after mixing. Care was taken not to exceed the manufacturer's stipulated working time by increasing the manpower. Depending on the type of the repair mortar, the mortars were placed as per manufacturer's recommendations. For flowing micro-concrete, the material was pourable and hence small holding cans were used to pour the material in the mould. No vibration was performed. For trowelable material, the repair mortar was placed in the mould and pressed firmly by hand to force the plastic mortars into corners. The mortars were also compacted using a vibrating table in certain cases. For thicker specimens, repair mortar was placed in two layers and each layer was compacted thoroughly on a vibrating table. Leveling and initial finishing was carried out using a wooden float wherever required. In

shrinkage compensated flowable microconcrete, a light pressure was applied on the surfaces to prevent unrestricted expansion in exposed surface, as per manufacturer's recommendations.

Placing of Embedded Strain Gauges

Strain gauges were inserted in the repair mortar at the time of casting. In flowing microconcrete gauges were placed after some time to allow the mortar to set. In trowelable mortar the mortar was place up to desired level, strain gauge was placed and then the remaining mortar was placed.

3.1.6 CURING REGIME FOR TEST SPECIMENS

All specimens used in this test series were kept in moulds for 24 hours after casting. The surface of the specimens were covered with layers of plastic sheet and then covered with wet towels. A plastic sheet was placed over the wetted towel to ensure that it remains wet for 24 hours. After 24 hours, the specimens were removed from the moulds. The specimens were then kept moist under wet towels and covered by plastic sheets for a period of 7 days. After 7 days, the specimen were removed from the wet cloth and allowed to cure in air at 65 ± 5% humidity and 23 ± 2°C temperature for the entire duration of test.

3.1.7 TEST PROCEDURE FOR COMPRESSIVE STRENGTH TEST

The compressive strength tests of the two repair materials were carried out using 50x50x40mm cubes (ASTM C-579) and 75Øx150mm cylinders (ASTM C-39). For concrete only cylinders 75Øx150mm were used. The 75Øx150 mm repair mortar

cylinders were prepared to make the ends flat and the edges of the specimens were made smooth by using sulfur cap. Tests on cubes were conducted on a hydraulic machine with a load capacity of 200 kN. Tests on cylinders were conducted on a hydraulic machine with a load capacity of 3000 kN. The loading rate was kept at 1.1 kN/sec for all tests. The load was measured by load cell built in the equipment. Tests were conducted at various ages 1, 3, 7, 14, 28, 60, and 180 days after casting, for repair materials and 7, 14, 28, 60, and 180 days for concrete. Three specimens were tested at each age to take their average. If the strength values differ from the mean by more than 15%, the farthest value from the mean was rejected and average of the remaining two samples was recorded as the compressive strength of the material at that age.

3.1.8 TEST PROCEDURE FOR TENSILE STRENGTH TEST

The direct tensile strength of repair mortars was determined using the standard briquette tests as per ASTM C-307. The tests on briquettes were performed on standard testing machine. Tests were conducted at various ages 1, 3, 7, 14, 28, 60, and 180 days after casting. Five specimens were tested at each age to take their average. If the strength values differ from the mean by more than 15%, the farthest value from the mean was rejected and average of the remaining four samples was recorded as the tensile strength of the material at that age.

3.1.9 TEST PROCEDURE FOR BOND STRENGTH TEST

The bond strength tests were conducted using cylinders 75Øx150mm and cores 75mm Ø from slabs 350x350mm and tested in direct tension.

Preparation of Samples

The concrete cylinders 75Øx150mm were cut to two equal halves and the circular surface cut was sandblasted. The concrete cylinders now 75Øx75mm were kept wet in the cylindrical moulds of size 75Øx150mm and the remaining half was filled with repair material. The specimens before testing were prepared by roughening the flat surfaces of cylinders and applying high strength epoxy to attach steel plates. The details of specimens used are shown in Figure 3.1.

The same test was also performed by using cores. Concrete slabs of size 350x350x100mm were cast and its surface was sandblasted. After wetting the sandblasted surface 50mm thick repair was cast on it. Four cores of size 75mm Ø were taken from these slabs for testing at each age. The cored specimens before testing were prepared using the same procedure as used for cylinders. The details of these specimens used are also shown in Figure 3.1.

Testing apparatus

A special grip consisting of plates and hooks was used to hold the test specimens. The test specimens were attached to the plate using high strength epoxy. The grip was mounted onto the close loop Electro-hydraulic loading machine of 200 kN capacity. To minimize eccentricity, hooks were used to simulate pin connections. The testing arrangement is shown in Figure 3.2.

Test procedure

The testing machine has a top block, which moves upward/downward. The tensile load was applied to the specimen by the upward movement of the top block at rate of 1 mm/minute till failure. The load was measured by load cell built in the equipment. The

highest load taken by the specimen to fail at the interface of repair and concrete was recorded and the bond strength evaluated for that age. Tests were conducted at various ages 3, 7, 28, and 60 days after casting the repair material. Three replicate specimens for cylinders and four replicate specimens for cores were tested at each age for each material.

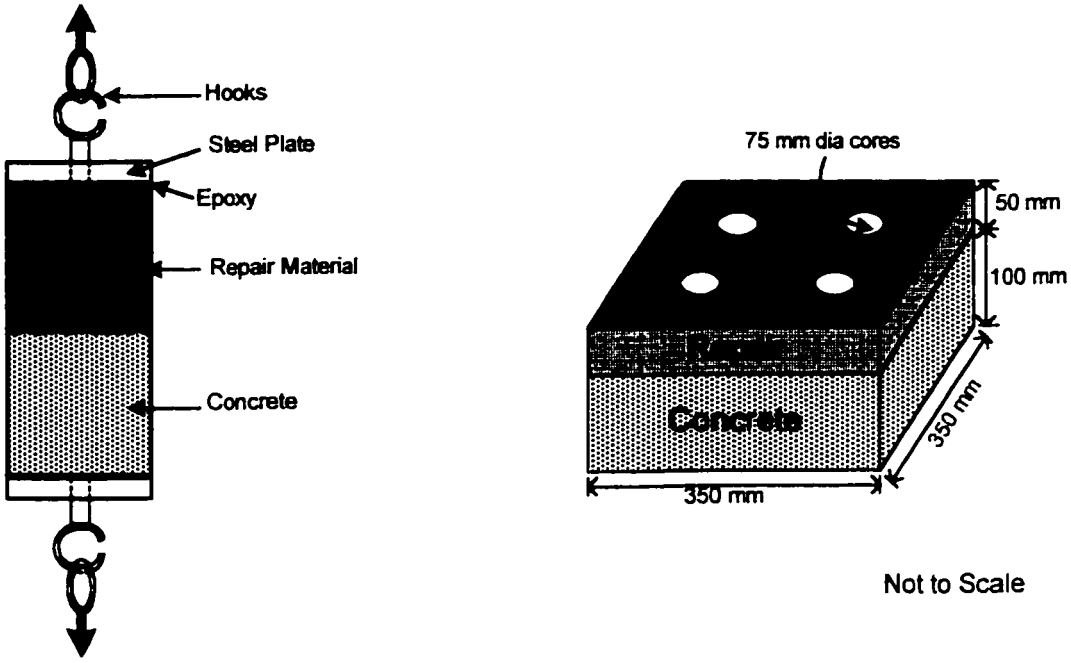

Figure 3.1: Details of bond strength test specimens

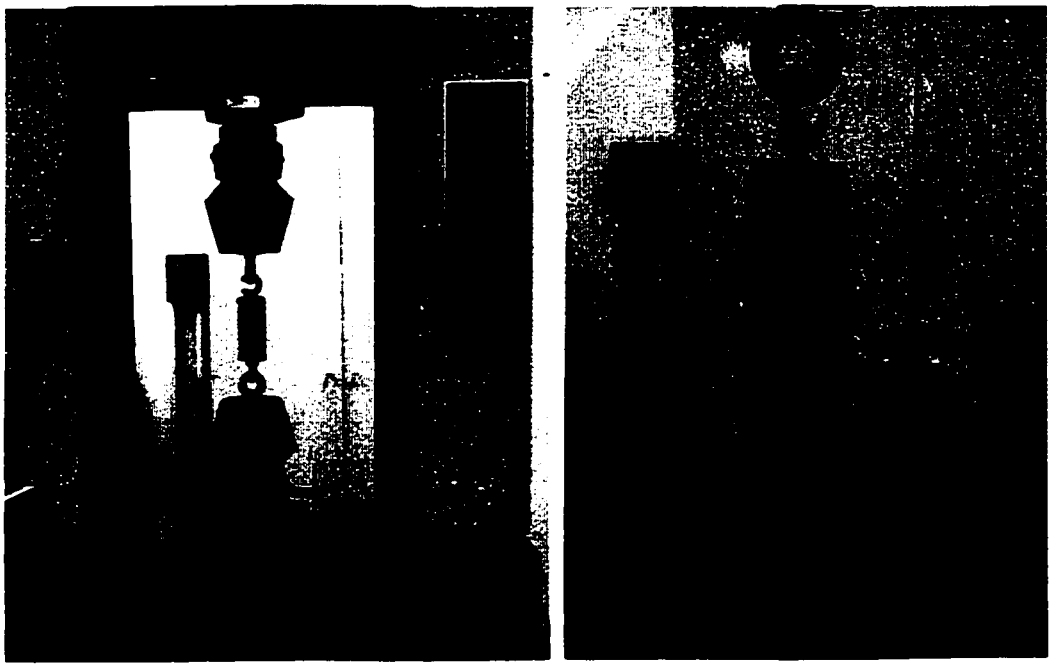

(a) Test on cylinder **(b) Test on core**

Figure 3.2: Testing arrangement for Bond strength tests

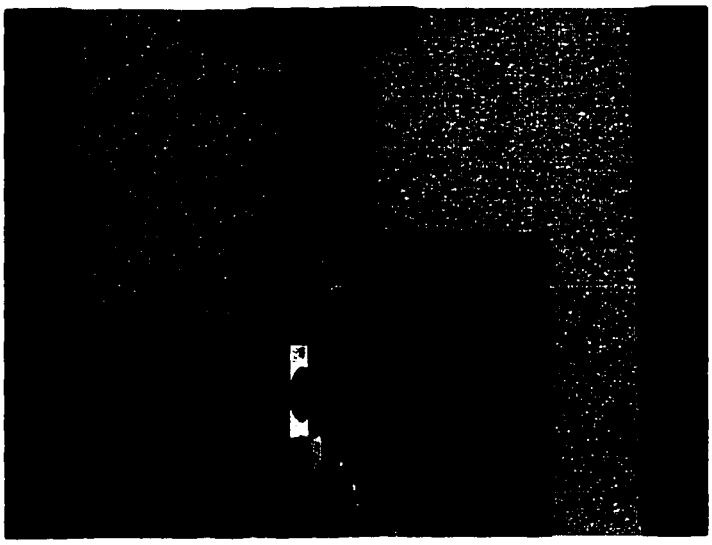

Figure 3.3 Bond test specimen failure at the interface of repair and concrete

3.1.10 TEST PROCEDURE FOR COMPRESSIVE MODULUS OF ELASTICITY AND POISON'S RATIO

The compressive modulus of elasticity and poisons ratio of the two repair materials and concrete were carried out using 75Øx150mm cylinders. The standard test method specified by the ASTM C-469 was used.

Preparation of sample

The 75Øx150mm repair mortar and concrete cylinders were prepared to make the ends flat and the edges of the specimens were made smooth by using sulfur cap. The specimens from curing tank were first dried by a towel and then allowed to dry in air for 2-4 hours before being tested. An internal embedded gauge was already placed in the specimen while casting. Strain gauges were glued using a quick set epoxy when the surface of the specimens was dry. The details of test sample are shown in Figure 3.4.

Testing apparatus

The load applied on the specimen was measured using a close loop Electro-hydraulic loading Instron machine of 200 kN capacity. The testing arrangement is shown in Figure 3.5.

Loading measurements

The testing machine has a top block, which moves upward/downward, and has a load cell attached to it. The compressive load was applied to the specimen by the downward movement of the top block at a rate of 1 mm/minute.

Deformation measurements

The longitudinal strains were assessed by means of electrical embedded TML strain gauges of Type PMLS-45, having a gauge length of 40 mm and TML type PL-60-11 surface gauges attached to the surface. These surface strain gauges having a gauge length of 60 mm were attached on opposite sides of the test specimens. For measuring the transverse strain, surface gauges were attached to the cylinder in the horizontal direction. Lead wires from strain gauges and load cell of Instron machine were connected to a data logger.

Test procedure

The compressive load was applied to the specimen, initially at a very slow rate at about 10% of the ultimate compressive strength of the material. Strain and deformation readings were taken. If the individual strains were not within 10% of the mean value then the specimens was unloaded and the specimen and plates were adjusted. The specimen was loaded again to check strain variation. This process is repeated until essentially similar strains are achieved on the sides. For measuring elastic modulus, load was applied at a controlled longitudinal deformation rate of 2 mm/min till failure. All load and deformation data were recorded at load increments of 5 kN using automated computer controlled data loggers.

Test parameters

- The tests were carried out under normal laboratory conditions with 23 ± 2°C temperature and 60 ± 5% relative humidity.
- Minimum of two replicate specimens were used for each material. At early ages, three replicate specimens were tested.

- The tests were carried out at following ages: 1, 3, 7, 14, 28, 60, and 180 days.

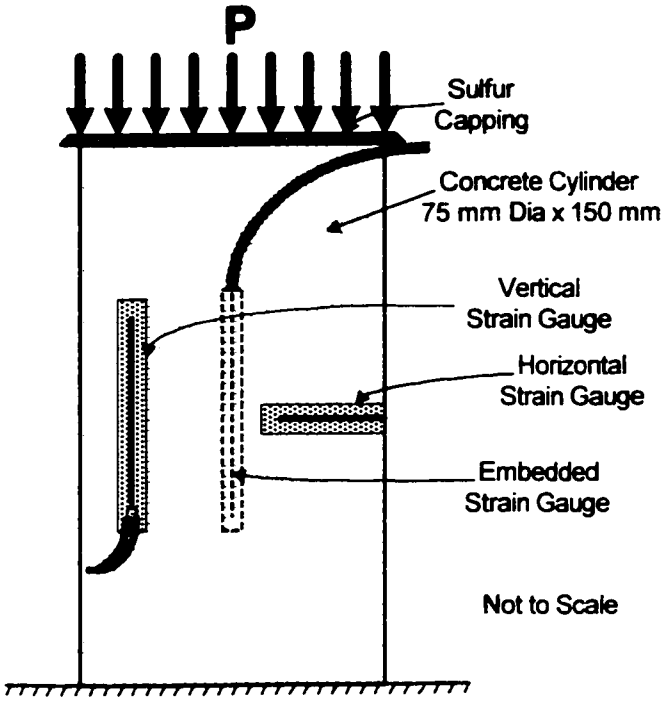

Figure 3.4: Details of Compressive Modulus specimen

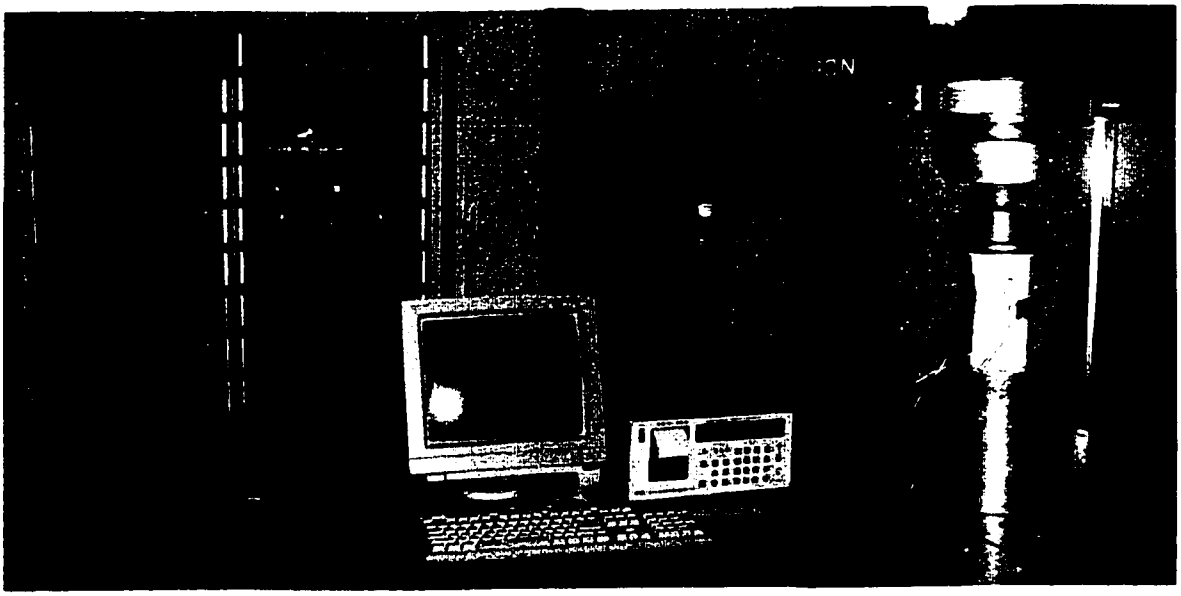

Figure 3.5: Testing arrangement for compressive modulus of elasticity test

3.1.11 TEST PROCEDURE FOR TENSILE MODULUS OF ELASTICITY

The tensile modulus of elasticity of the two repair materials was carried out using 40x40x160mm prisms.

Preparation of sample

The 40x40x160mm repair mortar prisms were prepared to make the ends flat and the edges of the specimens were made smooth. The specimens from curing tank were first dried by a towel and then allowed to dry in air for 2-4 hours before applying high strength epoxy to attach steel plates. Strain gauges were glued on opposite faces using a quick set epoxy when the surface of the specimens was dry. The detail of test specimen is shown in Figure 3.6.

Testing apparatus

A special grip consisting of plates and hooks was used to hold the test specimens. The test specimens were attached to the plate using high strength epoxy. The grip was mounted onto the close loop Electro-hydraulic loading machine of 200 kN capacity. To minimize eccentricity, hooks were used to simulate pin connections. The testing arrangement is shown in Figure 3.7.

Loading measurements

The testing machine has a top block, which moves upward/downward, and has a load cell attached to it. The tensile load was applied to the specimen by the upward movement of the top block at a rate of 1 mm/minute.

Deformation measurements

The longitudinal strains were assessed by means of electrical strain gauges TML type PL-60-11. These strain gauges having a gauge length of 60 mm are attached on opposite sides of the test specimens. Lead wires from strain gauges and load cell of Instron machine were connected to a data logger.

Test procedure

The tensile load was applied to the specimen, initially at a very slow rate at about 10% of the ultimate tensile strength of the material. Strain and deformation readings were taken. If the individual strains were not within 10% of the mean value then the specimen was unloaded and hooks adjusted to ensure that the eccentricity is minimized. The specimen was loaded again to check strain variation. This process is repeated until essentially similar strains are achieved on the sides. For measuring elastic modulus, load was applied at a controlled longitudinal deformation rate of 1 mm/minute till failure. All load and deformation data were recorded at load increments of 0.5 kN using automated computer controlled data loggers.

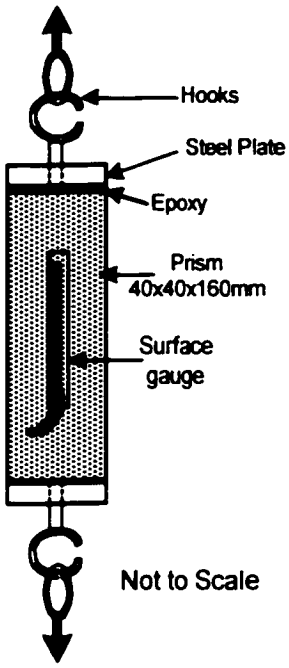

Figure 3.6: Details of tensile modulus specimen

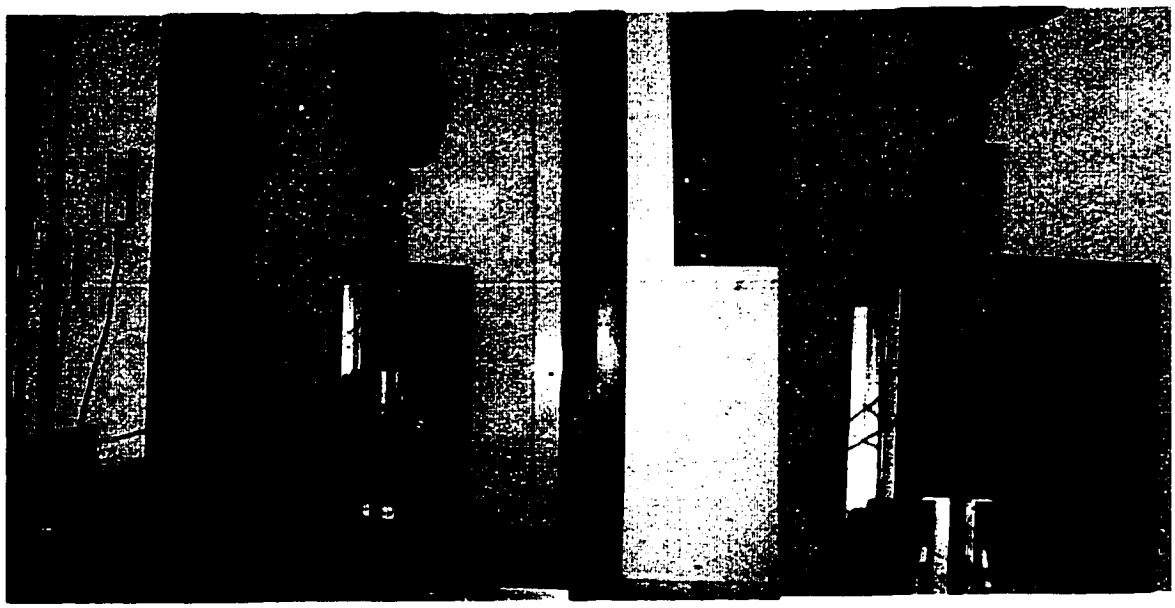

Figure 3.7: Testing arrangement for tensile modulus test

Test parameters

- The tests were carried out under normal laboratory conditions with 23 ± 2°C temperature and 60 ± 5% relative humidity.
- A minimum of three replicate specimens was used for each material. At early ages, five replicate specimens were tested.
- The tests were carried out at following ages: 3, 7, 28, and 60 days.

3.1.12 TEST PROCEDURE FOR SHRINKAGE TEST

The free expansion and shrinkage tests for two types of repair materials and concrete on three sizes of specimens were carried out in a test series in which strain evolution was captured right from the stage of initial setting of the material. The expansion in the repair materials results from the addition of shrinkage compensating agents, which initiates in plastic state and initial hardening state (up to 3-4 days).

These tests were carried out on prismatic specimens of three sizes 40x40x160mm, 25x25x285mm and 300x250x75mm. The 300x250x75mm specimens were covered by aluminum foil on three faces to avoid moisture loss from those faces to simulate its condition when in a patch repair of column, used in this research. The detail of this specimen is shown in figure 3.8 and 3.9. The expansion and shrinkage strains were captured from 2 hours after casting up to 8-12 weeks by using embedded strain gauges. The specimens were placed in moist conditions till the curing period and then subjected to drying at room temperature and humidity.

Curing regime

Expansion and shrinkage were measured on the same specimen with a replicate of two specimens. The specimens were cured in moulds for 24 hours as described in earlier

section. The specimens for expansion/shrinkage were covered in plastic sheet and kept under wet towel for 7 days and expansion was measured. After 7 days the wet towel was removed and the specimens were allowed to dry in a room at 23 ± 2°C temperature and 65 ± 5% relative humidity and shrinkage was monitored.

Deformation measurements

The expansion/shrinkage strain evolution was measured by embedded strain gauges. TML strain gauges of Type PMLS-45, having a gauge length of 40 mm were used for this purpose. The gauges were embedded in the samples at the time of casting the specimens at a depth of approximately half the width of specimens. from the surface of the specimens. All strain gauges were connected to a data logger and extension box. A computer connected to the data logger took the measurements automatically. The complete setup and specimens attached to data logging system are shown in Figure 3.10.

Test procedure

The specimens for capturing the strain evolution (expansive/shrinkage strain) had an embedded strain gauge that was placed at the time of casting the specimen. While the specimen was still in the mould, the strain gauges were connected to the data logger. The strain measurements were initiated soon after the initial setting of the repair mortar, after nearly 2 hours. During the measurements in the mould, the top surface of the specimen was covered with plexiglass sheet, wet towel and then a plastic sheet. In this stage, strain measurements were taken at 15-min intervals for 2 hours and then at 30 min and 60 min intervals. The specimens were demolded after 24 hours. The samples were immediately placed under curing under wet towel covered with plastic. Strain measurements were

taken at intervals of 30 minutes for the first four hours. An interval of 1 hour, 2 hours and 6 hours were used subsequently until the removal of the samples from curing.

The specimens were removed from curing after 7 days and then allowed to dry in the air up to the end of the testing period. When subjected to air drying, the strain measurements were initially taken at intervals of 1 hour for 12 hours, subsequently the time interval was progressively increased in a preprogrammed data acquisition control to 2 hours, 6 hours and finally once a day up to at least 2 months. The readings were subsequently taken till the end of the testing period.

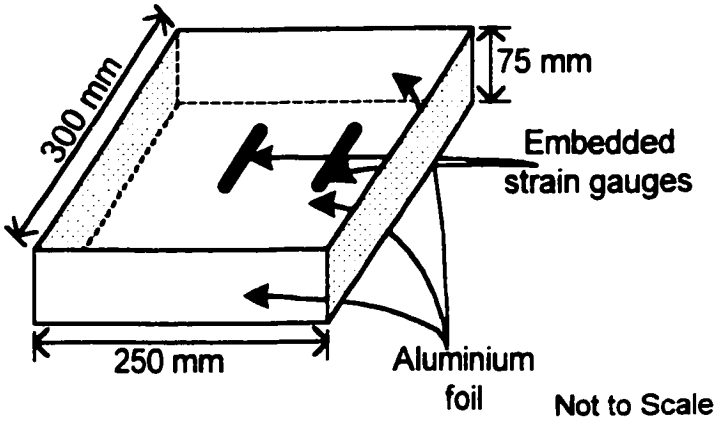

Figure 3.8: Details of Shrinkage specimen 300x250x75mm with embedded gauges and three faces covered by aluminum foil

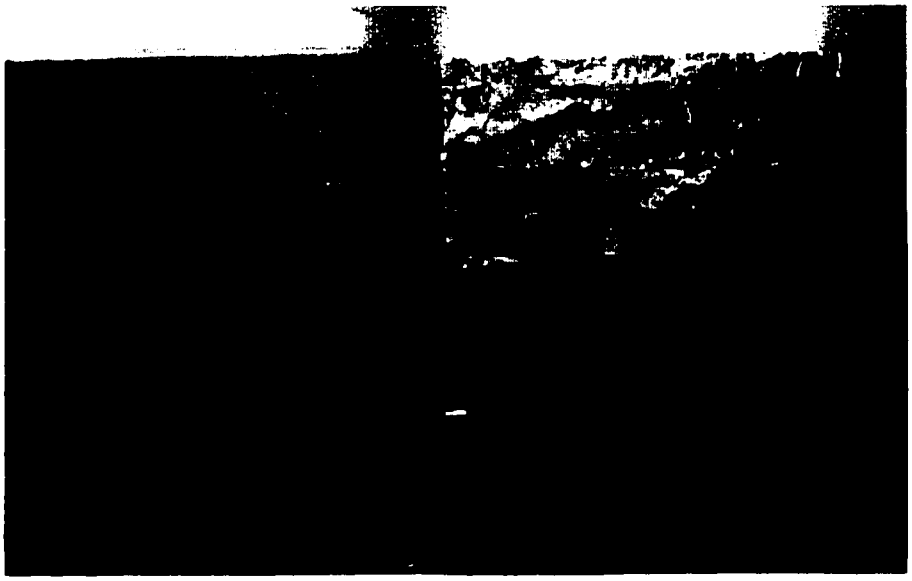

Figure 3.9: Shrinkage specimens 300x250x75mm with embedded gauges and covered with aluminum foil

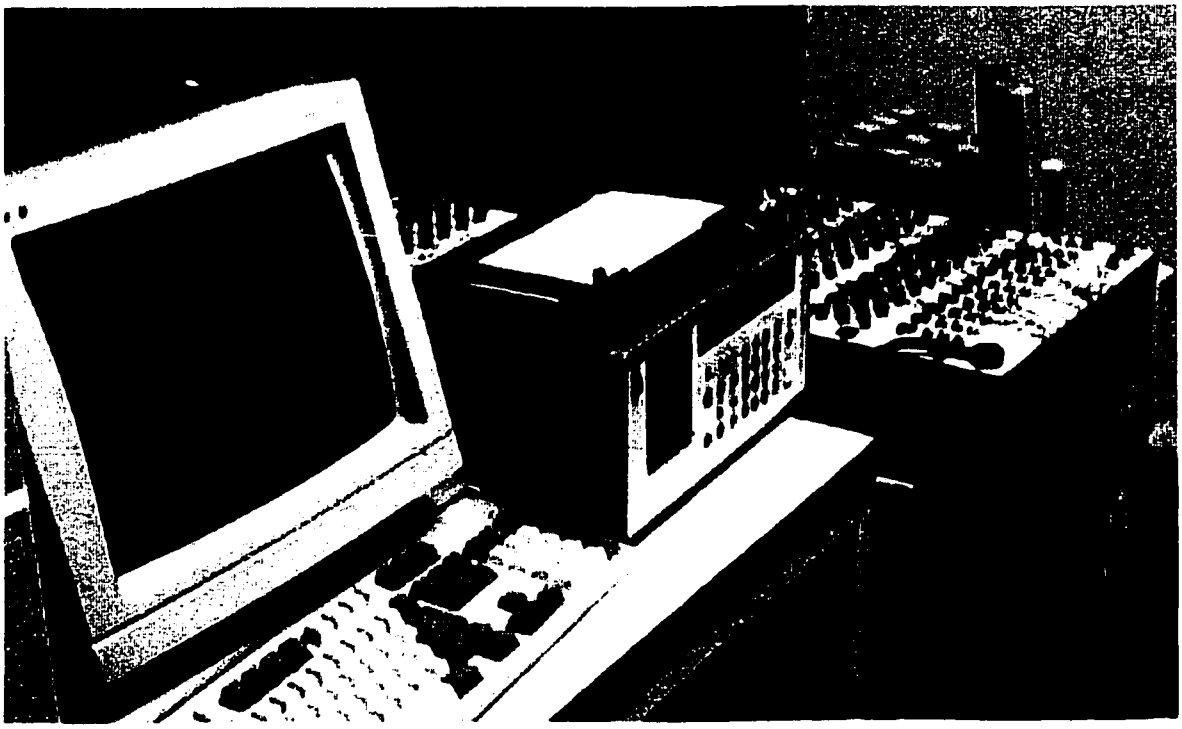

Figure 3.10: Shrinkage specimens connected to data logging system and computer

3.1.13 TEST PROCEDURE FOR COMPRESSIVE CREEP TEST

An experimental investigation was conducted on compressive creep for two repair materials selected for this study and the concrete used for test columns. These tests were conducted on repair materials PFSM and FMCX and concrete. Cylindrical specimens having a diameter of 150 mm and a length of 300 mm were used for this purpose according to ASTM C-512. Prismatic specimens 300x250x75mm of both repair materials were also used for creep tests. The dimensions of these specimens is the same as the repair patch in columns used in this study. Tests were conducted on specimens, which were loaded after 28 days of casting. Strains in these samples were measured by strain gauges embedded inside the specimen and surface gauges.

3.1.13.1 Fabrication of Creep Rigs

Creep test and long-term testing of repaired columns under uniaxial compressive load needs special rigs for conducting the tests on multiple columns and/or cylinders. Two rigs were manufactured in the University research workshop, whose detailed drawings are shown in figures 3.11 and 3.12. These rigs were designed to apply concentric force to the columns and creep specimens and preclude any moment transfer to the columns and specimens. These rigs were used to evaluate the compressive creep characteristics of the selected repair materials and to monitor the performance of patch-repaired and un-repaired columns under sustained compressive loads.

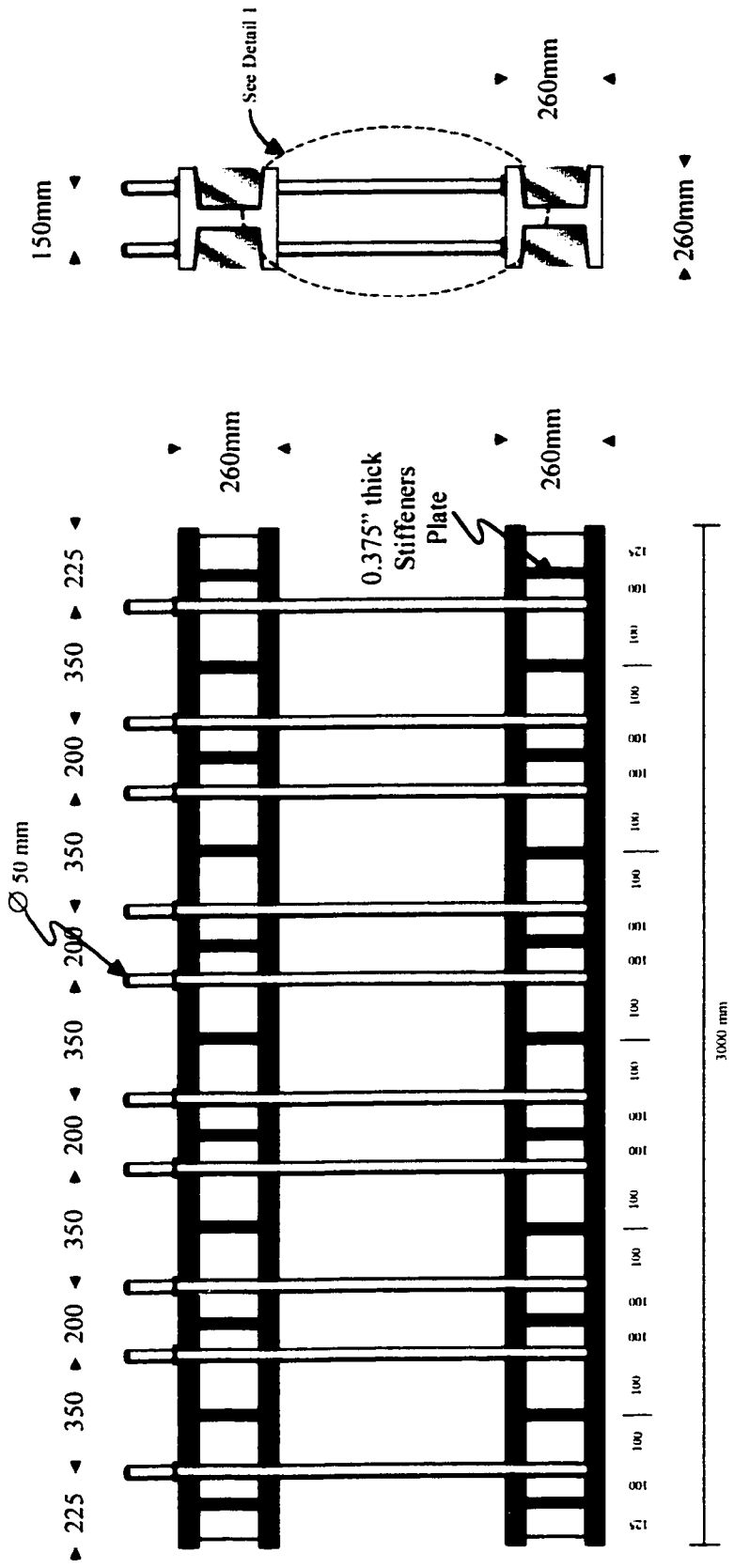

Figure 3.11. General arrangement of the Creep Rig.

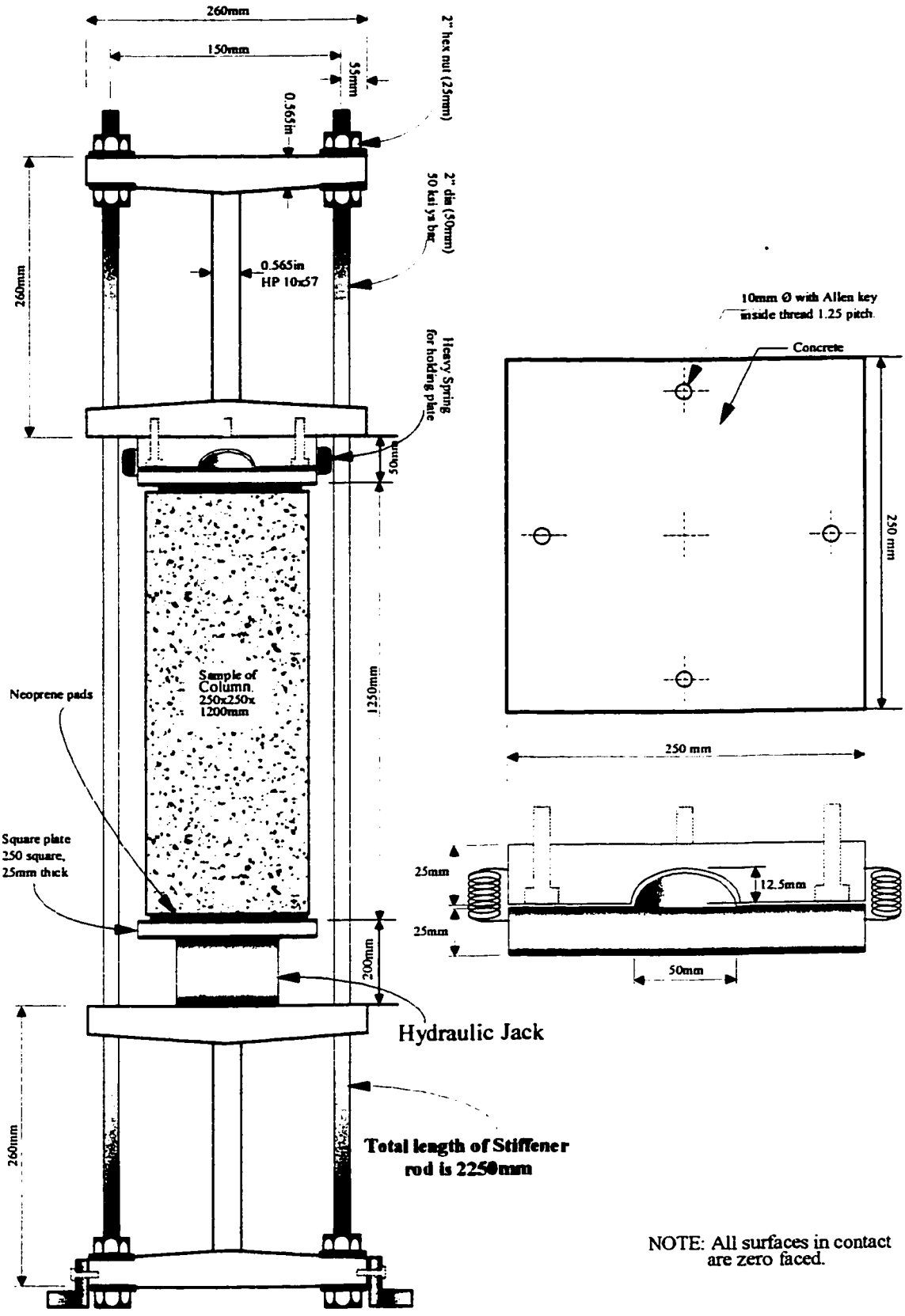

Figure 3.12. Sectional elevation of the rig.

The testing rig comprises of two steel I-sections having a depth of 260mm and a height of 260mm. The steel sections are spaced at a distance of the height of the columns to be tested by high strength steel bars of 50 mm diameter and nuts at appropriate locations as shown in the figure 3.11 and 3.12. The 50 mm diameter bars are threaded at appropriate locations to accommodate the nuts. The top I-beam can be adjusted to any height by placing the nuts at appropriate locations. The I-section has stiffeners at locations where high compressive load will be generated in both the top and the bottom I-section. The length of the I-sections 3 meters has been selected to accommodate five columns or creep samples. Steel plates having provision for ball and socket type of joint was fabricated by using computer controlled CNC machine in the research workshop. The ball and socket joint is provided to transfer pure axial loads to the columns.

Hydraulic jacks with provision for mechanical locks for holding long-term load on the columns and creep samples are used for the application of loads. The jacks have capacity of 70 tons and 100 tons. The hydraulic jacks are placed on grooves made for placing the jacks on the lower I-section. A steel plate with grooves is placed on the top of the hydraulic jack. The columns/ creep test cylinders are placed at the top of this plate. The loading plate of the hydraulic jack has a ball and socket joint. Five hydraulic jacks are placed on each rig. The high-pressure tubes from these hydraulic jacks are connected to a manifold. A manual pump is connected to the manifold that can be used for applying and maintaining compressive loads on the sample by operating the valves on the manifold.

Specimen preparation

The cylindrical specimens 150Øx300mm for compressive creep tests were removed from moist curing after 7 days and then allowed to cure in air till the time of testing. The top

surface of the specimen was capped by sulfur. The locations of externally bonded strain gauges were then marked on all specimens. The gauge application area on concrete was scrubbed and cleaned and then the strain gauges were bonded to the concrete using rapid strength resin based compatible bonding agent. After curing of resin, the exposed area and the strain gauges were covered with clear silicone to protect from the environment and damage. The prismatic specimens 300x250x75mm were prepared by embedding strain gauges during casting, whose locations are shown in figure 3.8. Three faces of the specimen were covered with aluminum foil to avoid moisture loss from those faces to simulate the situation of repair in the column. These specimens were loaded at an age of 7 days after casting.

Load and deformation measurements

A load cell having a capacity of 200 tons was used to calibrate the pressure gauge on the hydraulic jacks. The loads applied to various specimens were subsequently measured from the pressure gauge attached to the hydraulic pump. Total strains in the specimen were measured using embedded strain gauges of type TML PML-60 having a gauge length of 60 mm, which were already embedded in the specimens during casting. Strain gauges of type TML PL-60-11 having a gauge length of 60 mm also bonded on surface on opposite side of the specimen. The external strain gauges were attached to the middle portion of the specimen length at the center of each face in longitudinal direction. The strain gauges were connected to a data logger capable of storing continuous strain data at preprogrammed intervals.

Test Procedure

A total of 15 cylinders (150∅x300 mm) were prepared using the above procedure. This included six cylinders each for FMCX and PFSM and three cylinders for concrete of same mix used in the column. Uniaxial compressive load corresponding to 25% and 35% of the 28-days strength was applied to the specimens for each repair material. In a single column of the rig three specimen of each material were stacked one above another as shown in Figure 3.13. A uniaxial compressive load corresponding to 35% of the 28 days strength was applied to the concrete specimen. By using the hydraulic pump and the manifold each columns of specimens in the testing rig was loaded to the specified value. Figure 3.13 shows the hydraulic pumps and the manifold together with hydraulic jacks used for applying compressive stress on the specimen. The specimen were initially loaded to about 10% of the sustained load, strain readings were taken. If the strain readings were not within ±5% of their mean value, adjustments were made and readings were retaken. This process was repeated till the individual strains were within the stipulated limit. The sample was then further loaded slowly to the stipulated limits and the strains were monitored.

Two specimens 300x250x75mm for each repair material were used to capture the creep strains. The specimens were kept one over the other in a creep rig as can be seen in figure 3.15, over which a plate was provided on which a load cell was kept and a second plate was kept on the load cell. The nuts above the second plate were tightened simultaneously to apply the load on the specimens till the specified load is reached and the load on the specimens was measured using the load cell.

During the loading process, load and strains were recorded at small intervals till the sustained load is achieved. The strain readings for creep were taken at an interval of 15 minutes for 2 hours, hourly interval for the next 22 hours, 2 hours interval for the next 24 hours and then at 4 hours interval till the end of testing period. Due to elastic compression the pressure on the sample is lost. The pressure was initially checked everyday and the constant pressure was maintained throughout the duration of the test. About 40 strain gauges attached to various samples were connected to data logger for automated recording of data. Figure 3.14 shows the setup with data logger.

The strain measured on a loaded specimen includes the creep strain, the elastic strain and the shrinkage strain due to simultaneous drying of the sample under no load. The shrinkage strain was measured on a companion sample of same shape and size with strain gauges. This was started once sustained loading was in place.

The creep rigs were placed in a room where the temperature was kept at 21 ± 2°C and the relative humidity was kept at 65 ± 5%. The relative humidity and temperature however varied significantly during the testing period when the main doors of the reaction floor where the equipment is housed were left open. The temperature and humidity of the environment was however measured at one-hour interval during the duration of the test.

Figure 3.13: Creep specimens loaded in the creep rig using jacks and hydraulic pumps

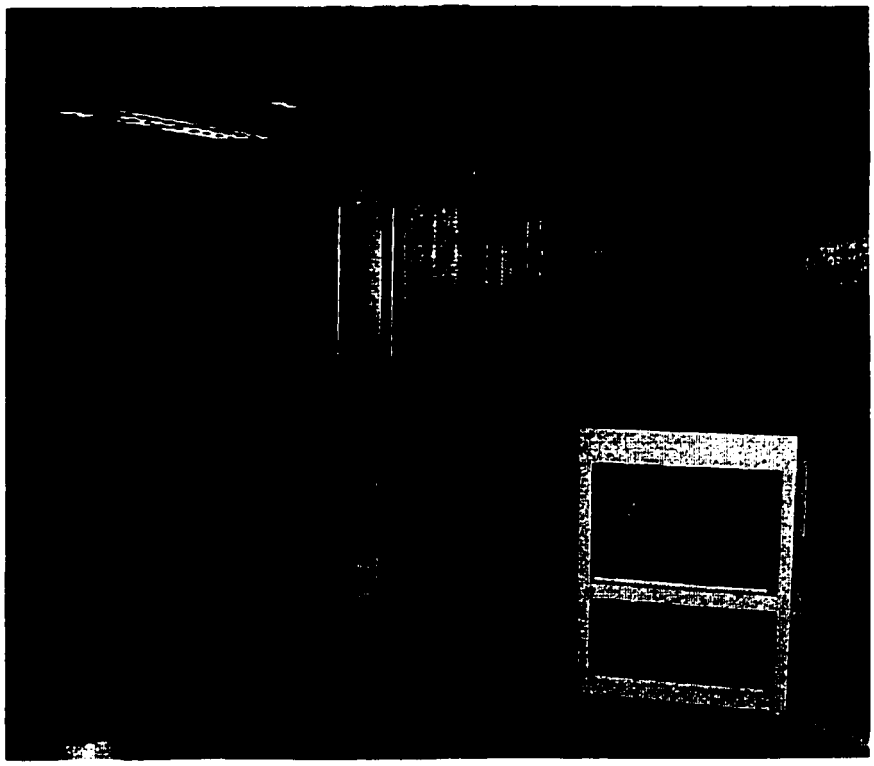

Figure 3.14: Creep setup with the data logger with 40 strain gauges attached

Figure 3.15: Creep test setup for prismatic specimens 300x250x75mm

3.1.14 TEST PROCEDURE FOR CHLORIDE PENETRABILITY

The resistance of concrete and repair materials to the ingress of chloride ions is being measured using ASTM: C-1202 "Standard Test Method for Electrical Indication of Concrete's Ability to Resist Chloride Ion Penetration." The specimens were prepared by cutting cylindrical disks of 50 mm thick from 75mm ∅ cylinders. The age of testing for concrete and repair materials is 28 days after casting. A rapid set epoxy coating was applied on the curved surfaces of the discs to make them impermeable. The samples were, then, saturated with water, under vacuum as per the procedures outlined in ASTM C-1201. The specimen was then clamped between the two halves of the cell, schematically shown in Figure 3.16. Figures 3.17 and 3.18 show the actual setup for the test. One half portion of the cell contained a reservoir, filled with 3% sodium chloride solution. This portion was connected to the positive terminal of a DC power source. The other half of the cell was filled with 0.3 molar sodium hydroxide solution, and was connected to the negative terminal of the DC power source. One copper mesh was provided on each side of the cell for impressing the current on the specimen and rubber shims were used to prevent leakage.

A DC power source was utilized to apply a potential of 60 V. The intensity of current flowing across the sample was calculated by determining the potential drop over the two terminals of a resister connected as part of the power line. The current was recorded for 6 hours at intervals of 30 minutes and plotted against time. The area under the curve provides the total charge passed in Coulombs (ampere-seconds). Higher values of total charge indicate lower electrical resistivity of concrete and repair materials.

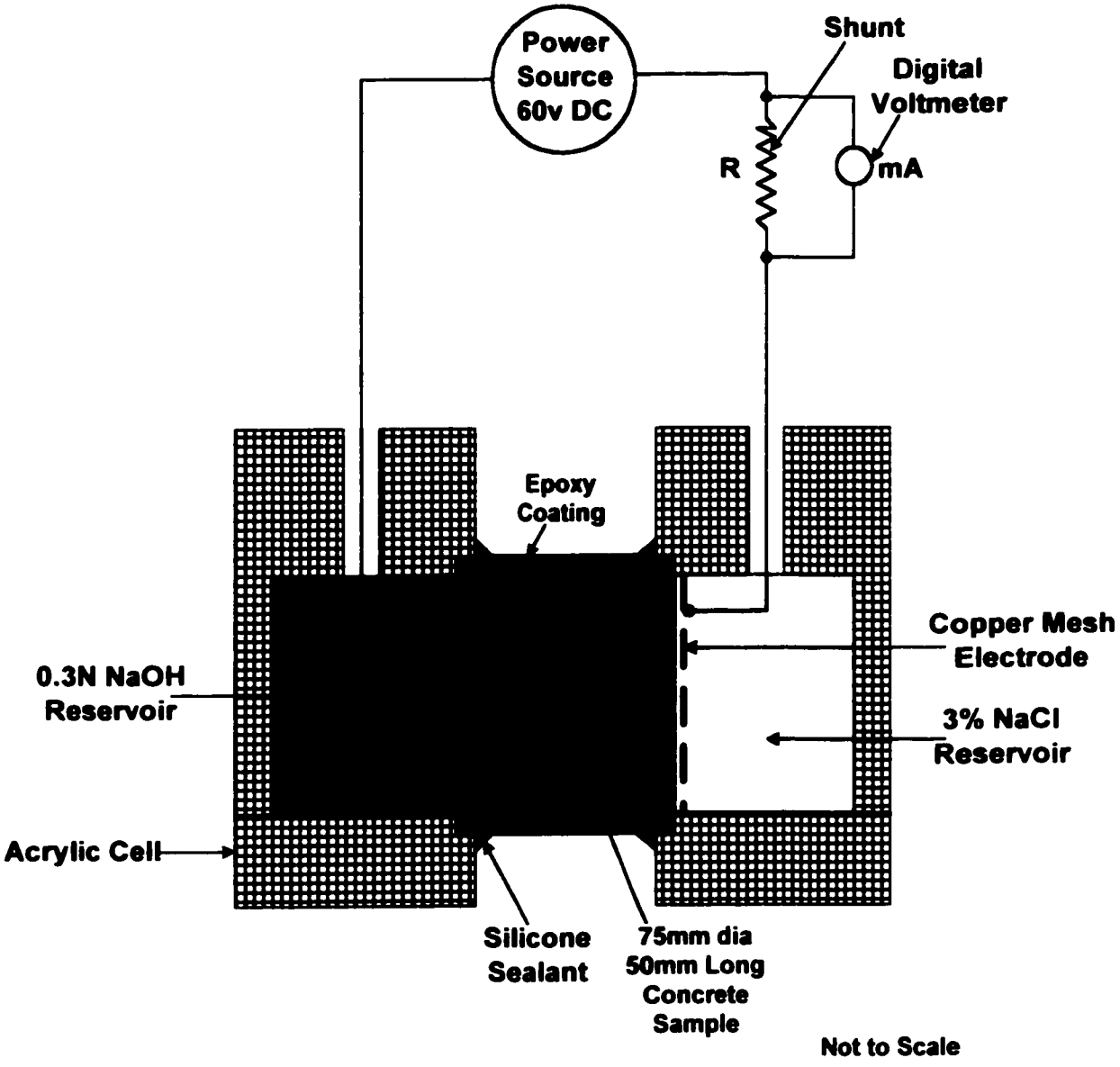

Figure 3.16: Chloride ion Penetrability setup

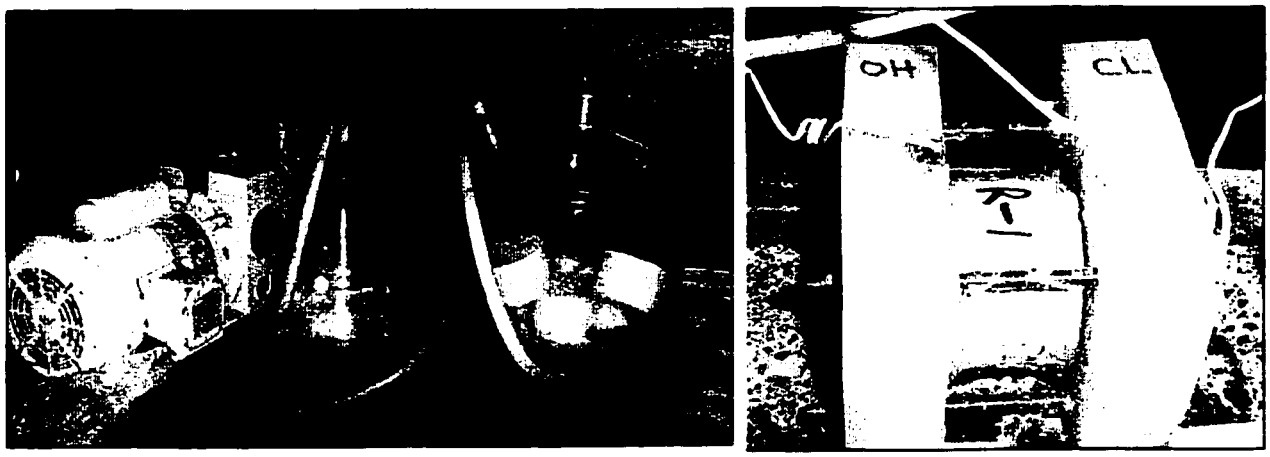

Figure 3.17: Specimens soaked in water under vacuum and then fixed in the cell

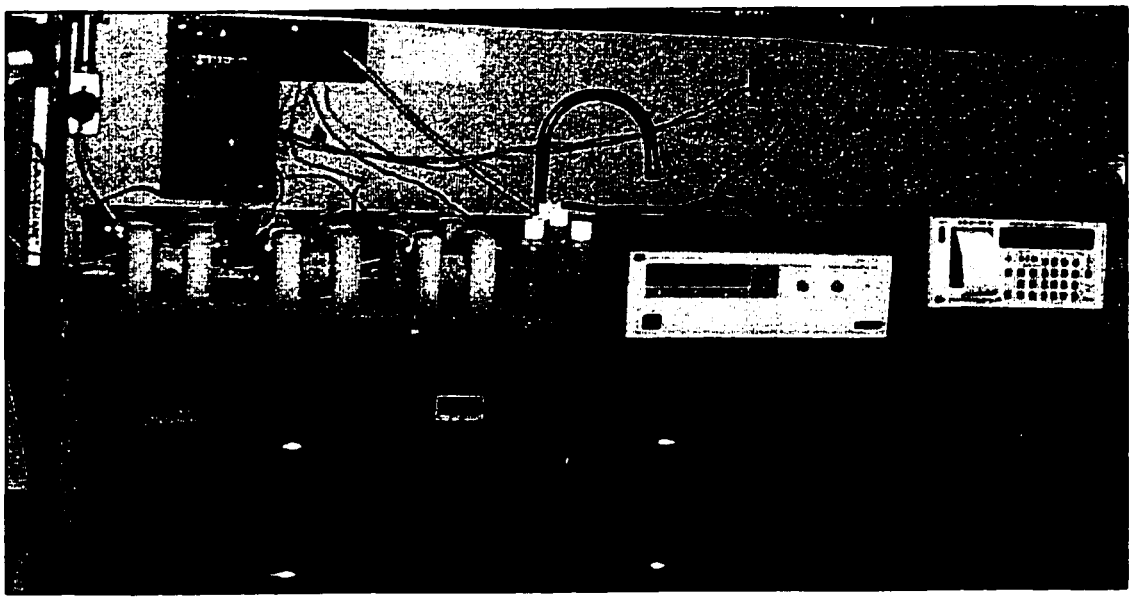

Figure 3.18: Chloride ion penetrability test set-up

3.1.15 TEST PROCEDURE FOR EVALUATING SULFATE ATTACK

The durability of selected repair materials subjected to sulfate attack on repair materials is investigated by subjecting the cubes of selected repair materials to concentrated sulfate solution and monitoring the depletion of strength with time.

Concrete as well as Repair material cubes 50x50x50 mm were tested by placing them in sulfate solution to record any reduction in strength. The cubes were first cured for 7 days, concrete mortar cubes being cured under water where as the repair material cubes were cured under wet cloth. After 7 days of curing, cubes were tested for their compressive strength. Then to simulate the conditions of Sabkha soil the 50% of cubes were placed in salt water having the compositions of a Sabkha soil and the other 50% in water. The sulfate concentration in the solution was 5.5% contributed equally by Magnesium sulfate and Sodium sulfate. The cubes both in water and sulfate solution were tested for their compressive strengths at interval of one month. At each age of testing three specimens were removed from water and three from sulfate solution and allowed to dry for an hour before testing them in the compression testing machine. The testing has been completed up to 9 months.

3.2 PREPARATION OF COLUMN TEST SPECIMENS

The principal objective of this research is to ascertain the effectiveness of the patch repair that is carried out in deteriorated concrete columns. A total of 20 columns have been cast for conducting the tests. The concrete mix design used for these columns is given in section 3.1.2 of this chapter which was delivered by a ready mix concrete truck on the field, where the casting was performed.

3.2.1 SPECIMEN SHAPE AND SIZE

Short columns of size 250x250mm c/s and length of 1200mm were used for carrying out the tests. The recess for repair was preformed in the specimens on the opposite faces at mid height using Styrofoam attached to the reinforcement cage. The size of recess is 300mm along the length, 250mm width and a depth of 75mm. Reinforcement used in the columns was 1 percent of the cross-sectional area. Eight 10 mm diameter bars were used as main bars and 8 mm diameter bars spaced at 150 mm were used as lateral ties. The cover to the center of the main reinforcement is 60 mm with a clear cover of about 50 mm. The repair recess extends 10 mm beyond the main reinforcement. Figures 3.19 to 3.21 shows the details of the columns to be tested.

3.2.2 MANUFACTURE OF SPECIMENS

The manufacture of column specimens for the tests was programmed and planned carefully. First the steel reinforcement cages were made as per the requirements of clear cover 50mm, whose details can be seen in Figure 3.19. The columns to be manufactured with recess were made by attaching Styrofoam blocks on the opposite faces of the reinforcement cage. Then the next step was attachment of gauges on the reinforcing steel. Figure 3.22 shows the reinforcement cage with Styrofoam blocks and gauge on steel attached placed in mould.

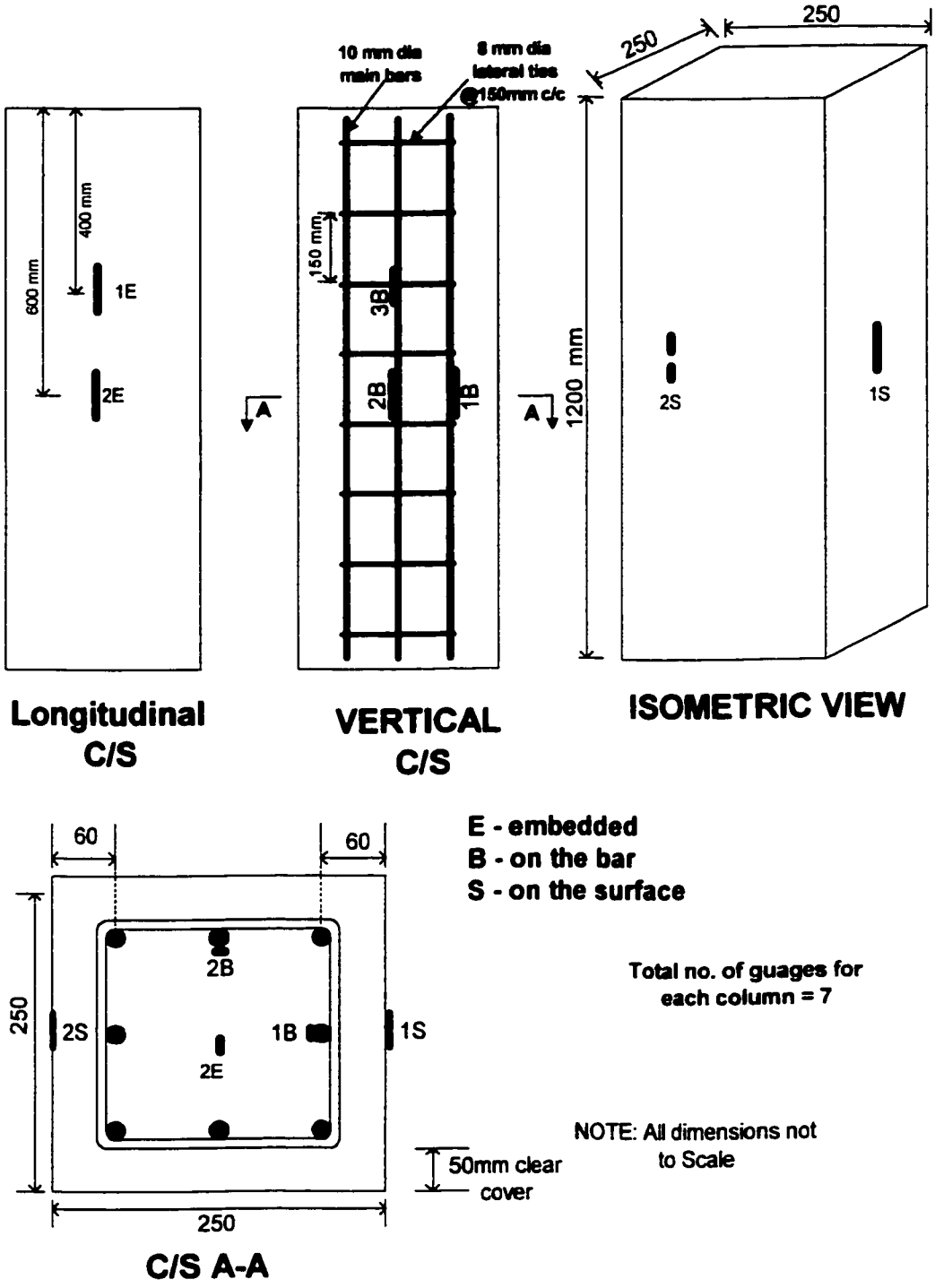

Figure 3.19: Columns without recess

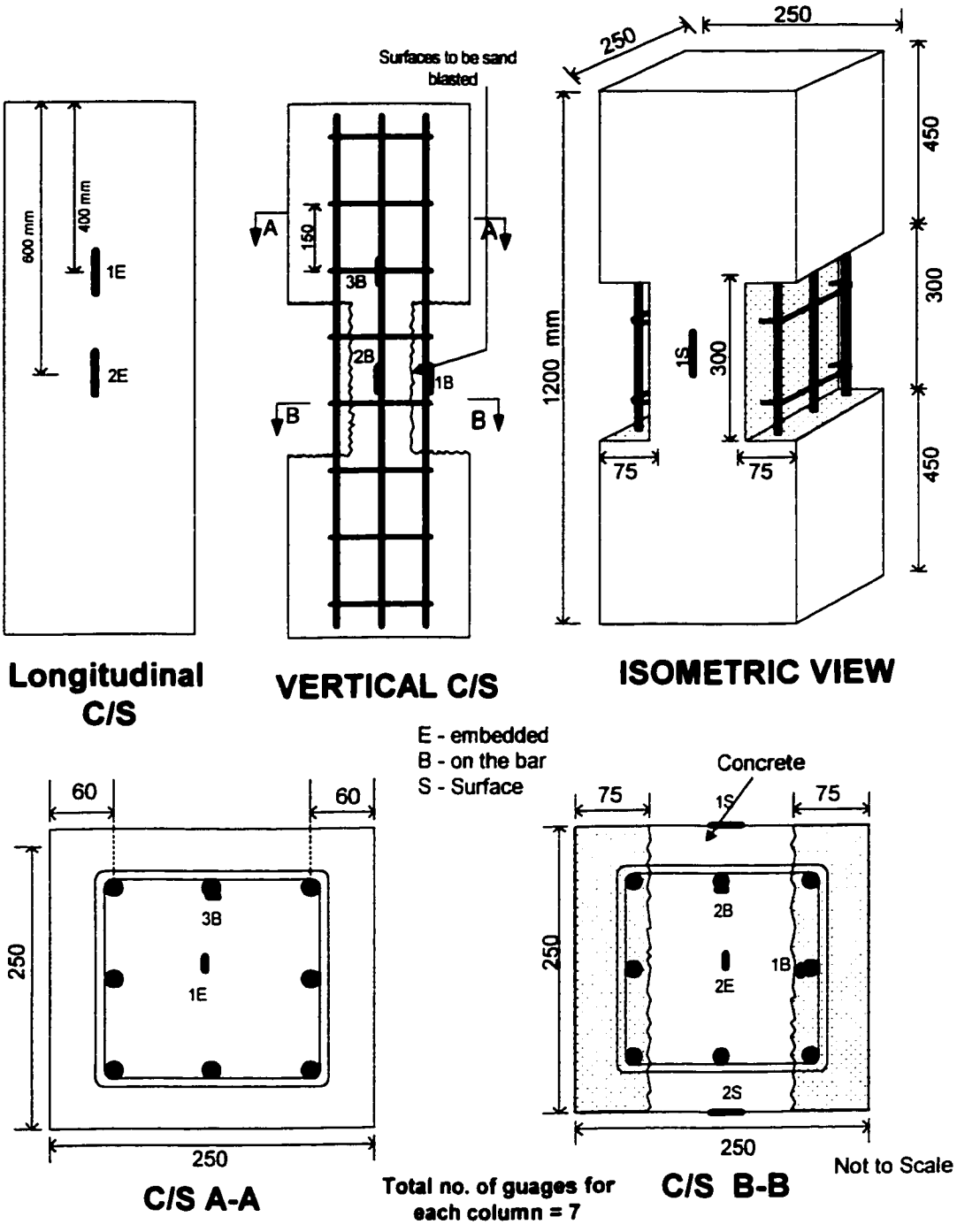

Figure 3.20: columns un-repaired and with recess

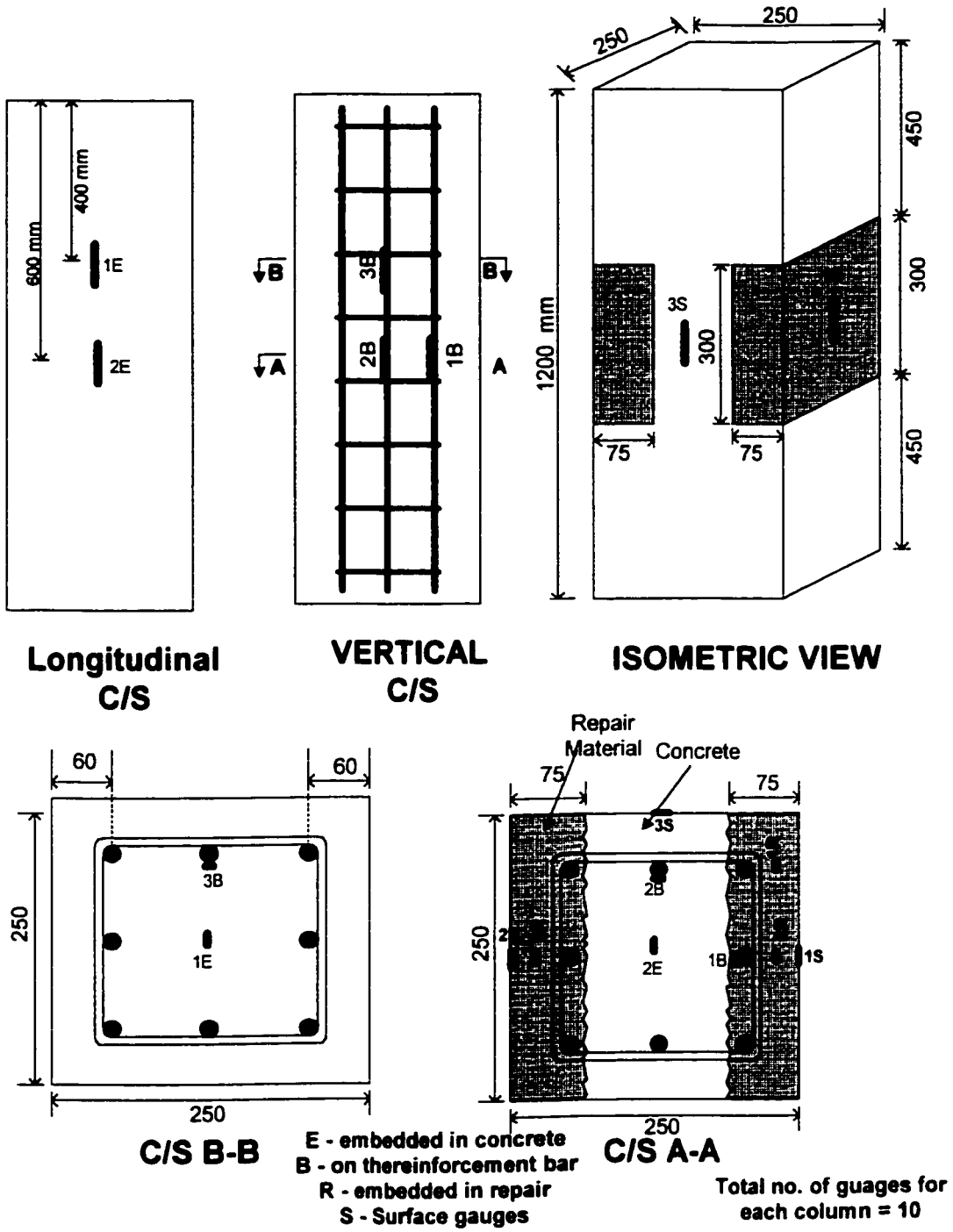

Figure 3.21: Columns with recess and repaired

Wooden moulds were used as formwork for casting columns. The wooden moulds were oiled in the inner faces for its easy removal after the concrete hardens. The reinforcement cage was placed in the moulds with Styrofoam attached and sufficient spacers were used for providing proper spacing to the reinforcing bars from the walls of moulds.

The concrete was filled up to half height of mould and vibrated and then the embedded gauges were placed at appropriate locations. The concrete was then filled completely and vibrated for the second time taking precaution not to disturb the embedded gauges. Leveling and finishing was performed using a wooden float and the top surface was made smooth before covering the specimens with a plastic sheet. Plastic sheet was used to avoid moisture loss from the freshly placed concrete as can be seen in Figure 3.23.

3.2.3 CURING REGIME FOR THE SPECIMENS

All the column specimens cast were kept in moulds for 24 hours after casting. The surface of the specimens were covered with layers of plastic sheet and then covered with wet hessian. A plastic sheet was placed over the wet hessian to ensure that it remains wet for 24 hours. After 24 hours, the forms were stripped off from sides and the wooden block was removed. The specimens were then kept moist under wet hessian and covered by plastic sheets for a period of 21 days. After 21 days, the specimen were removed from under the wet hessian and allowed to cure in air at 65 ± 5% humidity and 33 ± 10°C temperature for a period of next three weeks. The specimens were, then, brought from field to the laboratory for conducting tests.

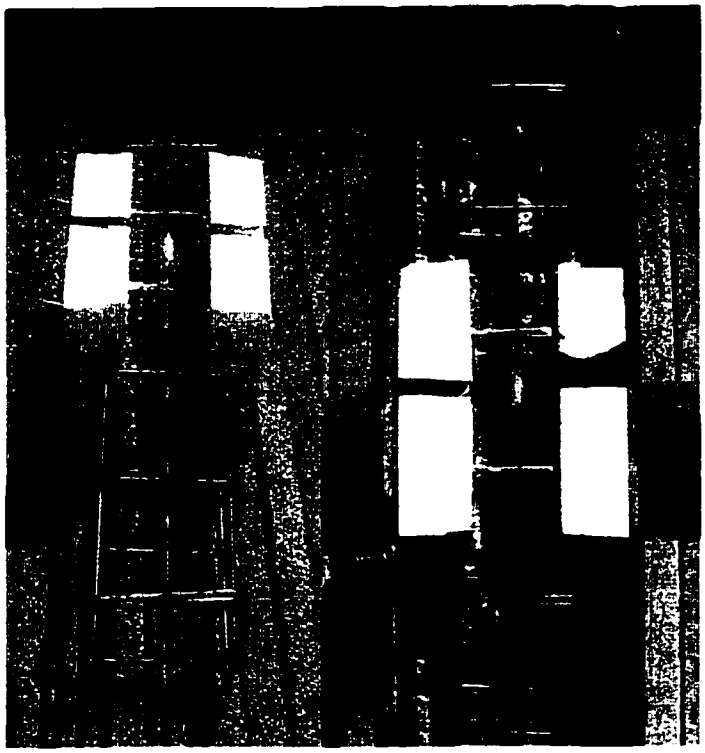

Figure 3.22: Reinforcement cage with Styrofoam and gauge on steel attached and placed in mould

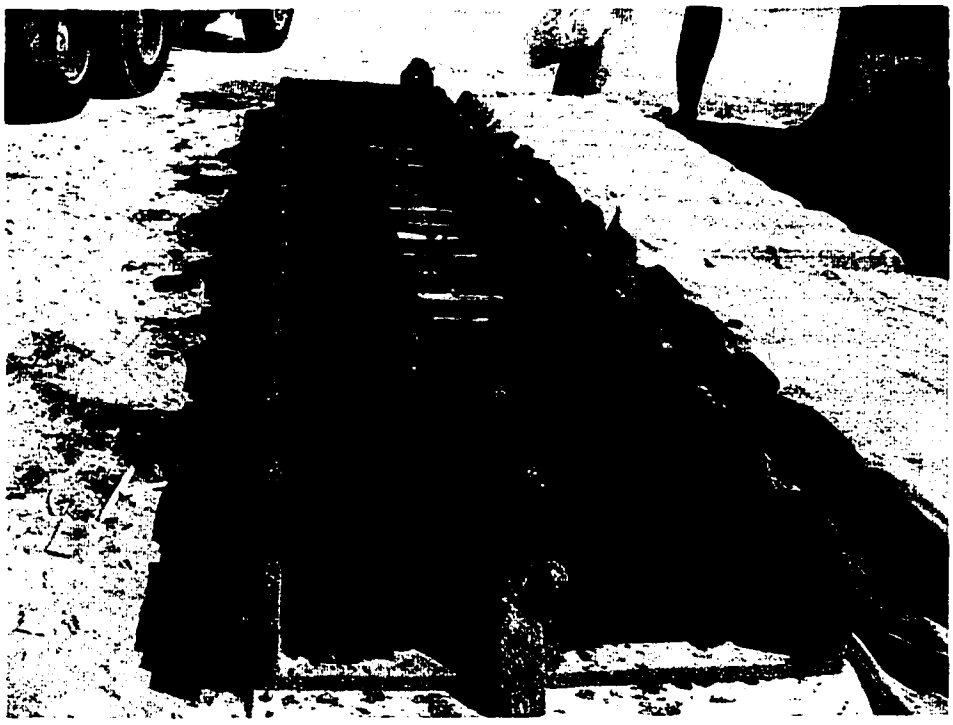

Figure 3.23: Column specimens after casting and before covering with plastic sheet

3.2.4 PREPARATION OF SPECIEMNS

Before transporting the specimens to the laboratory, the Styrofoam was removed from sides of column specimens to form the recess. On the field itself the surfaces of concrete in the recess, which are going to receive repair materials later, were sandblasted. During the process of sandblasting the exposed reinforcement of the specimens was also sandblasted. To avoid corrosion of the reinforcement Zincrich was painted on the exposed reinforcement. The specimens were transported to the lab. The locations of externally bonded strain gauges on surface were then marked on all specimens. The gauge application area on concrete was scrubbed and cleaned and then the strain gauges were bonded to the concrete using rapid strength resin based compatible bonding agent. Another gauge on the exposed reinforcement was also attached to the reinforcing bar. The locations of strain gauges for the specimens are shown in Figures 3.19 to 3.21.

3.2.5 PATCH REPAIR OF COLUMN SPECIMENS WITH RECESS

The column specimens with recess were repaired using two types of repair materials. The procedures adopted for repairing the specimens is described below:

3.2.5.1 Repairing columns with FMCX

FMCX is a flowing micro concrete which requires a watertight formwork for performing the patch repair on columns. The Figure 3.24 shows the details of formwork designed for columns to be repaired with FMCX.

Before attaching the formwork to the columns, the strain gauges that are to be embedded in the repair were attached to the reinforcing bars using a thick steel wire at proper location and the strain gauge was hanged from that wire.

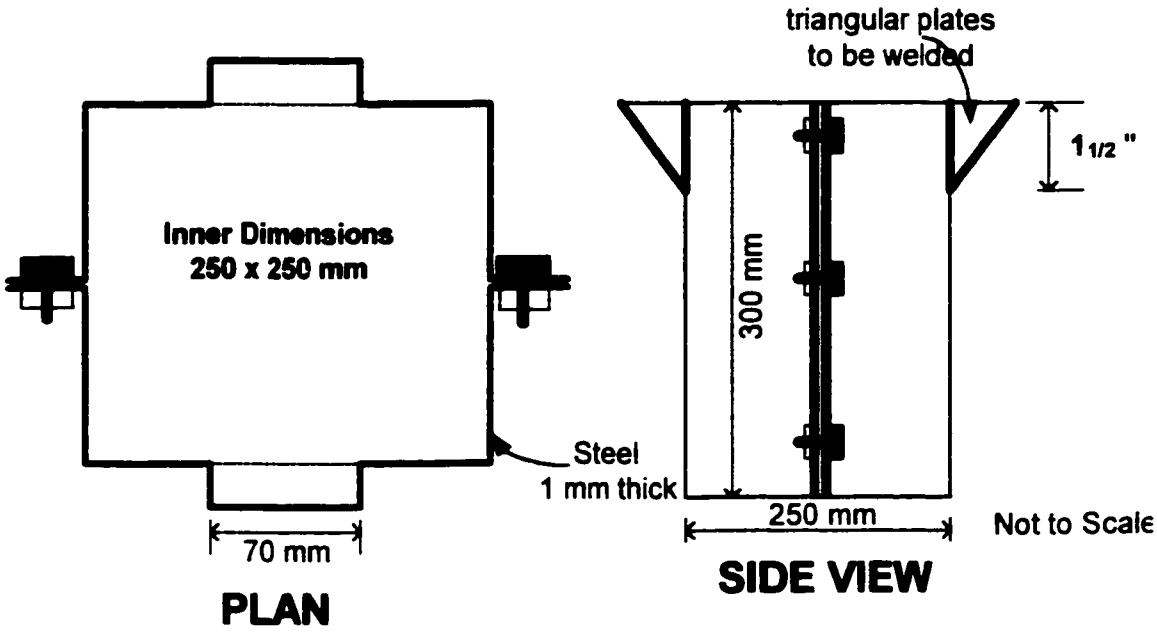

Figure 3.24: Watertight formwork for columns to be repaired with FMCX

To ensure that the strain gauge does not move during the repair process, very thin wires were used to keep the gauge in place. Figure 3.25 shows the embedded strain gauges hanging from the thick steel wire attached to the exposed reinforcing bar.

The formwork was then oiled in the inner surface and fixed to the column around the recess and sealed with silicone to make it watertight. Figure 3.26 shows the column specimen fixed with formwork. After the silicone has set the formwork was filled with water to ensure that the concrete surfaces in the recess are wet. The water was kept in the formwork for 24 hours to ensure that the concrete surfaces are moist enough. Before pouring the repair material the water inside the formwork was drained out thoroughly. The repair material FMCX was mixed as specified in the section 3.1.5. The material was poured in recess using small scoops from the openings provided on the top of formwork. The formwork was tampered slowly using a rod to vibrate the repair material poured inside to ensure proper settlement without formation of voids.

Figure 3.25: Column specimen with embedded strain gauges attached

Figure 3.26: Column specimen fixed with formwork around recess and filled with water

3.2.5.2 Repairing columns with PFSM

PFSM is a trowelable mortar, which also requires a formwork for covering the patch repair on columns after the application. The Figure 3.27 shows the details of formwork designed for columns to be repaired with PFSM.

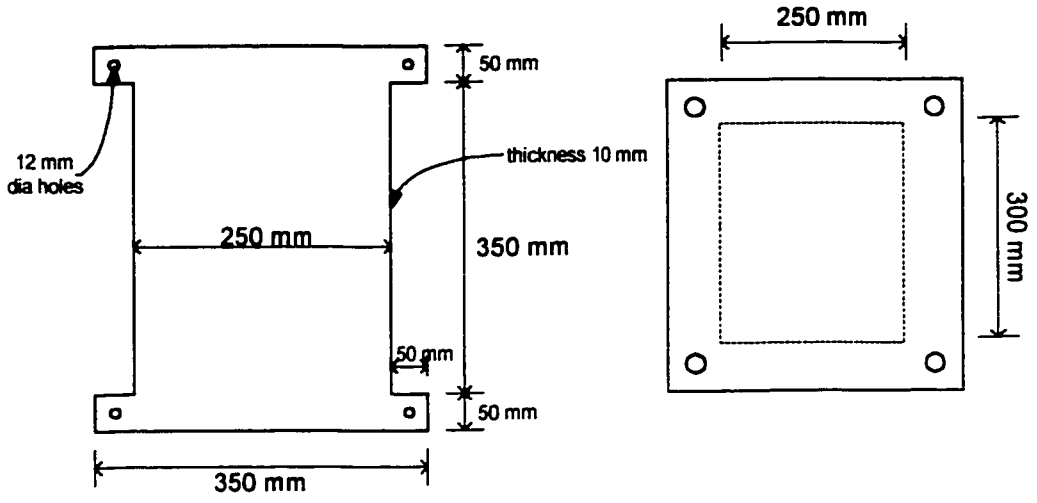

Figure 3.27: Formwork for covering the patch repaired PFSM columns

The column specimens to be repaired with PFSM were first attached with formwork shown in Fig. 3.26 and filled with water to ensure the concrete surfaces in the recess are wet. After 24 hours the water was drained and formwork removed. Now when the concrete surfaces are wet the formwork shown in Fig. 3.27 was attached using threaded steel rods and bolts. Figure 3.28 shows the formwork attached on sides of column before the application of repair material. The repair material PFSM was mixed as specified in the section 3.1.5. The repair material was then placed with hand and by pressing it behind the reinforcement. Initially half the depth of recess was filled with repair material and then embedded strain gauges were placed at appropriate locations as shown in Fig. 3.29. The second layer of repair material was applied to fill the remaining half portion. The

surface was prepared using a wooden float and then the repair was covered with the other wooden panel and fixed in place using threaded rods and bolts as shown in Figure 3.30.

Figure 3.28: Column specimen fixed with formwork to be repaired with PFSM

Figure 3.29: Embedded strain gauges placed in the repair

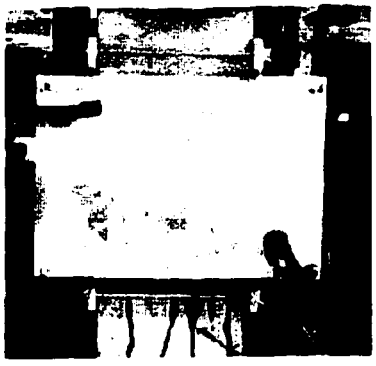

Figure 3.30: Column specimen repaired with PFSM and covered with formwork

3.2.5.3 Curing Regime for Patch Repair of Columns

The formwork covering the patch repair was removed after 24 hours after casting. Immediately after the removal of formwork a first coat of curing compound was applied. The second coat was applied after 4 hours after application of first coat. After a period of 7 days the curing compound on the patch repair surface was removed using sandpaper attached to an electric mortar.

3.3 DESTRUCTIVE TESTING OF REPAIRED/UN-REPAIRED COLUMNS

Out of 20 columns cast, 10 were used for testing their ultimate load capacities. The breakdown for the number of columns tested is as follows:

(a)	Columns without recess	3
(b)	Columns un-repaired and with recess	3
(c)	Columns with recess and repaired with FMCX	2
(d)	Columns with recess and repaired with PFSM	2

3.3.1 FABRICATION OF LOADING FRAME

For conducting destructive tests on columns with recess and without recess and repaired columns, a setup comprising of a 250-ton capacity frame and hydraulic jack for applying up to 250 tons of load has been fabricated. This frame was fabricated from an existing heavy-duty creep-testing frame that was not in working condition. The details of testing frame are shown in figure 3.31. The original load application system was dismantled and a 250 ton hydraulic jack with electrical pump, a 200 tons load cell and two 50 mm thick

plates were assembled for conducting destructive tests on column. This loading frame has an upper plate with adjustable screw heads, which can be adjusted to tilt the upper plate such that it is in the same plane as of the column specimen to apply axial force without any eccentricity.

3.3.2 LOADING MEASUREMENTS

The hydraulic jack has a top block that can move upwards/downwards. On the top block there is a steel plate placed on which the 200 capacity load cell is placed. The compressive loads on the column specimens were measured by the upward movement of hydraulic jack. The reaction to the specimens was provided by the top block of the frame, which has adjustable screw heads for axial load application.

3.3.3 DEFORMATION MEASUREMENTS

The compressive strains on the surface were assessed by means of electrical strain gauges TML type PL-60-11. These strain gauges having a gauge length of 60 mm were attached on opposite sides of the column specimens. The strains inside concrete and repair material were assessed by means of embedded electrical strain gauges TML type PML-60. The strains in the reinforcing steel were assessed by means of electric strain gauges TML type GFLA-3-50-2LDA. Lead wires from strain gauges and load cell were connected to a data logger to record the strains.

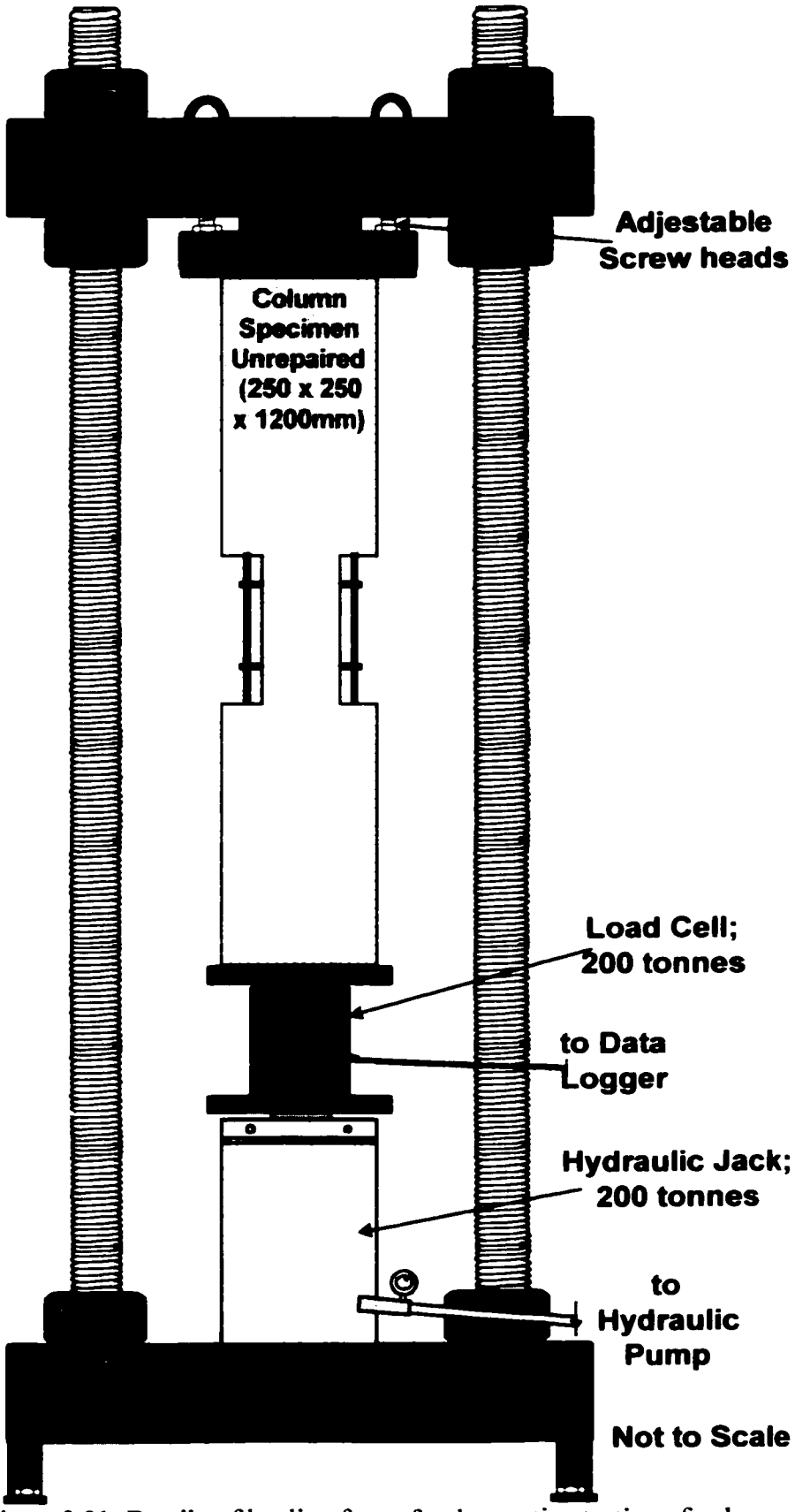

Figure 3.31: Details of loading frame for destructive testing of column specimens

3.3.4 PREPARATION OF COLUMN SPECIMENS

The column specimens without recess as shown in Fig. 3.19 were prepared by attaching surface strain gauges on opposite faces using a quick set epoxy. After the epoxy has set the columns were placed in the loading frame and tested for their ultimate capacity.

The column specimens un-repaired and with recess as shown in Fig. 3.20 were prepared by attaching surface strain gauges on opposite faces using a quick set epoxy. An additional strain gauge was also attached to the exposed reinforcement bar in the recess area, whose location is also shown in Fig.3.20. After the epoxy has hardened the columns were placed in the loading frame and tested for their ultimate capacity as can be seen in Fig. 3.31.

The column specimens with recess and repaired with two types of repair materials as shown in Fig. 3.21 were tested for their ultimate load capacities after monitoring the shrinkage strains for a period of 4 months. Surface strain gauges were attached on opposite faces using a quick set epoxy. After the epoxy has hardened the columns were placed in the loading frame and tested for their ultimate load capacities.

3.3.5 TEST PROCEDURE

The column specimens were placed in the loading frame as shown in Fig. 3.32 and the compressive load was applied through Hydraulic jack using an electric control. The speed of application of load was maintained at a constant speed of 5 kN/sec. Initially a load of 25-30 kN was applied and the strains on opposite faces of the specimen were monitored to check the eccentricity of load. If the strains on opposite faces differed by more than 5 percent, the screw heads on the top block of the loading frame were adjusted accordingly

till the strains were within the stipulated range. All load and deformation data were recorded at load increments of 10 kN using automated computer controlled data loggers.

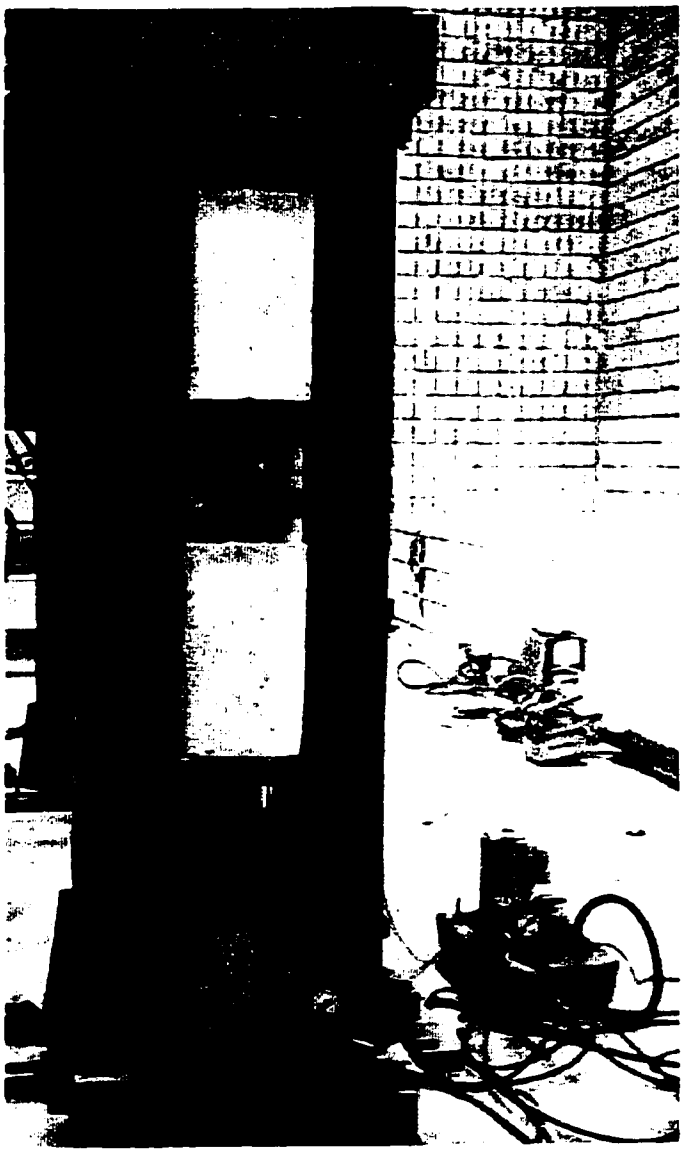

Figure 3.32: Column specimen with recess being tested for its ultimate load capacity

3.4 LONG TERM TESTING OF REPAIRED/UN-REPAIRED COLUMNS UNDER CONSTANT LOAD

Out of 20 columns cast the remaining 10 were used for monitoring strains under constant load. The breakdown for the number of columns tested is as follows:

(a)	Columns without recess	2
(b)	Columns repaired with FMCX and loaded after 7 days	2
(c)	Columns repaired with PFSM and loaded after 7 days	2
(d)	Columns repaired with FMCX in loaded state	2
(e)	Columns repaired with PFSM in loaded state	2

The fabrication of creep rigs for the purpose of conducting long-term tests on repaired/un-repaired columns is discussed in the section 3.1.13.1 of this chapter. The detailed drawings are shown in Figures 3.11 and 3.12.

3.4.1 LOADING AND DEFORMATION MEASUREMENTS

A load cell having a capacity of 200 tons was used to calibrate the pressure gauge on the hydraulic jacks. The loads applied to various specimens were subsequently measured from the pressure gauge attached to the hydraulic pump. The strains in the specimen were measured using embedded strain gauges of type TML PML-60 having a gauge length of 60 mm, which were already embedded in the specimens during casting. Strain gauges of type TML PL-60-11 having a gauge length of 60 mm also bonded on surface on opposite side of the specimen. To capture the strains in the reinforcing steel strain gauges of type

TML GFLA-3-50-2LDA were used. The surface strain gauges were attached to the middle portion of the specimen length at the center of each face in longitudinal direction. The strain gauges were connected to a data logger capable of storing continuous strain data at preprogrammed intervals.

3.4.2 SPECIMEN PREPARATION

The column specimens without recess as shown in Fig. 3.19 were prepared by attaching surface strain gauges on opposite faces using a quick set epoxy. After the epoxy has set the columns were placed in the creep rig and tested for their long-term behavior under constant load.

For the column specimens that are to be repaired with FMCX and PFSM and loaded in the creep rig, the procedures described in section 3.2.5 were adopted for repair. The patch repair in the column specimens were allowed to cure for 7 days and then surface strain gauges were attached on opposite faces using a quick set epoxy. After the epoxy has set the columns were placed in the creep rig and tested for their long-term behavior under constant load.

For the column specimens that are to be repaired with FMCX and PFSM under loaded state, the procedures described in section 3.2.5 were adopted for repair. The column specimens with formwork attached were first loaded in the creep rig to the specified value and then the patch repair of these specimens was performed.

3.4.3 TEST PROCEDURE

A total of 10 column specimens were tested in two creep rigs. By using the hydraulic pump and the manifold each column specimen in the rig was loaded to the specified

value of 400 kN, which is 20% of the Ultimate Crushing Strength of column specimens. The specimen was initially loaded to about 10% of the sustained load and strain readings were taken. If the strain readings were not within ±5% of their mean value, adjustments were made and readings were retaken. This process was repeated till the individual strains were within the stipulated limit. The sample was then further loaded slowly to the stipulated limits and the strains were monitored.

During the loading process, load and strains were recorded at small intervals till the sustained load is achieved. The strain readings were taken at an interval of 15 minutes for 2 hours, hourly interval for the next 22 hours, 2 hours interval for the next 24 hours and then at 4 hours interval till the end of testing period. Due to elastic compression the pressure on the sample is lost. The pressure was initially checked everyday and the constant pressure was maintained throughout the duration of the test. Figure 3.33 shows the test setup for one creep frame and Figure 3.34 shows the complete test setup.

The creep rigs were placed in a room where the temperature was kept at 21 ± 2°C and the relative humidity was kept at 65 ± 5%. The relative humidity and temperature however varied significantly during the testing period when the main doors of the reaction floor where the equipment is housed were left open. The temperature and humidity of the environment was however measured at one-hour interval during the duration of the test.

Figure 3.33: Test setup showing five columns in a creep rig under constant load

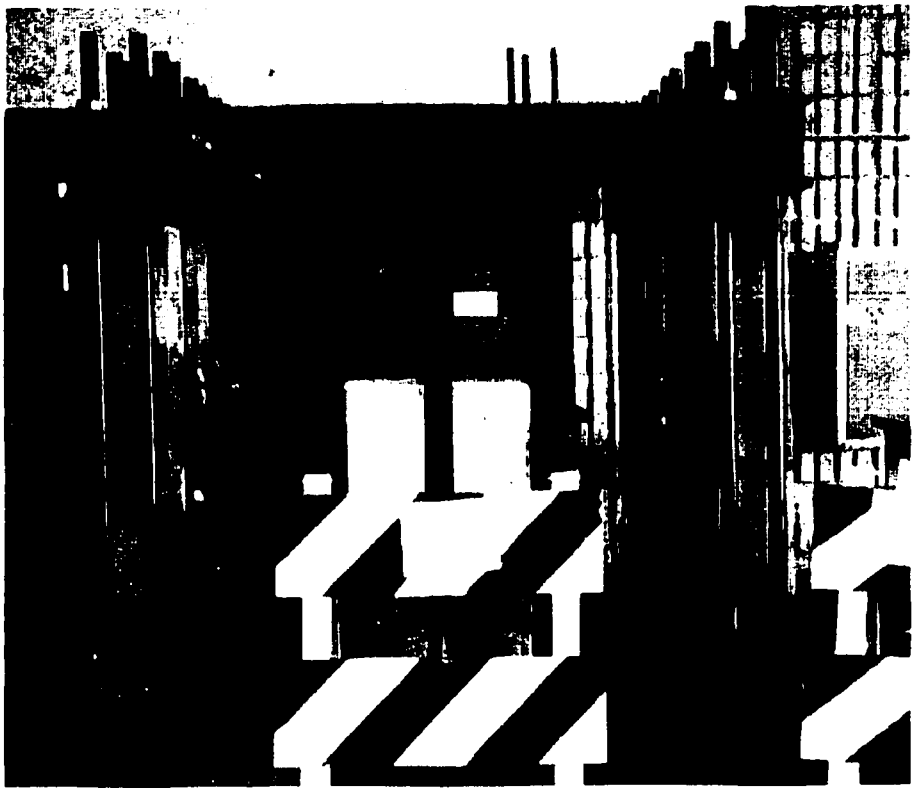

Fig. 3.34: Test setup showing both creep rigs with 10 column specimens loaded

CHAPTER 4

RESULTS AND DISCUSSION

4.1 CONCRETE AND REPAIR MATERIAL PROPERTIES

As discussed in chapter 3, the knowledge of evolution of key properties of concrete and repair materials is important to analyze and predict the performance of repair materials when used for patch repair of corrosion damaged columns.

4.1.1 COMPRESSIVE STRENGTH

Figures 4.1 shows the evolution of cylinder compressive strength versus time for concrete and the two repair materials FMCX and PFSM. Figure 4.2 shows the development of cube compressive strength for FMCX and PFSM. The results obtained are shown in Tables 4.1 and 4.3. The compressive strength values of all the materials were obtained up to a period of 6 months (180 days). All the materials were cured for 7 days under wet towel. It can be observed from the results that FMCX has the higher increase in compressive strength, than concrete and PFSM.

Table 4.1: Cylinder compressive strength (MPa)

Material	AGE (Days)							
	0	1	3	7	14	28	60	180
Concrete	0	NA*	NA*	40.32	47.92	53.30	55.15	55.21
FMCX	0	22.50	40.45	50.37	56.30	62.66	66.80	67.13
PFSM	0	11.73	22.11	32.97	42.11	50.41	52.11	52.19

*(Not available because the specimens were cast at field and transported to lab for testing after initial curing period of 7 days)

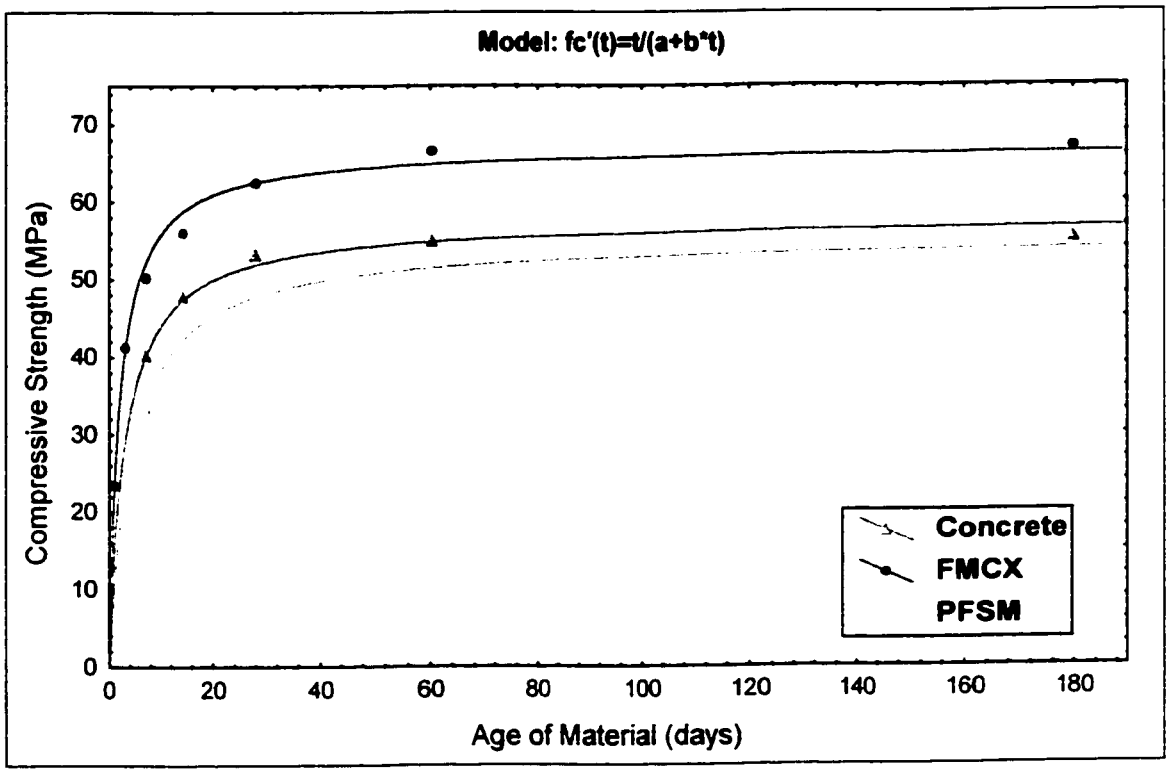

Figure 4.1: Evolution of cylinder compressive strength

Table 4.2: Regression coefficients (a, b) and coefficient of determination (R^2) for evolution of cylinder compressive strength.

Material	a	b	R^2
Concrete	0.052924	0.017324	99.843%
FMCX	0.029748	0.014898	99.595%
PFSM	0.077742	0.018096	99.517%

Table 4.3: Cube compressive strength (MPa)

Material	AGE (Days)							
	0	1	3	7	14	28	60	180
FMCX	0	22.15	40.73	52.26	58.90	64.63	67.58	68.16
PFSM	0	12.65	22.35	33.16	43.11	52.85	53.50	53.74

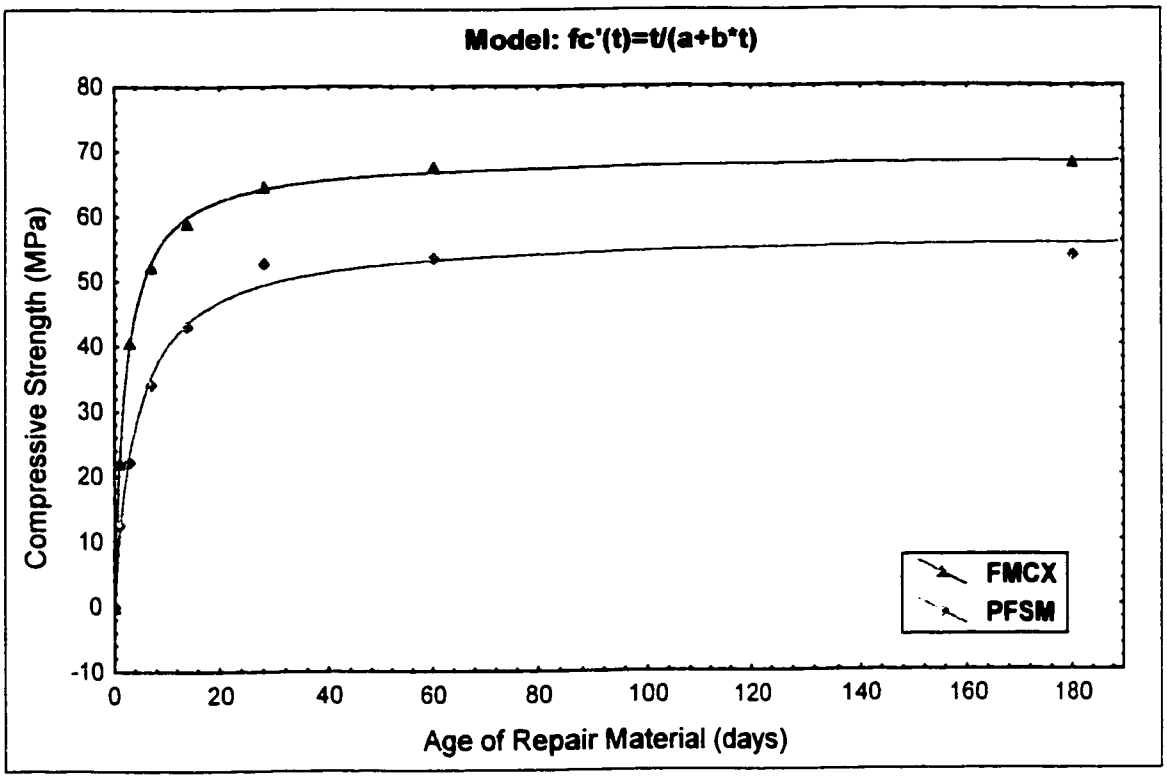

Figure 4.2: Evolution of Cube compressive strength

Table 4.4: Regression coefficients (a, b) and coefficient of determination (R^2) for evolution of cube compressive strength

Material	a	b	R^2
FMCX	0.031200	0.014458	99.938%
PFSM	0.075259	0.017531	99.257%

The 28-day cube compressive strength is higher by 3-5% (around 2-3 MPa) compared to 28-day cylinder compressive strength for the repair materials. The 28-day cylinder compressive strength of Concrete is 53 MPa, FMCX is 62 MPa and PFSM is 50 MPa.

The evolution of compressive strength shows Concrete achieved 75% and 90% of the 28-day strength at 7 and 14 days respectively. Only 3-4% increase in strength was observed after 28 days up to an age of 180 days. FMCX achieved 36%, 65%, 80% and 90% of 28-day strength at 1, 3, 7 and 14 days respectively. About 6-7% increase in strength was observed after 28 days up to an age of 180 days. PFSM achieved 23%, 44%, 65% and 84% of 28-day strength at 1, 3, 7 and 14 days respectively. About 3-4% increase in strength was observed after 28 days up to an age of 180 days.

FMCX achieved 36% whereas PFSM achieved 23% of its 28-day strength at an age of 1 day. The early age strength evolution of FMCX is quite higher than PFSM, and the increase in strength after 28-days is also higher in FMCX compared to that of PFSM and Concrete. A comparison of strengths and their evolution shows that FMCX have the higher strength than the others.

The evolution of compressive strength can be predicted using ACI strength evolution equation [29], which is given as

$$f_c'(t) = \frac{t}{a + bt}$$

The regression parameters 'a' (days/MPa) and 'b' (1/MPa) for these materials are however, significantly different. The regression coefficients and the coefficient of determination are shown in Table 4.2 and 4.4. The coefficient of determination R^2 for all the curves are above 99%.

4.1.2 TENSILE STRENGTH

Figures 4.3 shows the evolution of briquette tensile strength versus time for the two repair materials FMCX and PFSM. The results obtained are shown in Table 4.5. The tensile strength values of all the materials were obtained up to a period of 6 months (180 days). All the materials were cured for 7 days under wet towel. It can be observed from the results that PFSM has the higher increase in tensile strength, than FMCX.

The 28-day briquette tensile strength of FMCX is 3.47 MPa and PFSM is 4.7 MPa. The evolution of tensile strength shows FMCX achieved 50%, 84%, 95% and 97% of 28-day strength at 1, 3, 7 and 14 days respectively. About 3-4% increase in strength was observed after 28 days up to an age of 180 days. PFSM achieved 40%, 49%, 67% and 90% of 28-day strength at 1, 3, 7 and 14 days respectively. About 1-2% increase in strength was observed after 28 days up to an age of 180 days.

FMCX achieved 50% whereas PFSM achieved 40% of its 28-day strength at an age of 1 day. The early age strength evolution of FMCX is higher than PFSM, and the increase in strength after 28-days is also higher in FMCX compared to that of PFSM. There is sudden increase in the tensile strength of PFSM after 7 days which is due to formation of polymer matrix due to fibers present in it, when exposed to air after curing period of 7 days.

The evolution of briquette tensile strength can also be predicted using ACI strength evolution equation [29], which is given as

$$f_t(t) = \frac{t}{a+bt}$$

Table 4.5: Briquette tensile strength (MPa)

Material	AGE (days)							
	0	1	3	7	14	28	60	180
FMCX	0	1.74	2.90	3.30	3.35	3.47	3.59	3.60
PFSM	0	1.87	2.29	3.13	4.24	4.70	4.75	4.73

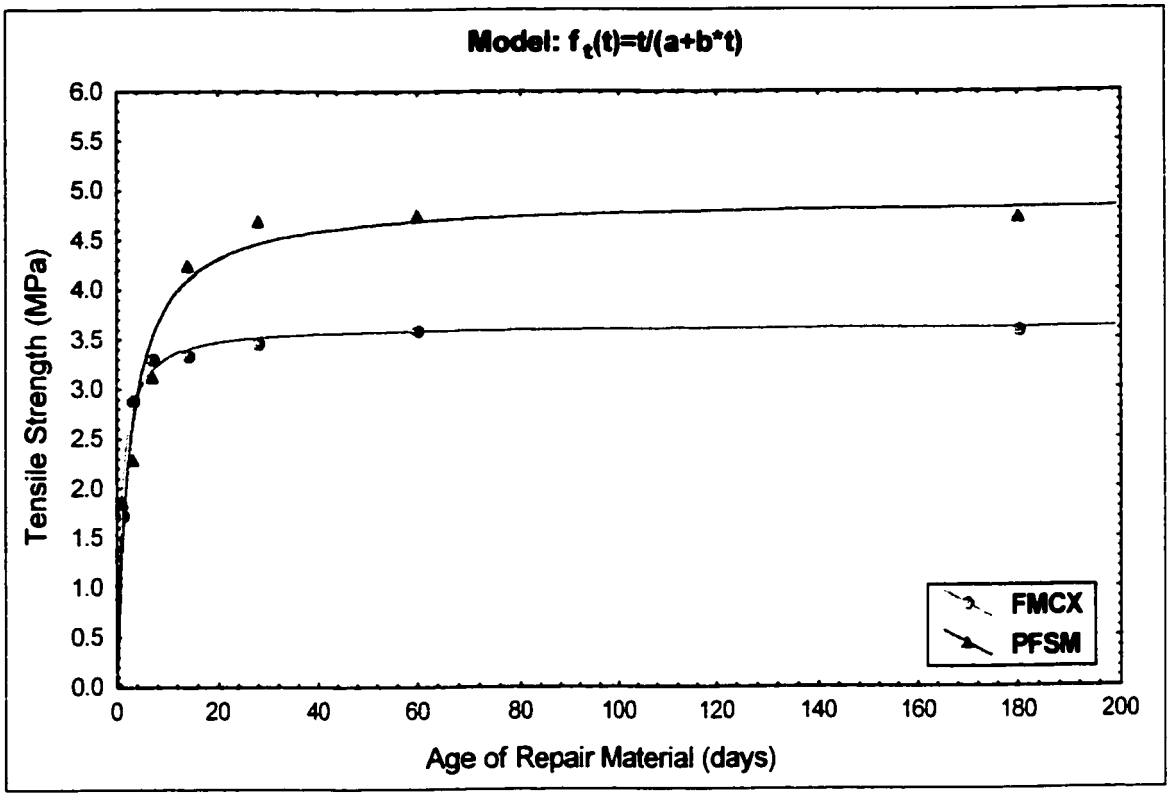

Figure 4.3: Evolution of briquette tensile strength

Table 4.6: Regression coefficients (a, b) and coefficient of determination (R^2) for evolution of briquette tensile strength

Material	a	b	R^2
FMCX	0.263245	0.274370	99.558%
PFSM	0.559474	0.203760	96.990%

The regression parameters 'a' (days/MPa) and 'b' (1/MPa) for these materials are however, significantly different. The regression coefficients and the coefficient of determination are shown in Table 4.6. The coefficient of determination R^2 for FMCX is 99%, whereas for PFSM is 97%.

4.1.3 BOND STRENGTH

Figures 4.4 shows the evolution of bond strength versus time for the two repair materials FMCX and PFSM using cylinders. Figure 4.5 shows the development of bond strength for FMCX and PFSM using cores taken from slab specimens. The results obtained are shown in Tables 4.7 and 4.9. The bond strength values of all the materials were obtained up to a period of 2 months (60 days). All the materials tested were cured for 7 days under wet towel. It can be observed from the results that FMCX has the higher bond strength compared to that of PFSM.

The bond strength using cylinders is higher by 8-10% (around 0.2-0.3 MPa) compared to bond strength using cores for the repair materials. The 28-day bond strength of FMCX is 2.73 MPa and PFSM is 1.84 MPa tested using cylinders.

The evolution of bond strength shows FMCX achieved 83% and 90% of 28-day strength at 3and 7 days respectively. About 2-3% increase in strength was observed after 28 days up to an age of 60 days. PFSM achieved 78% and 90% of 28-day strength at 3 and 7 days respectively. About 2-3% increase in strength was observed after 28 days up to an age of 60 days.

Table 4.7: Bond strength (MPa) using cylinders

Material	AGE (days)				
	0	3	7	28	60
FMCX	0	2.27	2.41	2.73	2.81
PFSM	0	1.43	1.67	1.84	1.88

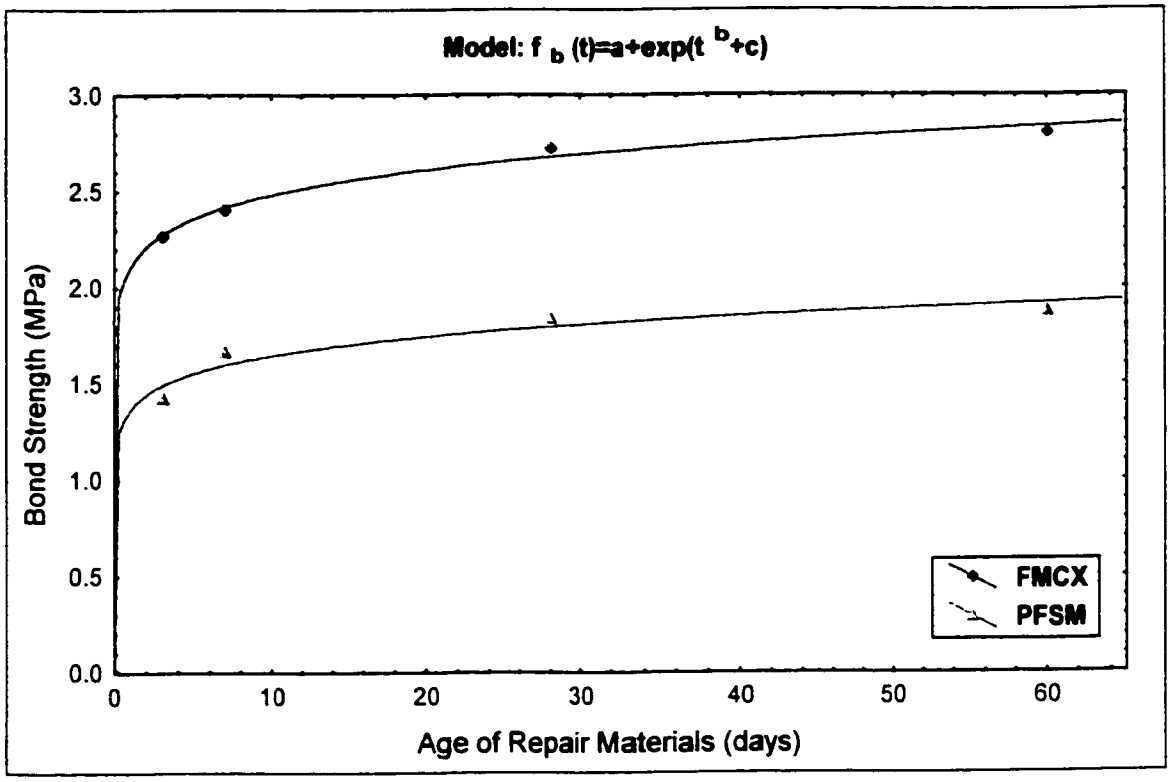

Figure 4.4: Evolution of bond strength using cylinders

Table 4.8: Regression coefficients (a, b, & c) and coefficient of determination (R^2) for evolution of bond strength using cylinders

Material	a	b	c	R^2
FMCX	-1.22609	0.04438	0.203637	99.937%
PFSM	-0.79843	0.04998	-0.226175	99.503%

Table 4.9: Bond strength (MPa) using cores

Material	AGE (days)				
	0	3	7	28	60
FMCX	0	1.97	2.21	2.48	2.50
PFSM	0	1.31	1.43	1.63	1.69

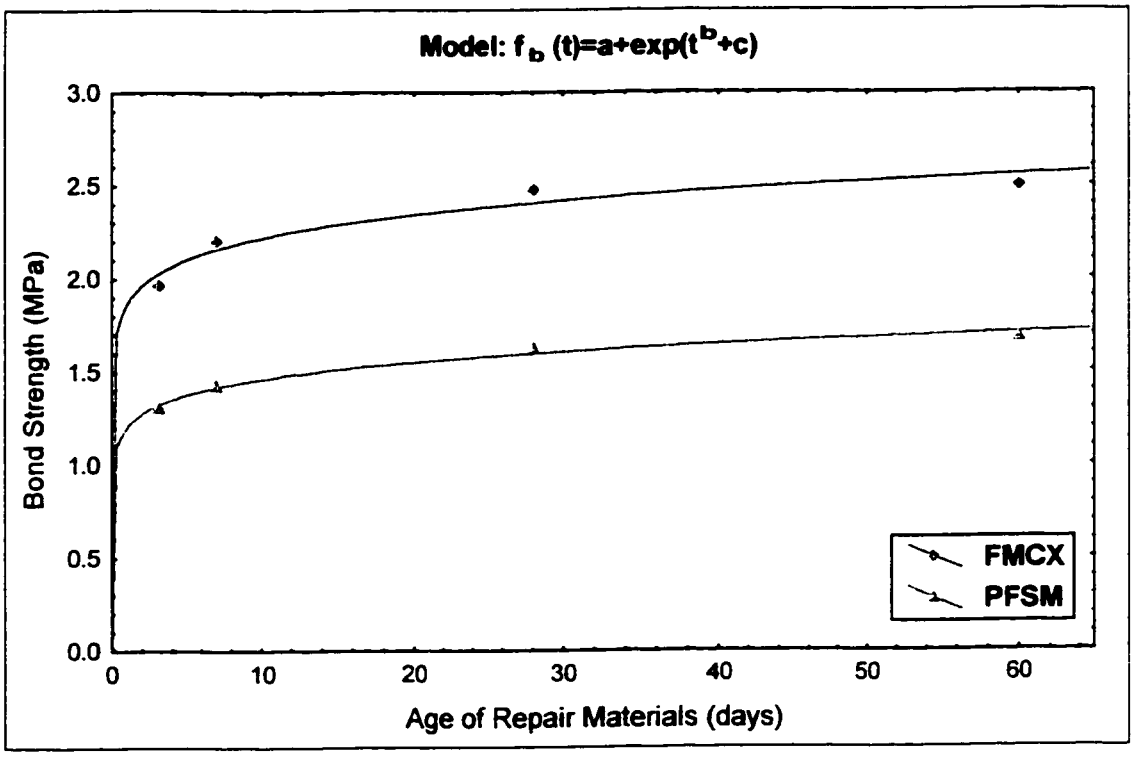

Figure 4.5: Evolution of bond strength using cores

Table 4.10: Regression coefficients (a, b, & c) and coefficient of determination (R^2) for evolution of bond strength using cores

Material	a	b	c	R^2
FMCX	-1.08937	0.046469	0.084862	99.676%
PFSM	-0.70586	0.050854	-0.348768	99.917%

FMCX achieved 83% whereas PFSM achieved 78% of its 28-day strength at an age of 3 day. The early age strength evolution of FMCX is higher than PFSM, and the increase in strength after 28-days is equal in FMCX compared to that of PFSM. A comparison of strengths and their evolution shows that FMCX have the higher strength than PFSM.

For the purpose of modeling, an exponential 3-parameter evolution curve gives a good fit for both repair materials, which is given as

$$f_b(t) = a + exp(t^b + c)$$

The regression parameters a, b, and c, and the coefficient of determination R^2 are shown in Table 4.8 and 4.10. The coefficient of determination R^2 for all the curves are above 99%.

4.1.4 COMPRESSIVE MODULUS OF ELASTICITY & POISON'S RATIO

The compressive modulus of elasticity and poison's ratio are the most important structural properties of repair materials. The stress generation in a repair layer is dependent on the evolution of this material parameter.

Figures 4.6, 4.7, and 4.8 show the stress strain curves for concrete, FMCX, and PFSM respectively. The 1-day and 3-day stress strain curves are not available for concrete, because the specimens were cast at field and transported to lab for testing after initial curing period of 7 days. The modulus of elasticity and poison's ratio were evaluated from these curves using the procedure specified in ASTM C-469.

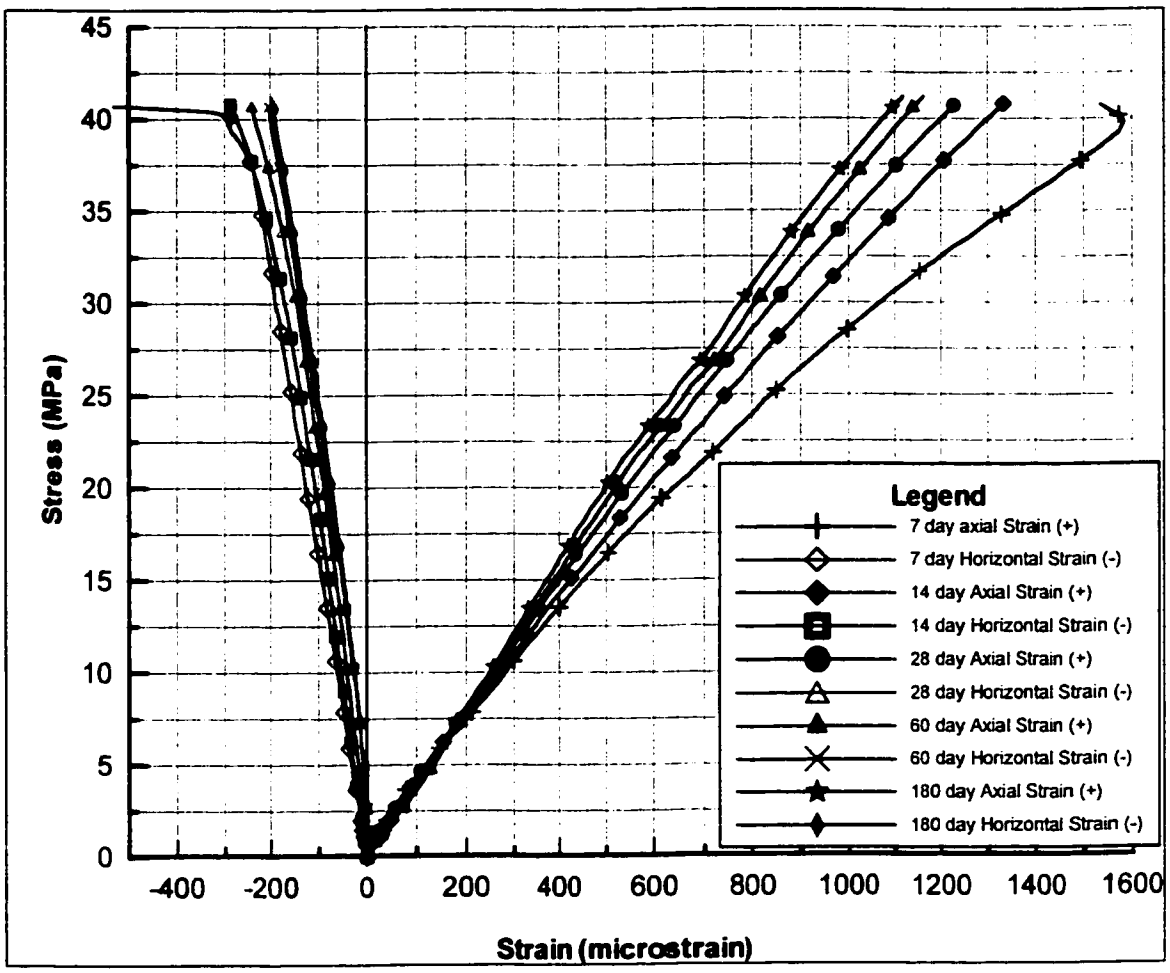

Figure 4.6: Compressive stress - strain curves for concrete

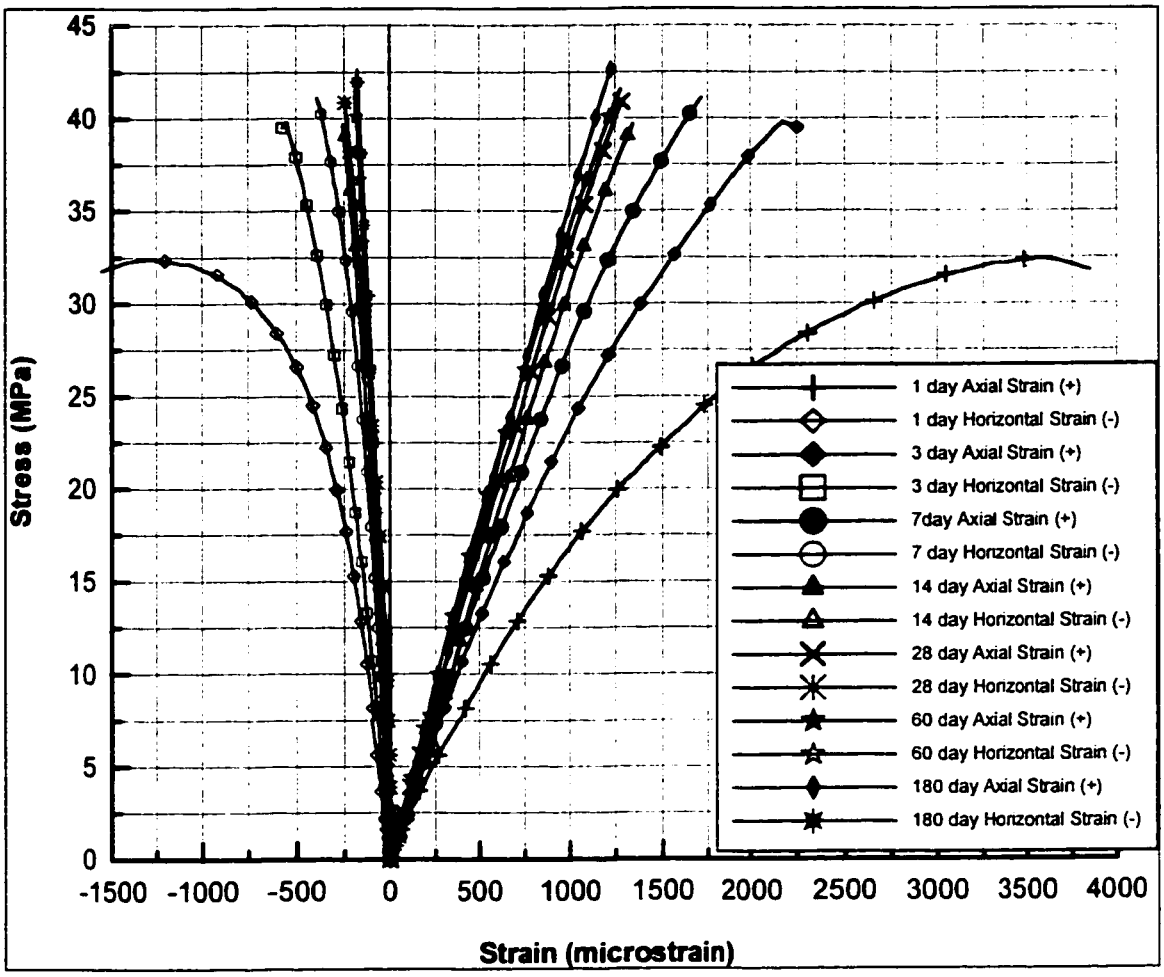

Figure 4.7: Compressive stress - strain curves for FMCX

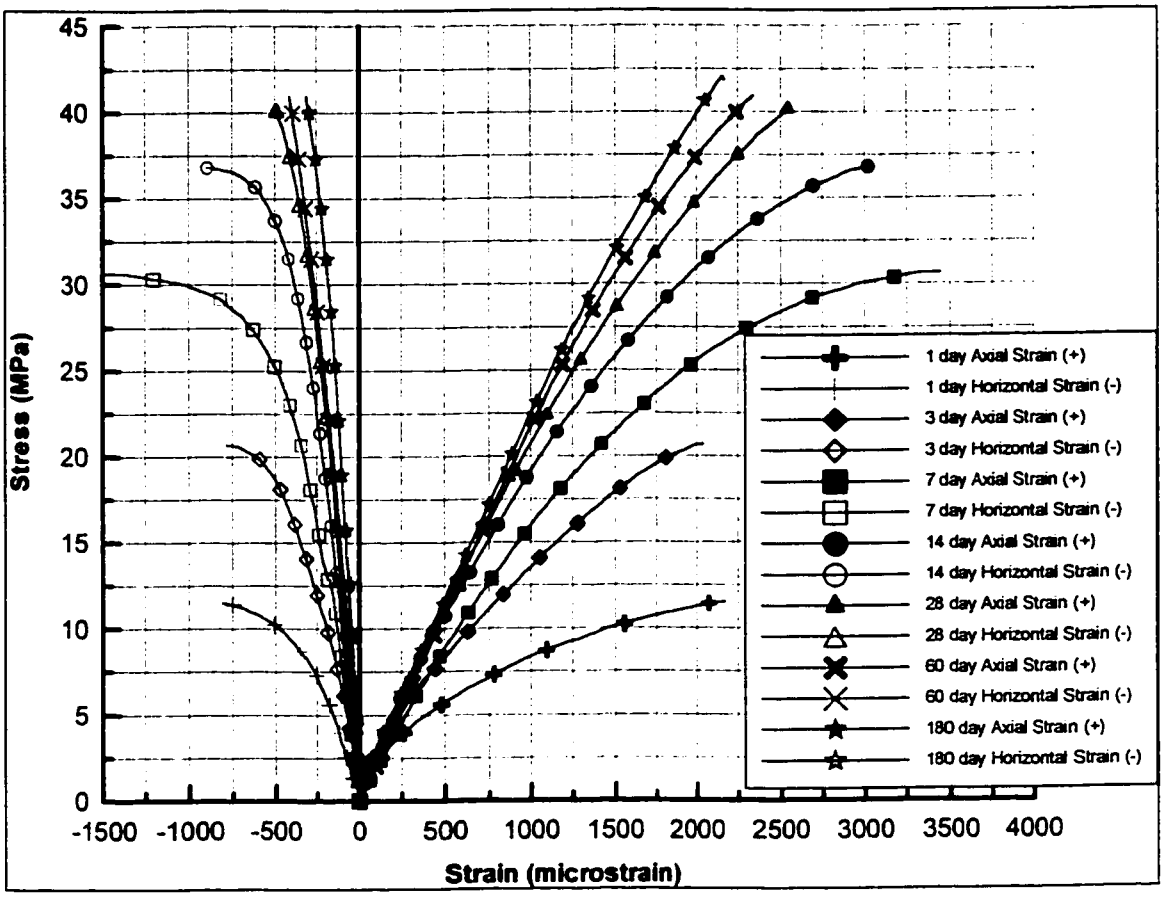

Figure 4.8: Compressive stress - strain curves for PFSM

Table 4.11: Compressive modulus of elasticity (GPa)

Material	AGE (Days)							
	0	1	3	7	14	28	60	180
Concrete	0	NA*	NA*	25.77	28.83	30.55	31.74	32.18
FMCX	0	18.15	23.81	28.35	31.44	33.46	35.13	35.27
PFSM	0	10.03	14.19	16.81	18.91	20.87	21.76	22.14

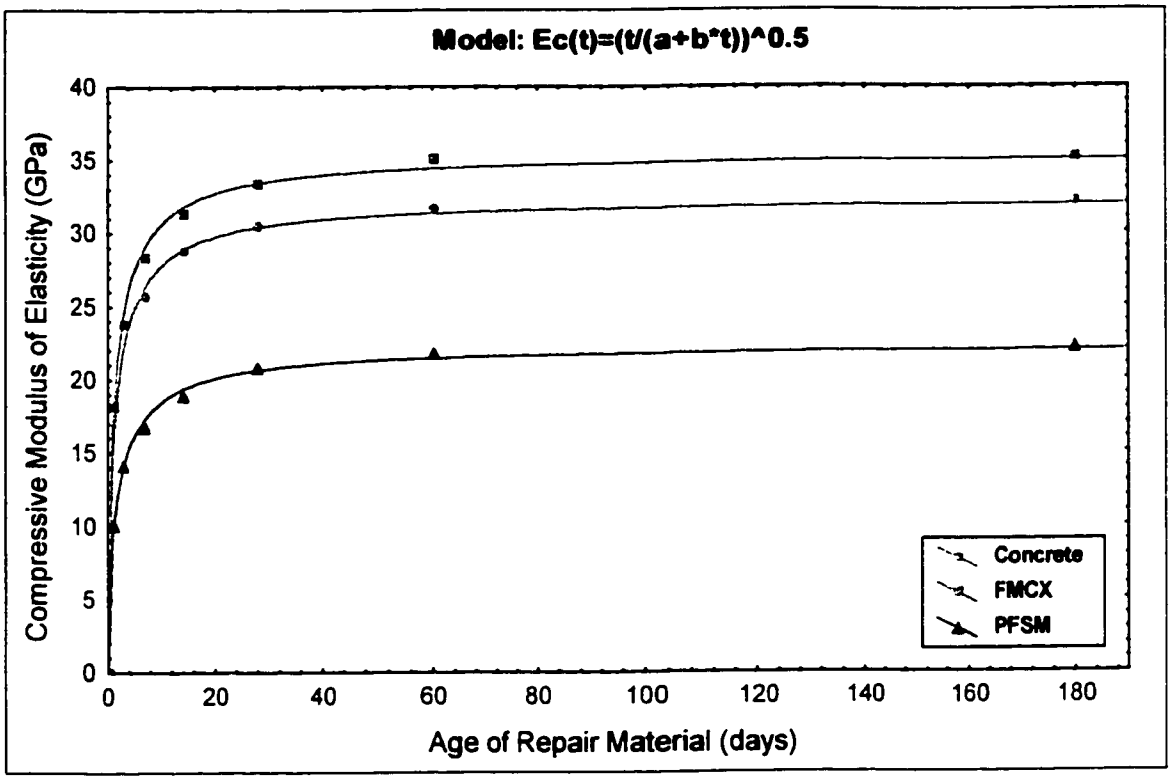

Figure 4.9: Evolution of compressive modulus of elasticity

Table 4.12: Regression coefficients (a, b) and coefficient of determination (R^2) for evolution of compressive modulus of elasticity

Material	a	b	R^2
Concrete	0.003315	0.000960	99.671%
FMCX	0.002656	0.000799	99.713%
PFSM	0.009084	0.002014	99.756%

Table 4.13: Poison's ratio

Material	AGE (Days)						
	1	3	7	14	28	60	180
Concrete	NA*	NA*	0.192	0.1782	0.1637	0.1581	0.1502
FMCX	0.214	0.197	0.183	0.1716	0.1590	0.1535	0.1498
PFSM	0.350	0.280	0.236	0.2056	0.1806	0.1780	0.1762

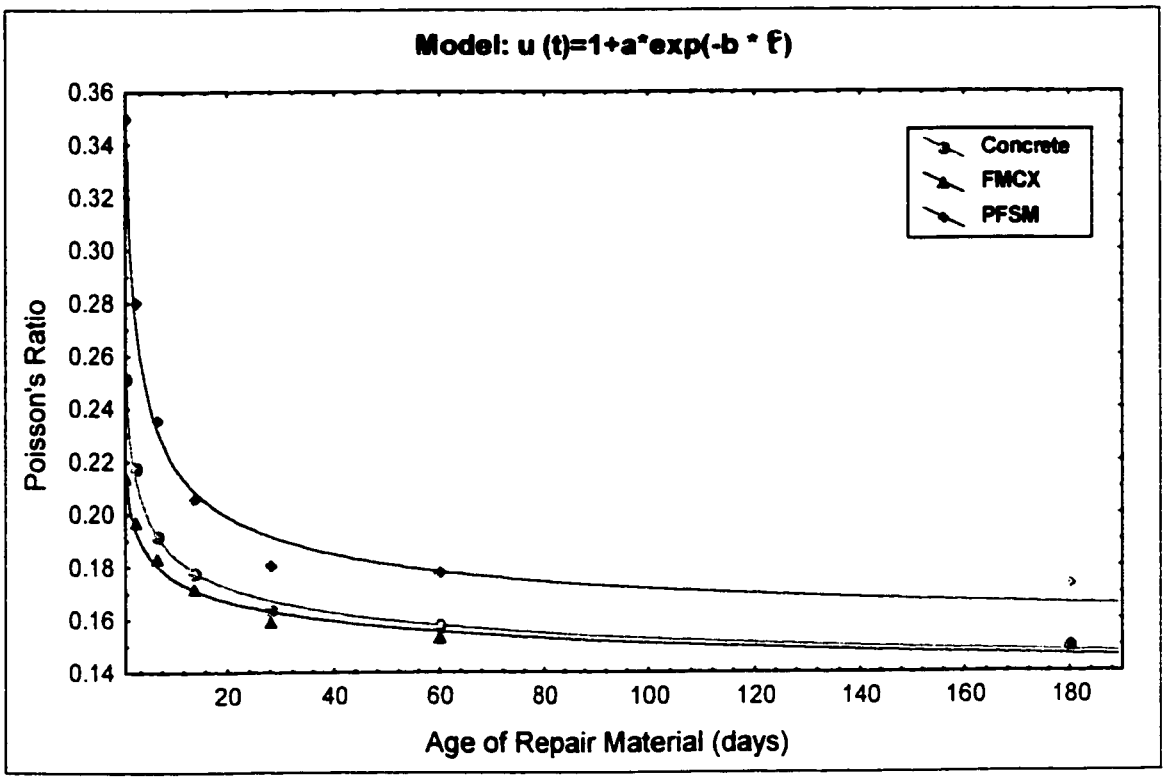

Figure 4.10: Evolution of poison's ratio

Table 4.14: Regression coefficients (a, b, c) and coefficient of determination (R^2) for evolution of poison's ratio

Material	a	b	c	R^2
Concrete	-0.872399	0.155439	-0.360497	99.568%
FMCX	-0.885543	0.121255	-0.227892	98.575%
PFSM	-0.850714	0.273826	-0.503961	99.030%

Figures 4.9 shows the evolution of compressive modulus of elasticity versus time for concrete and the two repair materials FMCX and PFSM. Figure 4.10 shows the evolution of poison's ratio for concrete and the two repair materials FMCX and PFSM. The results obtained are shown in Tables 4.11 and 4.13. The compressive modulus and poison's ratio for all the materials were obtained up to a period of 6 months (180 days). All the materials were cured for 7 days under wet towel. It can be observed from the results that FMCX is a stiff material and develops a high compressive modulus at an early age.

The evolution of compressive modulus shows Concrete achieved 84% and 94% of the 28-day modulus at 7 and 14 days respectively. Only 4-5% increase in modulus was observed after 28 days up to an age of 180 days. FMCX achieved 54%, 71%, 85% and 94% of 28-day modulus at 1, 3, 7 and 14 days respectively. About 5-6% increase in modulus was observed after 28 days up to an age of 180 days. PFSM achieved 48%, 68%, 80% and 91% of 28-day modulus at 1, 3, 7 and 14 days respectively. About 4-6% increase in modulus was observed after 28 days up to an age of 180 days. The evolution of modulus rate of concrete and FMCX is nearly similar and is rather little slower in PFSM.

The poison's ratio for FMCX is the lowest as compared to the other material PFSM and concrete at early ages but as the time progresses the material FMCX and concrete have the same values. FMCX and concrete are stiff materials as compared to PFSM. It can be seen from Figure 4.10 that the material PFSM has high poison's ratio, which shows it as a soft material that bulges in the lateral directions when subjected to compressive loads.

The poison's ratio for concrete and FMCX are around 0.16 at 28 days of age and reduces to 0.15 at 180 days, whereas for PFSM it is 0.18 at 28 days of age and then reduces a little to 0.175 at 180 days.

For the purpose of modeling, the ACI two-parameter regression equation gives a reasonably good fit for observed values of compressive modulus for all materials, which is given as

$$E_c(t) = \sqrt{\frac{t}{a+bt}}$$

For poison's ratio, a three parameter exponential curve gives a good fit for all the materials, which is given as

$$\mu(t) = 1 + a\,exp(-b\,t^c)$$

The regression parameters a, b, and c, and the coefficient of determination R^2 are shown in Table 4.12 and 4.14. The coefficient of determination R^2 for all the curves are above 99%.

4.1.5 TENSILE MODULUS

The tensile modulus of elasticity is one of the most important structural properties of repair materials. The stress generation in a repair layer due to shrinkage is dependent on the evolution of this material parameter.

Figures 4.11 shows the evolution of tensile modulus of elasticity versus time for the two repair materials FMCX and PFSM. The results obtained are shown in Table 4.15. The tensile moduli for the repair materials were obtained up to a period of 2 months (60

days). The materials were cured for 7 days under wet towel. It can be observed from the results that FMCX is a stiff material under tension and develops a high tensile modulus at an early age.

The evolution of tensile modulus shows FMCX achieved 78% and 92% of 28-day modulus at 3 and 7 days respectively. About 2.5% increase in modulus was observed after 28 days up to an age of 60 days. PFSM achieved 66% and 85% of 28-day modulus at 3 and 7 days respectively. About 3-4% increase in modulus was observed after 28 days up to an age of 60 days. The early age evolution of modulus of elasticity of FMCX is quite higher than PFSM.

For the purpose of modeling, a three parameter exponential curve gives a good fit for all the materials, which is given as

$$E_t(t) = a \exp(1 + b f)$$

The regression parameters a, b, and c, and the coefficient of determination R^2 are shown in Table 4.16. The coefficient of determination R^2 for all the curves are above 99%.

Table 4.15: Tensile modulus of elasticity (GPa)

Material	AGE (days)				
	0	3	7	28	60
FMCX	0	27.53	32.19	35.05	35.94
PFSM	0	15.19	19.37	22.92	23.73

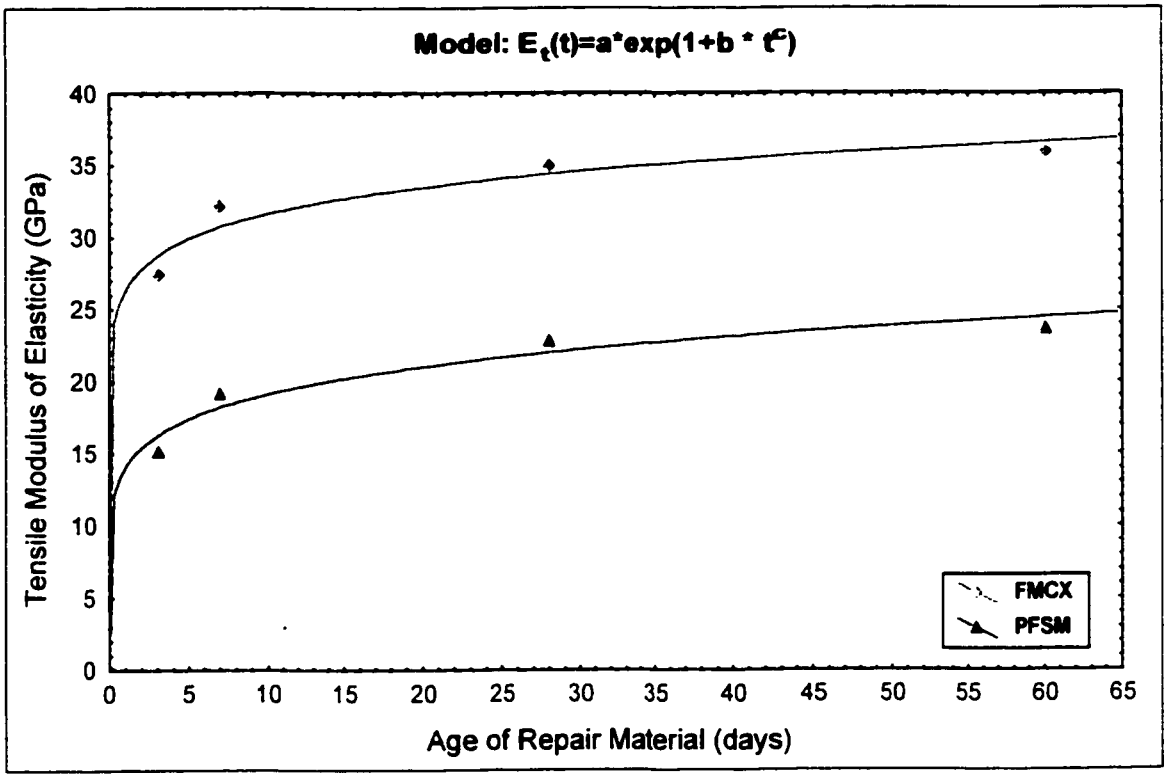

Figure 4.11: Evolution of tensile modulus of elasticity

Table 4.16: Regression coefficients (a, b, c) and coefficient of determination (R^2) for evolution of tensile modulus of elasticity

Material	a	b	c	R^2
FMCX	0.000691	9.549604	0.008287	99.513%
PFSM	0.000518	9.212907	0.014218	99.039%

4.1.6 SHRINKAGE

The critical role of shrinkage-induced stresses at early ages in a repair system necessitates the monitoring of the shrinkage strains after initial setting of the mortar. The importance of monitoring the history of strain evolution in a repair material gains more importance in view of the shrinkage compensating additives in these materials. The expansion of these materials in plastic and early ages plays a critical role in overall stress history of the system.

In view of the above, strains were measured in specimens of two sizes, 25x25x285 mm and 40x40x160 mm soon after initial setting in the mold up to a period of three months (90 days). The strains were measured using embedded strain gauges. Figure 4.12 shows the evolution of strains in two specimens 25x25x285 and 40x40x160 of material FMCX, and Figure 4.13 shows the strains in material PFSM.

The total strain evolution in FMCX (Figure 4.12) shows an initial expansion of 350 με and 460 με in specimens of size 25x25x285 and 40x40x160 respectively, during the initial hardening stage up to 7 days. The expansion in this material kept on increasing till it is removed from curing and subjected to laboratory atmosphere. After 7 days, when the specimen is exposed to drying with moisture diffusing from 5 faces of prism at 65 ± 5% relative humidity, a steep fall in shrinkage-time curve can be seen in both size specimens. The total strain drops from +350 με to +20 με (net 330 με) in the first week after exposure, and a net shrinkage strain of –320 με (gross 670 με) takes place in 90 days for specimen of size 25x25x285.

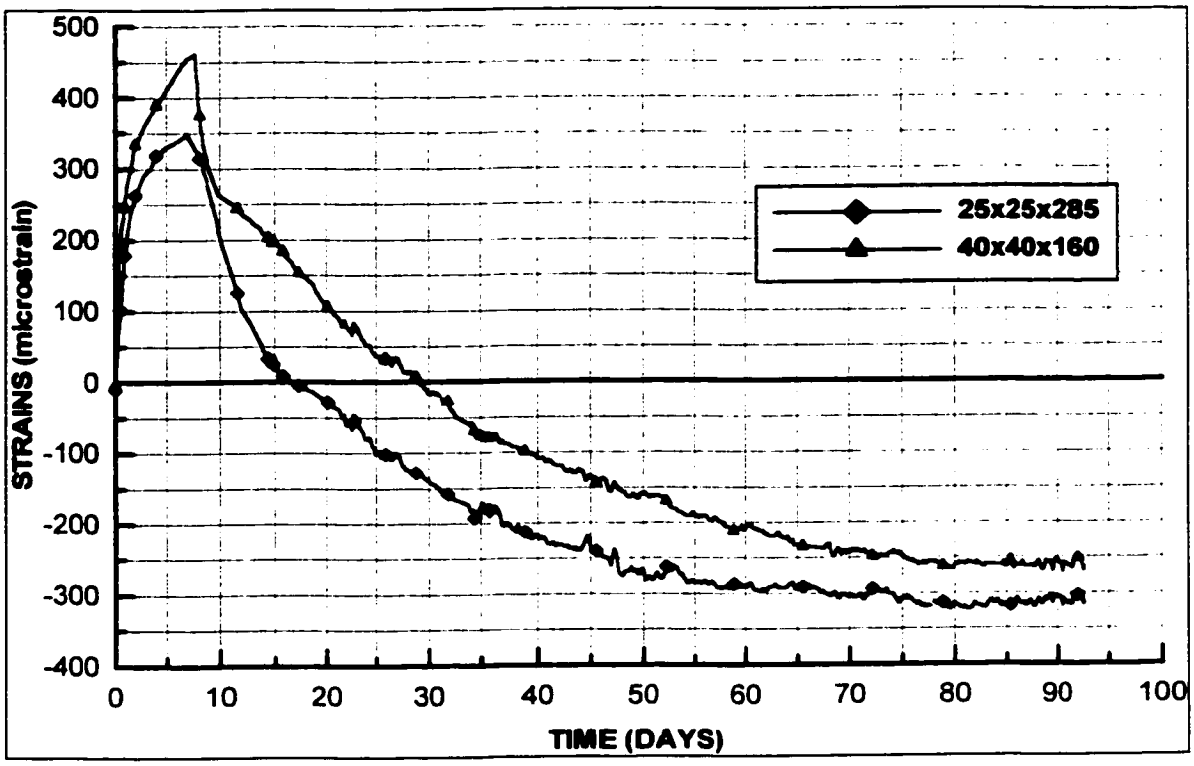

Figure 4.12: Expansion-Shrinkage strain in FMCX

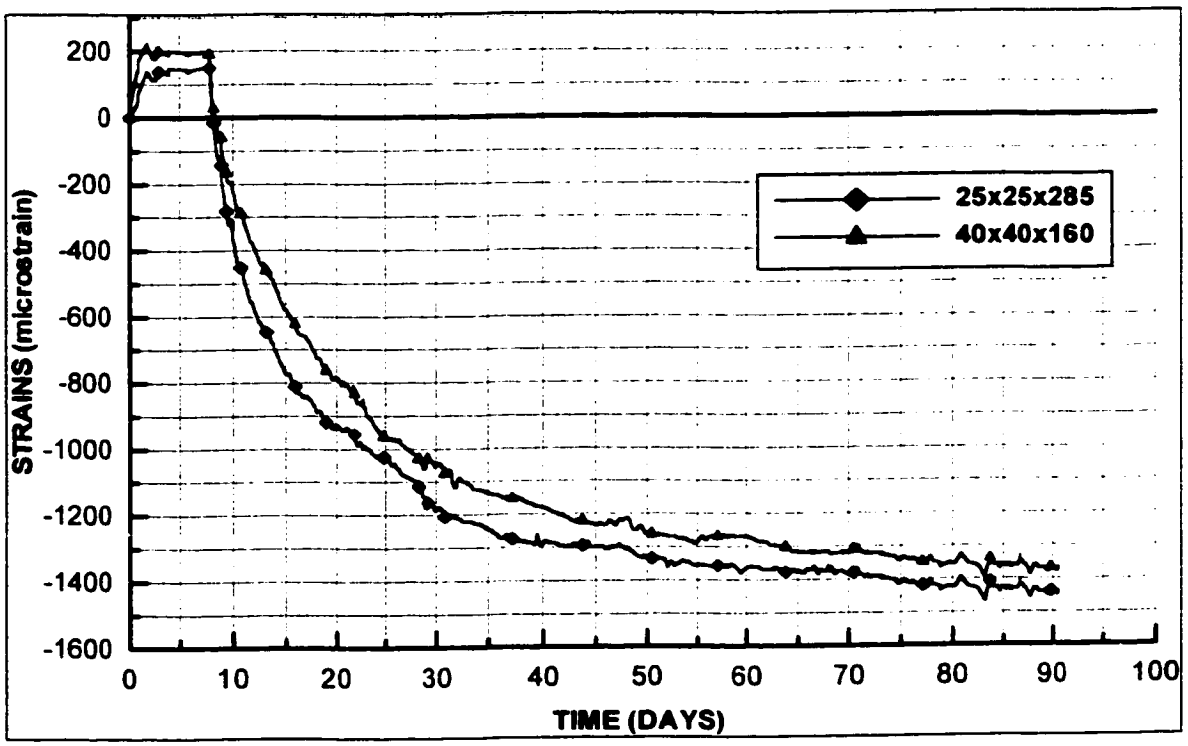

Figure 4.13: Expansion-Shrinkage strain in PFSM

The total strain drops from +460 με to +200 με (net 260 με) in the first week after exposure, and a net shrinkage strain of –260 με (gross 720 με) takes place in 90 days for specimen of size 40x40x160.

The total strain evolution in PFSM (Figure 4.13) shows an initial expansion of 150 με and 200 με in specimens of size 25x25x285 and 40x40x160 respectively, during the initial hardening stage up to 1-2 days. The expansion in this material was constant up to 7 days. After the curing period of 7 days the specimens were exposed to drying with moisture diffusing from 5 faces of prism at 65 ± 5% relative humidity, a steep fall in shrinkage-time curve can be seen in both size specimens. The total strain drops from +150 με to -760 με (net 910 με) in the first week after exposure, and a net shrinkage strain of –1440 με (gross 1590 με) takes place in 90 days for specimen of size 25x25x285. The total strain drops from +200 με to -580 με (net 780 με) in the first week after exposure, and a net shrinkage strain of –1360 με (gross 1560 με) takes place in 90 days for specimen of size 40x40x160.

Table 4.17: Strains at key points for both materials and two sizes

Material		Strain on demoulding (με)	Strain after curing (7 days) (με)	Maximum expansion strain (με)	Final strain (90 days) (με)	Gross Shrinkage strain (με)
FMCX	25x25x285	+ 240	+350	+350	-320	670
	40x40x160	+300	+460	+460	-260	720
PFSM	25x25x285	+150	+150	+150	-1440	1590
	40x40x160	+200	+200	+200	-1360	1560

4.1.7 COMPRESSIVE CREEP

An experimental investigation was conducted on compressive creep for two repair materials selected for this study and the concrete used for test columns. Cylindrical specimens having a diameter of 150 mm and a length of 300 mm were used for this purpose according to ASTM C-512. Tests were conducted on specimens, which were loaded after 28 days of casting. Uniaxial compressive strength (UCS) corresponding to 25% and 35% of the 28-days strength was applied to the specimens. The strain measured on a loaded specimen includes the elastic strain and the creep strain. The compressive creep strain is given as

$$\varepsilon_{exp}(t,t_o) = \varepsilon_{el}(t_o) + \varepsilon_{cr}(t,t_o)$$

where,

$\varepsilon_{exp}(t,t_o)$ is the measured strain at time t due to applied load at time t_0

$\varepsilon_{el}(t_o)$ is the elastic strain at t_o due to applied load

$\varepsilon_{cr}(t,t_o)$ is the total creep strain.

The compressive creep curves for concrete, FMCX and PFSM are shown in Figures 4.14 to 4.16. The sign convention is positive (+) for all compressive strains used in these Figures. A non-linear regression analysis was carried out for the three materials. A functional form shown below gave a good fit to the experimental creep strain data

$$\varepsilon_{exp}\ (t,\ t_o) = a + b\ exp(1 + t^c)$$

Where a, b, and c are the regression parameters given in Table 4.18 for concrete and the two repair materials.

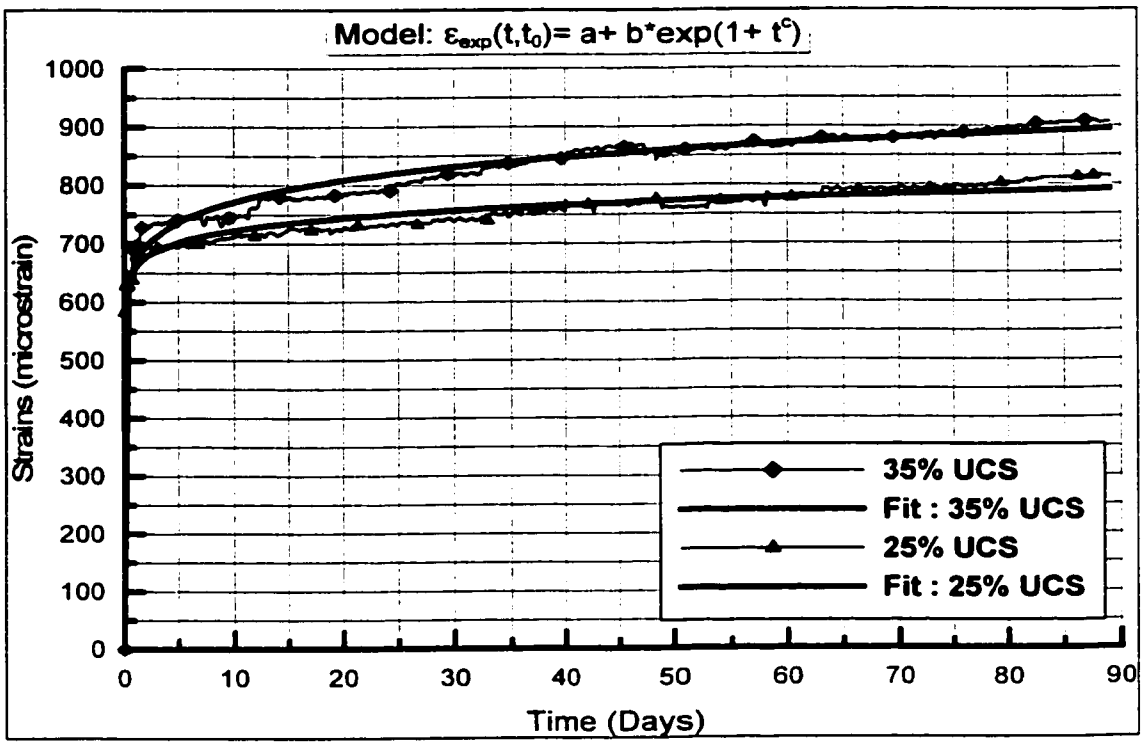

Figure 4.14: Compressive creep in concrete

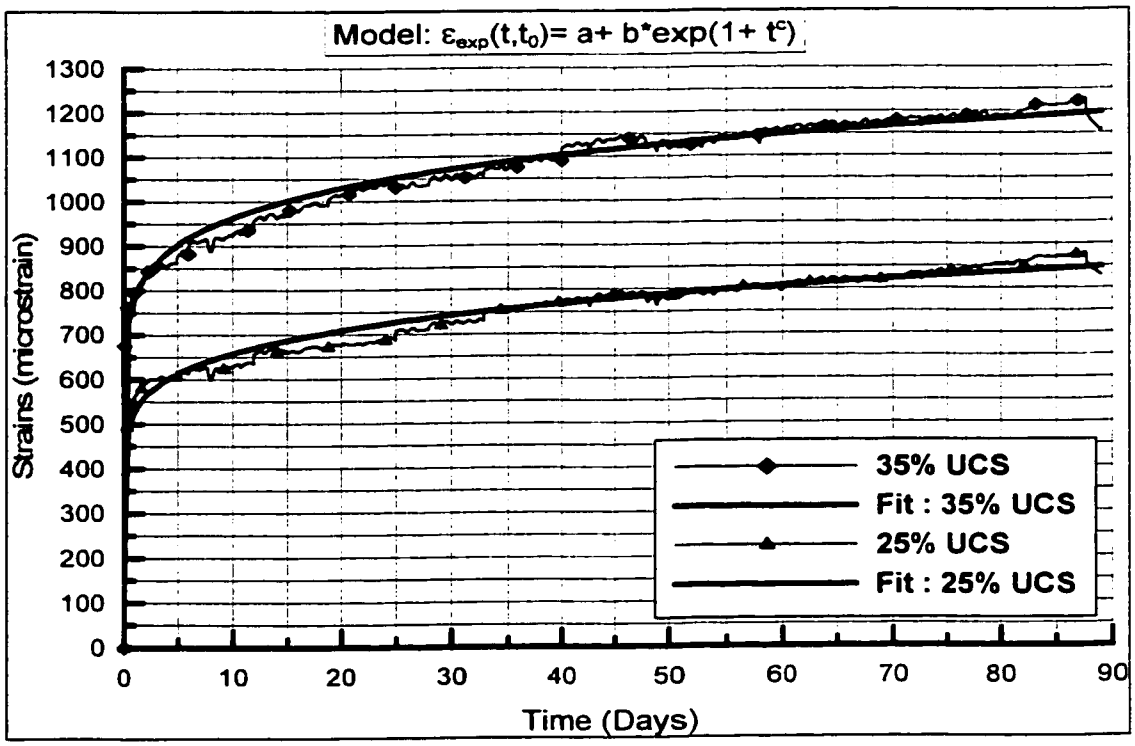

Figure 4.15: Compressive creep in FMCX

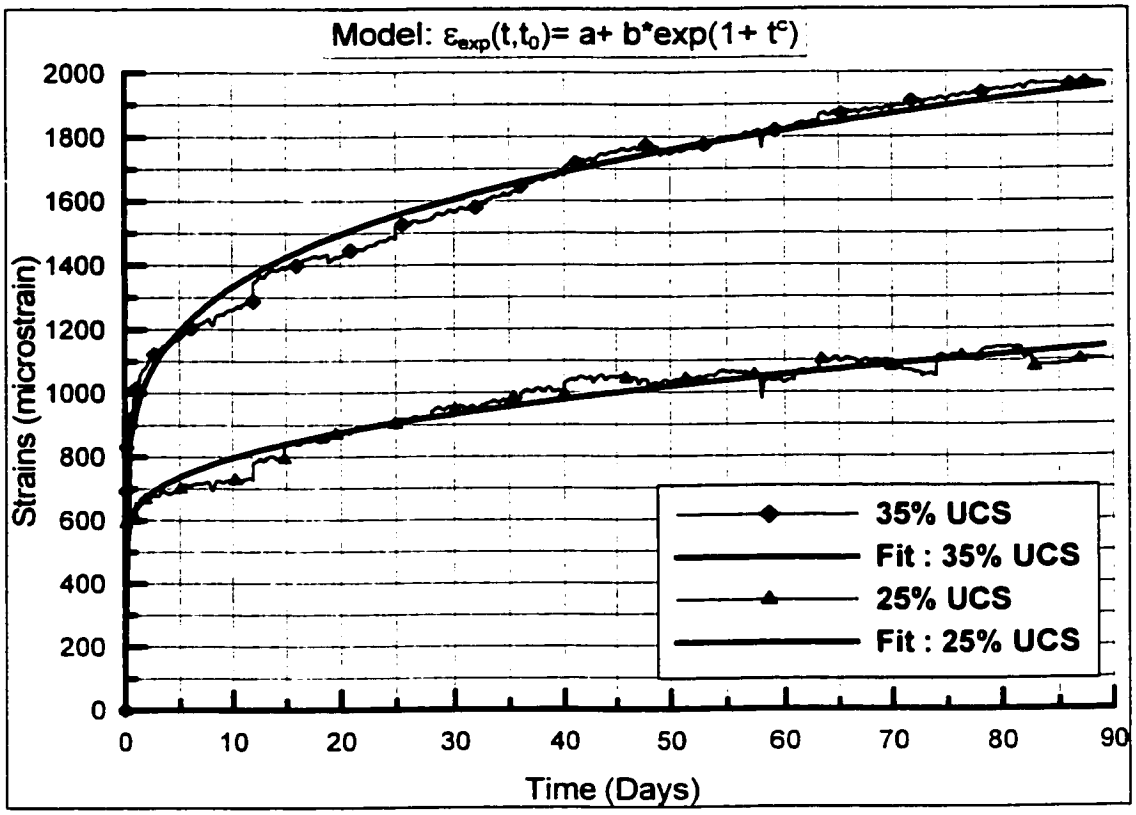

Figure 4.16: Compressive creep in PFSM

Table 4.18: Regression coefficients (a, b, c) and coefficient of determination (R^2) for compressive creep

Material	Load	a	b	c	R^2
Concrete	25% UCS	-348.791	136.278	0.02616	90.79
	35% UCS	-512.75	158.968	0.0371	91.85
FMCX	25% UCS	-51.842	78.694	0.07973	95.10
	35% UCS	-355.99	153.767	0.0605	95.15
PFSM	25% UCS	359.06	38.181	0.15742	95.86
	35% UCS	-349.382	174.85	0.10183	97.63

Table 4.19: Compressive creep strains at key points

Material	Load	$\varepsilon_{el}(t_o)$ (με)	$\varepsilon_{exp}(90\text{-days})$ (με)	$\varepsilon_{cr}(90\text{-days})$ (με)
Concrete	25% UCS	580	815	235
	35% UCS	620	910	290
FMCX	25% UCS	450	850	400
	35% UCS	660	1220	560
PFSM	25% UCS	530	1140	610
	35% UCS	770	1960	1190

It can be seen from the Figures 4.14 to 4.16 and Table 4.19 that the magnitude of compressive creep stresses in concrete are very low compared to that of the two repair materials. The repair material PFSM shows a very high creep up to the age of 90 days. The creep strains under 25% uniaxial compressive strength are lower than those under 35%. It can be observed from the Figures that most of the creep strains are recorded in the first week after loading the specimens.

4.1.8 CHLORIDE PENETRABILITY

The selected two repair materials and concrete was tested for chloride penetrability as per the procedures outlined in ASTM C-1202. The intensity of the current flowing across the sample was determined by measuring the potential drop between the two leads of a resistor connected in the power line. The current data was recorded for six hours at intervals of 30 minutes and this was plotted against time as shown in Figure 4.17.

Table 4.20: ASTM C-1202 indication of chloride ion penetrability based on total charge passed (coulombs)

Charge Passed (coloumbs)	Chloride Ion Penetrability
>4000	High
2000-4000	Moderate
1000-2000	Low
100-1000	Very Low
<100	Negligible

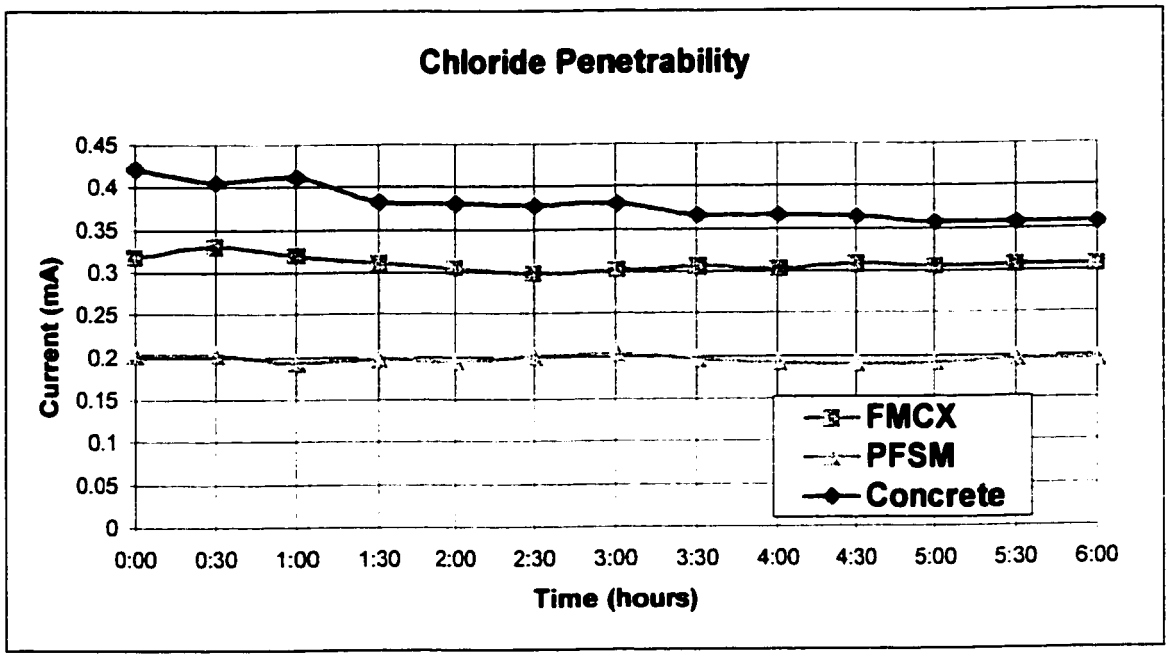

Figure 4.17: Time-current curves for concrete, FMCX and PFSM

Table 4.21: Charge passed through the specimens in the chloride penetrability test

Material	Charge Passed (coulombs)	ASTM C-1202 classification
Concrete	523	Very Low
FMCX	428	Very Low
PFSM	273	Very Low

The area under the curve is the total charge passed in Coulombs (ampere-seconds). The total charge passed through the specimen for a period of 6 hours gives an indication of the electrical resistivity to chloride ion penetrability of the material as shown in Table 4.20.

Figure 4.17 show the charge passed through the material for every 30 minutes. Table 4.21 shows the total charge passed through the materials and also shows the ASTM C-1202 classification for the materials based on the total charge passed. It can be seen from this table that all the materials allow 'Very Low' amount of chloride ions to penetrate. The highest ions are passing through concrete and the lowest through PFSM. As for comparison PFSM is the most resistant to chloride ion penetration and concrete is the less resistant.

4.1.9 SULFATE ATTACK

The selected repair materials were tested for resistance to sulfate attack by carrying out compressive strength tests on cubes made of concrete and repair materials FMCX and PFSM at an interval of one month for a total period of 9 months. Table 4.22 to 4.24 shows the results in tabular form and figures 4.18 and 4.19 shows the percent loss of strength with time.

It can seen be seen that when immersed in sulfate solution the loss of strength in concrete specimen over a period of 9 months is about 6.73 MPa. The repair material PFSM also loses 6.72 MPa in the same period, whereas, the repair material FMCX loses about 16.58 MPa. There is a decrease in compressive strength of about 11% in concrete, 13% in repair material PFSM and 20% in repair material FMCX.

Table 4.22: Loss of strength due to sulfate attack for concrete specimens

Immersion Period	Concrete			
	In Water (MPa)	In Sulfate (MPa)	Loss in Strength (MPa)	% Strength loss
1 Month	56.70	56.48	**0.22**	**0.39**
2 Months	59.32	59.07	**0.25**	**0.42**
3 Months	59.81	59.30	**0.51**	**0.85**
4 Months	59.43	58.20	**1.23**	**2.07**
5 Months	60.04	56.16	**3.88**	**6.46**
6 Months	60.17	56.42	**3.75**	**6.23**
7 Months	60.44	56.31	**4.13**	**6.83**
8 Months	61.51	56.25	**5.26**	**8.55**
9 Months	62.78	56.05	**6.73**	**10.72**

Table 4.23: Loss of strength due to sulfate attack in FMCX

Immersion Period	Repair Material FMCX			
	In Water (MPa)	In Sulfate (MPa)	Loss in Strength (MPa)	% Strength loss
1 Month	62.36	62.09	**0.27**	**0.43**
2 Months	65.12	64.81	**0.31**	**0.48**
3 Months	66.45	65.24	**1.21**	**1.82**
4 Months	71.17	69.14	**2.03**	**2.85**
5 Months	77.61	72.28	**5.33**	**6.87**
6 Months	79.92	69.64	**10.28**	**12.86**
7 Months	81.13	67.99	**13.14**	**16.20**
8 Months	81.75	65.66	**16.09**	**19.68**
9 Months	82.02	65.44	**16.58**	**20.21**

Table 4.24: Loss of strength due to sulfate attack in PFSM

Immersion Period	Repair material PFSM			
	In Water (MPa)	In Sulfate (MPa)	Loss in Strength (MPa)	% Strength loss
1 Month	44.35	44.03	**0.32**	**0.72**
2 Months	47.71	47.36	**0.35**	**0.73**
3 Months	48.19	47.35	**0.84**	**1.74**
4 Months	49.38	46.65	**2.73**	**5.53**
5 Months	50.11	46.93	**3.18**	**6.35**
6 Months	50.36	46.05	**4.31**	**8.56**
7 Months	51.22	46.69	**4.53**	**8.84**
8 Months	50.95	45.71	**5.24**	**10.28**
9 Months	51.38	44.66	**6.72**	**13.08**

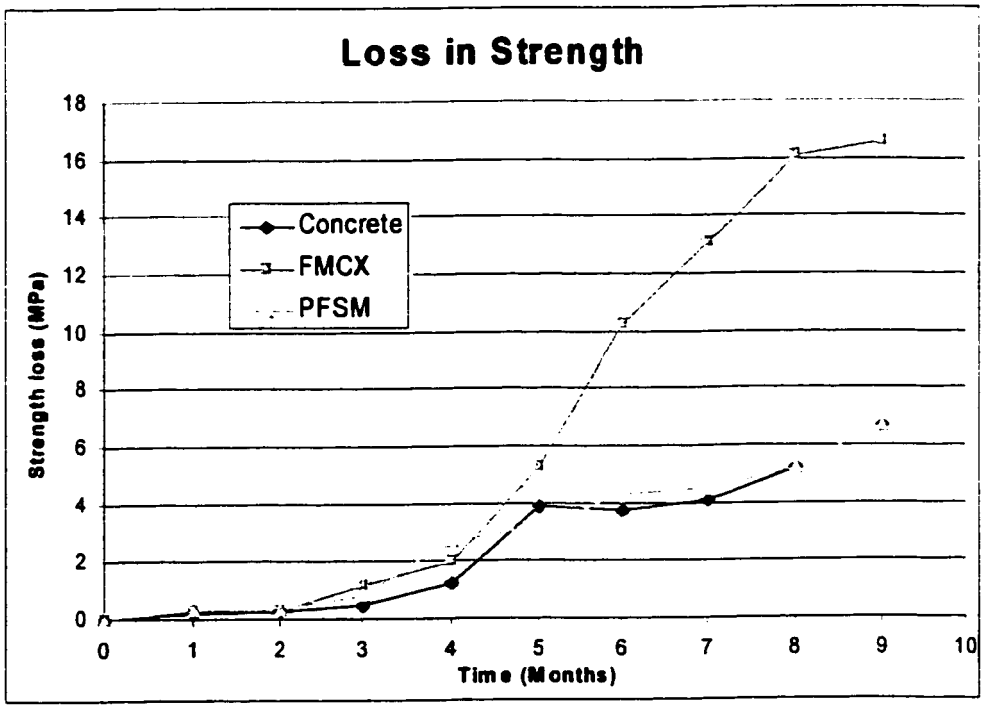

Figure 4.18: Loss of strength due to sulfate attack

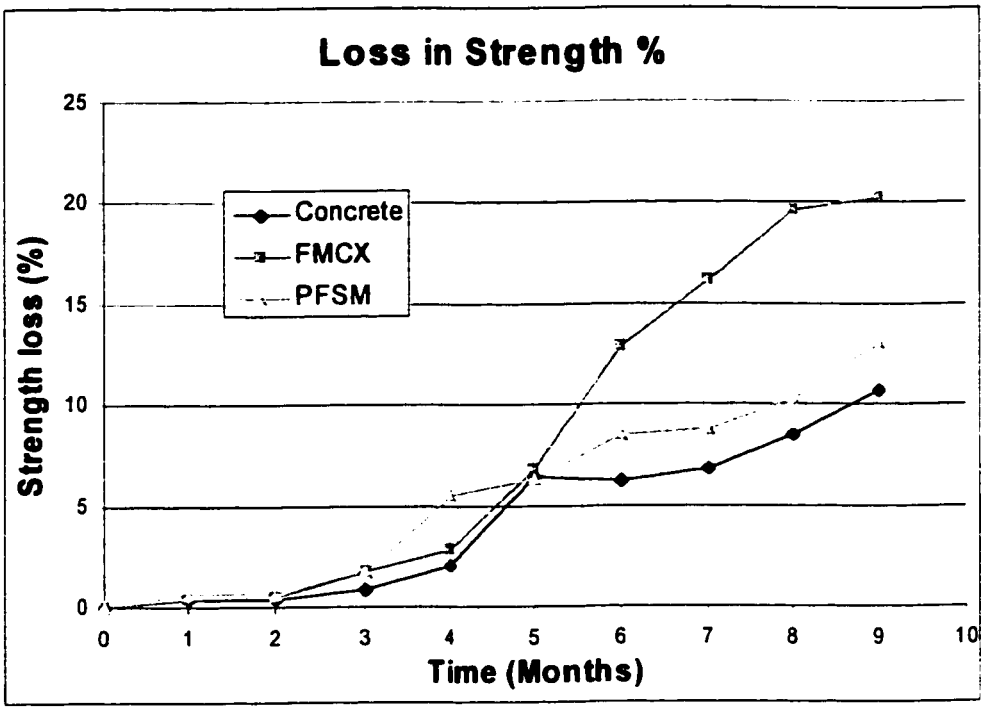

Figure 4.19: Percent Loss of strength due to sulfate attack

4.2 RESULTS AND DISCUSSION OF DESTRUCTIVE TESTS OF REPAIRED/UN-REPAIRED COLUMNS

The testing of 20 repaired/un-repaired columns consists of two parts in which 10 columns were tested for their ultimate load capacities and the remaining 10 columns were tested for their long-term performance under constant load. The breakdown for the number of columns tested is as follows:

(a)	Columns without recess	3
(b)	Columns un-repaired and with recess	3
(c)	Columns with recess and repaired with FMCX	2
(d)	Columns with recess and repaired with PFSM	2

4.2.1 COMPUTATION OF LOADS AND STRESSES FROM MEASURED STRAINS

CASE –I: COLUMNS WITHOUT RECESS

The column specimens without recess as shown schematically in Figure 3.19 were tested till failure using the procedure explained in section 3.3.5 of Chapter-3. The load applied on the specimen and the strains at different locations in the specimen were recorded and plotted against applied load. The location of strain gauges in the specimen is also shown in Figure 3.19.

The load distribution in columns without recess can be calculated using simple mechanics. The experimental data comprises of the load applied P, and the strains

measured in concrete ε_c and steel ε_s. The column specimen without recess is a composite section comprising concrete and steel.

P = Load applied on the specimen

P_c, P_s = Load taken by concrete and steel respectively

ε_c , ε_s = Axial strains measured in concrete and steel respectively

A_c, A_s = Cross-sectional area of concrete and steel respectively

E_c, E_s = Modulus of elasticity of concrete and steel respectively

$E_c = 0.85\ E_{c,exp}$, where $E_{c,exp}$ is the modulus of elasticity measured on a cylindrical specimen of concrete. Coefficient 0.85 is used to account for the difference between concrete in the column and that in a test cylinder

Let k_c, k_s = stiffness parameters of concrete and steel respectively,

where 'k_c' = A_cE_c, and 'k_s' = A_sE_s

The load applied on the specimen 'P' is the summation of load taken by concrete and steel.

$$P = P_c + P_s \qquad (1)$$

The equistrain requirements in the two elements detects the following compatibility conditions:

$$\frac{P_c}{k_c} = \frac{P_s}{k_s} \qquad (2)$$

Solving equations (1) and (2) gives the load components in concrete and steel:

$$P_c = \frac{k_c P}{k_c + k_s} \tag{3}$$

$$P_s = \frac{k_s P}{k_c + k_s} \tag{4}$$

From the measured strains ε_c and ε_s the load components in Concrete P_c and steel P_s can be obtained by multiplying the strains with the modulus of elasticity E_c and E_s respectively.

$$P_c = \varepsilon_c E_c \tag{5}$$

$$P_s = \varepsilon_s E_s \tag{6}$$

The total load on the specimen 'P' is the summation of loads taken by concrete and steel.

$$P = \varepsilon_c E_c + \varepsilon_s E_s \tag{7}$$

CASE –II: COLUMNS WITH RECESS

The column specimens with recess as shown schematically in Figure 3.20 were tested till failure using the procedure explained in section 3.3.5 of Chapter-3. The load applied on the specimen and the strains at different locations in the specimen were recorded and plotted against applied load. The location of strain gauges in the specimen is also shown in Figure 3.20.

The load distribution in columns with recess can be calculated using simple mechanics. The experimental data comprises of the load applied P, and the strains measured in concrete ε_c, steel in concrete ε_{sc} and steel exposed in recess ε_{se}. The column specimen with recess is a composite section comprising concrete and steel.

P = Load applied on the specimen

P_c, P_{sc}, P_{se} = Load taken by concrete, steel in concrete and steel exposed in recess

ε_c , ε_{sc}, ε_{se} = Axial strains measured in concrete, steel in concrete and steel exposed

A_c, A_{sc}, A_{se} = Cross-sectional area of concrete, steel in concrete and steel exposed

E_c, E_s = Modulus of elasticity of concrete and steel respectively

$E_c = 0.85\ E_{c,exp}$, where $E_{c,exp}$ is the modulus of elasticity measured on a cylindrical specimen of concrete. Coefficient 0.85 is used to account for the difference between concrete in the column and that in a test cylinder

Let k_c, k_{sc}, k_{se} = stiffness parameters of concrete, steel in concrete and steel exposed respectively,

where 'k_c' = A_cE_c ; 'k_{sc}' = $A_{sc}E_s$, and 'k_{se}' = $A_{se}E_s$

The load applied on the specimen 'P' is the summation of load taken by concrete, steel in concrete and steel exposed.

$$P = P_c + P_{sc} + P_{se} \qquad (1)$$

The equistrain requirements in the three elements detects the following compatibility conditions:

$$\frac{P_c}{k_c} = \frac{P_{sc}}{k_{sc}} = \frac{P_{se}}{k_{se}} \qquad (2)$$

Solving equations (1) and (2) gives the load components in concrete, steel in concrete and steel exposed in recess:

$$P_c = \frac{k_c P}{k_c + k_{sc} + k_{se}} \qquad (3)$$

$$P_{sc} = \frac{k_{sc} P}{k_c + k_{sc} + k_{se}} \qquad (4)$$

$$P_{se} = \frac{k_{se} P}{k_c + k_{sc} + k_{se}} \qquad (5)$$

From the measured strains ε_c, ε_{sc} and ε_{se} the load components in Concrete P_c, steel in concrete P_{sc} and steel exposed P_{se} can be obtained by multiplying the strains with the modulus of elasticity E_c and E_s respectively.

$$P_c = \varepsilon_c E_c \qquad (6)$$

$$P_{sc} = \varepsilon_{sc} E_s \qquad (7)$$

$$P_{se} = \varepsilon_{se} E_s \qquad (8)$$

The total load on the specimen 'P' is the summation of loads taken by concrete, steel in concrete and steel exposed.

$$P = \varepsilon_c E_c + \varepsilon_{sc} E_s + \varepsilon_{se} E_s \qquad (9)$$

CASE –III: REPAIRED COLUMNS

The column specimens with recess and repaired as shown schematically in Figure 3.21 were tested till failure using the procedure explained in section 3.3.5 of Chapter-3. The load applied on the specimen and the strains at different locations in the specimen were recorded and plotted against applied load. The location of strain gauges in the specimen is also shown in Figure 3.21.

The load distribution in repaired columns can also be calculated using simple mechanics. The experimental data comprises of the load applied P, and the strains measured in concrete ε_c, steel in concrete ε_{sc}, steel in repair ε_{se}, and repair mortar ε_r. The column specimen with recess is a composite section comprising concrete, steel and repair.

P = Load applied on the specimen

P_c, P_{sc}, P_{sr}, P_r = Load taken by concrete, steel in concrete, steel in repair and repair mortar respectively

ε_c , ε_{sc}, ε_{sr}, ε_r = Axial strains measured in concrete, steel in concrete, steel in repair and repair mortar respectively

A_c, A_{sc}, A_{sr}, A_r = Cross-sectional area of concrete, steel in concrete, steel in repair and repair mortar respectively

E_c, E_s, E_r = Modulus of elasticity of concrete, steel and repair mortar respectively

$E_c = 0.85\ E_{c,exp}$, and $E_r = 0.85\ E_{r,exp}$ where, $E_{c,exp}$ and $E_{r,exp}$ is the modulus of elasticity measured on a cylindrical specimen of concrete and repair

respectively. Coefficient 0.85 is used to account for the difference between concrete in the column and that in a test cylinder

Let k_c, k_{sc}, k_{sr}, k_r = stiffness parameters of concrete, steel in concrete, steel in repair and repair mortar respectively,

where 'k_c' = A_cE_c ; 'k_{sc}' = $A_{sc}E_s$; 'k_{sr}' = $A_{sr}E_s$; and 'k_r' = A_rE_r

The load applied on the specimen 'P' is the summation of load taken by concrete, steel in concrete, steel in repair and repair mortar.

$$P = P_c + P_{sc} + P_{sr} + P_r \qquad (1)$$

The equistrain requirements in the four elements detects the following compatibility conditions:

$$\frac{P_c}{k_c} = \frac{P_{sc}}{k_{sc}} = \frac{P_{sr}}{k_{sr}} = \frac{P_r}{k_r} \qquad (2)$$

Solving equations (1) and (2) gives the load components in concrete, steel in concrete, steel in repair and repair mortar:

$$P_c = \frac{k_c P}{k_c + k_{sc} + k_{sr} + k_r} \qquad (3)$$

$$P_{sc} = \frac{k_{sc} P}{k_c + k_{sc} + k_{sr} + k_r} \qquad (4)$$

$$P_{sr} = \frac{k_{sr} P}{k_c + k_{sc} + k_{sr} + k_r} \qquad (5)$$

$$P_r = \frac{k_r P}{k_c + k_{sc} + k_{sr} + k_r} \qquad (6)$$

From the measured strains ε_c, ε_{sc}, ε_{sr} and ε_r the load components in Concrete P_c, steel in concrete P_{sc}, steel in repair P_{sr} and repair mortar P_r can be obtained by multiplying the strains with the modulus of elasticity E_c, E_s and E_r respectively.

$$P_c = \varepsilon_c E_c \tag{7}$$

$$P_{sc} = \varepsilon_{sc} E_s \tag{8}$$

$$P_{sr} = \varepsilon_{sr} E_s \tag{9}$$

$$P_r = \varepsilon_r E_r \tag{10}$$

The total load on the specimen 'P' is the summation of loads taken by concrete and steel.

$$P = \varepsilon_c E_c + \varepsilon_{sc} E_s + \varepsilon_{sr} E_s + \varepsilon_r E_r \tag{11}$$

4.2.2 COLUMNS WITHOUT RECESS

The data recorded during the testing process was sorted out and some of the data that showed a deviation of more than 10% from the average value was discarded. Only the selected data from the experiment are shown in Figures 4.20 to 4.24.

The measured strains inside concrete ε_c and in steel ε_s were taken to be the average of all similar strains recorded at that location in different specimens. The obtained strains were substituted in the equations (5) and (6) shown in section 4.2.1 for case-I, to calculate the load components of concrete P_c and steel P_s. The total load 'P' coming on the column specimen was calculated by summing up the loads coming on concrete and steel. The applied load and the calculated load was compared and plotted against measured strains as shown in Figures 4.25 and 4.26 at two different locations in a column specimen.

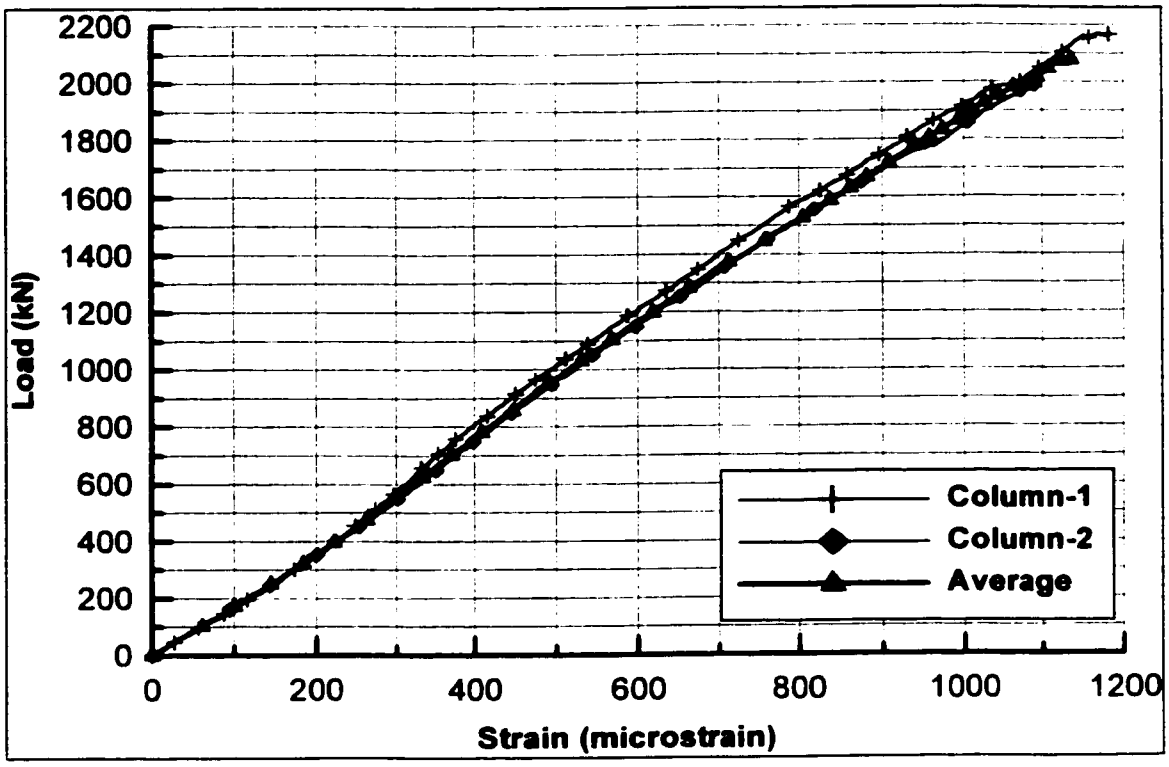

Figure 4.20: Load-strain curves in concrete at center and at 400 mm from top of Column (1E)

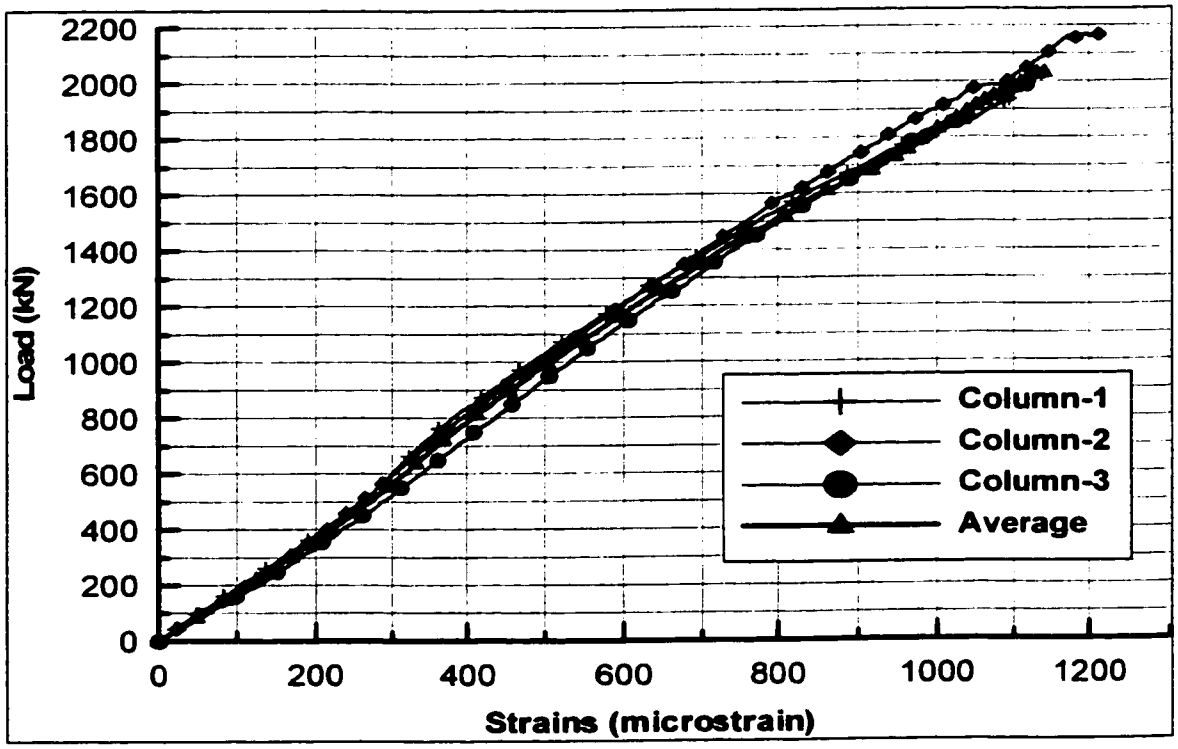

Figure 4.21: Load-strain curves in concrete at center and at mid-height of column (2E)

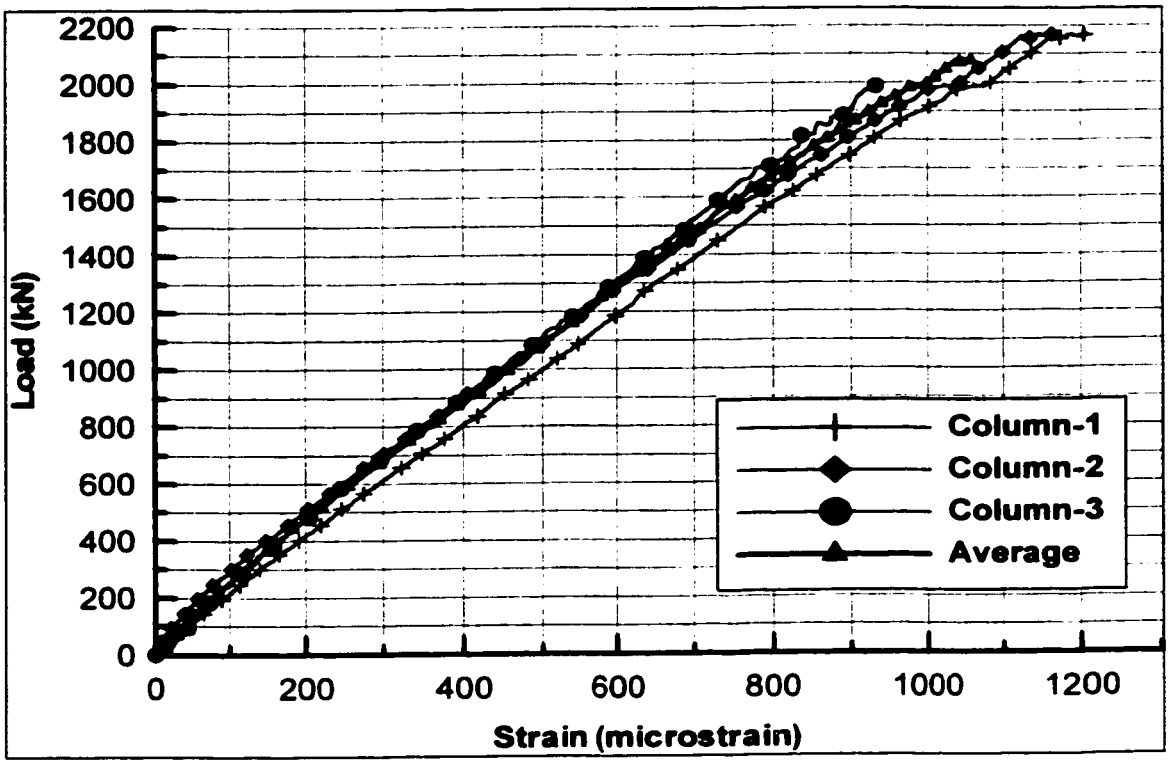

Figure 4.22: Load-strain curves in steel at mid-height of column (1B & 2B)

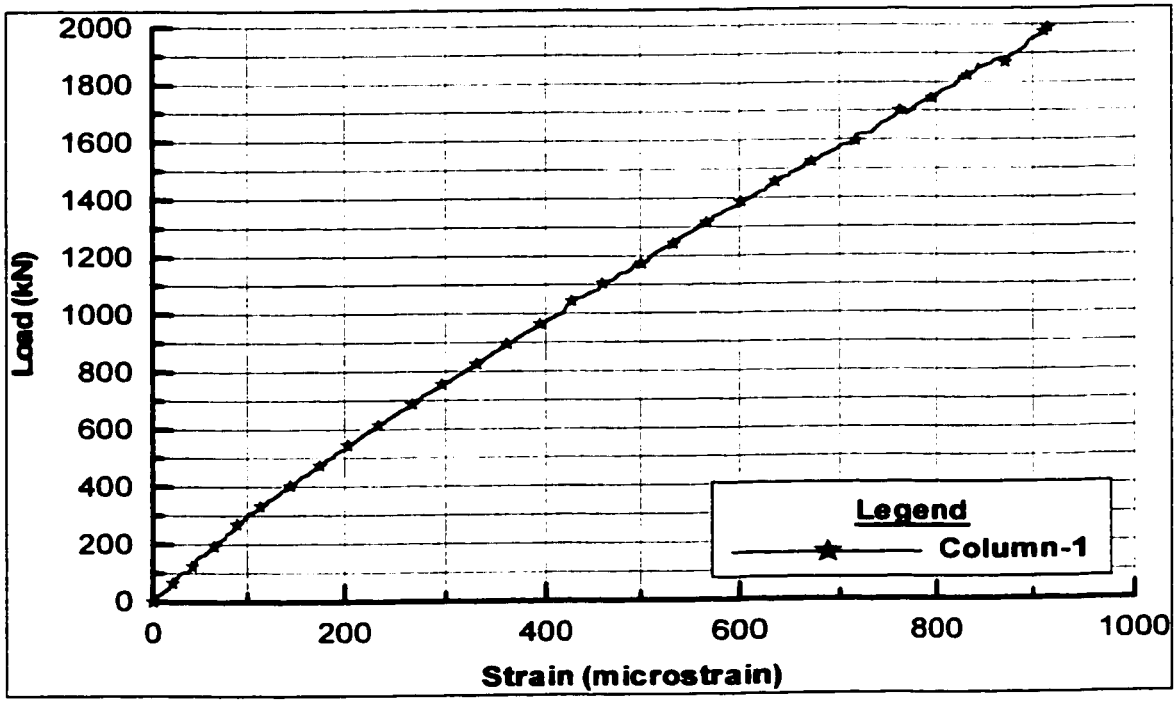

Figure 4.23: Load-strain curves in steel at 400 mm from top of column (3B)

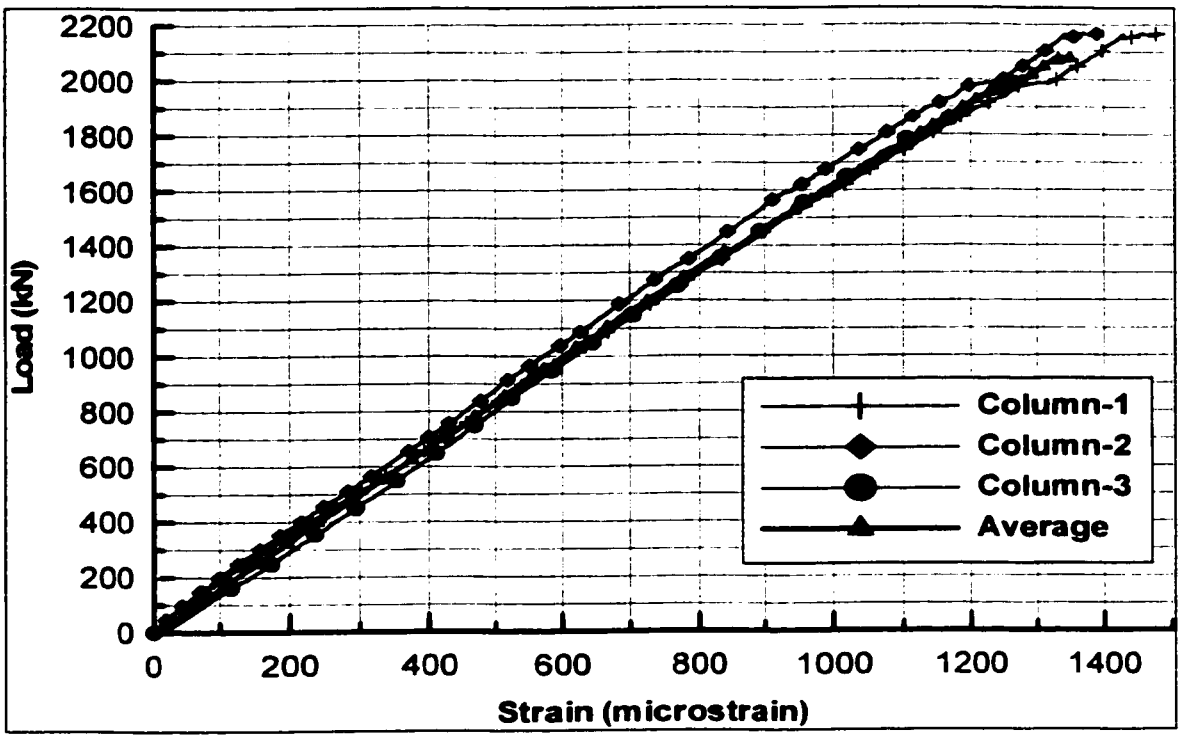

Figure 4.24: Load-strain curves on surface of concrete at center and at mid-height of column (1&2S)

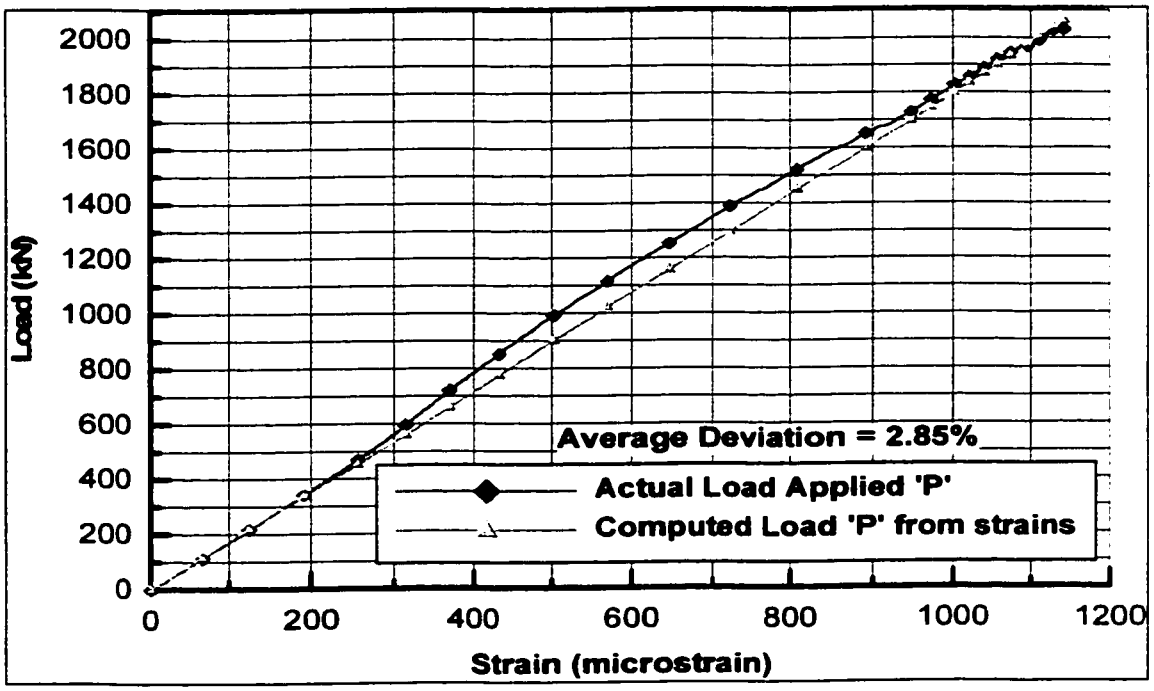

Figure 4.25: Comparison of Actual load applied and Computed load plotted against strains measured at mid-height of column specimen

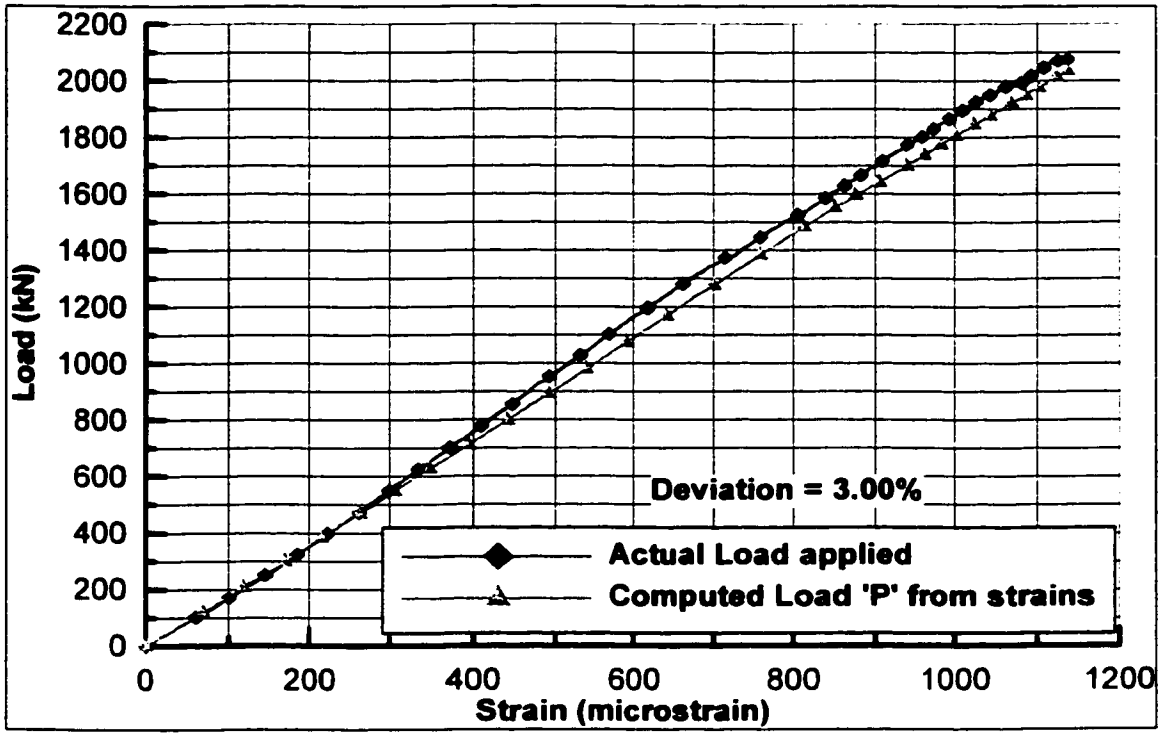

Figure 4.26: Comparison of Actual load applied and Computed load plotted against strains measured at 400 mm from top of column specimen

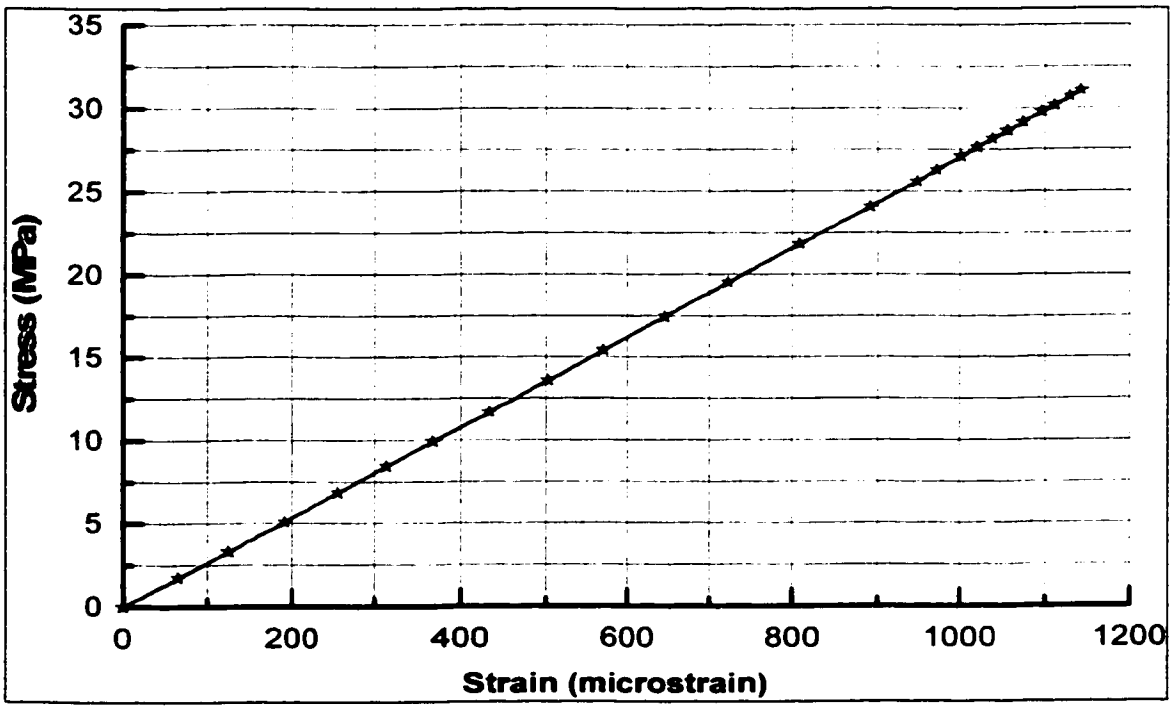

Figure 4.27: Stress-strain curve for concrete at center and at mid-height of column specimen without recess

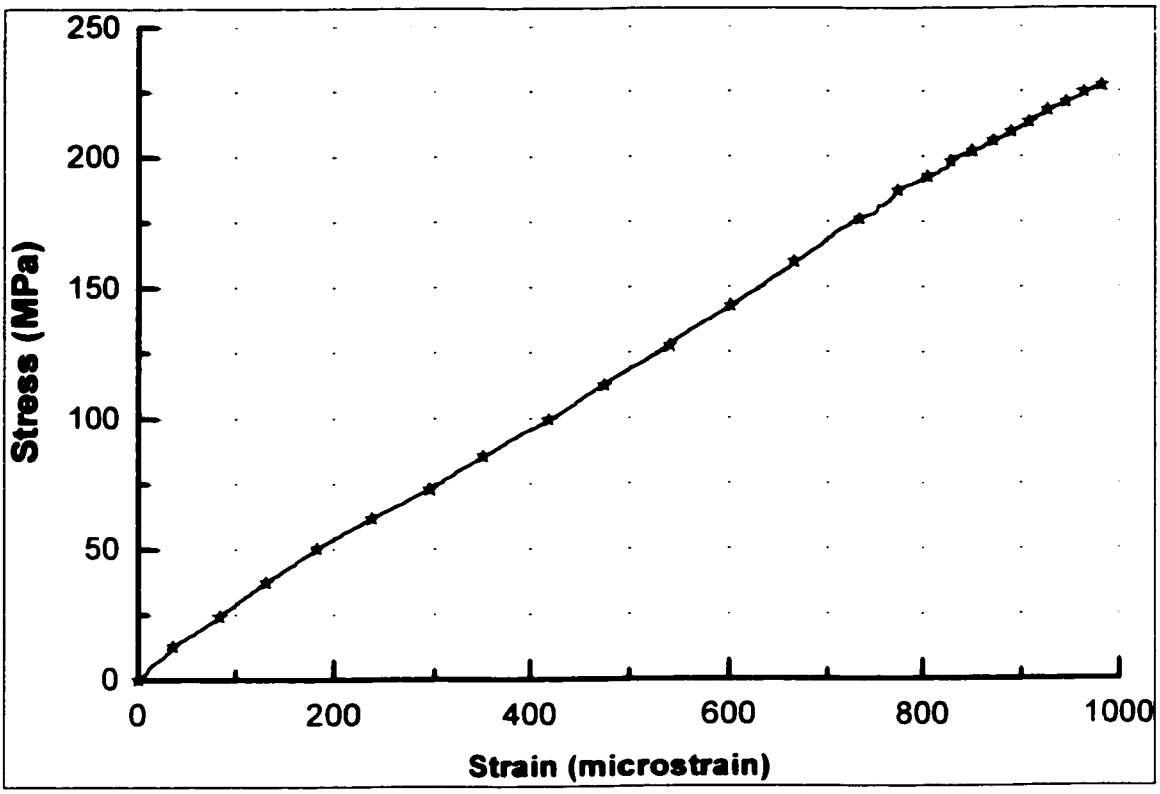

Figure 4.28: Stress-strain curve for steel at mid-height of column specimen without recess

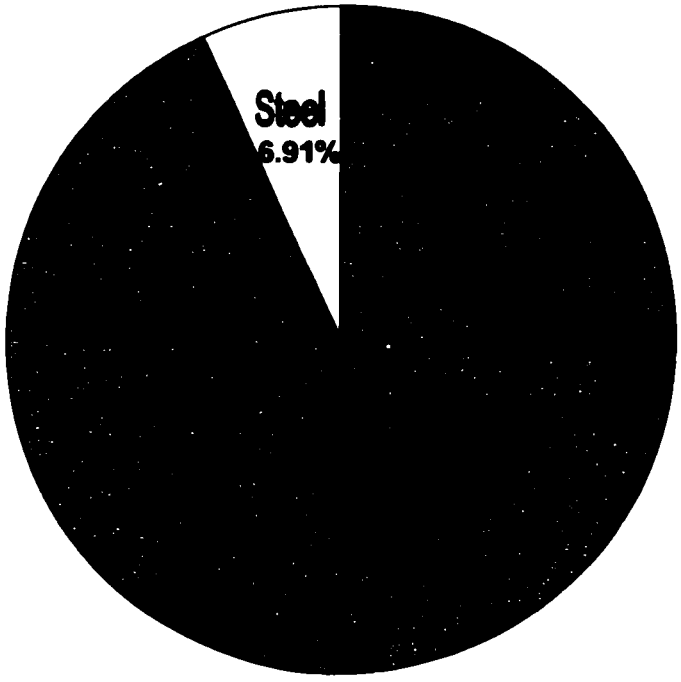

Figure 4.29: Load distribution between concrete and steel in columns without recess

The deviation of calculated values of load from the applied load was also calculated. Figure 4.29 shows the percentages of loads taken by concrete and steel. The components of load P_c and P_s were divided by their area of cross section to obtain the stresses in concrete and steel respectively. The stress-strain curves for concrete and steel are plotted in Figures 4.27 and 4.28 respectively. The deviation of calculated values of load from the applied loads as shown in Figures 4.25 and 4.26 are 2.85% and 3.00% at mid-height and at 400 mm from the top of the column specimen. Figure 4.29 shows the load distribution between concrete and steel in the column specimens. Concrete, which has 99% of the cross-sectional area takes about 93.09% of the total calculated load whereas the steel, which is only 1% of the cross-sectional area, takes 6.91% of the total calculated load.

Figures 4.30 and 4.31 show the failure mode of the column specimen tested. The specimen fails at the ends due to crushing of concrete, which is attributed due to stress concentration at these locations. The concrete at these locations has reached its crushing strength but the concrete in the remaining portion has not yet reached its crushing strength.

Figure 4.27 shows the stress-strain curve for concrete at mid-height of the column specimen, which varies linearly till it reaches a stress level of 33 MPa before failure of the specimen at its end. The concrete at this location did not reach its ultimate crushing strength of $0.85f_c'$ (45 MPa).

Figure 4.28 shows the stress-strain curve for steel at mid-height of the column specimen, which varies linearly till it reaches a stress level of 230 MPa before failure of the specimen. The steel at this location has not yet reached its yield stress of 415 MPa.

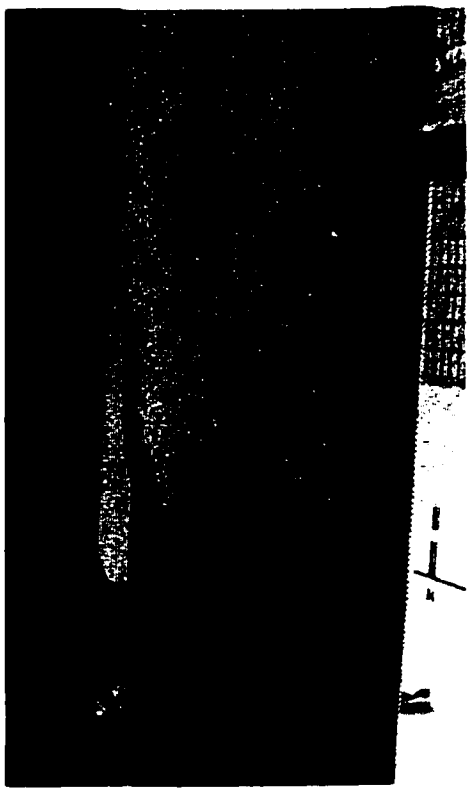

Figure 4.30: Failure of column without recess due to crushing of concrete at end

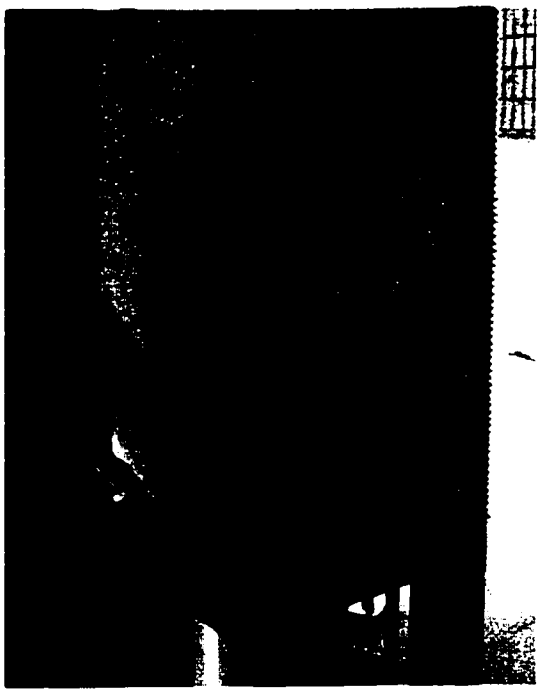

Figure 4.31: Close-up view of failure of column specimen without recess

4.2.3 COLUMNS WITH RECESS

The data recorded during the testing process was sorted out and some of the data that showed a deviation of more than 10% from the average value was discarded. Only the selected data from the experiment are shown in Figures 4.32 to 4.37.

The measured strains inside concrete ε_c, in steel in concrete ε_{sc} and steel exposed ε_{se} were taken to be the average of all similar strains recorded at that location in different specimens. The obtained strains were substituted in (6), (7) and (8) shown in section 4.2.1 for case-II, to calculate the load distribution between concrete P_c, steel in concrete P_{sc} and steel exposed P_{se}. The total load 'P' coming on the column specimen was calculated by summing up the loads coming on concrete, steel in concrete and steel exposed. The applied load and the calculated load was compared and plotted against measured strains as shown in Figures 4.38 and 4.39 at two different locations in a column specimen. The deviation of calculated values of load from the applied load was also calculated.

Figures 4.42 and 4.43 show the percentages of loads taken by concrete and steel. The components of load P_c, P_{sc} and P_{se} were divided by their area of cross section to obtain the stresses in concrete and steel respectively. The stress-strain curves for concrete and steel are plotted in Figures 4.40 and 4.41 respectively.

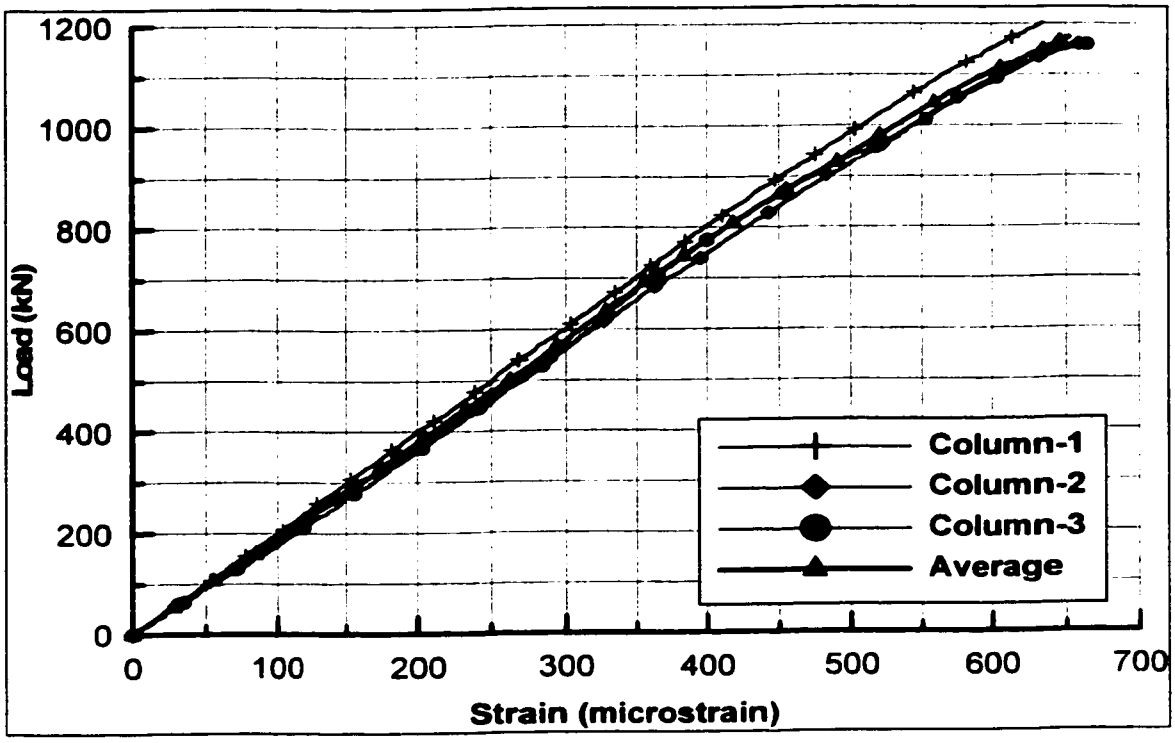

Figure 4.32: Load-strain curves in concrete at center and at 400 mm from top of Column (1E)

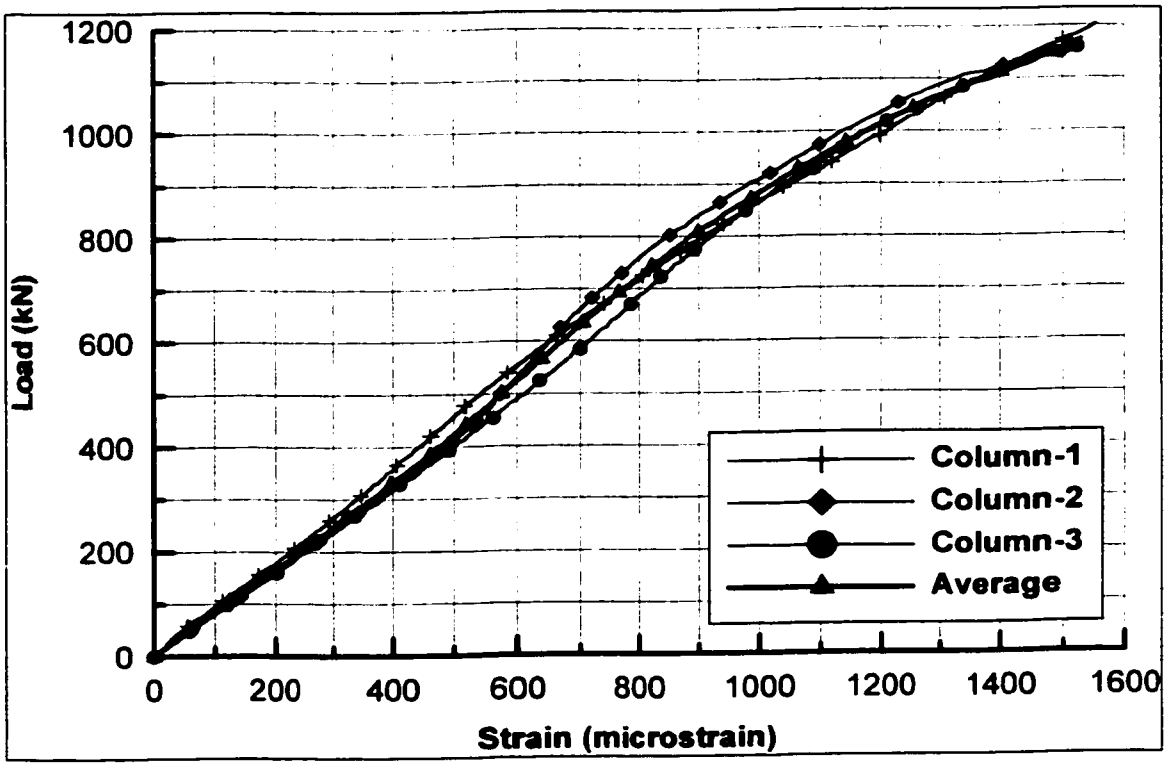

Figure 4.33: Load-strain curves in concrete at center and at mid-height of column (2E)

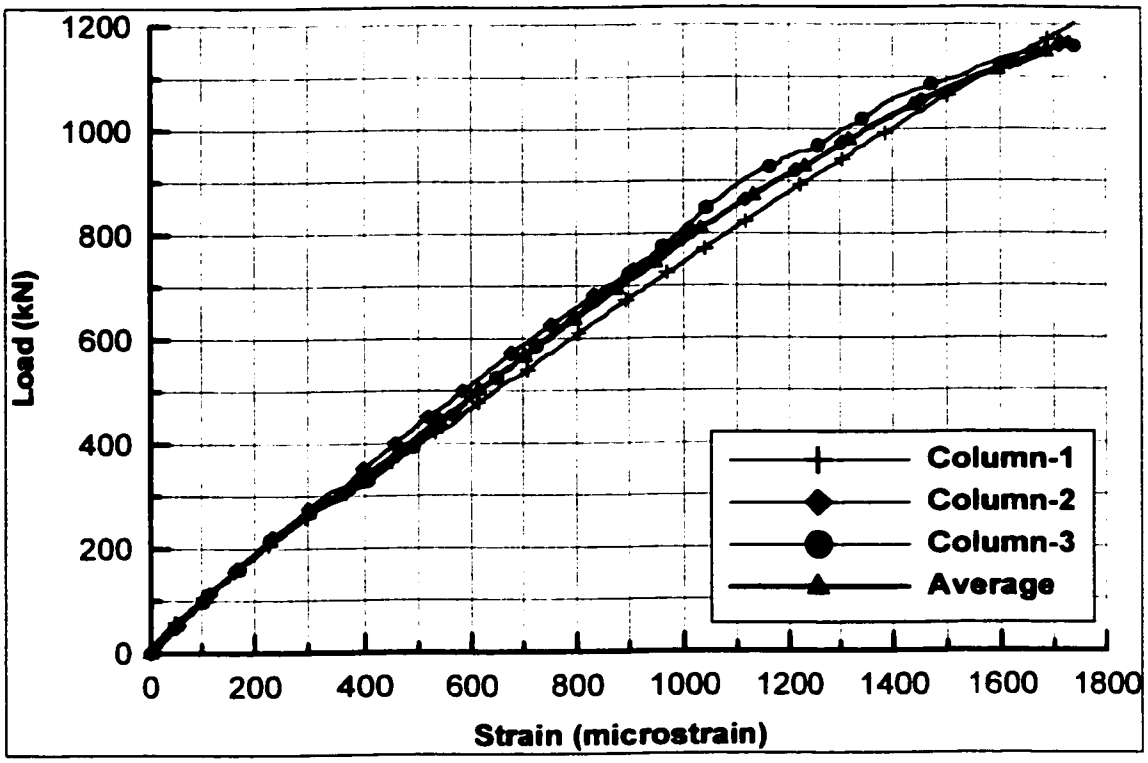

Figure 4.34: Load-strain curves in steel exposed in recess and at mid-height of column (1B)

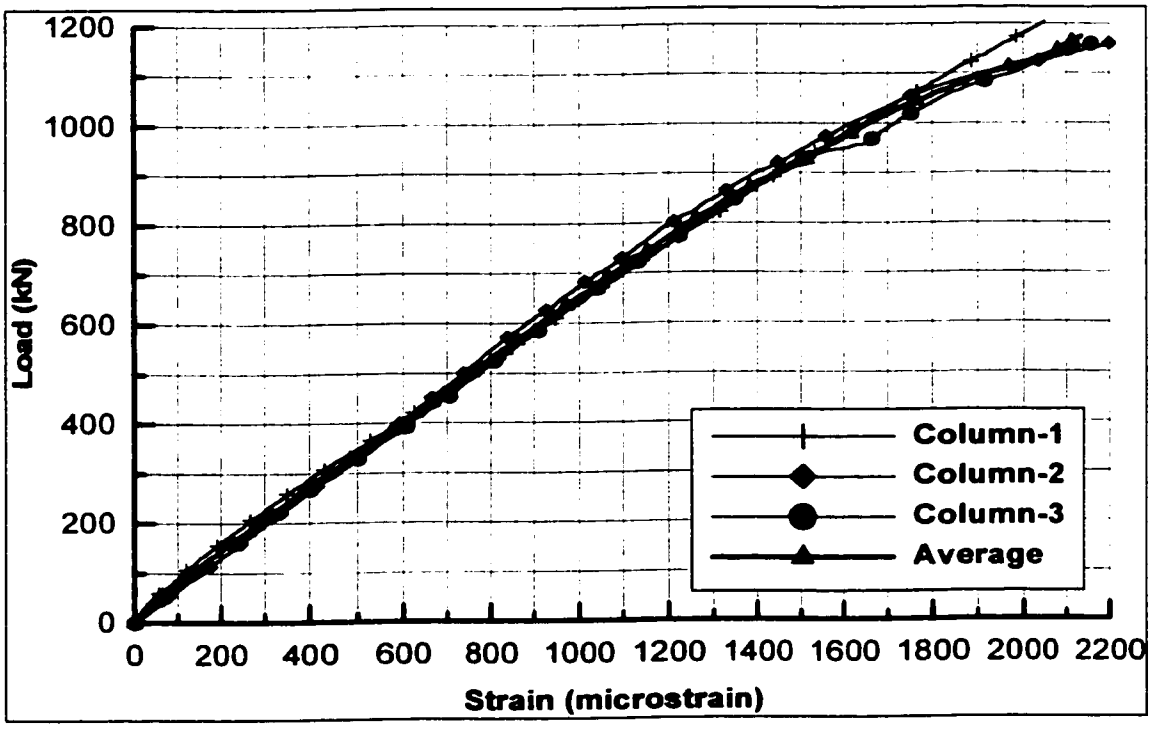

Figure 4.35: Load-strain curves in steel in concrete and at mid-height of column (2B)

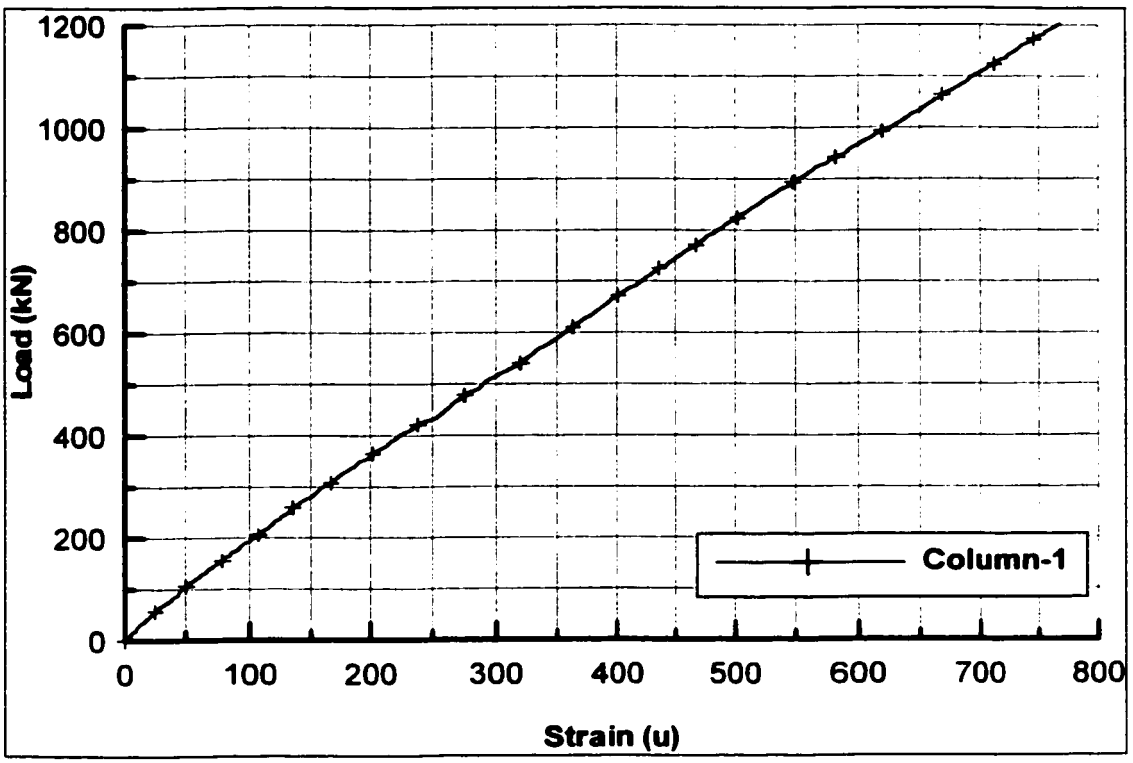

Figure 4.36: Load-strain curves in steel at 400 mm from top of column (3B)

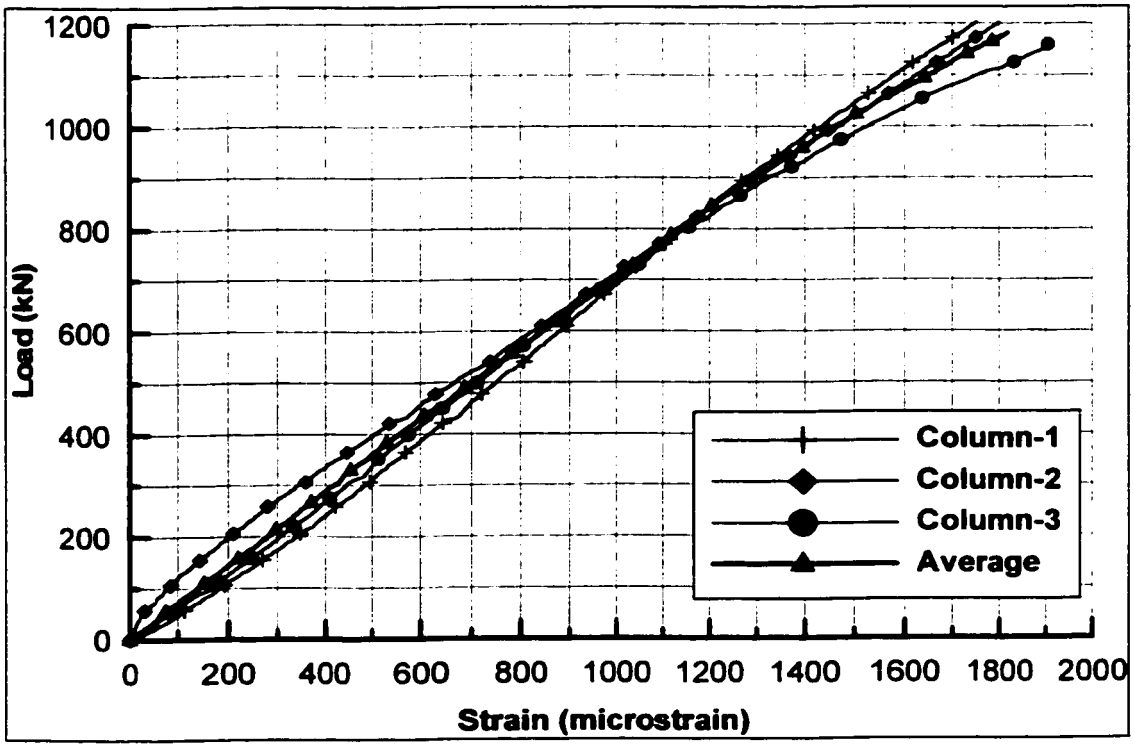

Figure 4.37: Load-strain curves on surface of concrete at center and at mid-height of column (1&2S)

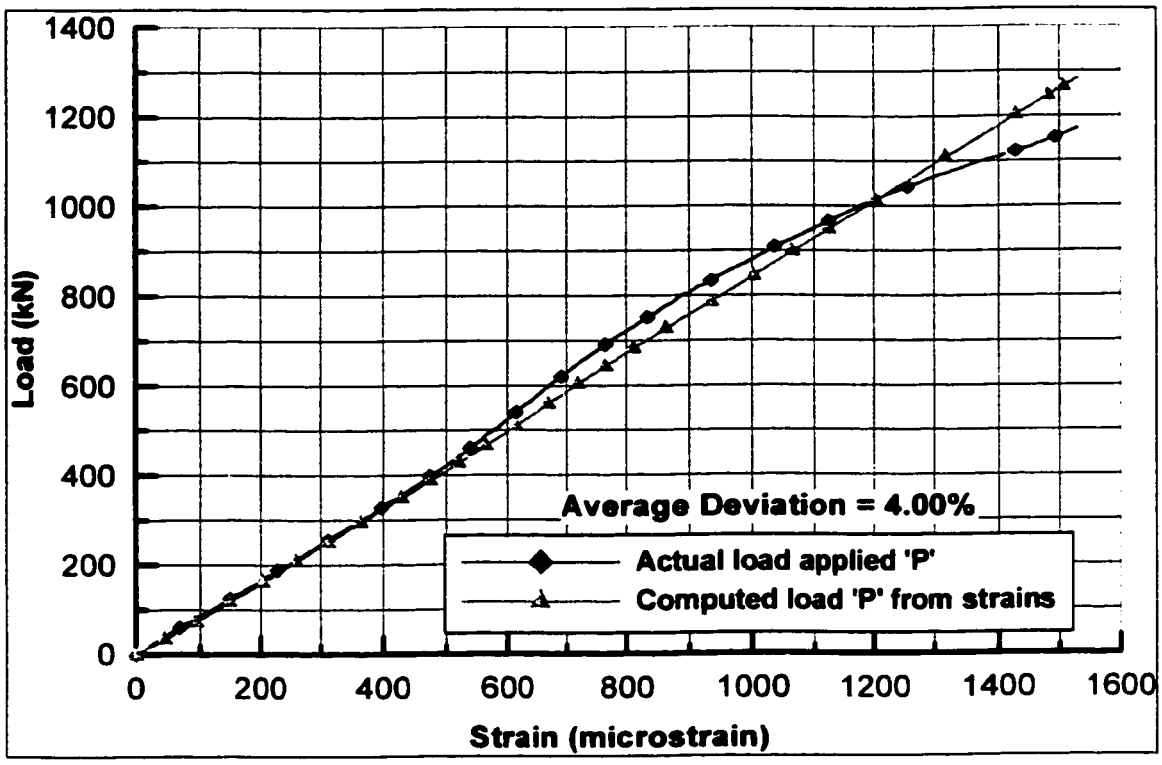

Figure 4.38: Comparison of Actual load applied and Computed load plotted against strains measured at mid-height of column specimen with recess

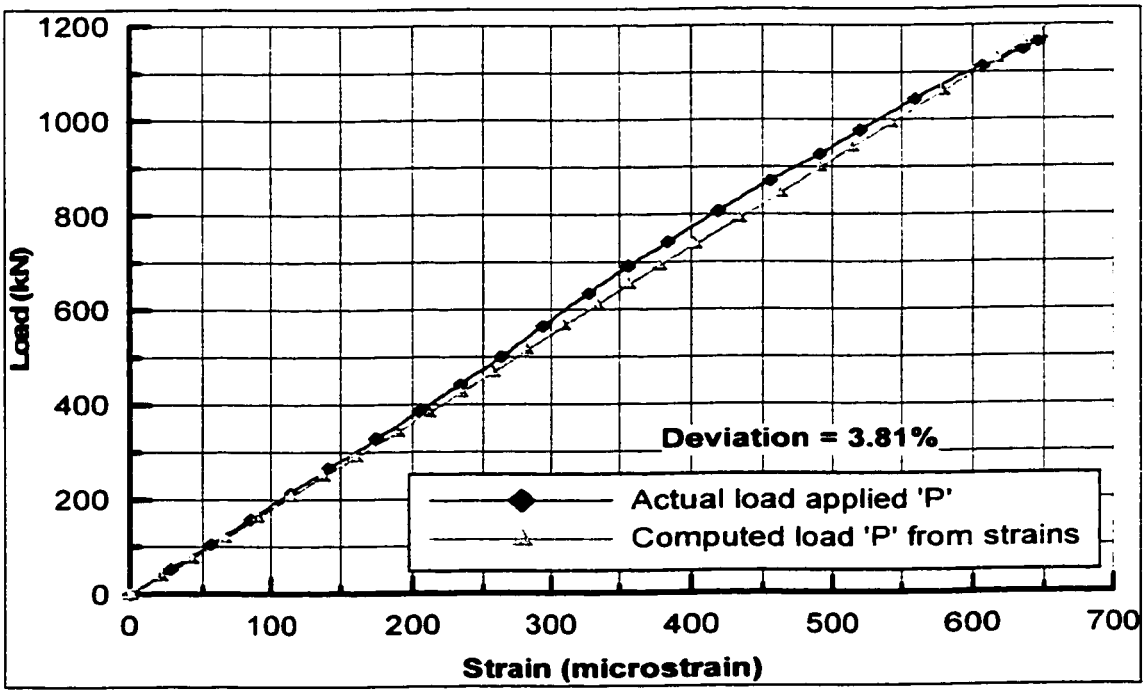

Figure 4.39: Comparison of Actual load applied and Computed load plotted against strains measured at 400 mm from top of column specimen with recess

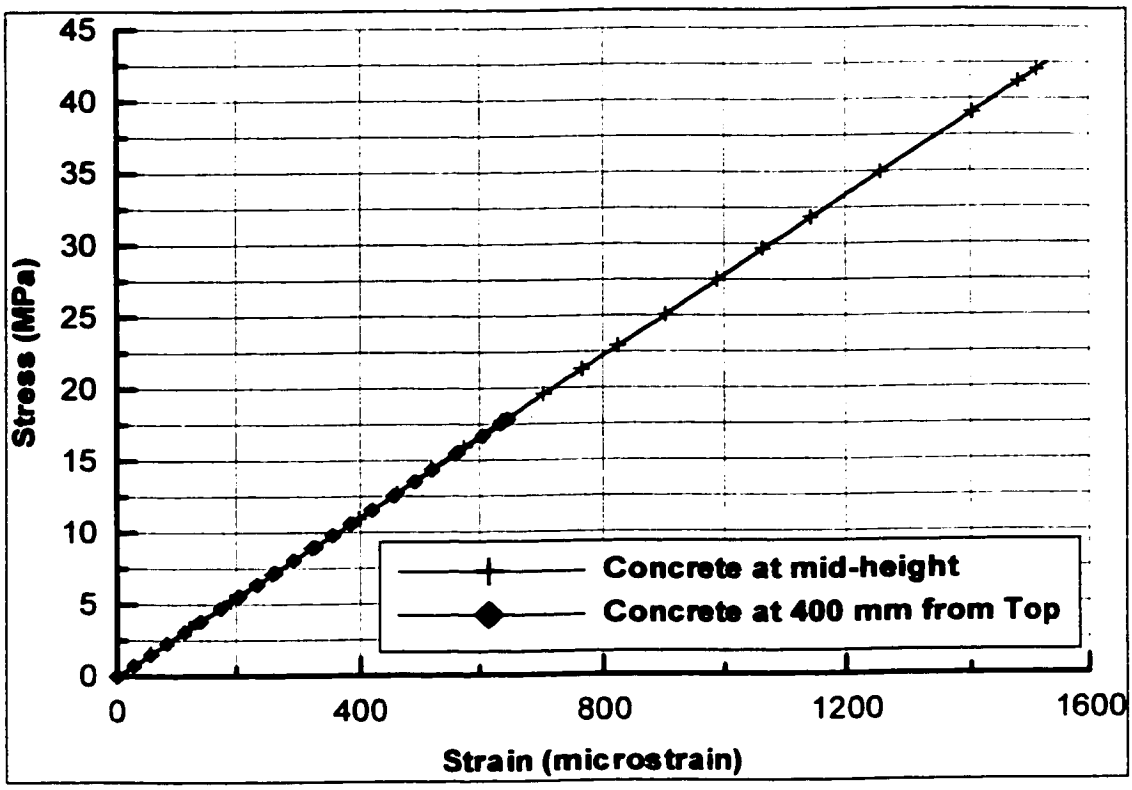

Figure 4.40: Stress-strain curve for concrete at mid-height and at 400 mm from top of column specimen with recess

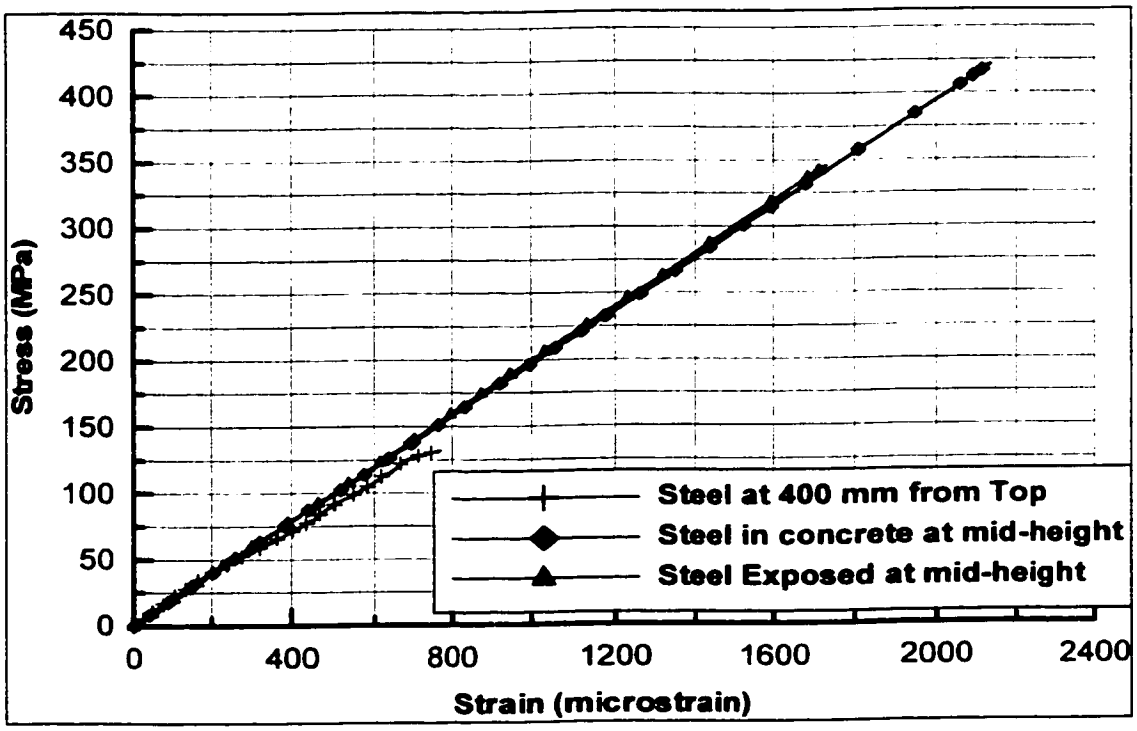

Figure 4.41: Stress-strain curve for steel in column specimen without recess

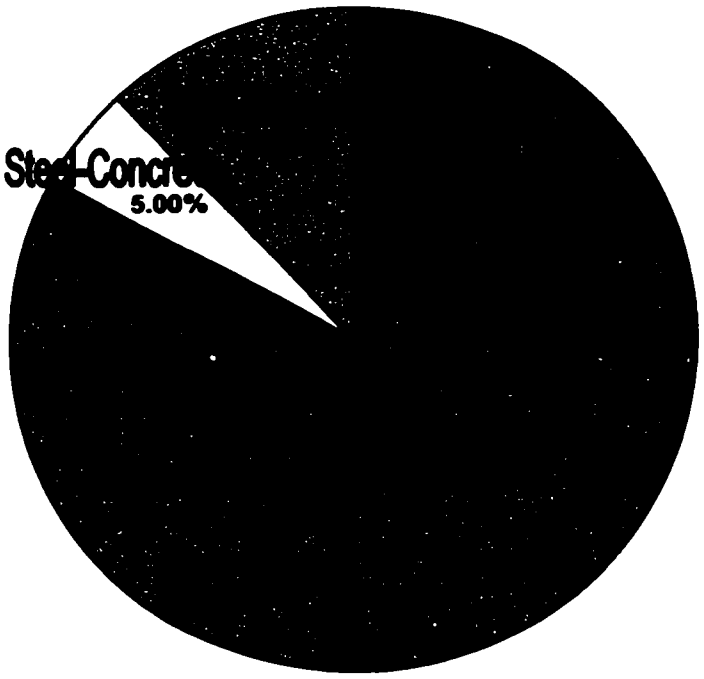

Figure 4.42: Load distribution between concrete and steel at mid-height in columns with recess

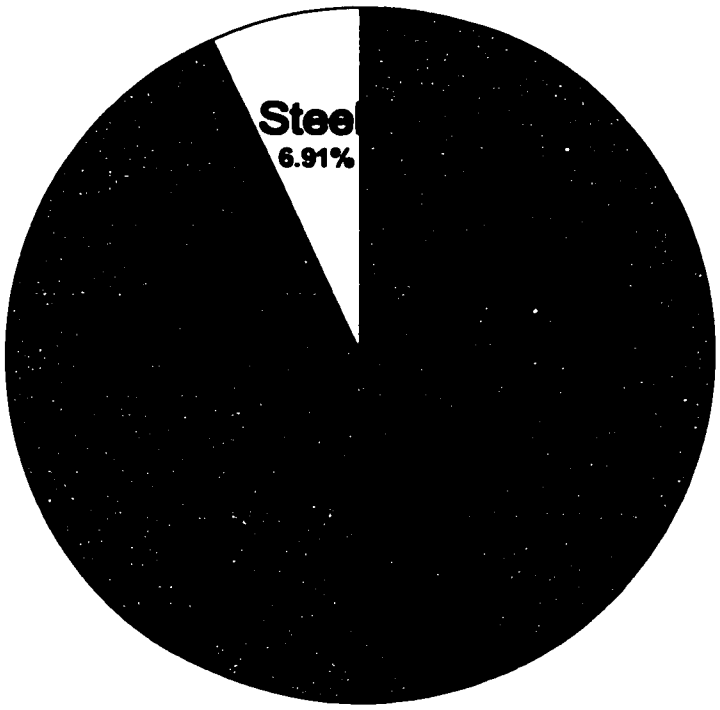

Figure 4.43: Load distribution between concrete and steel at 400 mm from top in columns with recess

The deviation of calculated values of load from the applied loads as shown in Figures 4.38 and 4.39 are 4.00% and 3.81% at mid-height and at 400 mm from the top of the column specimen. Figure 4.42 shows the load distribution between concrete and steel in the column specimens. Concrete core, which has 40% of the cross-sectional area remaining takes about 82.94% of the total calculated load whereas the steel in concrete, which is only 0.25% of the cross-sectional area, takes 5.00% of the total calculated load and the steel exposed in the recess, which is 0.75% of the cross-sectional area, takes 12.06% of the total calculated load. The steel inside concrete core is taking more load than the steel exposed in the recess.

Figure 4.43 shows the load distribution between concrete and steel in the column specimens at 400 mm from top. Concrete, which has 99% of the cross-sectional area takes about 93.09% of the total calculated load whereas the steel, which is only 1% of the cross-sectional area, takes 6.91% of the total calculated load.

Figures 4.44 and 4.45 show the failure mode of the column specimen tested. The specimen fails at the mid-height by buckling of steel and crushing of concrete by shear. The concrete at this location has reached its crushing strength and the steel has also reached its yielding strength.

Figure 4.40 shows the stress-strain curve for concrete at mid-height and at 400 mm from top of the column specimen. The stress at mid-height in the concrete core varies linearly till it reaches a stress level of 43 MPa before failure of the specimen. The concrete has almost reached its crushing strength of $0.85f_c'$ (45 MPa). The stress at 400 mm from top varies linearly till it reaches a stress level of 18 MPa before failure of the specimen. The concrete at this location did not reach its ultimate crushing strength of 45 MPa.

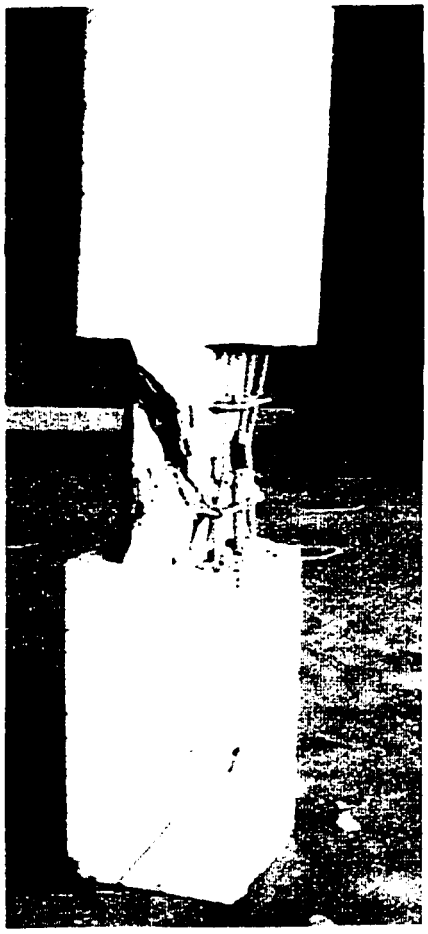

Figure 4.44: Failure of column specimen with recess

Figure 4.45: Close-up view of failure of column specimen with recess

Figure 4.41 shows the stress-strain curve for steel at mid-height and at 400 mm from top of the column specimen. The stress at mid-height in steel inside concrete varies linearly till it reaches a stress level of 420 MPa at failure of the specimen. The steel has reached its yielding strength at failure. The stress at mid-height in steel exposed in recess varies linearly till it reaches a stress level of 350 MPa. The steel at this location has not yet reached its yield stress of 415 MPa. The stress at 400 mm from top of column varies linearly till it reaches a stress level of 130 MPa. The steel at this location has not yet reached its yield stress of 415 MPa.

It can be concluded that the steel in concrete core and the concrete have reached their failure stresses at the point of failure of the specimen.

4.2.4 COLUMNS REPAIRED WITH FMCX

The column specimens with recess and repaired with FMCX as shown schematically in Figure 3.21 were tested till failure using the procedure explained in section 3.3.5 of Chapter-3. The load applied on the specimen and the strains at different locations in the specimen were recorded and plotted against applied load. The location of strain gauges in the specimen is also shown in Figure 3.21.

The data recorded during the testing process was sorted out and some of the data that showed a deviation of more than 10% from the average value was discarded. Only the selected data from the experiment are shown in Figures 4.46 to 4.53.

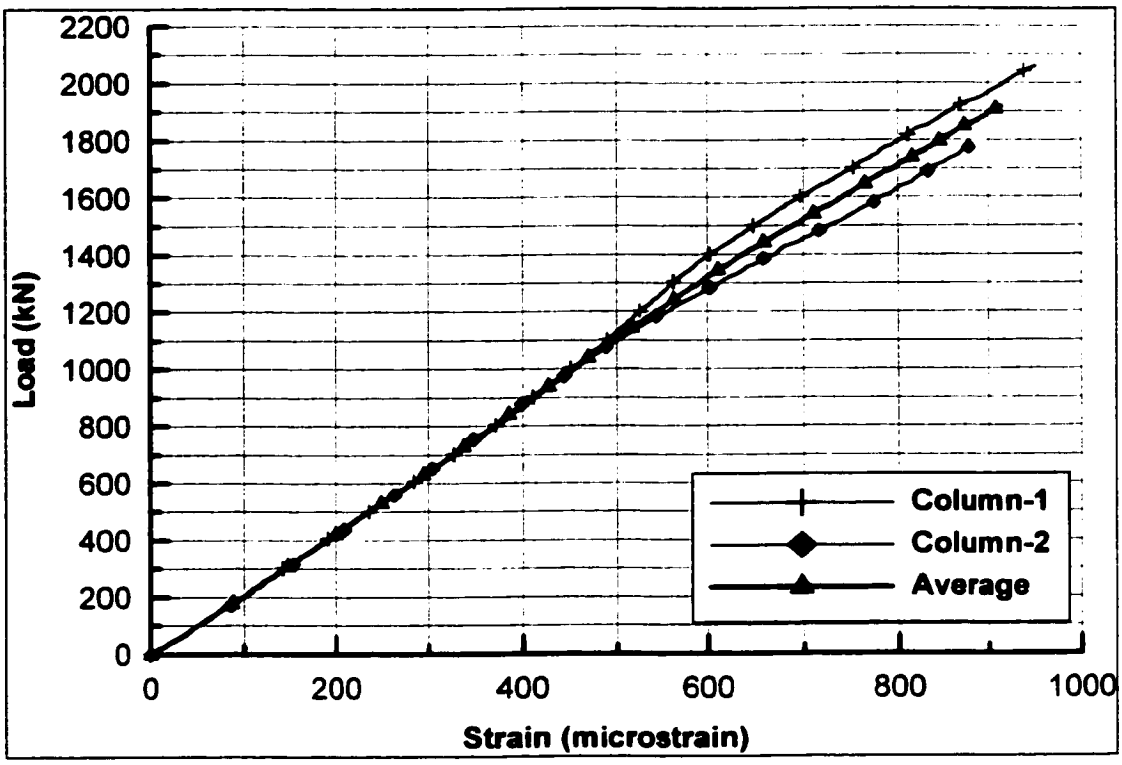

Figure 4.46: Load-strain curves in concrete at center and at 400 mm from top of Column (1E)

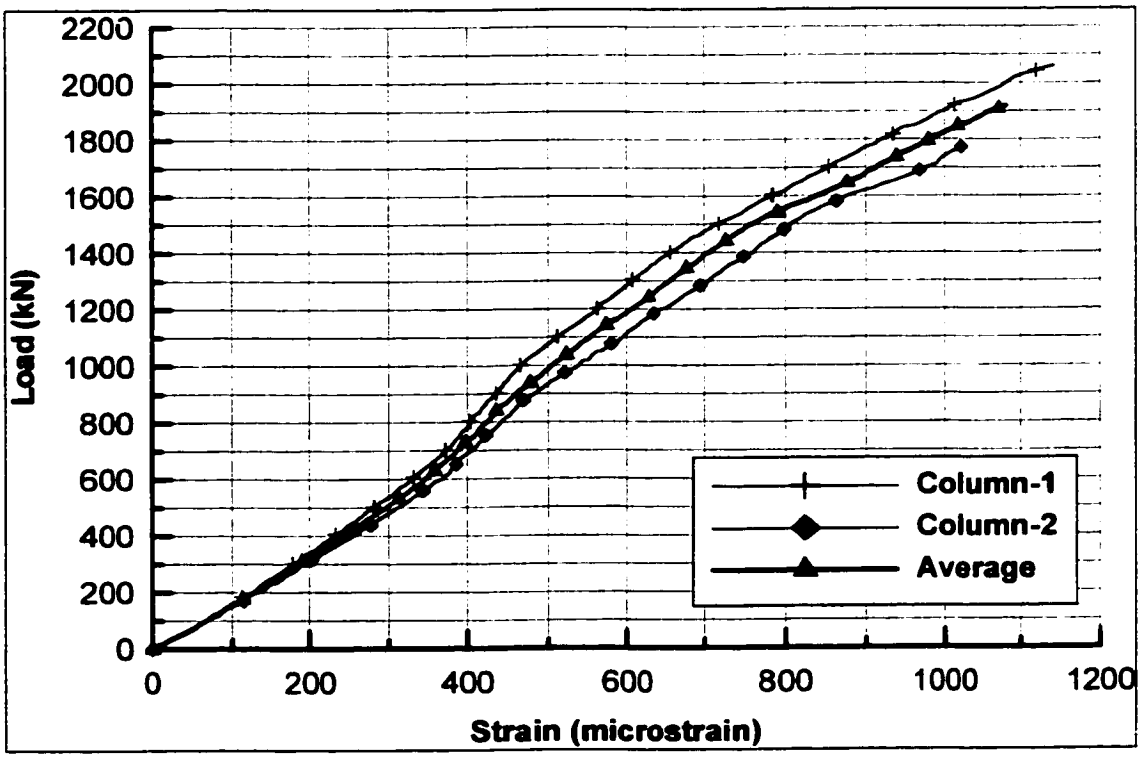

Figure 4.47: Load-strain curves in concrete at center and at mid-height of column (2E)

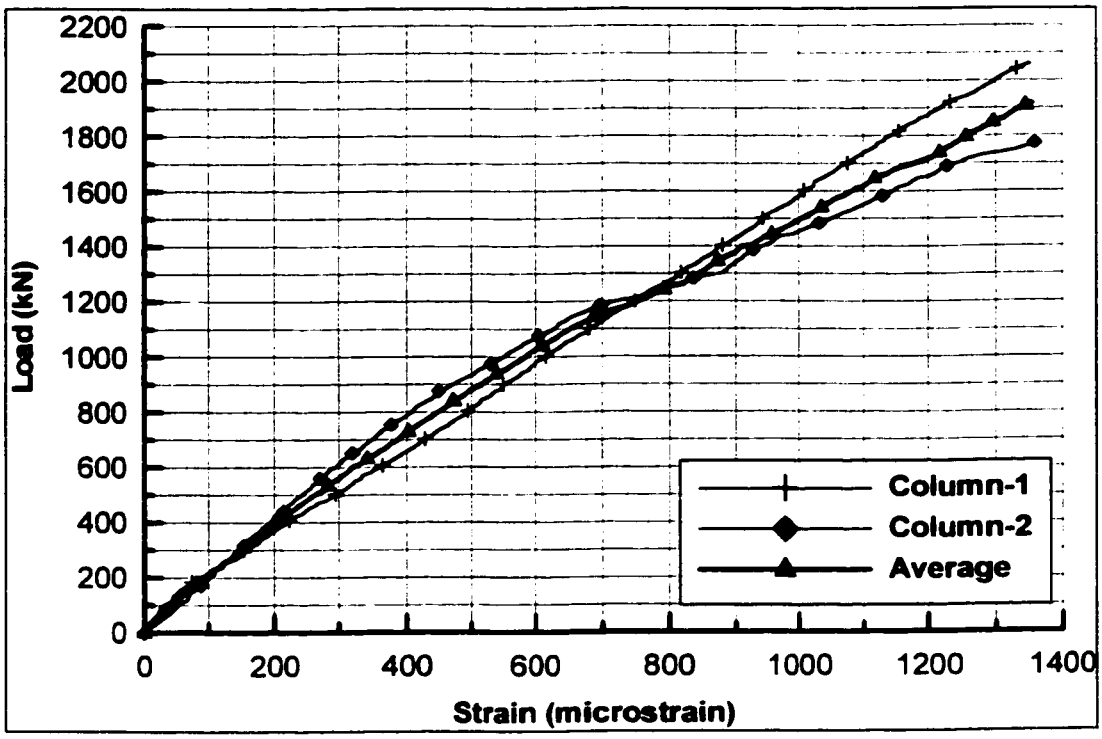

Figure 4.48: Load-strain curves in steel exposed in recess and at mid-height of column (1B)

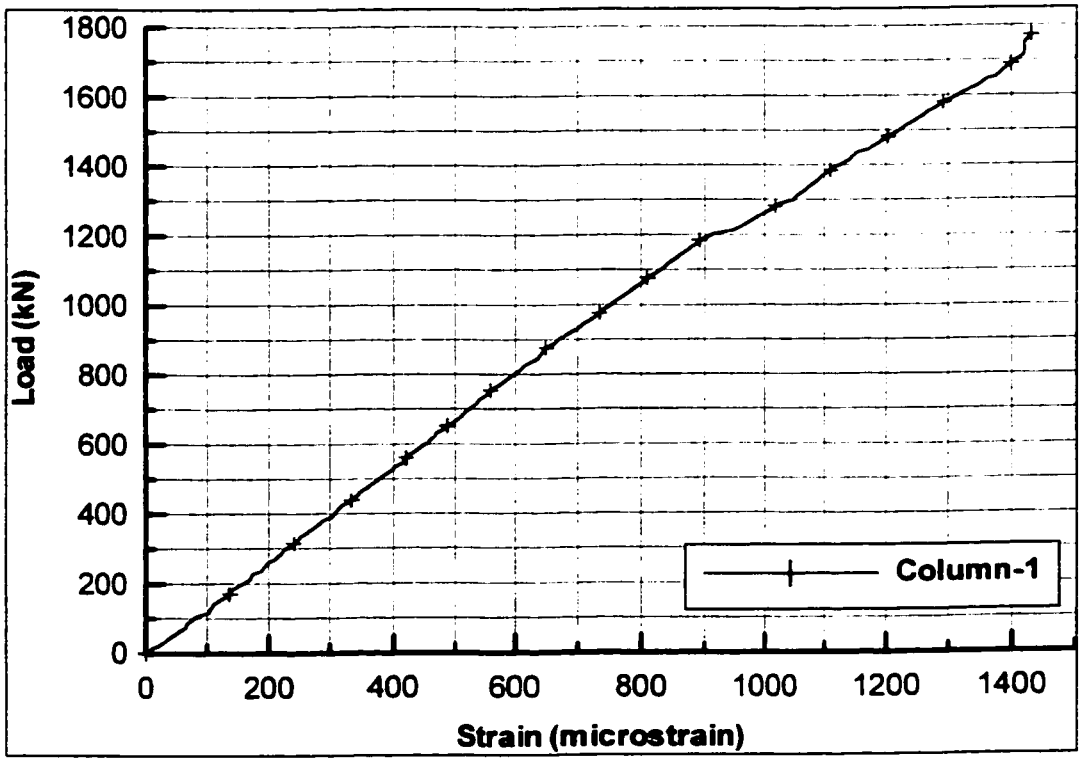

Figure 4.49: Load-strain curves in steel in concrete and at mid-height of column (2B)

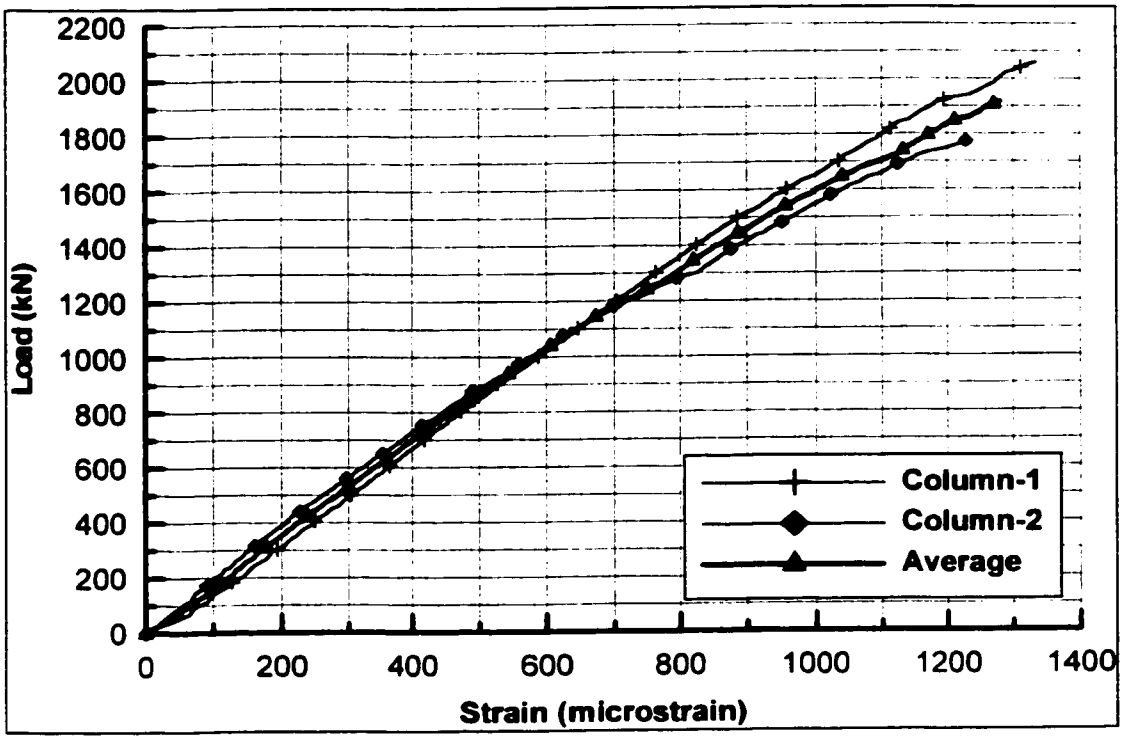

Figure 4.50: Load-strain curves on surface of concrete at center and at mid-height of column (3S)

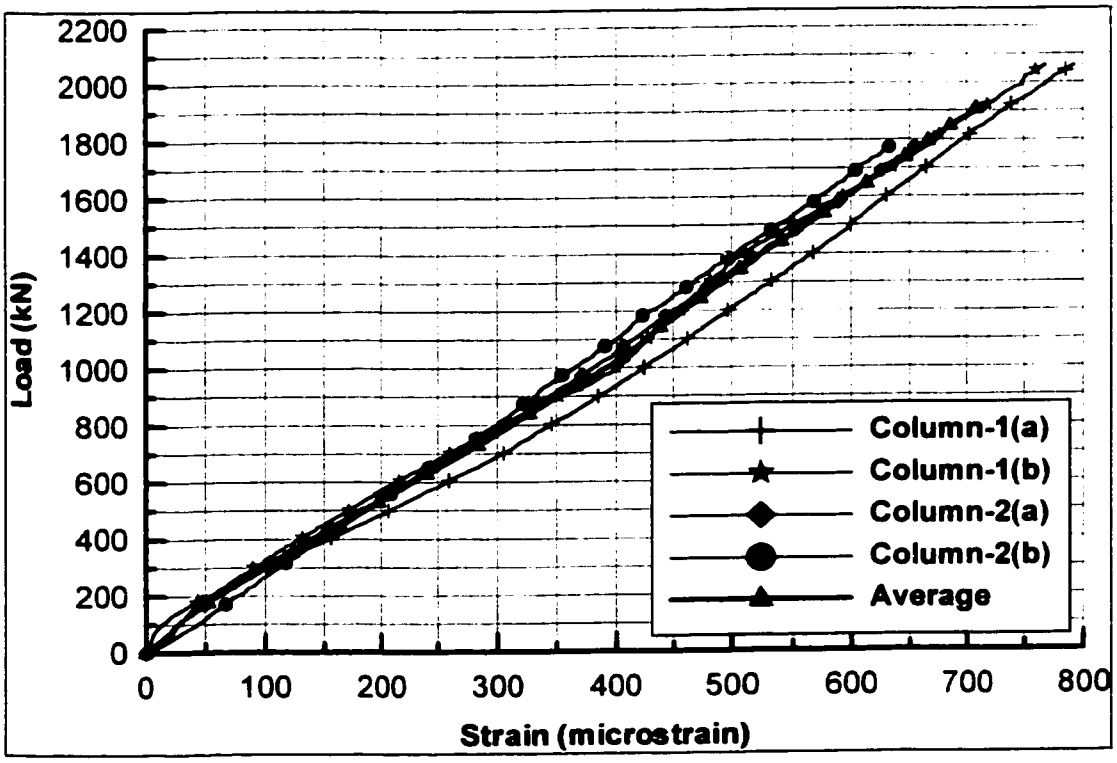

Figure 4.51: Load-strain curves on surface of repair at center and at mid-height of column (1&2S)

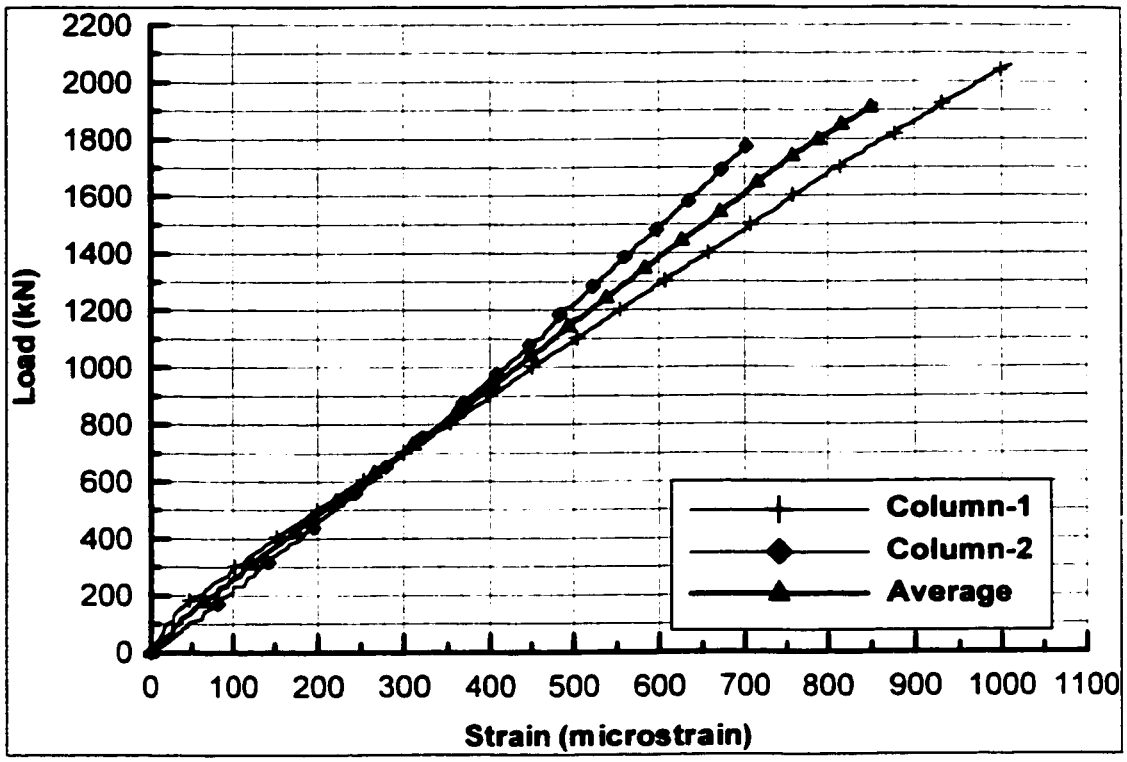

Figure 4.52: Load-strain curves in repair at edge and at mid-height of column (1R)

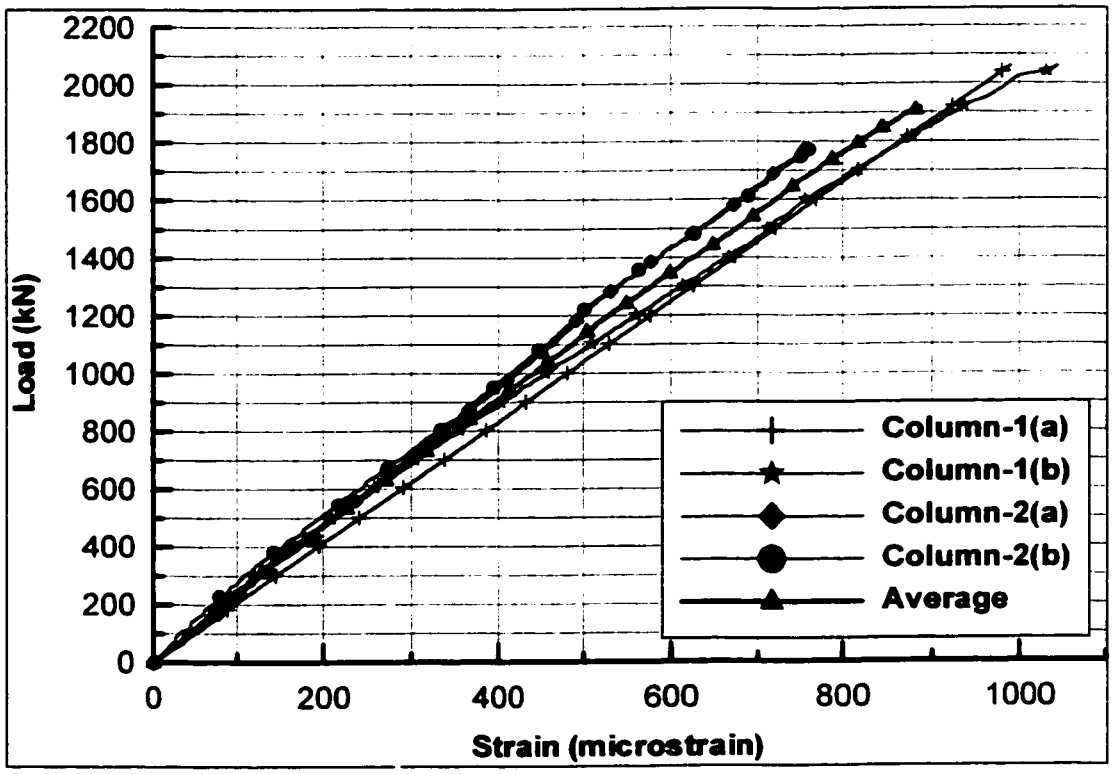

Figure 4.53: Load-strain curves in repair at center and at mid-height of column (2&3R)

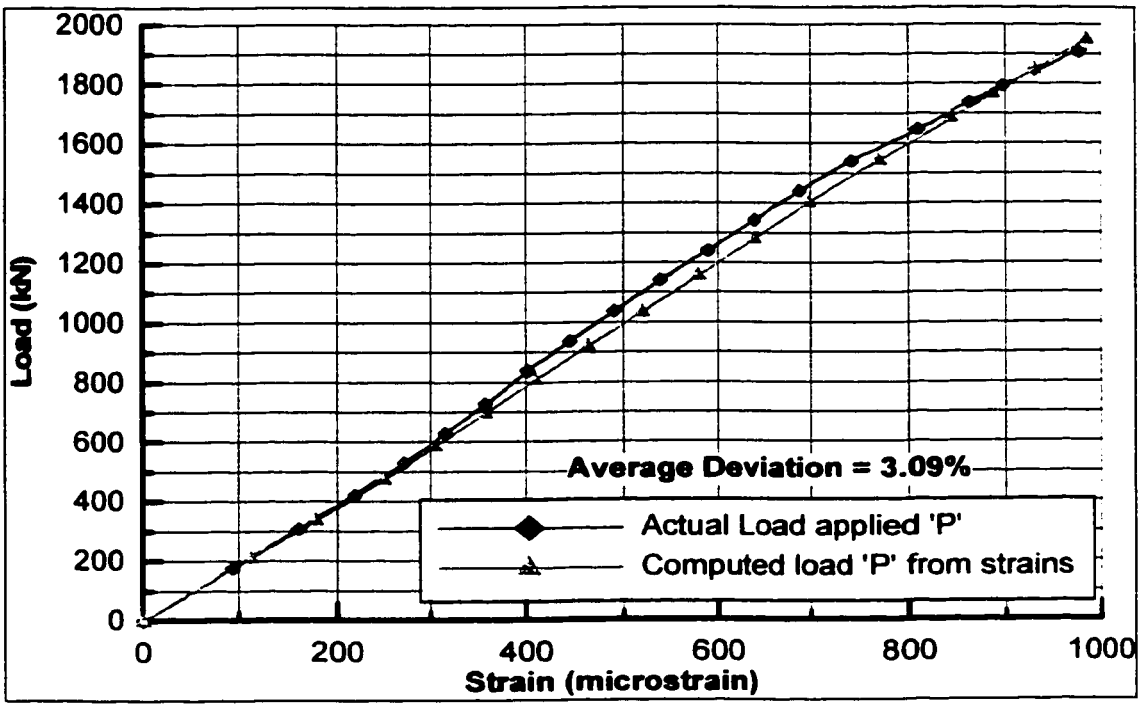

Figure 4.54: Comparison of Actual load applied and Computed load plotted against average strains measured at mid-height of column specimen repaired with FMCX

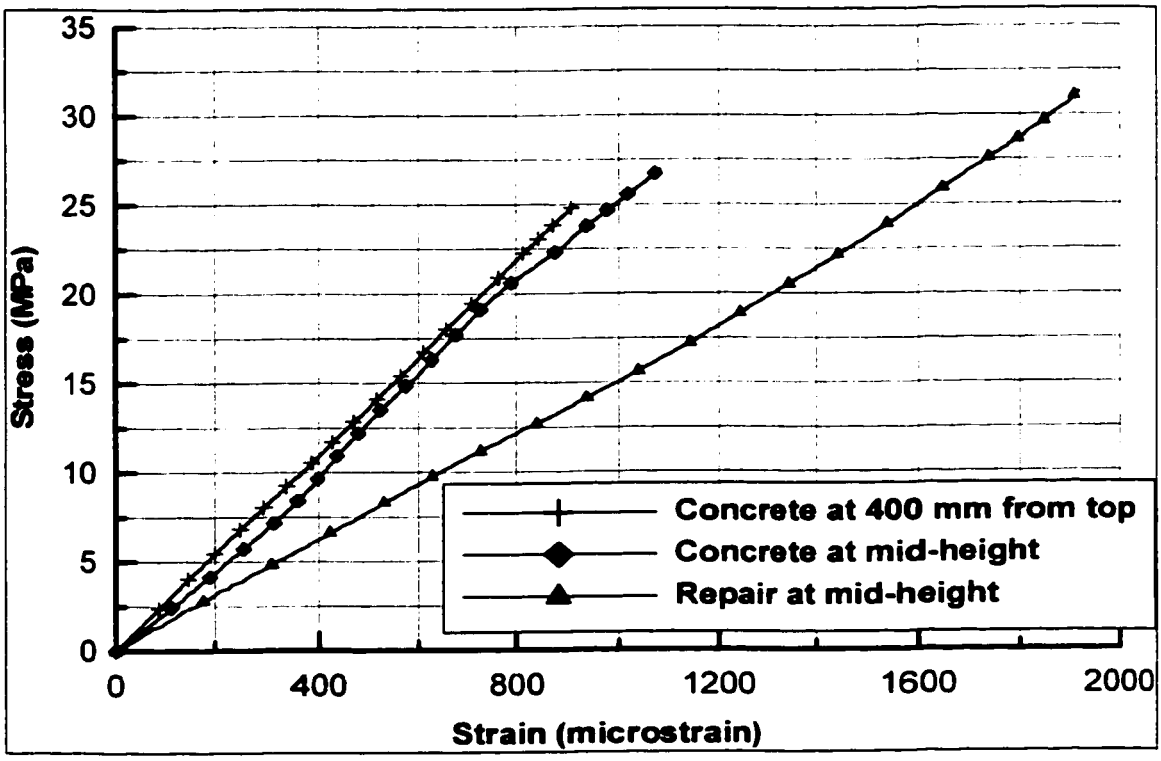

Figure 4.55: Stress-strain curve for concrete at two locations and in repair mortar for column specimen repaired with FMCX

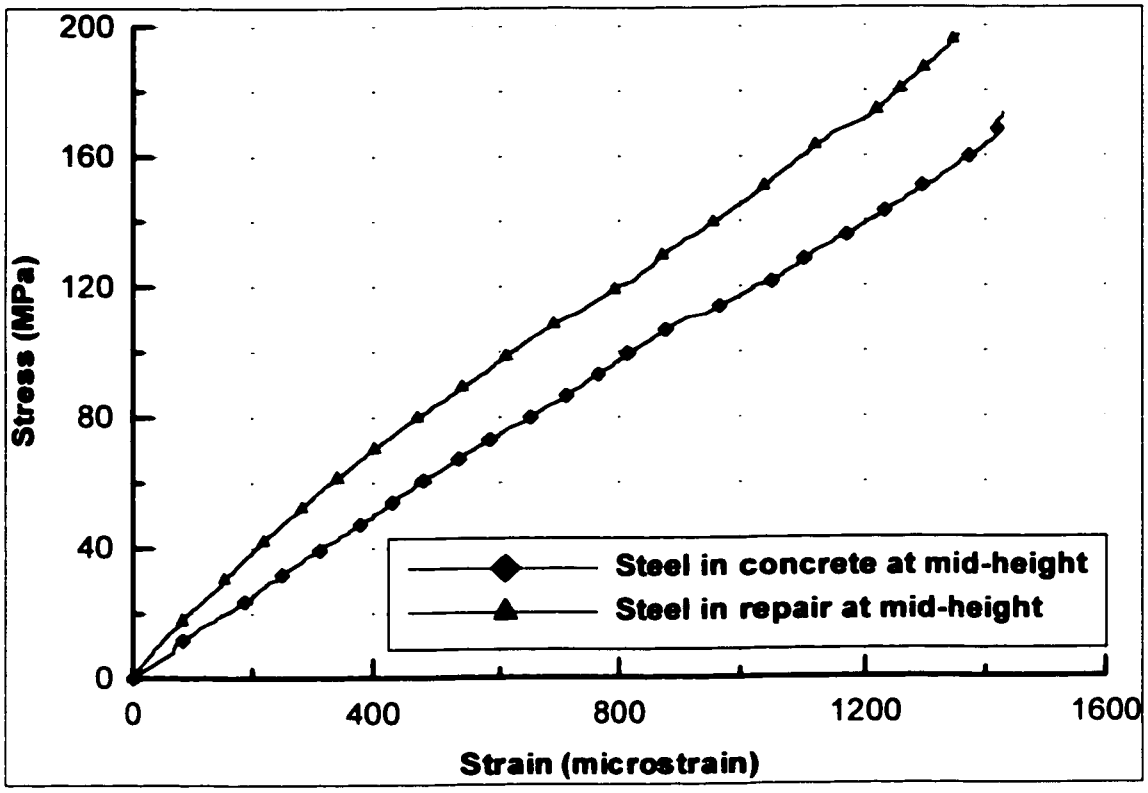

Figure 4.56: Stress-strain curve for steel in concrete and repair for column specimen repaired with FMCX

Figure 4.57: Load distribution between concrete, steel and repair at mid-height in columns repaired with FMCX

The measured strains inside concrete ε_c, in steel in concrete ε_{sc}, in steel in repair ε_{sr} and inside the repair mortar ε_r were taken to be the average of all similar strains recorded at that location in different specimens. The obtained strains were substituted in the equations (7) to (10) shown in section 4.2.1 for case-III, to calculate the load distribution between concrete P_c, steel in concrete P_{sc}, steel in repair P_{sr} and repair mortar P_r.

The total load 'P' coming on the column specimen was calculated by summing up the loads coming on concrete, steel in concrete, steel in repair and repair mortar. The applied load and the calculated load was compared and plotted against measured strains as shown in Figure 4.54 at mid-height of column specimen. The deviation of calculated values of load from the applied load was also calculated. Figure 4.57 shows the percentages of loads taken by concrete, steel and repair mortar. The components of load P_c, P_{sc}, P_{sr}, P_r and were divided by their area of cross section to obtain the stresses in concrete, steel in concrete, steel in repair and repair mortar respectively. The deviation of calculated values of load from the applied loads as shown in Figure 4.54 is 3.09% at mid-height of the column specimen. Figure 4.57 shows the load distribution between concrete, steel and repair mortar FMCX in the column specimens. Concrete core, which has 40% of the cross-sectional area takes about 34.31% of the total calculated load whereas the steel in concrete, which is only 0.25% of the cross-sectional area, takes 1.59% of the total calculated load and the steel in repair, which is 0.75% of the cross-sectional area, takes 4.76% of the total calculated load. The repair material FMCX, which is nearly 60% of the cross-sectional area, takes 59.35% of the total calculated load. The repair material FMCX is taking the larger portion of load than concrete because of its high modulus of elasticity.

Figure 4.58: Failure of column specimen repaired with FMCX

Figure 4.59: Close-up views of failure of column specimen repaired with FMCX

Figures 4.58 and 4.59 show the failure mode of the column specimen tested. The specimen fails at the ends due to crushing of concrete, which is attributed to stress concentration at these locations. The concrete at these locations has reached its crushing strength. The crushing of concrete at top causes cracks in concrete and these cracks develop longitudinally up to the repaired portion. The specimen at the end fails when chunks of concrete from top and some portion of repair mortar spalls off as can be seen in the figures provided.

Figure 4.55 shows the stress-strain curve for concrete at mid-height and at 400 mm from top of the column specimen and in repair mortar. The stress at mid-height in the concrete core varies linearly till it reaches a stress level of 27 MPa before failure of the specimen. The concrete has not yet reached its crushing strength of $0.85f_c'$ (45 MPa). The stress at 400 mm from top varies linearly till it reaches a stress level of 25 MPa before failure of the specimen. The concrete at this location has not yet reached its ultimate crushing strength of 45 MPa. The stress in repair material FMCX varies linearly till it reaches a stress level of 31.5 MPa before failure of specimen. The repair material has also not stressed up to its crushing strength of $0.85f_c'$ (51 MPa).

Figure 4.56 shows the stress-strain curve for steel in concrete and steel in repair at mid-height of the column specimen. The stress at mid-height in steel inside concrete varies linearly till it reaches a stress level of 175 MPa at failure of the specimen, and has not yet reached its yielding strength at failure. The stress at mid-height in steel in repair varies linearly till it reaches a stress level of 197 MPa. The steel at this location has not yet reached its yield stress of 415 MPa.

4.2.5 COLUMNS REPAIRED WITH PFSM

The column specimens with recess and repaired with PFSM as shown schematically in Figure 3.21 were tested till failure using the procedure explained in section 3.3.5 of Chapter-3. The load applied on the specimen and the strains at different locations in the specimen were recorded and plotted against applied load. The location of strain gauges in the specimen is also shown in Figure 3.21.

The data recorded during the testing process was sorted out and some of the data that showed a deviation of more than 10% from the average value was discarded. Only the selected data from the experiment are shown in Figures 4.60 to 4.67.

The measured strains inside concrete ε_c, in steel in concrete ε_{sc}, in steel in repair ε_{sr} and inside the repair mortar ε_r were taken to be the average of all similar strains recorded at that location in different specimens. The obtained strains were substituted in equations (7) to (10) shown in section 4.2.1 for case-III, to calculate the load distribution between concrete P_c, steel in concrete P_{sc}, steel in repair P_{sr} and repair mortar P_r. The total load 'P' coming on the column specimen was calculated by summing up the loads coming on concrete, steel and repair mortar. The applied load and the calculated load was compared and plotted against measured strains as shown in Figure 4.68 at mid-height of column specimen. The deviation of calculated values of load from the applied load was also calculated.

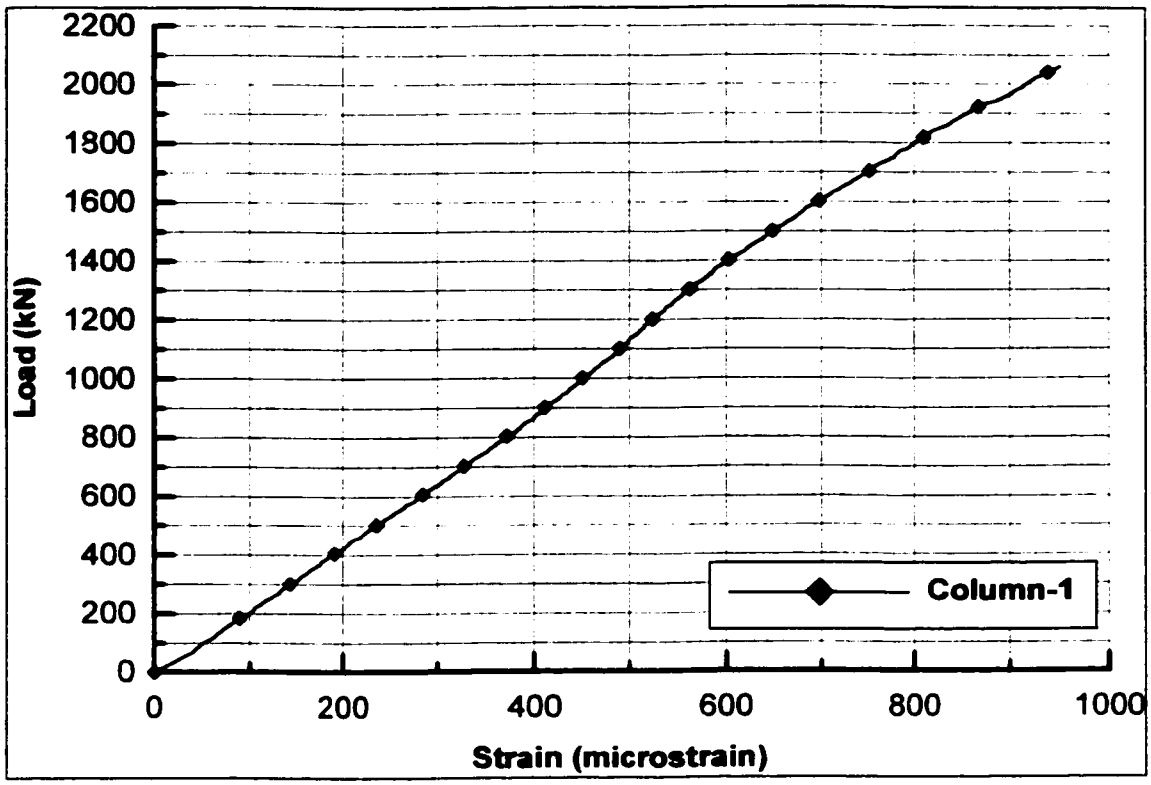

Figure 4.60: Load-strain curves in concrete at center and at 400 mm from top of Column (1E)

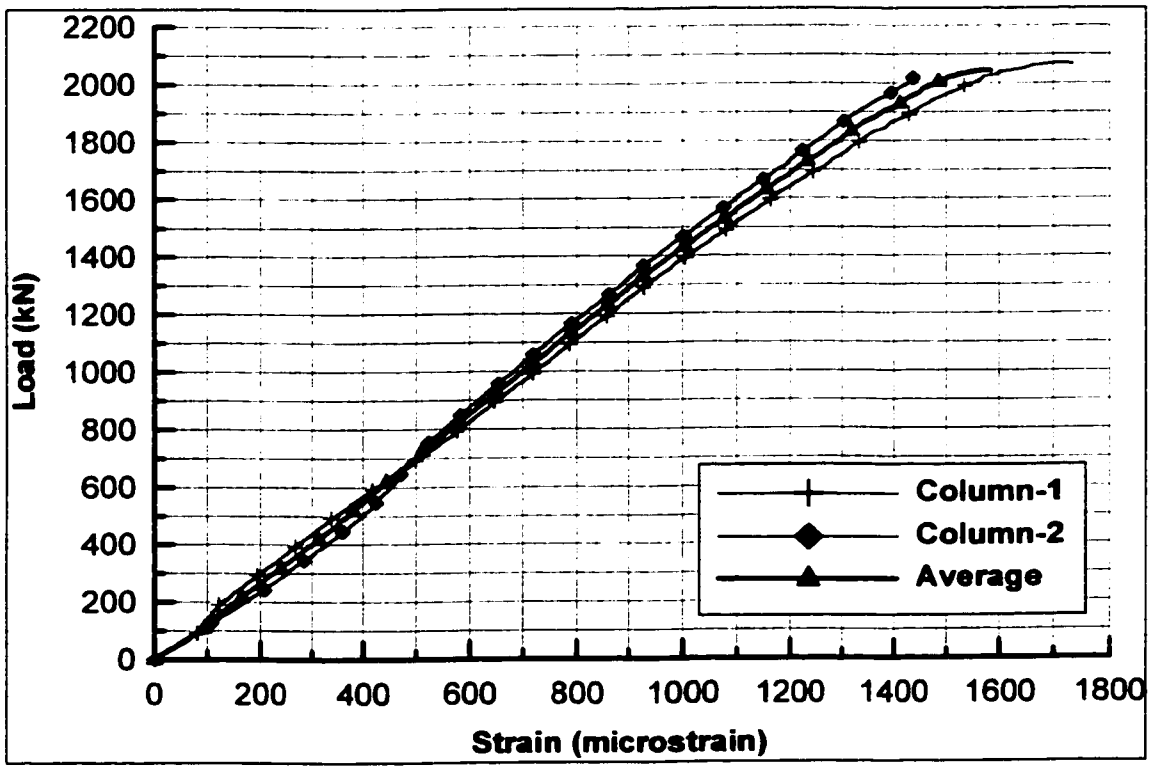

Figure 4.61: Load-strain curves in concrete at center and at mid-height of column (2E)

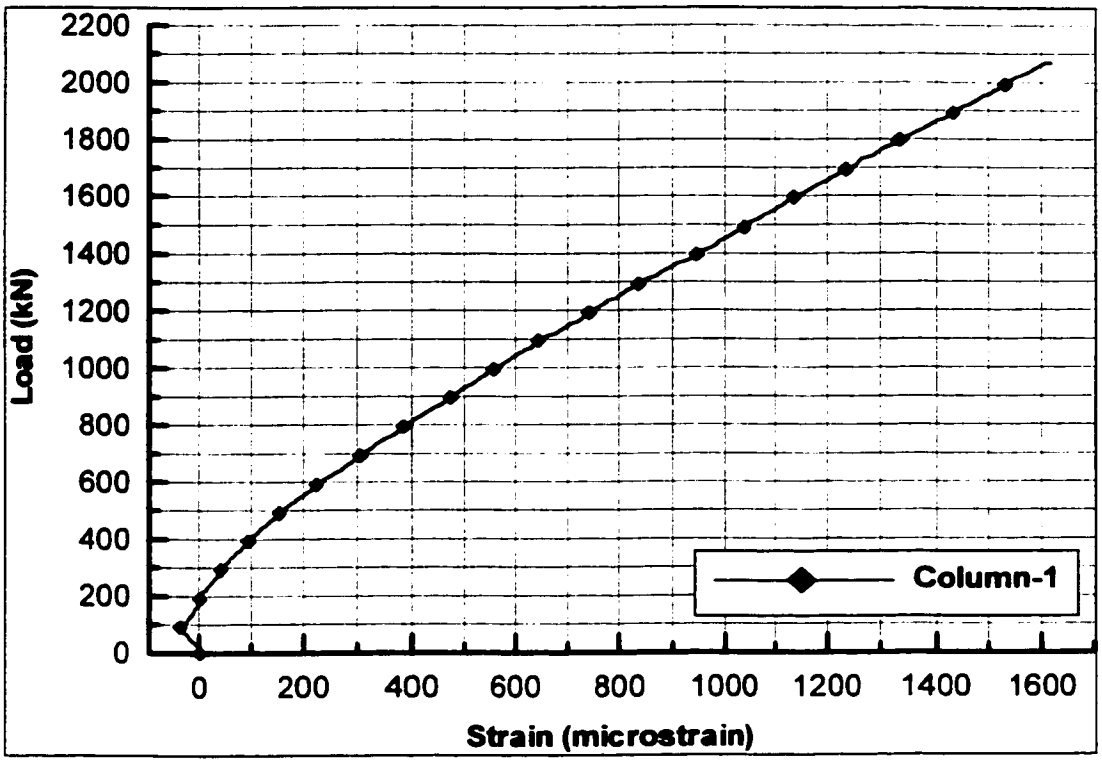

Figure 4.62: Load-strain curves in steel exposed in recess and at mid-height of column (1B)

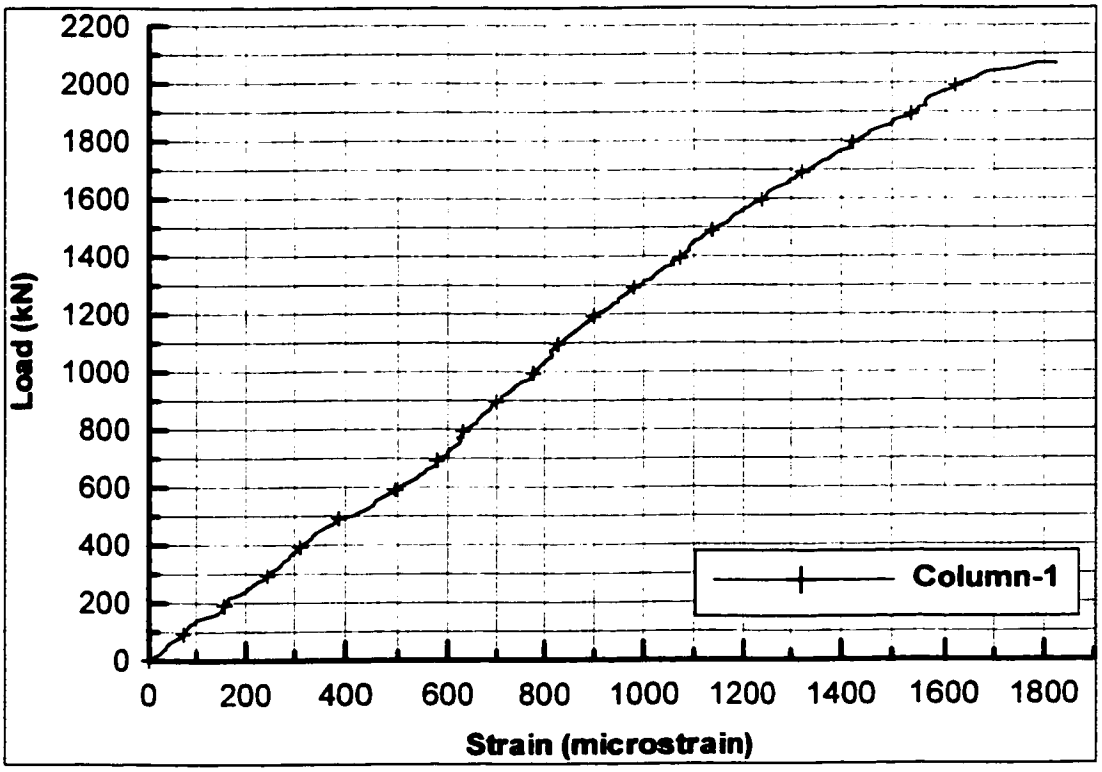

Figure 4.63: Load-strain curves in steel in concrete and at mid-height of column (2B)

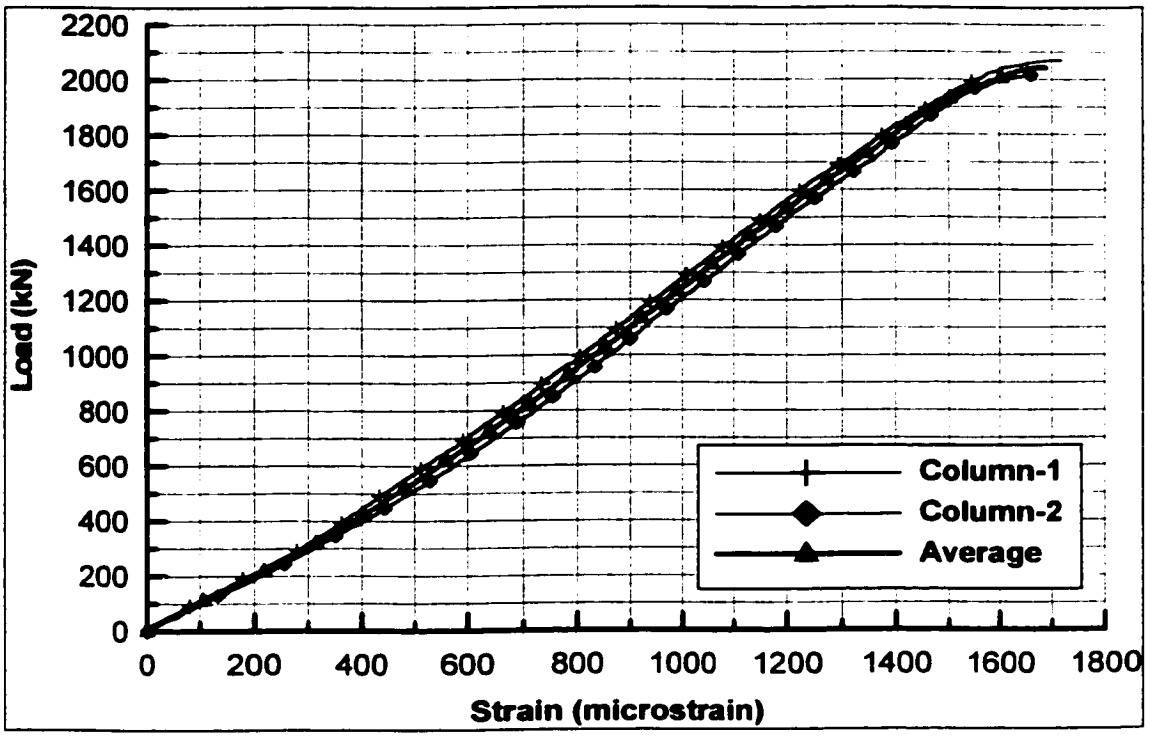

Figure 4.64: Load-strain curves on surface of concrete at center and at mid-height of column (3S)

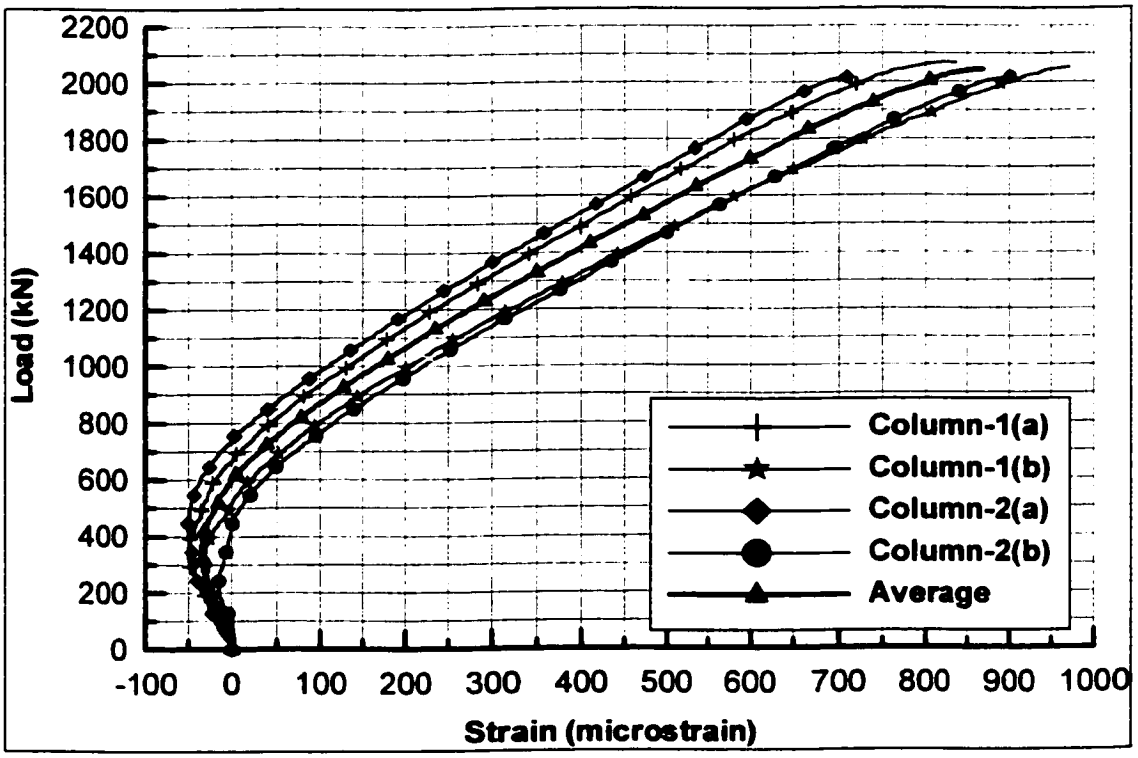

Figure 4.65: Load-strain curves on surface of repair at center and at mid-height of column (1&2S)

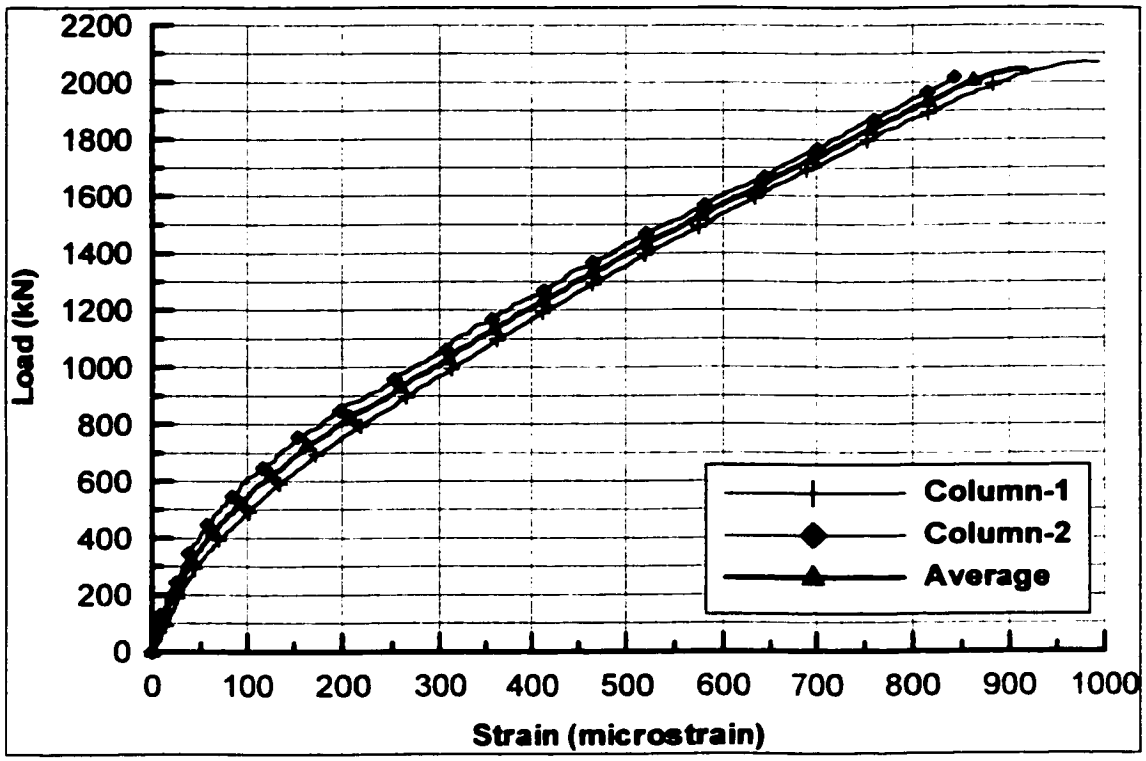

Figure 4.66: Load-strain curves in repair at edge and at mid-height of column (1R)

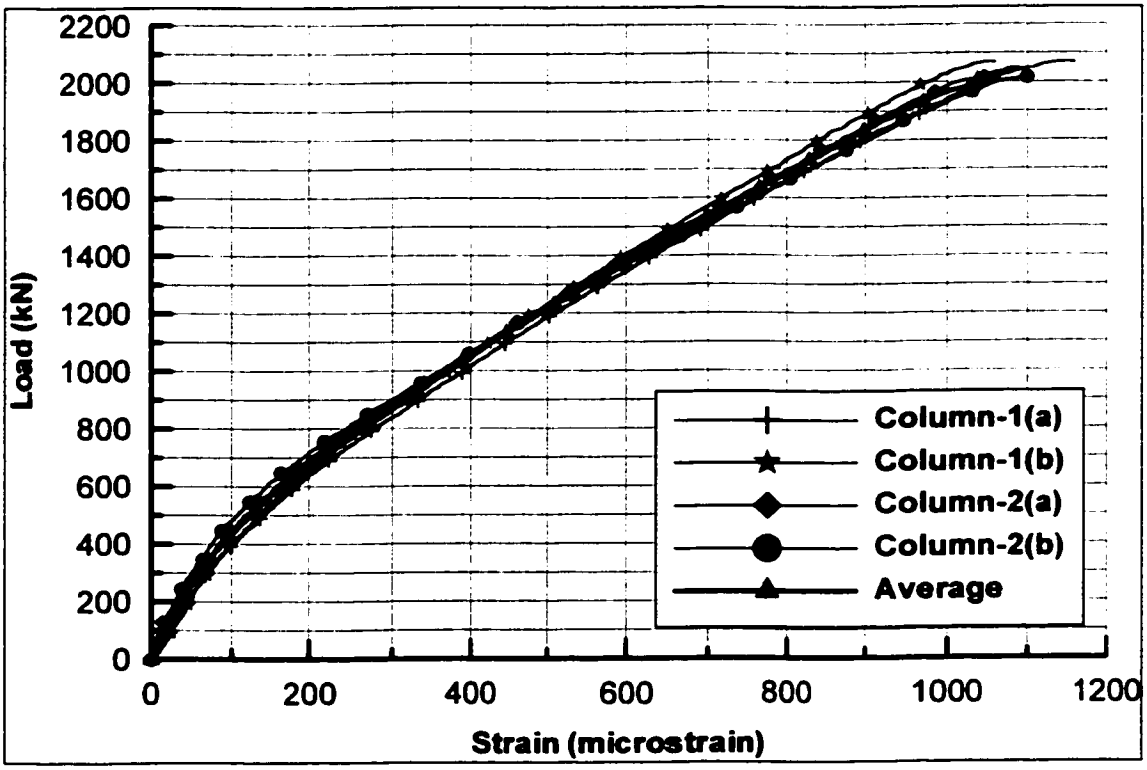

Figure 4.67: Load-strain curves in repair at center and at mid-height of column (2&3R)

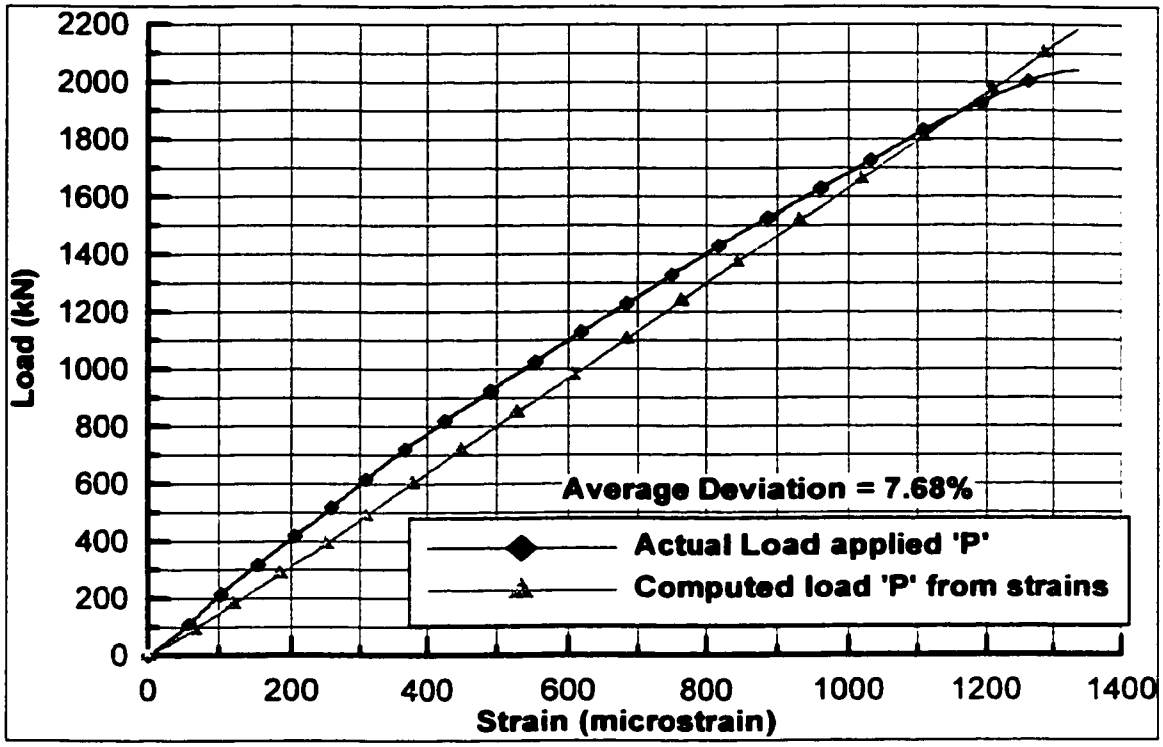

Figure 4.68: Comparison of Actual load applied and Computed load plotted against average strains measured at mid-height of column specimen repaired with PFSM

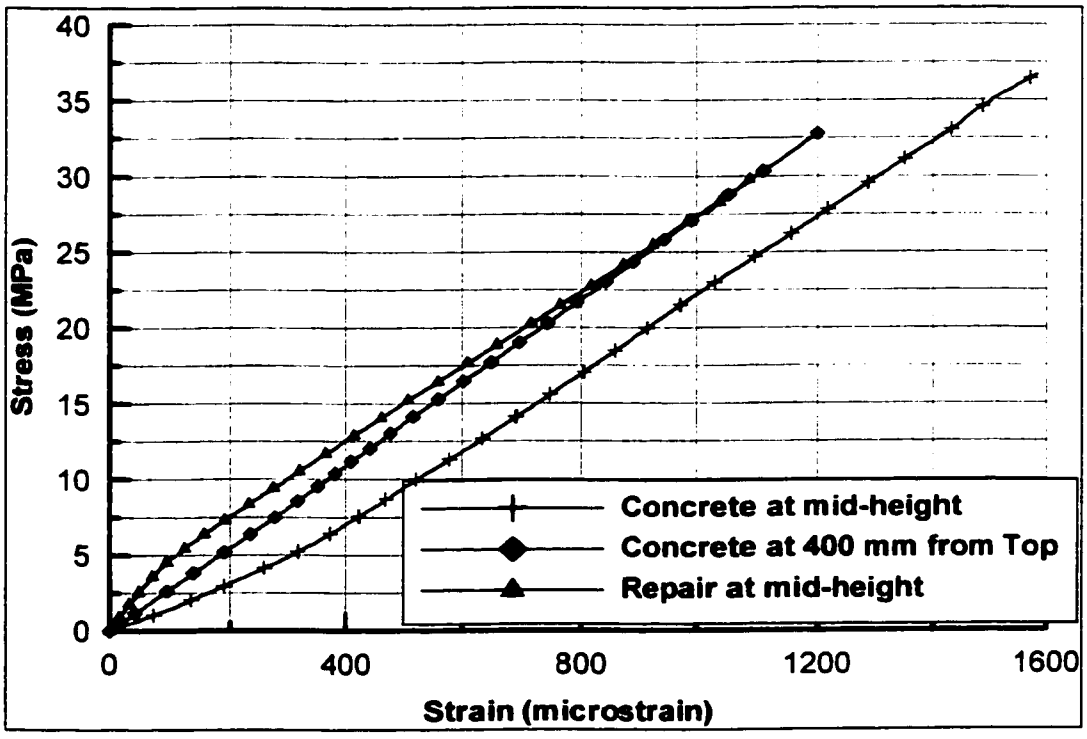

Figure 4.69: Stress-strain curve for concrete at two locations and in repair mortar for column specimen repaired with PFSM

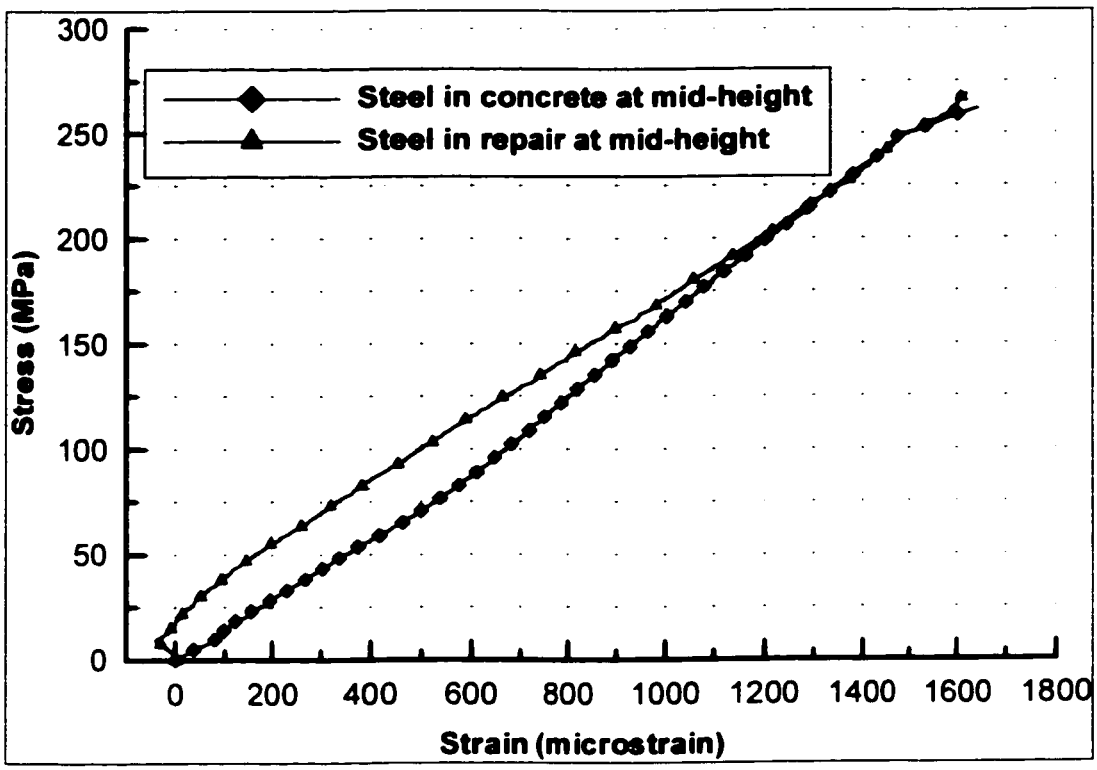

Figure 4.70: Stress-strain curve for steel in concrete and repair for column specimen repaired with PFSM

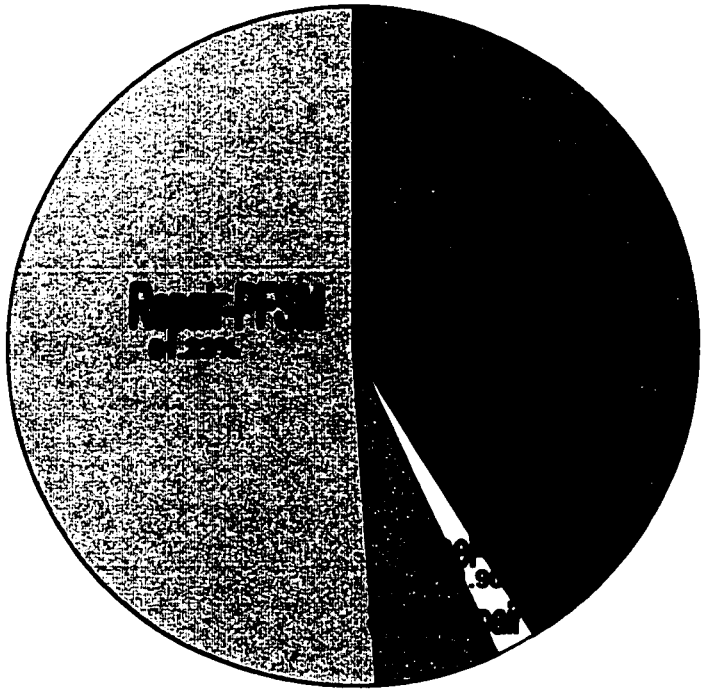

Figure 4.71: Load distribution between concrete, steel and repair at mid-height in columns repaired with PFSM

Figure 4.71 shows the percentages of loads taken by concrete, steel and repair mortar. The components of load P_c, P_{sc} P_{sr} P_r and were divided by their area of cross section to obtain the stresses in concrete, steel in concrete, steel in repair and repair mortar respectively. The strains measured on the surface of repair material PFSM under load as seen in Figure 4.65 shows the bulging of repair material in the initial stages. The strains on the surface have gone in tension. The strains measured inside the repair mortar at center and at edge also show the same pattern, but the material at these locations is not in tension. The bulging of material is attributed to its low elastic modulus.

The deviation of calculated values of load from the applied loads as shown in Figure 4.68 is 7.68% at mid-height of the column specimen. Here the deviation is large as compared to others because of the bulging of repair material. Figure 4.71 shows the load distribution between concrete, steel and repair mortar PFSM in the column specimens. Concrete core, which has 40% of the cross-sectional area takes about 41.16% of the total calculated load whereas the steel in concrete, which is only 0.25% of the cross-sectional area, takes 1.90% of the total calculated load and the steel in repair, which is 0.75% of the cross-sectional area, takes 5.71% of the total calculated load. The repair material PFSM, which is nearly 60% of the cross-sectional area, takes 51.23% of the total calculated load. The concrete core is taking the larger portion of load than repair material PFSM because concrete has high modulus of elasticity than PFSM.

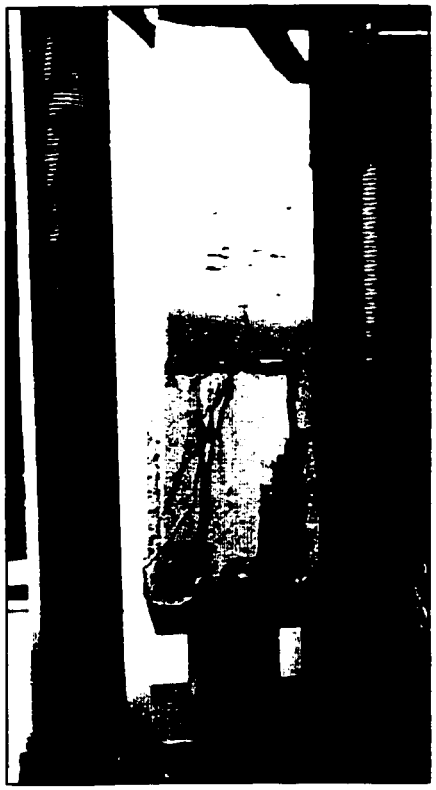

Figure 4.72: Failure of column specimen repaired with PFSM

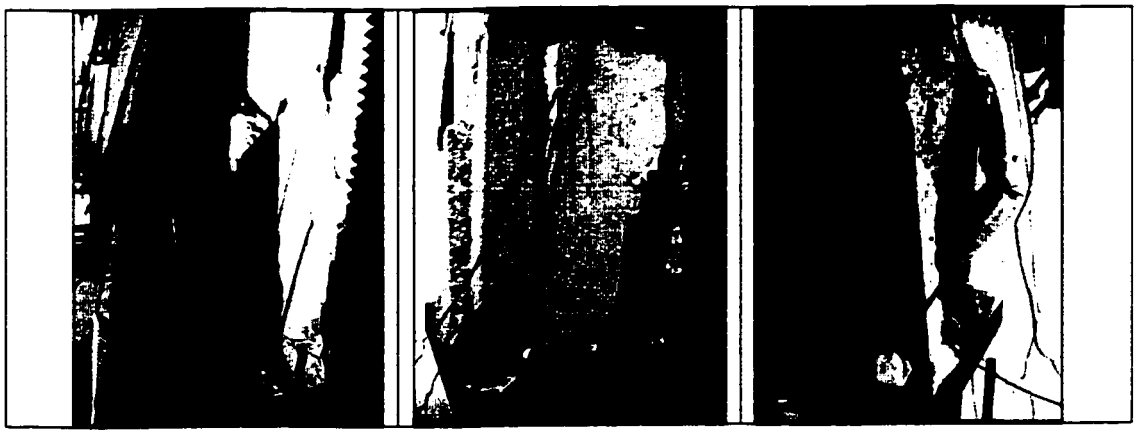

Figure 4.73: Close-up views of failure of column specimen repaired with PFSM

Figures 4.72 and 4.73 show the failure mode of the column specimen tested. The specimen fails at the ends due to crushing of concrete, which is attributed due to stress concentration at these locations. The concrete at these locations has reached its crushing strength. The crushing of concrete at top causes cracks in concrete and these cracks develop longitudinally up to the repaired portion. The specimen at the end fails when chunks of concrete from top and some portion of repair mortar spalls off as can be seen in the figures provided.

Figure 4.69 shows the stress-strain curve for concrete at mid-height and at 400 mm from top of the column specimen and in repair mortar. The stress at mid-height in the concrete core varies linearly till it reaches a stress level of 37 MPa before failure of the specimen. The concrete has not yet reached its crushing strength of $0.85f_c'$ (45 MPa). The stress at 400 mm from top varies linearly till it reaches a stress level of 33 MPa before failure of the specimen. The concrete at this location has not yet reached its ultimate crushing strength of 45 MPa. The stress in repair material PFSM does not vary linearly but after 5 MPa it varies linearly till it reaches a stress level of 30.0 MPa before failure of specimen. The repair material has also not stressed up to its crushing strength of $0.85f_c'$ (42 MPa).

Figure 4.70 shows the stress-strain curve for steel in concrete and steel in repair at mid-height of the column specimen. The stress at mid-height in steel inside concrete varies almost linearly till it reaches a stress level of 260 MPa at failure of the specimen, and has not yet reached its yielding strength at failure. The stress at mid-height in steel in repair varies linearly till it reaches a stress level of 270 MPa. The steel at this location has also not yet reached its yield stress of 415 MPa. It can be seen from the figure that the steel in

repair is taking more load initially than the steel in concrete but at higher loads the steel stresses are nearly equal.

4.2.6 STRESSES IN REPAIRED/UN-REPAIRED COLUMNS

For comparing the stresses obtained from the above four cases it was essential to plot curves showing the stresses developed in the materials with increase in load. Figures 4.74 to 4.78 show load-stress curves for different materials at different locations.

Figure 4.74 shows the load-stress curves for concrete at center and at mid-height of column specimen. It can be seen clearly in this figure that the stress in concrete is very high in the column specimen with recess. This is due to concentration of stress in core because of its small area. At a particular load level for example 1000 kN the stress in concrete should be around 13 MPa but the stress in the concrete of column specimen with recess has reached 32 MPa i.e., an increase of around 150%. The stresses in concrete core in column repaired with PFSM are higher than the column specimen repaired with FMCX, indicating that the core concrete in this case is taking more load. This is attributed to the low modulus of elasticity of PFSM than FMCX.

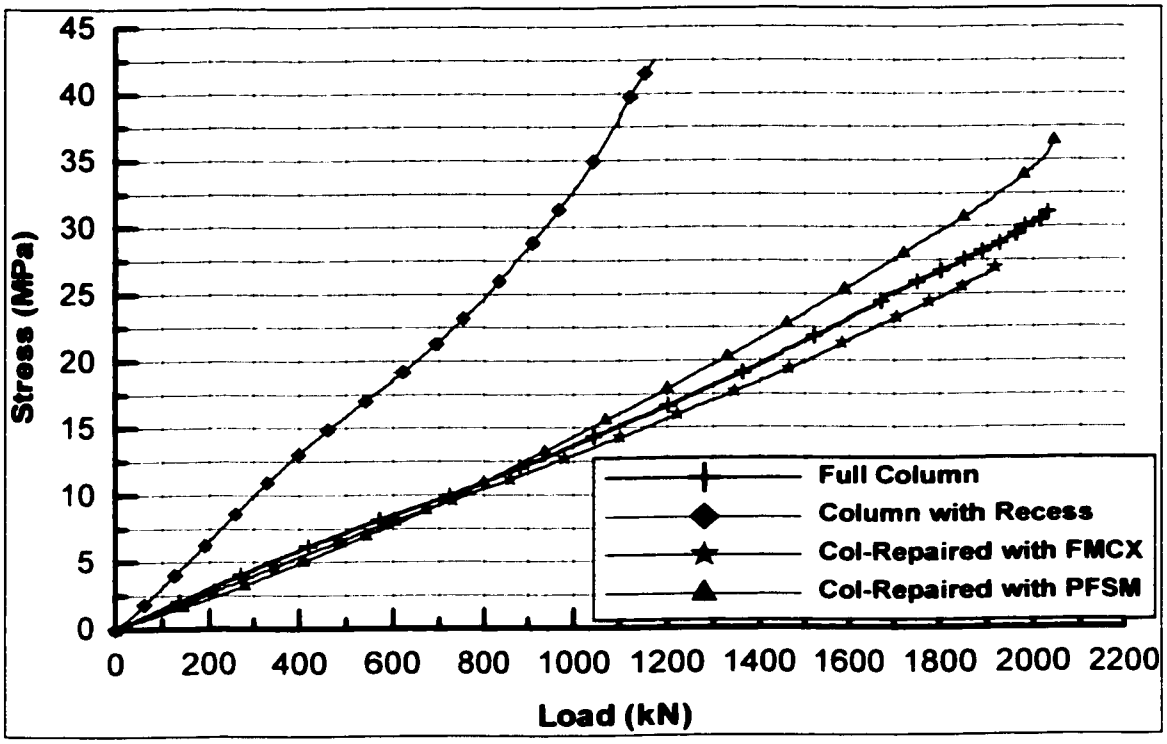

Figure 4.74: load-stress curves for concrete at center and at mid-height of column

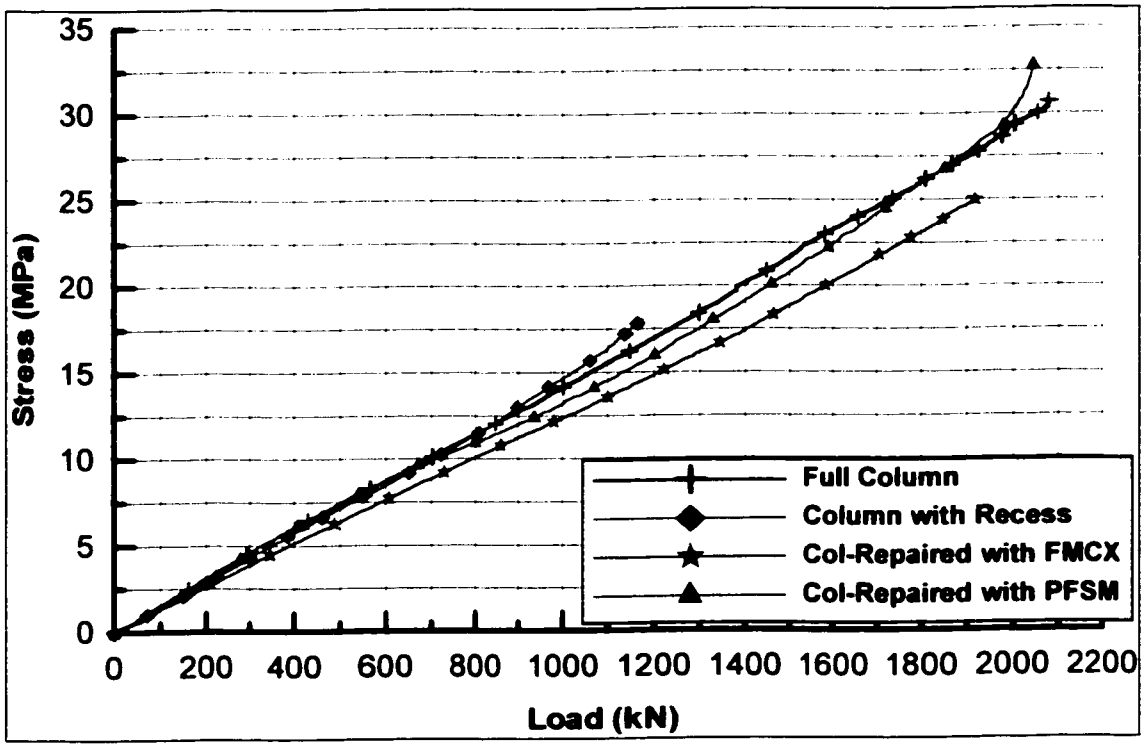

Figure 4.75: load-stress curves for concrete at center at 400 mm from top of column

Figure 4.75 shows the load-stress curves for concrete at center at 400 mm from top of column specimen. It can be seen clearly in this figure that the stresses in concrete at this location are nearly equal in all cases at low levels of load. The stresses in concrete at 400 mm from top of column repaired with FMCX are a little lower than the column specimen of other cases, indicating that the concrete in this case is taking less load. This is attributed to the high modulus of elasticity of FMCX.

Figure 4.76 shows the load-stress curves for concrete and repair materials at mid-height of column specimen. It can be seen clearly in this figure that the stress in repair material FMCX at this location is higher than those in concrete and PFSM. This indicates that the material FMCX is taking more load than concrete and PFSM, which is due to its high modulus of elasticity. The stress in repair material PFSM is low as compared to concrete and FMCX, which is due to its low modulus of elasticity.

Figure 4.77 shows the load-stress curves for Steel in concrete and at mid-height of column specimen. It can be seen clearly in this figure that the stress in steel is very high in the column specimen with recess. This is due to concentration of stress in remaining core and because of its small area. At a particular load level for example 1000 kN the stress in steel should be around 100 MPa but the stress in the steel of column specimen with recess has reached 325 MPa i.e., an increase of around 225%. The stresses in steel in core in column specimen repaired with PFSM are higher than the column specimen repaired with FMCX, indicating that the steel in concrete in this case is taking more load. This is attributed to the low modulus of elasticity of PFSM than FMCX.

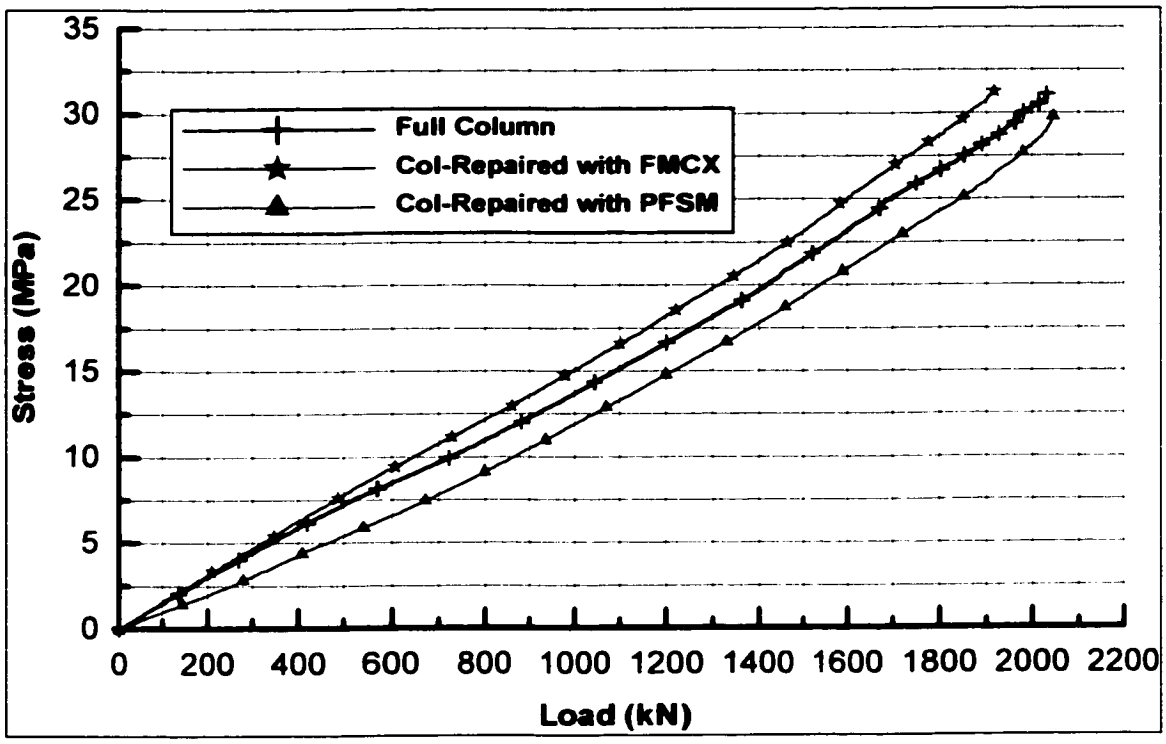

Figure 4.76: load-stress curves for concrete and repair materials at mid-height of column

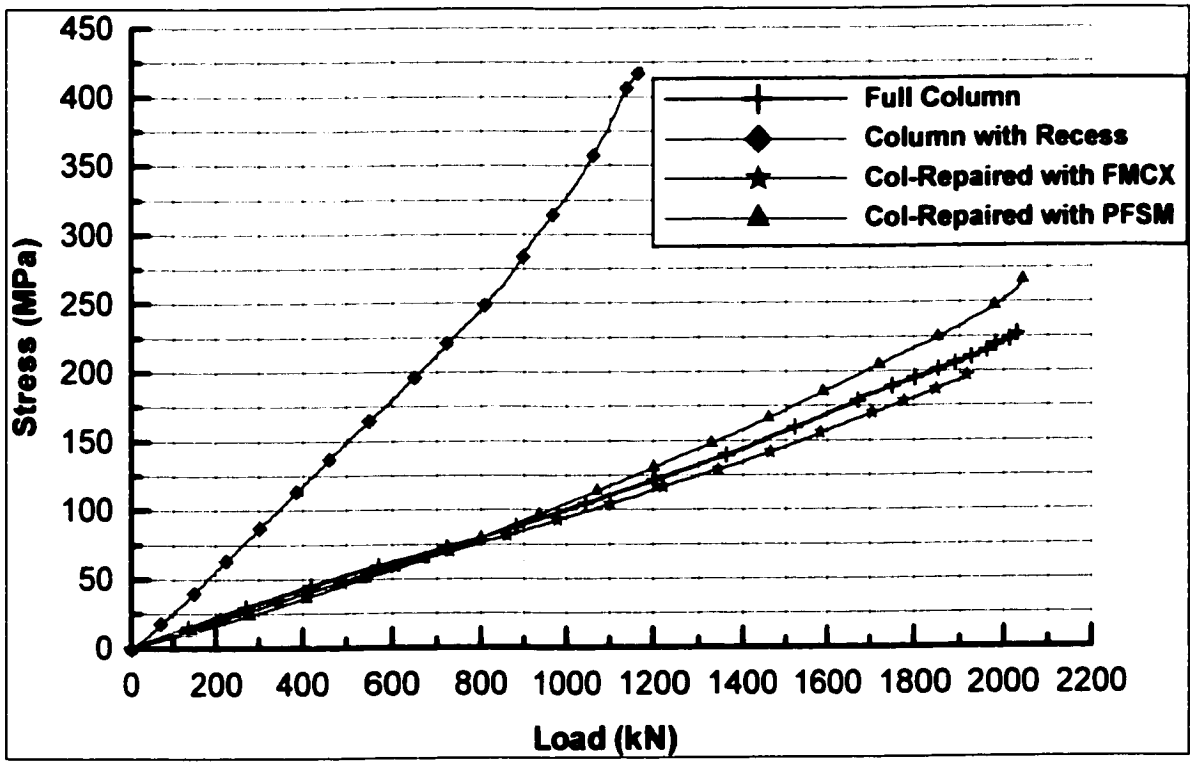

Figure 4.77: load-stress curves for steel inside concrete at mid-height of column

Figure 4.78 shows the load-stress curves for Steel in recess and in repair and at mid-height of column specimen. It can be seen clearly in this figure that the stress in steel is very high in the column specimen with recess. This is due to concentration of stress in remaining core and steel in recess and because of its small area. At a particular load level for example 1000 kN the stress in steel should be around 100 MPa but the stress in the steel of column specimen with recess has reached 270 MPa i.e., an increase of around 170%. The stresses in steel in repair in column specimen repaired with PFSM are higher than the column specimen repaired with FMCX, indicating that the steel in repair in this case is taking more load. This is attributed to the low modulus of elasticity of PFSM than FMCX.

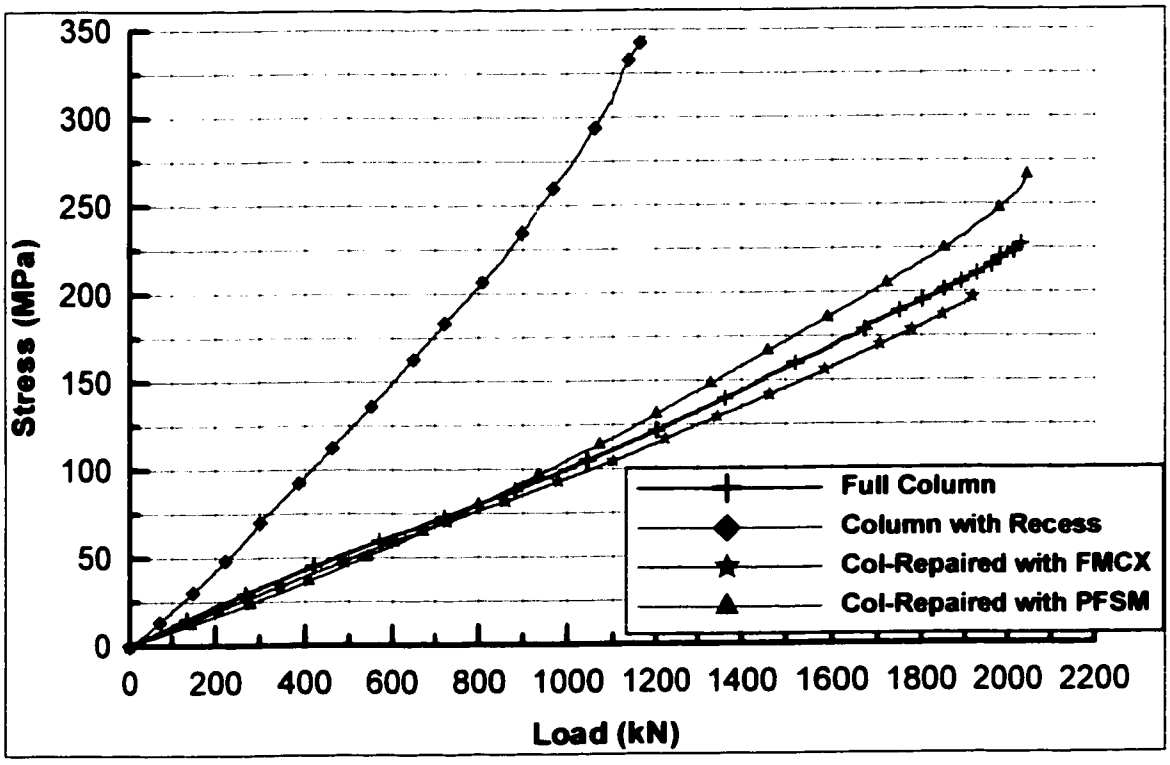

Figure 4.78: load-stress curves for steel in recess and in repair at mid-height of column

4.3 RESULTS OF LONG-TERM TESTING OF REPAIRED/UN-REPAIRED COLUMNS UNDER CONSTANT LOAD

Out of 20 columns cast the remaining 10 were used for monitoring strains under constant load. The breakdown for the number of columns tested is as follows:

(a) Columns without recess	2
(b) Columns repaired with FMCX and loaded after 7 days	2
(c) Columns repaired with PFSM and loaded after 7 days	2
(d) Columns repaired with FMCX in loaded state	2
(e) Columns repaired with PFSM in loaded state	2

4.3.1 SHRINKAGE AND CREEP MEASUREMENTS

The shrinkage and creep of repair materials play a significant role in the long-term behavior of repaired columns. The shrinkage and creep strains in repair materials were measured on specimens of size 300x250x75 mm. This geometry for the specimens was selected because of its same size as of patch repair on the column specimen. The procedures adopted for these tests are presented in sections 3.1.12 and 3.1.13 of chapter 3.

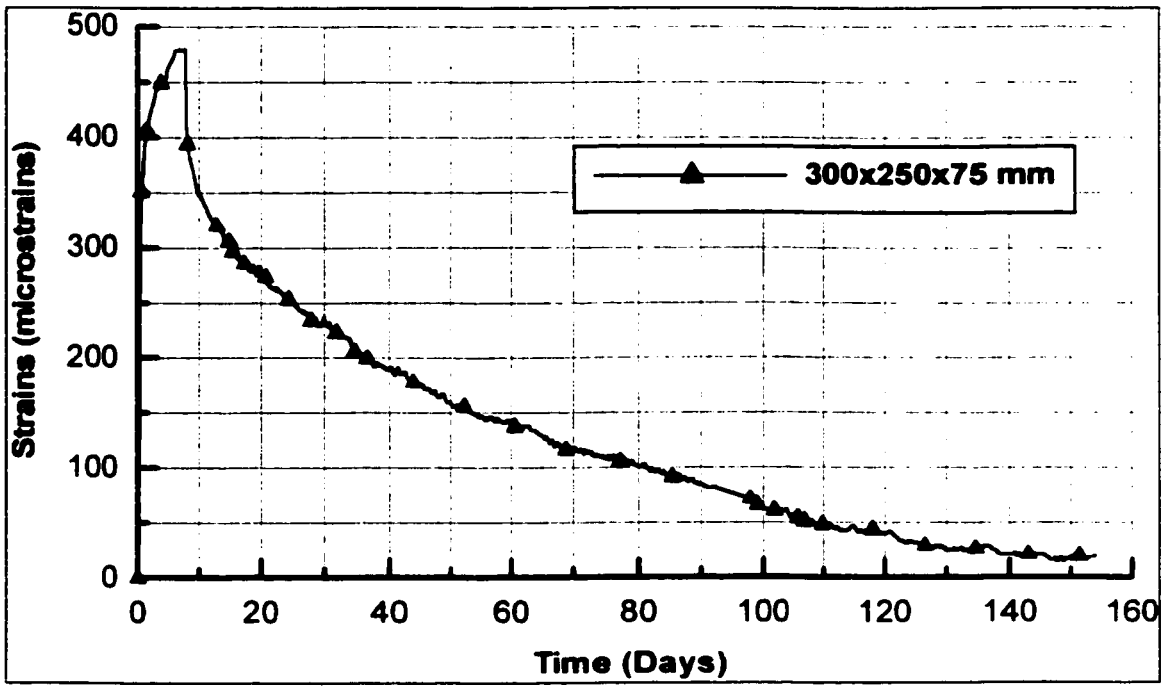

Figure 4.79: Expansion-shrinkage strains in FMCX

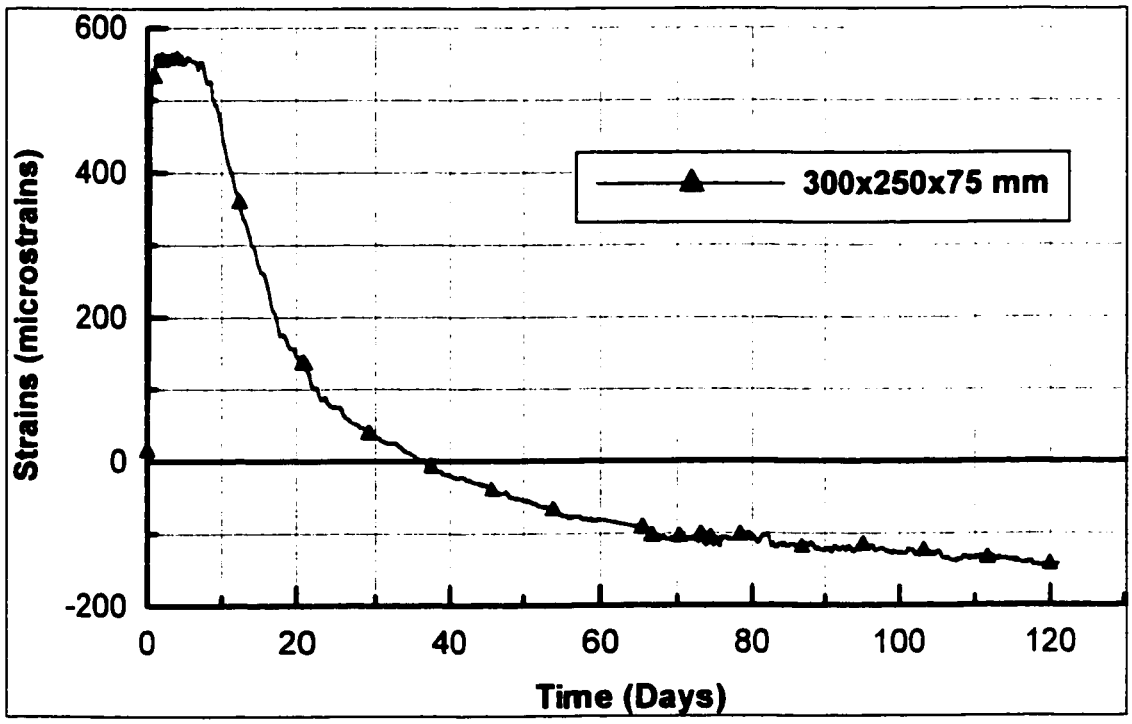

Figure 4.80: Expansion-shrinkage strains in PFSM

The total strain evolution in FMCX (Figure 4.79) shows an initial expansion of 480 με during the initial hardening stage up to 7 days. The expansion in this material kept on increasing till its removed from curing and subjected to laboratory atmosphere. After 7 days when the specimen is exposed to drying with moisture diffusing from 3 faces of prism at 65 ± 5% relative humidity, a steep fall in shrinkage-time curve can be seen in specimens. The total strain drops from +480 με to +310 με (net 170 με) in the first week after exposure, and a net shrinkage strain of +20 με (gross 460 με) takes place in 150 days for specimen of size 300x250x75.

The total strain evolution in PFSM (Figure 4.80) shows an initial expansion of 550 με during the initial hardening stage up to 7 days. The expansion in this material was constant till its removed from curing and subjected to laboratory atmosphere. After 7 days when the specimen is exposed to drying with moisture diffusing from 3 faces of prism at 65 ± 5% relative humidity, a steep fall in shrinkage-time curve can be seen in specimens. The total strain drops from +550 με to +280 με (net 270 με) in the first week after exposure, and a net shrinkage strain of -150 με (gross 700 με) takes place in 120 days for specimen of size 300x250x75.

Creep tests were conducted on repair material specimens of size 300x250x75 mm, which were loaded after 7 days of casting. The strain measured on a loaded specimen includes the elastic strain and the creep strain. The compressive creep strain is given as

$$\varepsilon_{exp}(t,t_o) = \varepsilon_{el}(t_o) + \varepsilon_{cr}(t,t_o) + \varepsilon_{sh}(t,t_o)$$

$\varepsilon_{exp}(t,t_o)$ is the measured strain at time t due to applied load at time t_o

$\varepsilon_{el}(t_o)$ is the elastic strain at t_o due to applied load

$\varepsilon_{cr}(t,t_o)$ is the total creep strain

$\varepsilon_{sh}(t,t_o)$ is the measured shrinkage strain in the companion sample.

The creep strain is therefore given as

$$\varepsilon_{cr}(t,t_o)=\varepsilon_{exp}(t,t_o)-\varepsilon_{el}(t_o)-\varepsilon_{sh}(t,t_o)$$

The creep coefficient can be written as

$$\phi(t,t_o)=\frac{\varepsilon_{cr}(t,t_o)}{\varepsilon_{el}(t,t_o)}=\frac{E_{ci}}{\sigma_t(t_o)}\varepsilon_{cr}(t,t_o)$$

where $\sigma_t(t_o)$ is the stress applied at time t_o and E_{ci} is the initial modulus of elasticity. The specific creep, $\varepsilon_{cr}^{sp}(t,t_o)$ which is the creep strain per unit stress, is given as:

$$\varepsilon_{cr}^{sp}(t,t_o)=\frac{\varepsilon_{cr}(t,t_o)}{\sigma_t(t_o)}$$

Figures 4.81 to 4.83 shows the specific creep curves for material FMCX, PFSM and concrete respectively. Concrete has a very low specific creep as compared to the two repair materials. The repair material PFSM shows very high specific creep strains compared to the other material FMCX.

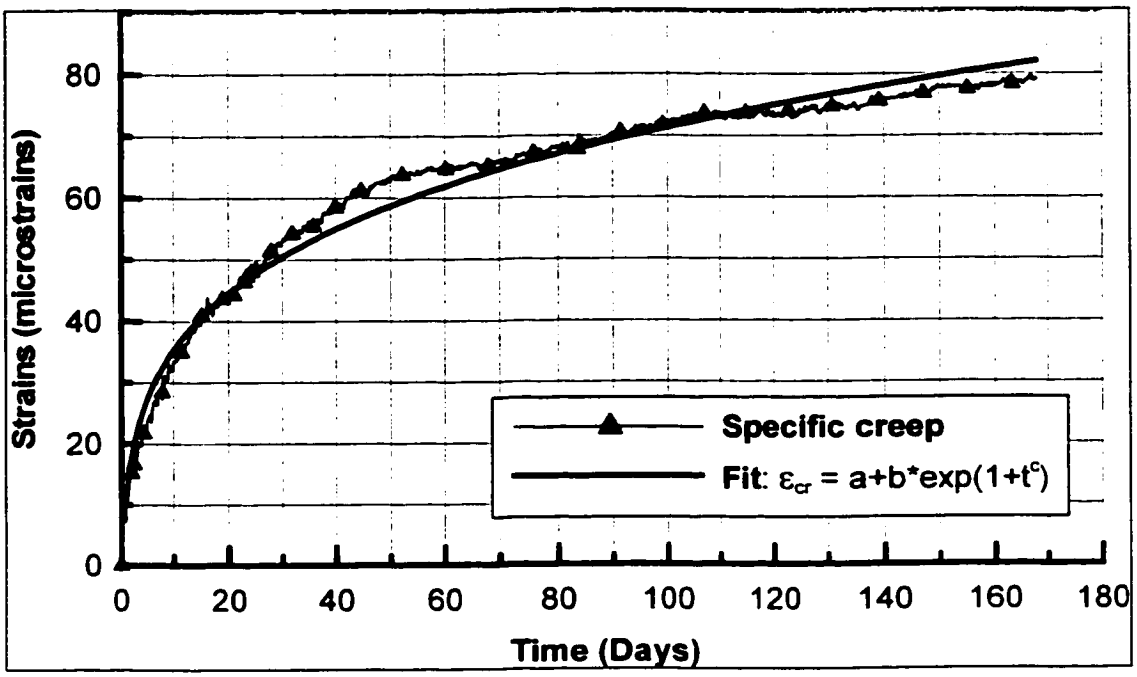

Figure 4.81: Specific creep in the material FMCX

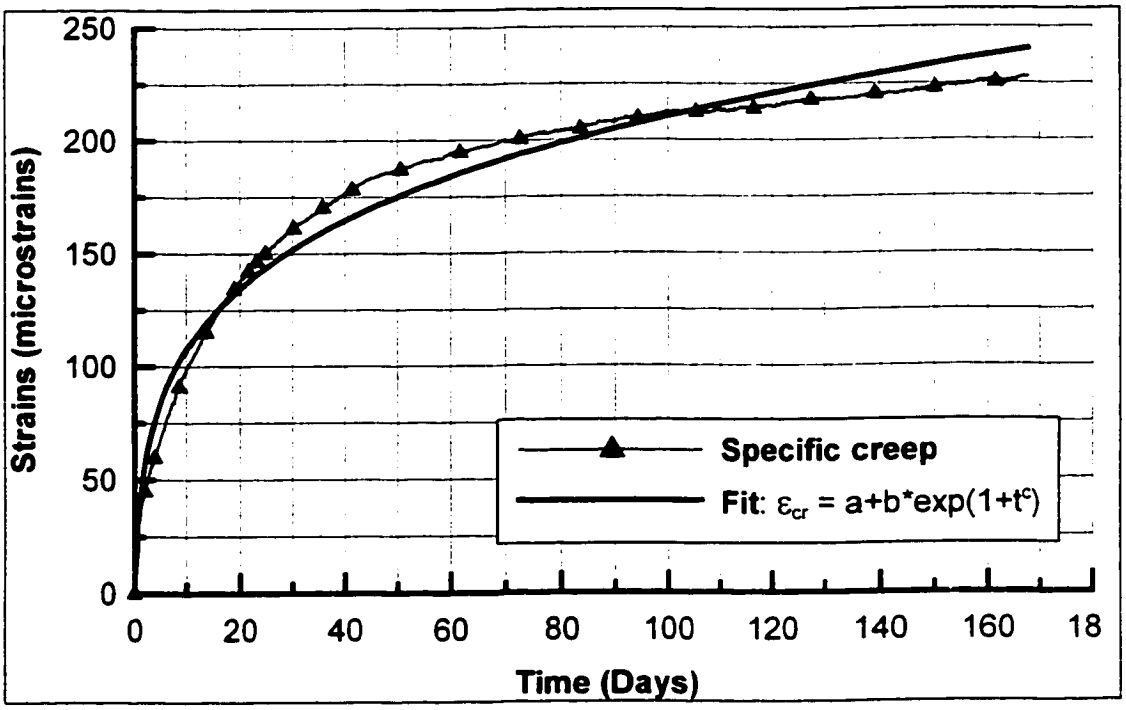

Figure 4.82: Specific creep in material PFSM

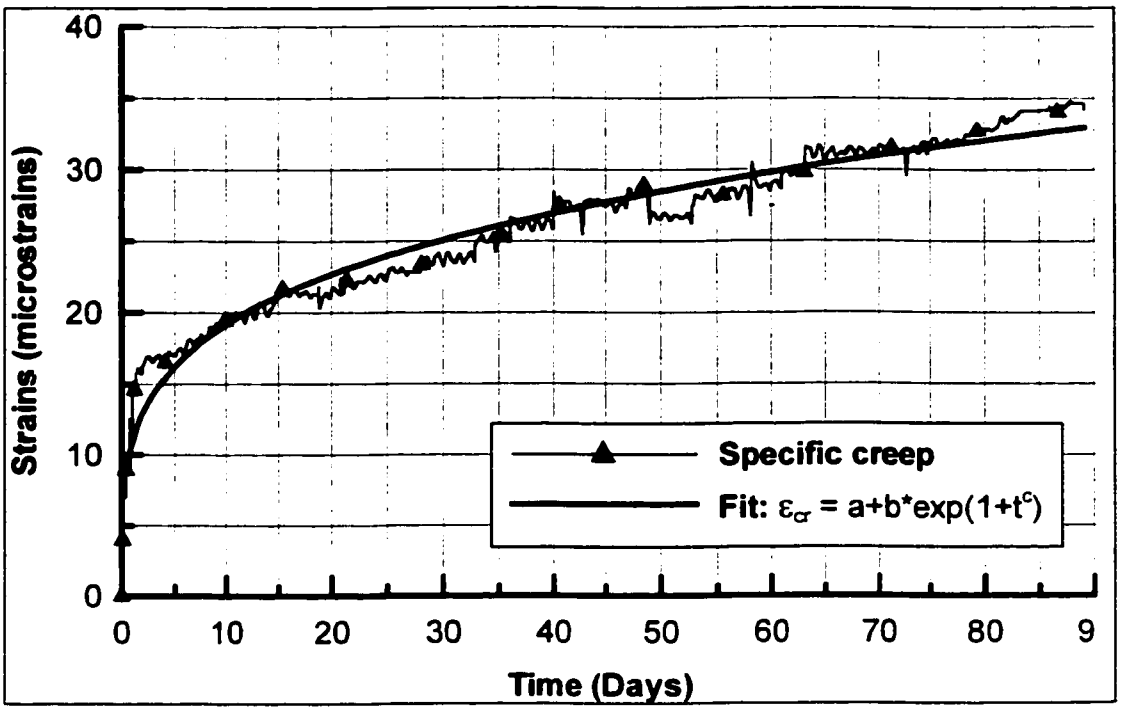

Figure 4.83: Specific creep in Concrete

4.3.2 COMPUTATION OF STRESSES AS A FUNCTION OF TIME

The stresses in concrete, steel and repair in column specimens repaired/un-repaired when subjected to constant load with respect to time are calculated from the measured strains in the respective materials at different locations.

The approach used for calculating stresses is described in this section.

4.3.2.1 Stresses in Concrete

The strains measured in concrete in column specimens include the strains due to initial elastic load, free creep and the restrained creep. The shrinkage in concrete is neglected, because the specimens were 6 months old at the age of testing and the concrete had shrunk already.

$$\varepsilon_c(t,t_o) = \varepsilon_c^{elo}(t_o) + \varepsilon_c^{fcr}(t,t_o) + \varepsilon_c^{ecr}(t,t_o)$$

where

$\varepsilon_c(t,t_o)$ is the measured strain in concrete at time t starting from time t_o

$\varepsilon_c^{elo}(t_o)$ is the elastic strain in concrete due to applied load at time t_o

$\varepsilon_c^{fcr}(t,t_o)$ is the strain due to free creep measured on a companion sample

$\varepsilon_c^{ecr}(t,t_o)$ is the elastic strain due to restrained creep (tensile).

The components of strains from the measured values, which contribute to the stresses in concrete, are due to the initial elastic load and due to the restrained creep. Therefore the strains, which are responsible for inducing stresses, are obtained by subtracting the free creep strains from the measured strains given by the equation

$$\varepsilon_c^{elo}(t_o)+\varepsilon_c^{ecr}(t,t_o)=\varepsilon_c(t,t_o)-\varepsilon_c^{fcr}(t,t_o)$$

The stress in concrete can be obtained by multiplying the strains with the modulus of elasticity of concrete given by the equation

$$\sigma_c(t,t_o)=\left[\varepsilon_c^{elo}(t_o)+\varepsilon_c^{ecr}(t,t_o)\right]* E_c(t,t_o)$$

where

$\sigma_c(t,t_o)$ is the stress in concrete at time t due to applied load at time t_o

$E_c(t,t_o)$ is the modulus of elasticity of concrete as a function of time t.

4.3.2.2 Stresses in Repair

The strains measured in repair in column specimens include the strains due to initial elastic load, free creep, restrained creep, free shrinkage and restrained shrinkage.

$$\varepsilon_r(t,t_o)=\varepsilon_r^{elo}(t_o)+\varepsilon_r^{fcr}(t,t_o)+\varepsilon_r^{ecr}(t,t_o)+\varepsilon_r^{fsh}(t,t_o)+\varepsilon_r^{esh}(t,t_o)$$

where

$\varepsilon_r(t,t_o)$ is the measured strain in repair at time t starting from time t_o

$\varepsilon_r^{elo}(t_o)$ is the elastic strain in repair due to applied load at time t_o

$\varepsilon_r^{fcr}(t,t_o)$ is the strain in repair due to free creep measured on a companion sample

$\varepsilon_r^{ecr}(t,t_o)$ is the elastic strain in repair due to restrained creep (tensile)

$\varepsilon_r^{fsh}(t,t_o)$ is the strain due to free shrinkage measured on a companion sample

$\varepsilon_r^{ecr}(t,t_o)$ is the elastic strain in repair due to restrained shrinkage (tensile).

The components of strains from the measured values, which contribute to the stresses in concrete, are due to the initial elastic load, restrained creep and due to the restrained shrinkage. Therefore the strains, which are responsible for inducing stresses, are obtained by subtracting the free creep strains and free shrinkage strains from the measured strains given by the equation

$$\varepsilon_r^{elo}(t_o)+\varepsilon_r^{ecr}(t,t_o)+\varepsilon_r^{esh}(t,t_o)=\varepsilon_r(t,t_o)-\varepsilon_r^{fcr}(t,t_o)-\varepsilon_r^{fsh}(t,t_o)$$

The stress in repair can be obtained by multiplying the strains with the modulus of elasticity of repair given by the equation

$$\sigma_r(t,t_o)=\left[\varepsilon_r^{elo}(t_o)+\varepsilon_r^{ecr}(t,t_o)+\varepsilon_r^{esh}(t,t_o)\right]* E_r(t,t_o)$$

where

$\sigma_r(t,t_o)$ is the stress in repair at time t due to applied load at time t_o

$E_r(t,t_o)$ is the modulus of elasticity of repair as a function of time t

4.3.2.3 Stresses in Steel

The stress in concrete can be obtained by multiplying the measured strains with the modulus of elasticity of steel given by the equation

$$\sigma_s(t,t_o)=[\varepsilon_s(t,t_o)]* E_s(t_o)$$

where

$\sigma_s(t,t_o)$ is the stress in steel at time t due to applied load at time t_o

$\varepsilon_s(t,t_o)$ is the measured strain in steel at time t starting from time t_o

$E_s(t_o)$ is the modulus of elasticity of steel

4.3.3 STRESSES IN COLUMNS WITHOUT RECESS

The columns without recess were loaded up to 20% (400 kN) of its ultimate load capacity and their behavior was monitored under constant load. The results for a period of 5 months are presented in this section. The strains developed in concrete and steel due to the applied load were captured and the stresses were calculated using the procedure described in section 4.3.2.

Figure 4.84 shows the variation of stress with respect to time in concrete. The concrete reached a stress level of 5.4 MPa at the time of loading. As time progresses the concrete started creeping and the steel provided restraint to its deformation. This restraint is responsible for relieving the stresses already present in concrete. Around 0.3 MPa is the reduction in stress in the first week after loading and it increases to 0.5 MPa over a period of 5 months.

Figure 4.85 shows the variation of stress with respect to time in steel. The steel reached a stress level of 41.5 MPa at the time of loading. As time progresses the stresses in steel increase because of its restraint provided to creep of concrete. The stress in steel increased to 91 MPa (almost 2.2 times the initial stress) at the end of 5 months under constant load. The increase in stress in steel after a period of 120 days is found to be negligible.

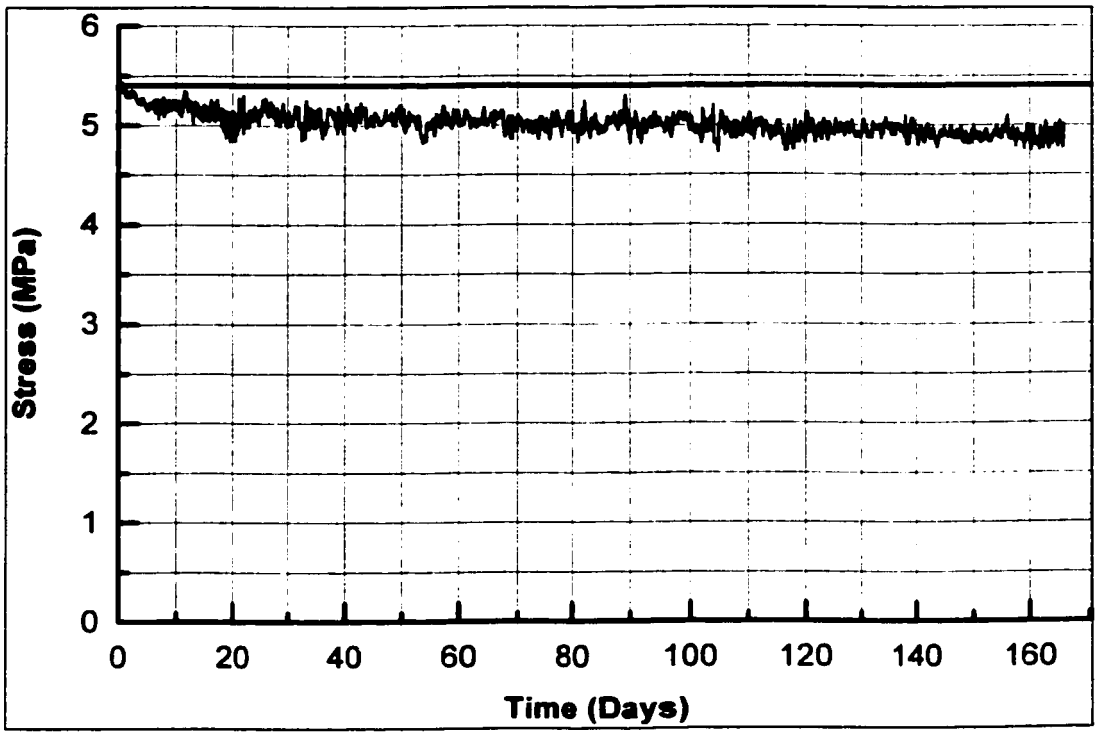

Figure 4.84: Stress-time curve for concrete in column specimens without recess

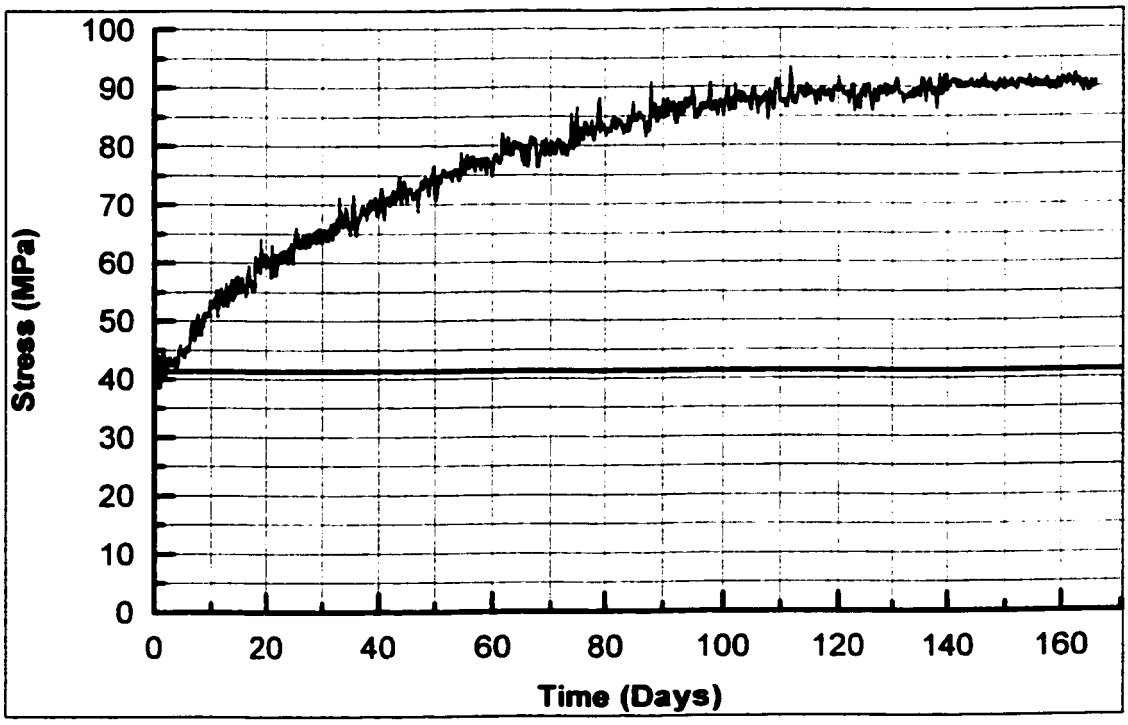

Figure 4.85: Stress-time curve for Steel in column specimens without recess

4.3.4 STRESSES IN COLUMNS REPAIRED WITH FMCX AND LOADED AFTER 7 DAYS

The columns repaired with FMCX were loaded up to 20% (400 kN) of its ultimate load capacity and their behavior was monitored under constant load. The results for a period of 5 months are presented in this section. The strains developed in concrete, repair and steel due to the applied load were captured and the stresses were calculated using the procedure described in section 4.3.2.

Figure 4.86 shows the variation of stress with respect to time in concrete core. The concrete reached a stress level of 5.9 MPa at the time of loading. As time progresses the concrete starts loosing stress due to restraint provided to creep of concrete by steel in concrete and the repair at the concrete-repair interface. This restraint is responsible for relieving the stresses already present in concrete. Around 0.6 MPa reduction in stress is observed over a period of 5 months.

Figure 4.87 shows the variation of stress with respect to time in repair. The repair reached a stress level of 5.5 MPa at the time of loading. As time progresses the time dependent phenomenon of shrinkage and creep comes in effect, which cause a significant reduction in stresses in repair due to the restraint provided by steel in repair and the bond between repair and concrete at the repair-concrete interface. The stress in repair decreases to 4.1 MPa at the end of 5 months under constant load. The decrease in stress in repair after a period of 120 days is found to be negligible.

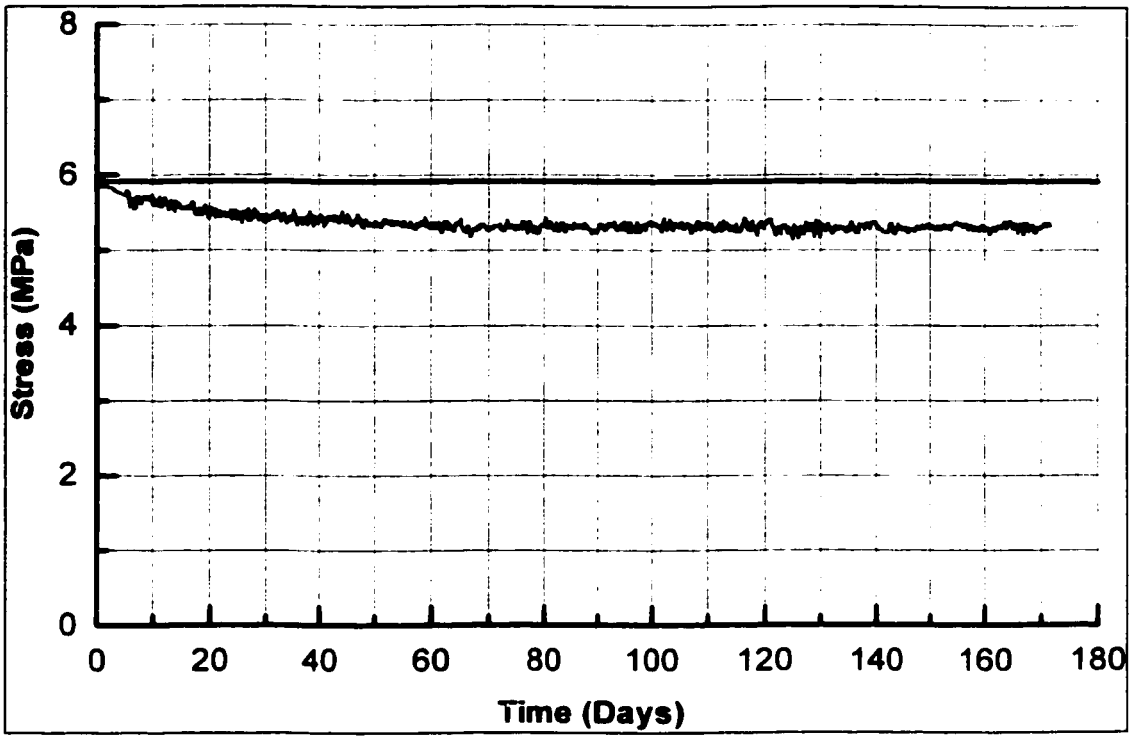

Figure 4.86: Stress-time curve for concrete at center and at mid-height of column specimen repaired with FMCX and loaded

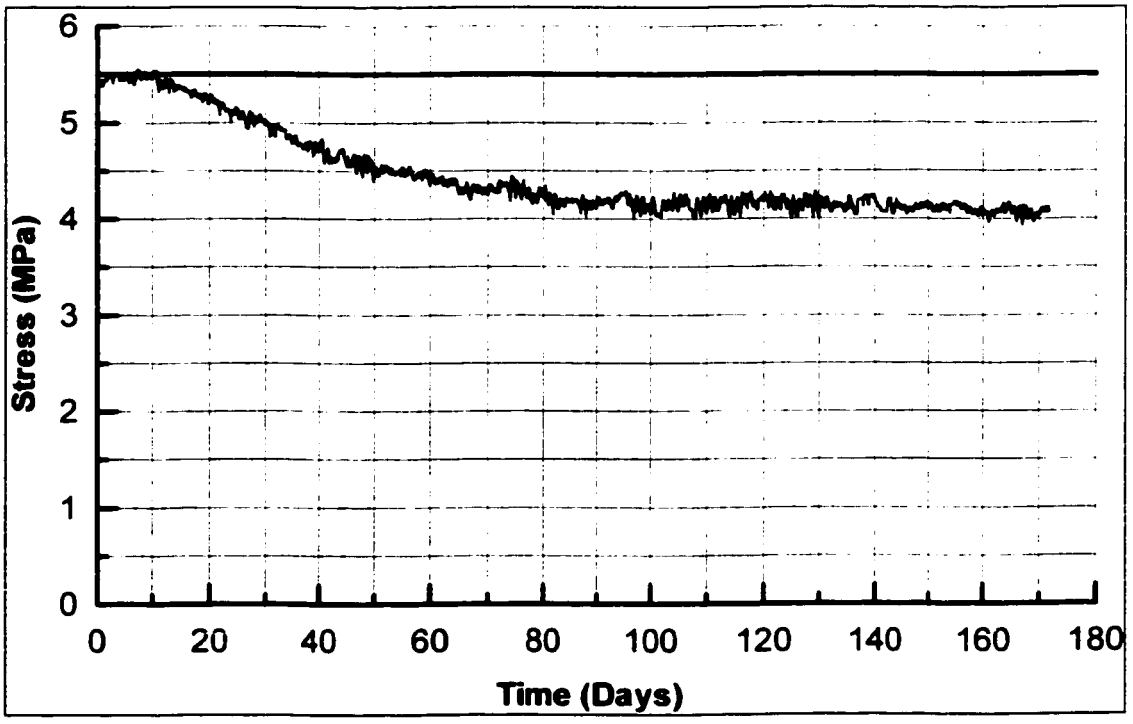

Figure 4.87: Stress-time curve for repair at center and at mid-height of column specimen repaired with FMCX and loaded

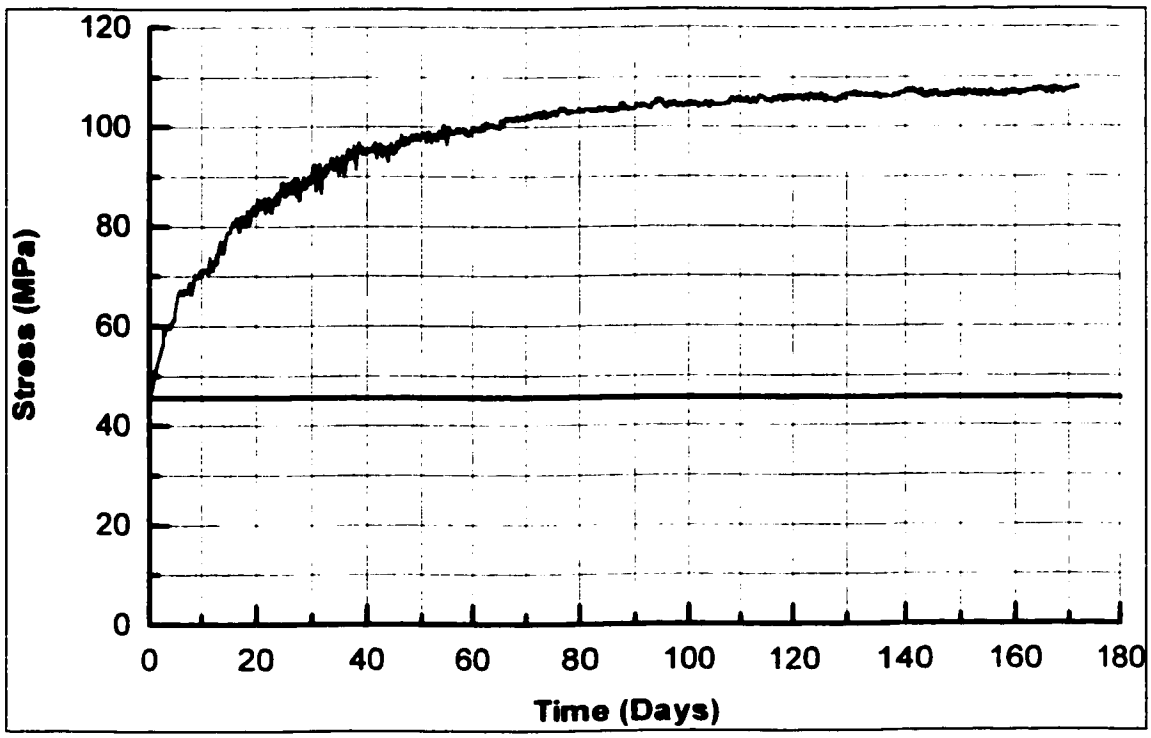

Figure 4.88: Stress-time curve for steel in concrete core at mid-height of column specimen repaired with FMCX and loaded

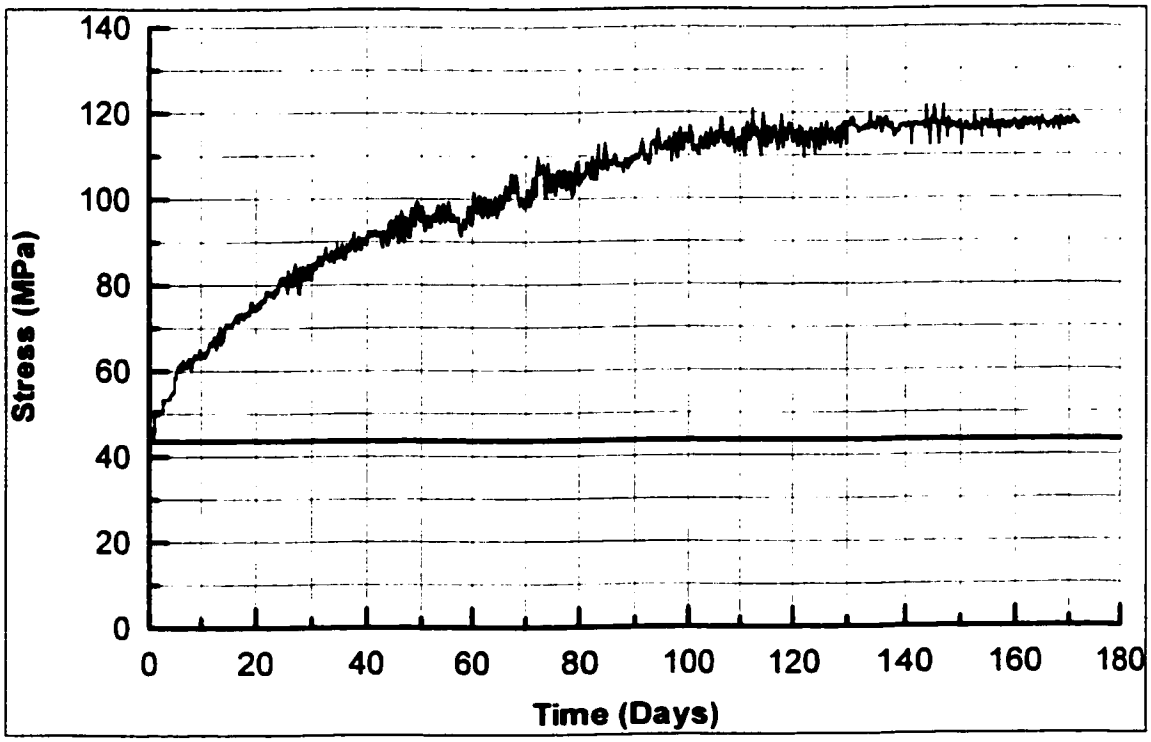

Figure 4.89: Stress-time curve for steel in repair at mid-height of column specimen repaired with FMCX and loaded

Figure 4.88 shows the variation of stress with respect to time in steel in concrete. The steel reached a stress level of 45 MPa at the time of loading. As time progresses the stresses in steel increase because of its restraint provided to creep of concrete. The stress in steel increased to 108 MPa (almost 2.4 times the initial stress) at the end of 5 months under constant load.

Figure 4.89 shows the variation of stress with respect to time in steel in repair. The steel reached a stress level of 42 MPa at the time of loading. As time progresses the stresses in steel increase because of its restraint provided to creep and shrinkage of repair. The stress in steel increased to 118 MPa (almost 2.8 times the initial stress) at the end of 5 months under constant load.

The modulus of elasticity of repair material FMCX was 28 GPa at the time of loading and 32 GPa for concrete. The stress in repair was 5.5 MPa and the stress in concrete was 5.9 MPa at the time of loading. The difference in stresses due to applied load is low because, the difference in modulus of elasticity of repair and concrete is also low.

4.3.5 STRESSES IN COLUMNS REPAIRED WITH PFSM AND LOADED AFTER 7 DAYS

The columns repaired with PFSM were loaded up to 20% (400 kN) of its ultimate load capacity and their behavior was monitored under constant load. The results for a period of 5 months are presented in this section. The strains developed in concrete, repair and steel due to the applied load were captured and the stresses were calculated using the procedure described in section 4.3.2.

Figure 4.90 shows the variation of stress with respect to time in concrete core. The concrete reached a stress level of 7.4 MPa at the time of loading. As time progresses the concrete starts loosing stress due to restraint provided to creep of concrete by steel in concrete and the repair at the concrete-repair interface. This restraint is responsible for relieving the stresses already present in concrete. Around 0.5 MPa reduction in stress is observed over a period of 5 months.

Figure 4.91 shows the variation of stress with respect to time in repair. The repair reached a stress level of 3.4 MPa at the time of loading. As time progresses the time dependent phenomenon of shrinkage and creep comes in effect, which cause a significant reduction in stresses in repair due to the restraint provided by steel in repair and the bond between repair and concrete at the repair-concrete interface. The stress in repair decreases to 2.07 MPa at the end of 5 months under constant load.

Figure 4.92 shows the variation of stress with respect to time in steel in concrete. The steel reached a stress level of 45 MPa at the time of loading. As time progresses the stresses in steel increase because of its restraint provided to creep of concrete. The stress in steel increased to 121 MPa (almost 2.6 times the initial stress) at the end of 5 months under constant load.

Figure 4.93 shows the variation of stress with respect to time in steel in repair. The steel reached a stress level of 46 MPa at the time of loading. As time progresses the stresses in steel increase because of its restraint provided to creep and shrinkage of repair. The stress in steel increased to 143 MPa (almost 3.1 times the initial stress) at the end of 5 months under constant load.

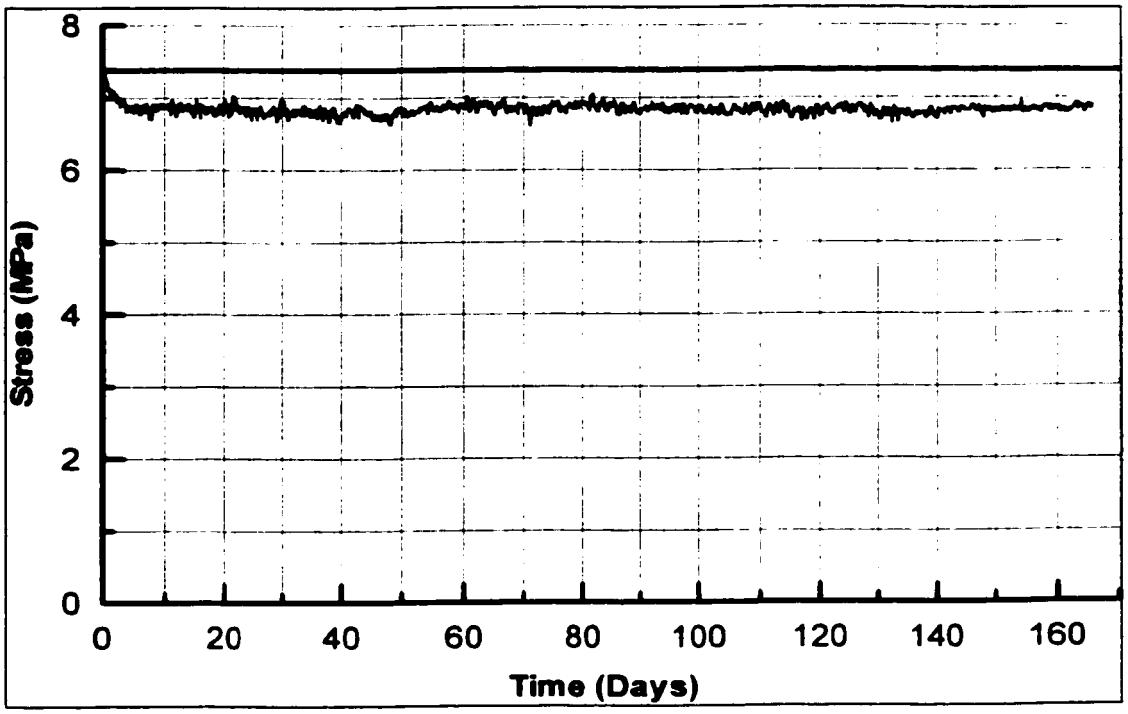

Figure 4.90: Stress-time curve for concrete at center and at mid-height of column specimen repaired with PFSM and loaded

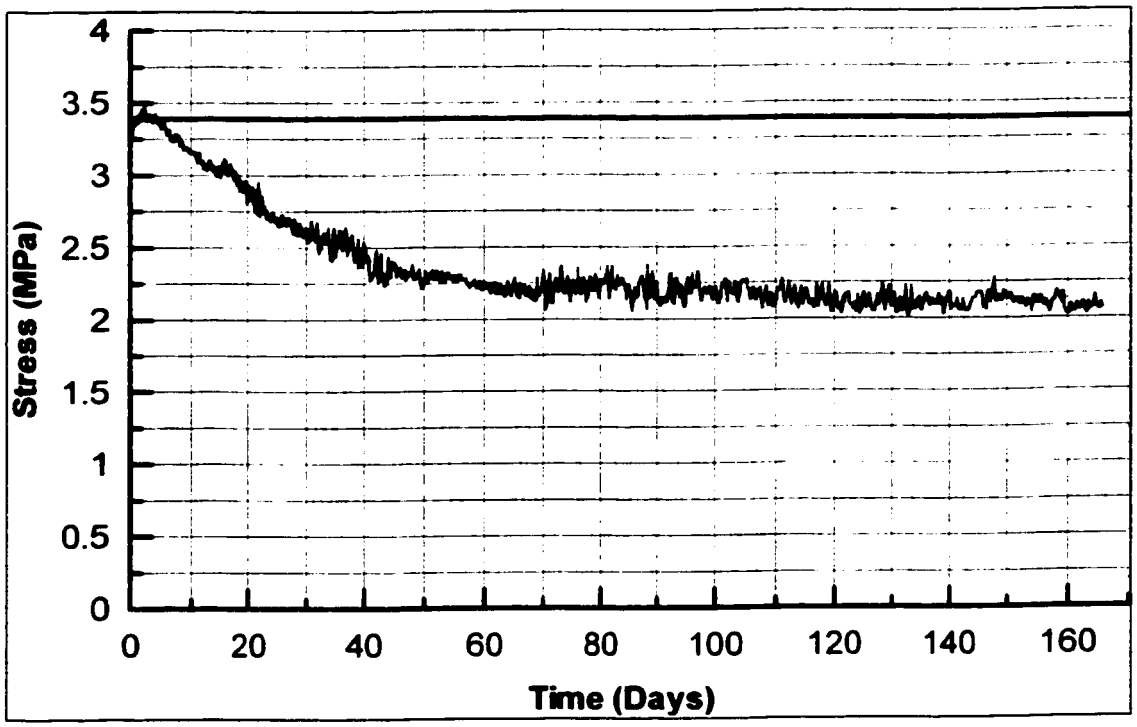

Figure 4.91: Stress-time curve for repair at center and at mid-height of column specimen repaired with PFSM and loaded

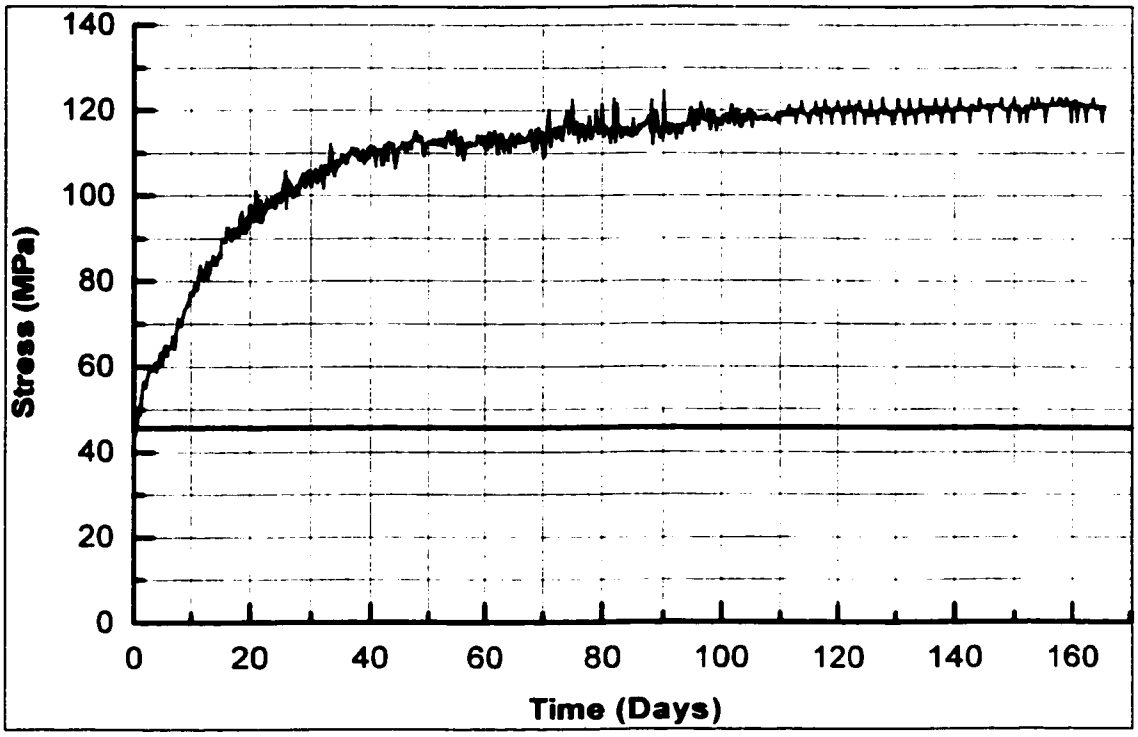

Figure 4.92: Stress-time curve for steel in concrete core at mid-height of column specimen repaired with PFSM and loaded

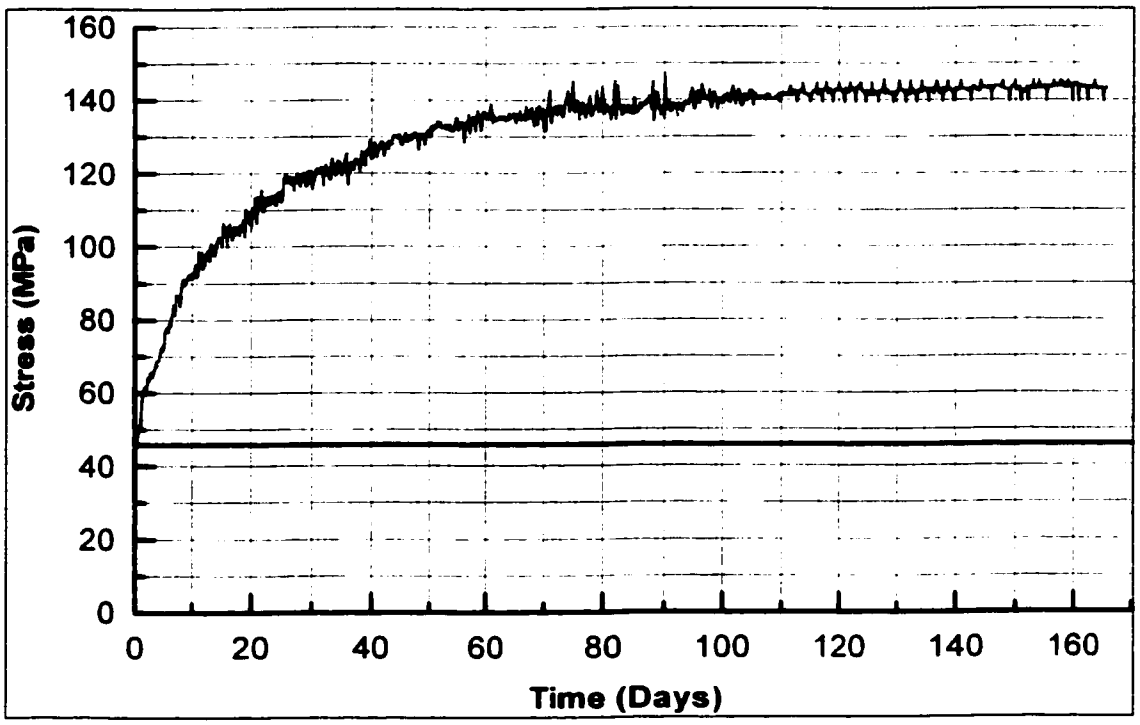

Figure 4.93: Stress-time curve for steel in repair at mid-height of column specimen repaired with PFSM and loaded

The modulus of elasticity of repair material PFSM was 17 GPa at the time of loading and 32 GPa for concrete. The stress in repair was 3.4 MPa and the stress in concrete was 7.4 MPa at the time of loading. The difference in stresses due to applied load is high because the difference in modulus of elasticity of repair and concrete is also high. The lower the modulus of repair material the lower the stresses coming in it.

4.3.6 STRESSES IN COLUMNS REPAIRED WITH FMCX IN LOADED STATE

The columns were first loaded up to 20% (400 kN) of its ultimate load capacity and then repaired with FMCX in loaded state and their behavior was monitored under constant load. The results for a period of 5 months are presented in this section. The strains developed in concrete, repair and steel due to the applied load were captured and the stresses were calculated using the procedure described in section 4.3.2. Any secondary tensile creep in the repair layer due to shrinkage induced tensile stresses has been neglected.

Figure 4.94 shows the variation of stress with respect to time in concrete core. The concrete in the core was under high stress level of 14.3 MPa at the time of repair. As time progresses the concrete looses very little stress due to restraint provided to creep of concrete by steel in concrete. This restraint is responsible for relieving the stresses already present in concrete. Around 1.0 MPa reduction in stress is observed over a period of 5 months.

Figure 4.95 shows the variation of stress with respect to time in repair. No stresses are developed in the repair due to the applied load even after the repair layer achieves its

strength and stiffness. As time progresses the time dependent phenomenon of shrinkage comes in effect. The stresses developed in repair are due to the restraint provided to shrinkage of repair by steel in repair and the bond between repair and concrete at the repair-concrete interface. Due to this restraint tensile stress of 1.6 MPa is developed in repair, which is less than the tensile strength of the material. If the tensile stress developed in repair exceeds the tensile strength of the repair material then cracking of repair may occur.

Figure 4.96 shows the variation of stress with respect to time in steel in concrete. The steel is under a stress level of 117 MPa at the time of loading. As time progresses the stresses in steel increase because of its restraint provided to creep of concrete. The stress in steel increased to 190 MPa (almost 1.6 times the initial stress) at the end of 5 months under constant load.

Figure 4.97 shows the variation of stress with respect to time in steel in repair. The steel is under a stress level of 96 MPa at the time of loading. As time progresses the stresses in steel increase because of its restraint provided to shrinkage of repair. The stress in steel increased to 164 MPa (almost 1.7 times the initial stress) at the end of 5 months under constant load.

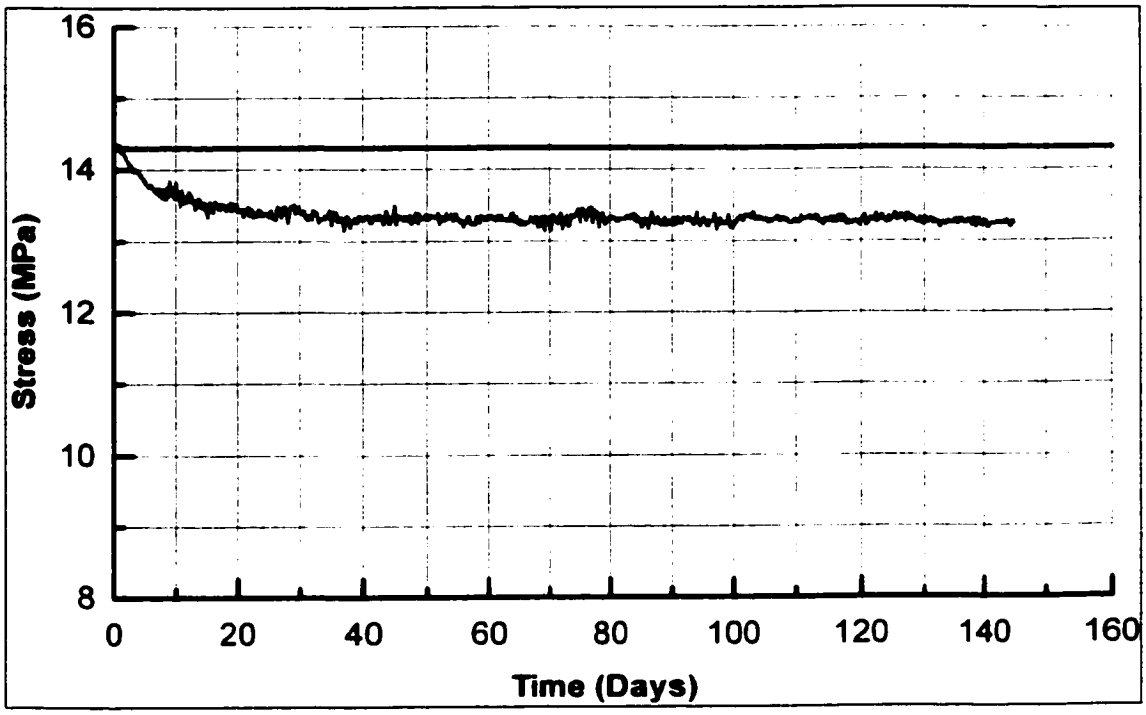

Figure 4.94 specimen repaired with FMCX in loaded state

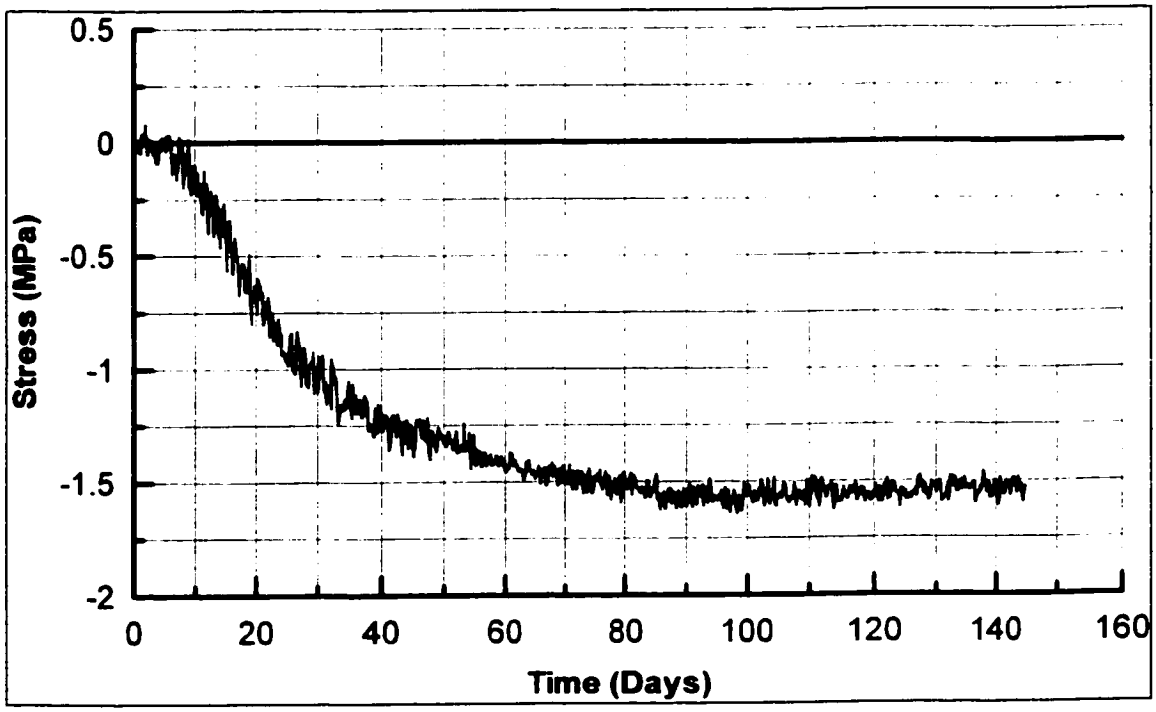

Figure 4.95: Stress-time curve for repair at center and at mid-height of column specimen repaired with FMCX in loaded state

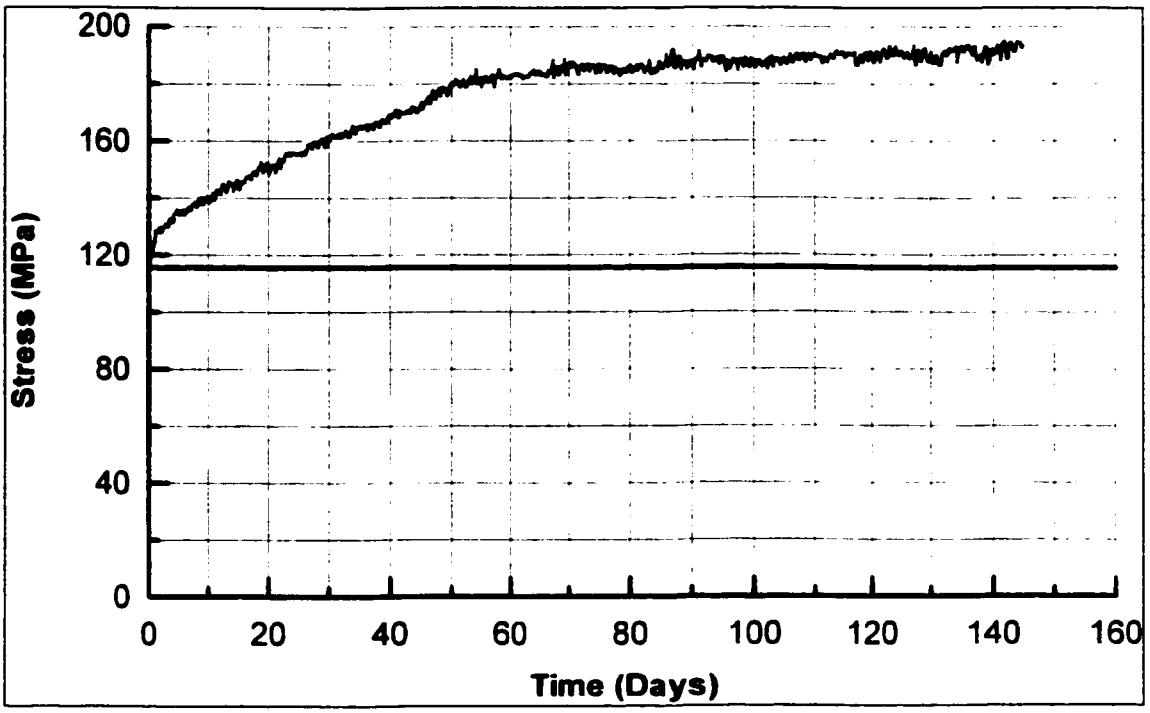

Figure 4.96: Stress-time curve for steel in concrete core at mid-height of column specimen repaired with FMCX in loaded state

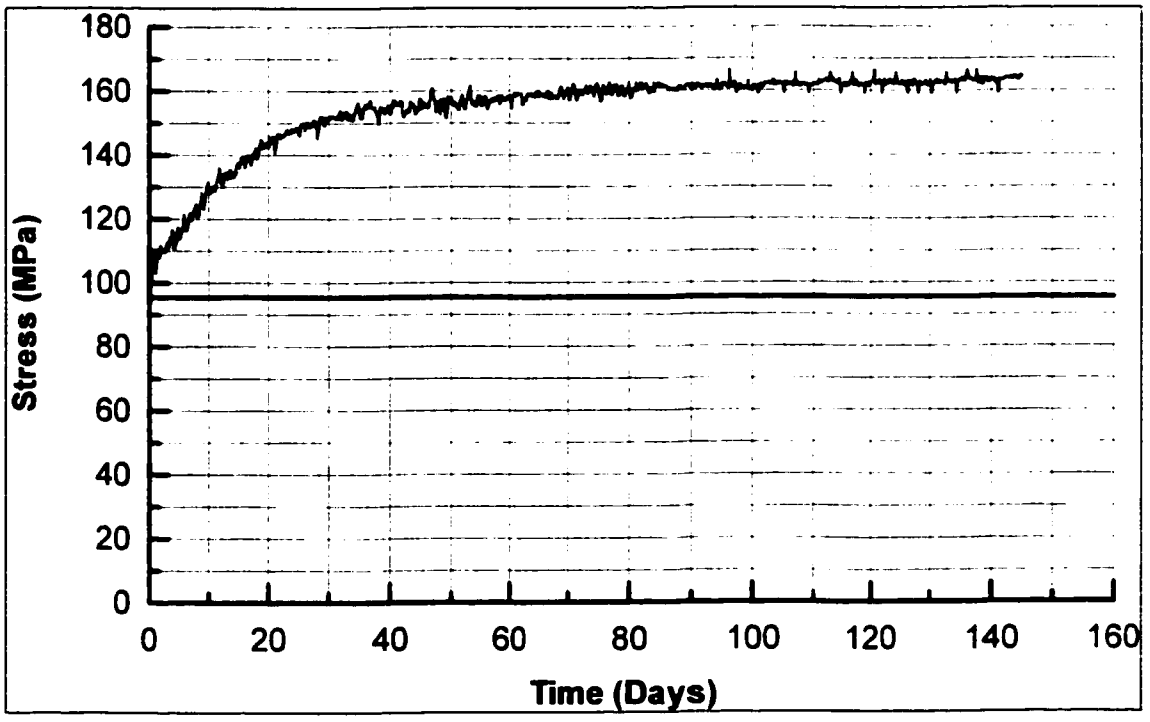

Figure 4.97: Stress-time curve for steel in repair at mid-height of column specimen repaired with FMCX in loaded state

4.3.7 STRESSES IN COLUMNS REPAIRED WITH PFSM IN LOADED STATE

The columns were first loaded up to 20% (400 kN) of its ultimate load capacity and then repaired with PFSM in loaded state and their behavior was monitored under constant load. The results for a period of 5 months are presented in this section. The strains developed in concrete, repair and steel due to the applied load were captured and the stresses were calculated using the procedure described in section 4.3.2. Any secondary tensile creep in the repair layer due to shrinkage induced tensile stresses has been neglected.

Figure 4.98 shows the variation of stress with respect to time in concrete core. The concrete in the core was under high stress level of 14.2 MPa at the time of repair. As time progresses the concrete looses very little stress due to restraint provided to creep of concrete by steel in concrete. This restraint is responsible for relieving the stresses already present in concrete. Around 1.4 MPa reduction in stress is observed over a period of 5 months.

Figure 4.99 shows the variation of stress with respect to time in repair. No stresses are developed in the repair due to the applied load even after the repair layer achieves its strength and stiffness. As time progresses the time dependent phenomenon of shrinkage comes in effect. The stresses developed in repair are due to the restraint provided to shrinkage of repair by steel in repair and the bond between repair and concrete at the repair-concrete interface.

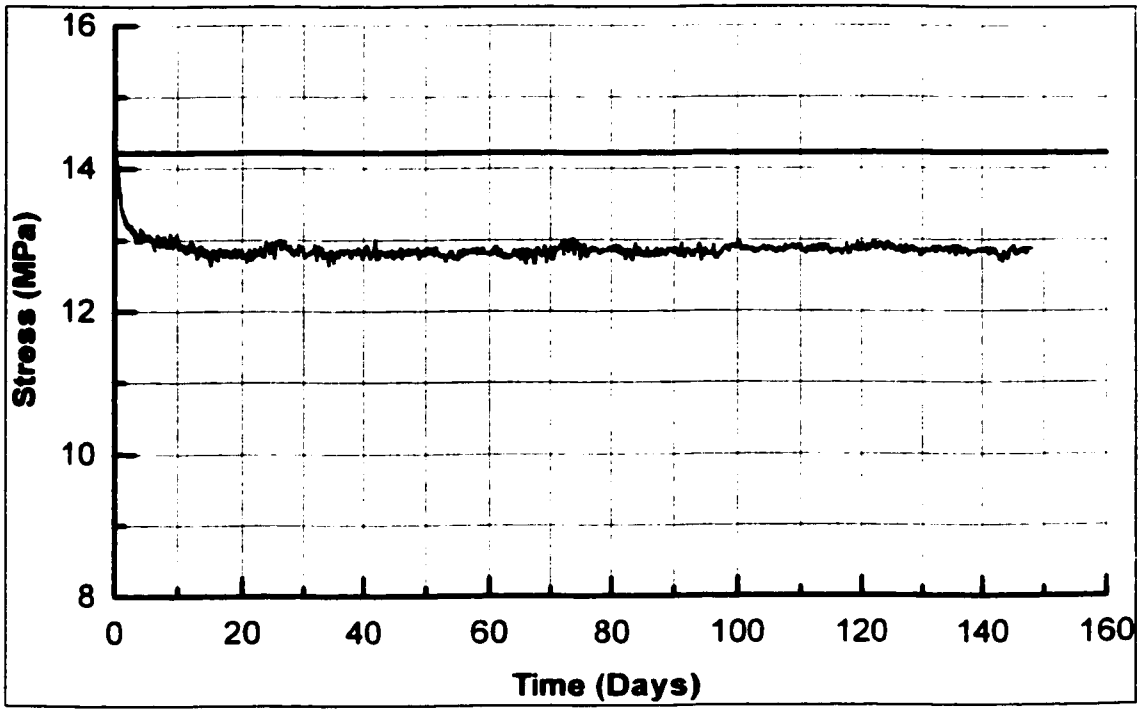

Figure 4.98: Stress-time curve for concrete at center and at mid-height of column specimen repaired with PFSM in loaded state

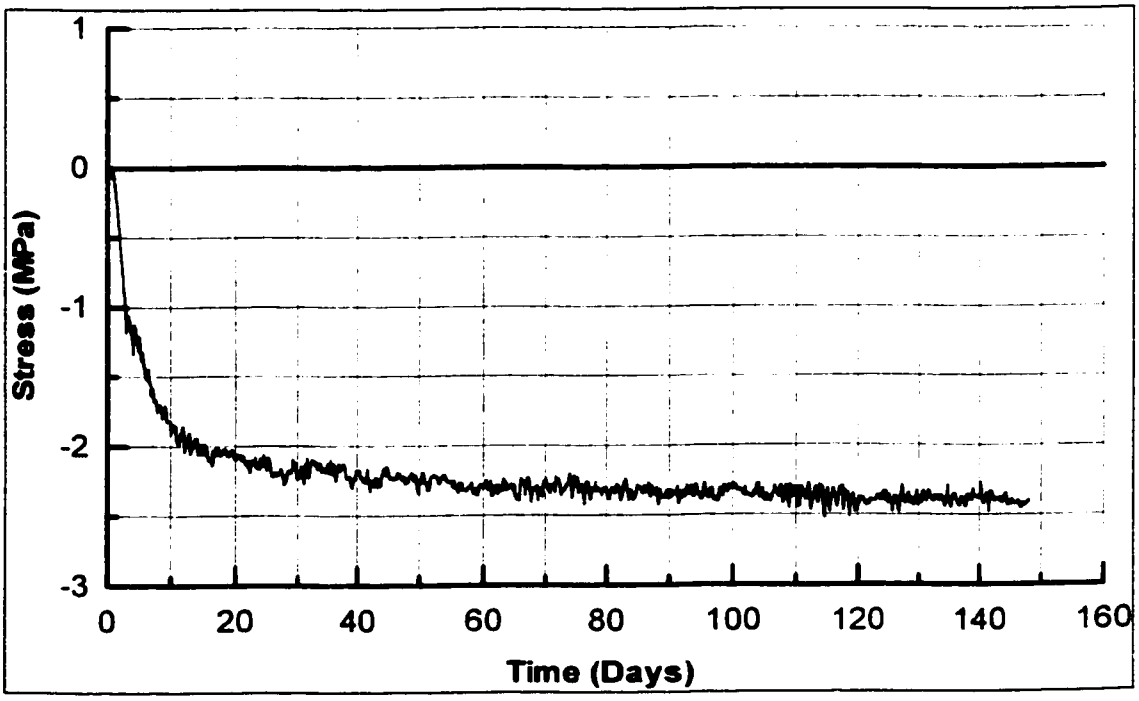

Figure 4.99: Stress-time curve for repair at center and at mid-height of column specimen repaired with PFSM in loaded state

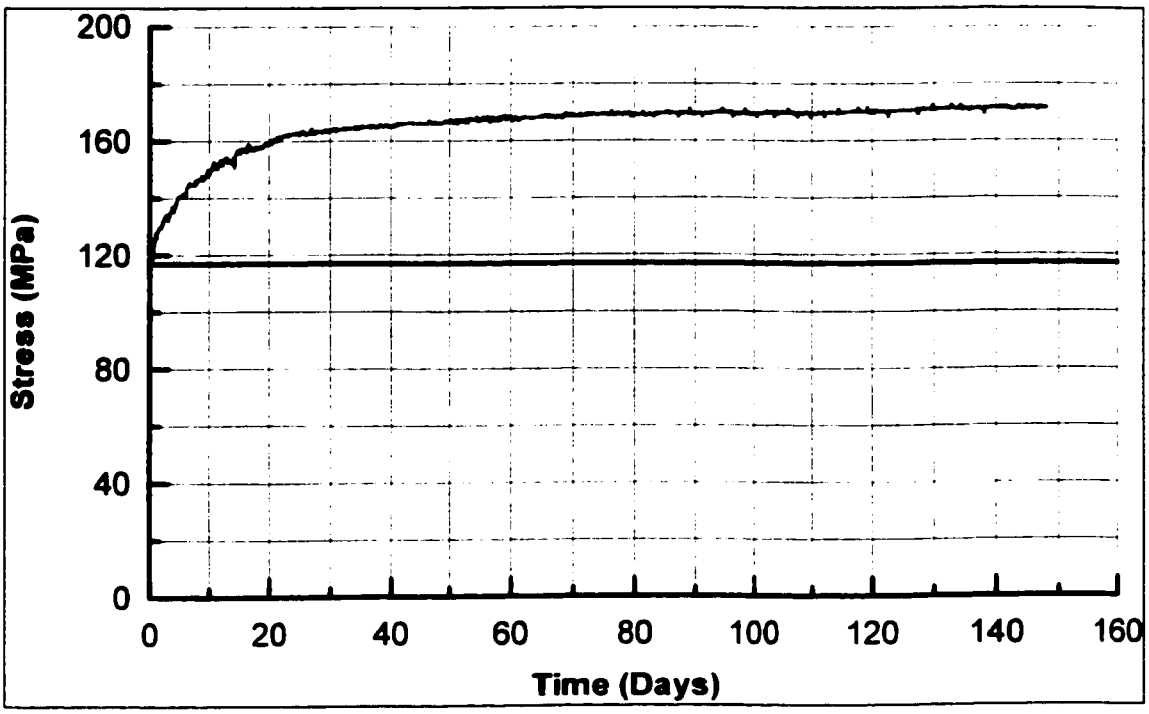

Figure 4.100: Stress-time curve for steel in concrete core at mid-height of column specimen repaired with PFSM in loaded state

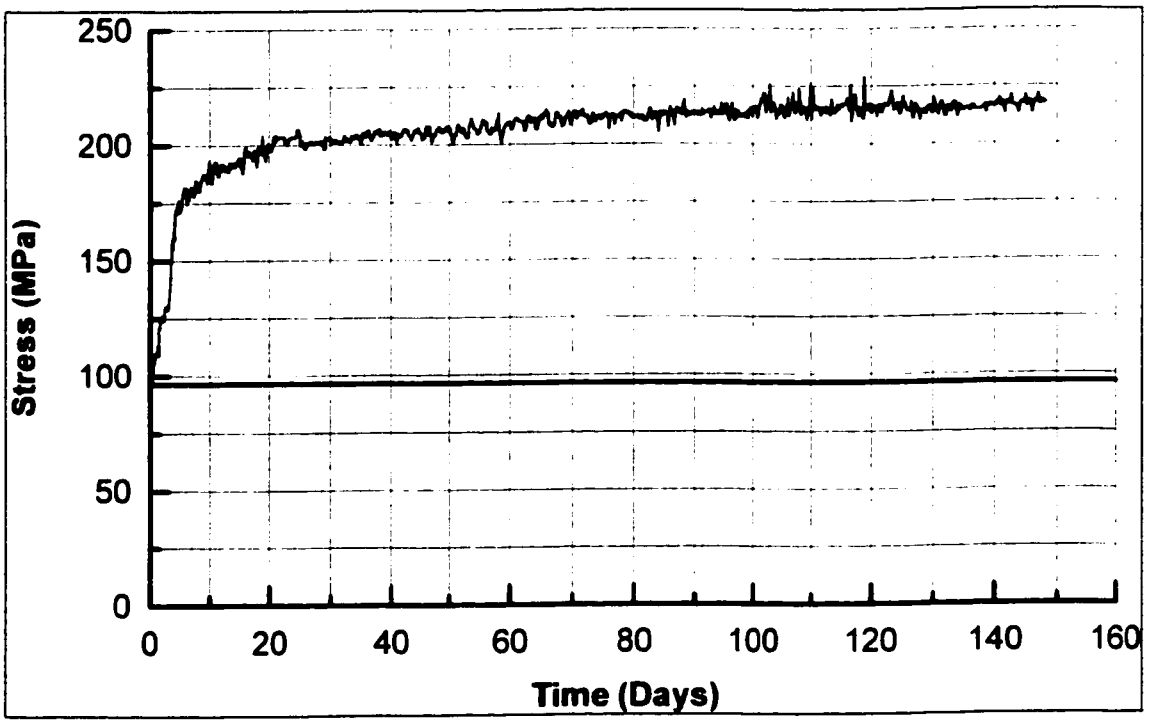

Figure 4.101: Stress-time curve for steel in repair at mid-height of column specimen repaired with PFSM in loaded state

Due to this restraint tensile stress of 2.4 MPa is developed in repair, which is less than the tensile strength of the material. If the tensile stress developed in repair exceeds the tensile strength of the repair material then cracking of repair may occur.

Figure 4.100 shows the variation of stress with respect to time in steel in concrete. The steel is under a stress level of 117 MPa at the time of loading. As time progresses the stresses in steel increase because of its restraint provided to creep of concrete. The stress in steel increased to 172 MPa (almost 1.5 times the initial stress) at the end of 5 months under constant load.

Figure 4.101 shows the variation of stress with respect to time in steel in repair. The steel is under a stress level of 96 MPa at the time of loading. As time progresses the stresses in steel increase because of its restraint provided to shrinkage of repair. The stress in steel increased to 217 MPa (almost 2.3 times the initial stress) at the end of 5 months under constant load.

CHAPTER 5

CONCLUSIONS AND RECOMMENDATIONS

The main conclusions drawn from this research based on the experimental results are presented below.

1) In columns, which are repaired after the loads are relieved by jacking, it is found that:

   (a) The patch repair is effective in carrying loads.

   (b) The distribution of load between concrete core and repair depends on modulus of elasticity of repair material at the age of loading,

   (c) In repair layer, there is stress relaxation with time due to the effect of restrained shrinkage and creep,

   (d) The stress in concrete core also relaxes with time due to creep effect, and

   (e) The stress in steel increases substantially (2.5 times the initial stress), due to relaxation of stress in concrete and repair.

2) In columns, which are repaired in loaded state, it is found that:

   (a) Deterioration of concrete results in a substantial increase in stress in concrete core and steel.

   (b) The patch repair is not effective in load redistribution showing it to be cosmetic,

   (c) The stresses in patch repair are tensile rather than compressive due to the effect of restrained shrinkage. The tensile stresses thus developed may lead to cracking of the repair layer,

   (d) The stress in steel embedded in repair increases substantially (2-3 times the initial stress).

3) For performing effective patch repair in deteriorated columns, it is highly recommended to relieve the structure from loads and proceed for repairs. At least a portion of the load must be relieved to counteract the tensile stresses developed in the patch repairs.

4) The columns repaired with two repair materials having high and low modulus of elasticity, when loaded to failure shows that:

   - The load taken by high modulus repair material is 59% of load applied. The repair is covering 60% of cross-sectional area. 34% of load is taken by the concrete core, which covers an area of 40%. The remaining 7 % of load is taken by steel (ρ = 1%).

   - The load taken by low modulus repair material is 51% of load applied. The repair is covering 60% of cross-sectional area. 41.5% of load is taken by the

concrete core, which covers an area of 40%. The remaining 7.5% of load is taken by steel (ρ = 1%).

5) The load distribution in concrete, steel and repair mainly depends on stiffness of the material. The ratio of stiffness of the material to the total stiffness of all materials located at that cross-section play a significant role in the load/stress distribution.

6) The two repair materials studied shows that the material having high early strength and stiffness development combined with low shrinkage and creep characteristics performs better in the load distribution in repaired columns.

7) The key repair material parameters, which play a central role in the distribution of loads in a patch repair and its long-term behavior are:

- Compressive modulus of elasticity E_c
- Free compressive creep strain ε_{cr}
- Free shrinkage strain ε_{sh}
- Tensile strength f_t

RECOMMENDATIONS FOR FUTURE STUDY

1) The effect of bending and eccentric loads on load distribution in patch-repaired columns should be investigated.

2) Finite element model needs to be developed for predicting the stresses and loads in concrete, steel and repair due to applied load incorporating the effect of shrinkage and creep.

3) The effect of loss of steel cross-sectional area due to corrosion on load carrying capacity of columns and the effect of reinforcing the damaged bars by new bars before performing patch repair should also be evaluated.

4) It is also recommended to investigate the effect of a wider range of repair materials including low cost materials and concrete on repaired. The long-term durability of these repair materials should also be investigated.

REFERENCES

1. Rahman, M.K., "Simulation and Assessment of Concrete Repair Systems," *Ph.D. Dissertation*, King Fahd University of Petroleum and Minerals, Dhahran, Saudi Arabia, May 1999, p 510.

2. Al-Amoudi, O. S. B., Rasheeduzzafar, Maslehuddin, M., and Al-Musallam, A.A., "Improving Concrete Durability in the Arabian Gulf," *Proceedings of 4th International Conference on Deterioration and repair of Reinforced Concrete in the Arabian gulf*, Vol. II, October 1993, pp. 927-941.

3. Al-Gahtani, A.S., Rasheeduzzafar, and Al-Musallam, A.A., "Performance of Repair Materials exposed to Fluctuation of Temperature," *Journal of Materials in Civil Engineering*, Vol. 7, No. 1, 1995.

4. Czarnecki, L., Vaysburd, A.M., Mailvaganam, N.P., Emmons, P.H. and McDonald, J.E., "Repair and Rehabilitation of Structures – Some Random Thoughts" *The Indian Concrete Journal*, Technical Papers, Jan. 2000.

5. FIP Guide to good practice, "Repair and Strengthening of Concrete Structures," Thomas Telford, London.

6. Mailvaganam, N.P., "Repair and Protection of Concrete Structures," CRC Press, Inc. 1992.

7. Vaysburd, A.M., Sabnis, G.M., Emmons, P.H., and McDonald, J.E., "Interfacial bond and surface preparation in concrete repair," *The Indian Concrete Journal*, Technical Papers, Jan. 2001.

8. Kay, E.A., "Concrete Society Working Party on Patch Repair of Concrete," *Proceedings of 3rd International Conference on Deterioration and repair of Reinforced Concrete in the Arabian Gulf*, Vol. II, October 1989, pp. 51-61.

9. Emberson, N.K., and Mays, G.C., "Significance of Property Mismatch in the Patch Repair of Structural Concrete - Part I: Properties of Repair Systems," *Magazine of Concrete Research*, Vol. 42, No. 152, 1990, pp. 147-160.

10. Emmons, P.H., and Vaysburd, A.M., "The Total System Concept - Necessary for Improving the Performance of Repaired Structures," *Concrete International*, Vol. 17, No. 3, March 1995, pp. 31-36.

11. Emmons, P.H., and Vaysburd, A.M., "System Concept in Design and Construction of Durable Concrete Repairs," *Construction and Building Materials*, Vol. 10, No. 1, 1996, pp. 69-75.

12. Shaw, J.D.N., "Materials for Concrete Repair," *Proceedings of 1st International Conference on Deterioration and repair of Reinforced Concrete in the Arabian Gulf*, Vol. I, October 1985, pp. 127-138.

13. Fontenay, C. de, "Testing of and Documentation for Concrete Repair Materials – A Consultant's Experience," *Proceedings of 3rd International Conference on Deterioration and repair of Reinforced Concrete in the Arabian Gulf*, Vol. II, October 1989, pp. 63-83.

14. Rizzo, E.M., and Sobelman, M.B., "Selection Criteria for Concrete Repair Materials," *Concrete international*, September 1989, pp. 46-49.

15. Coppola, Luigi, "Concrete Durability and Repair Technology" *Fifth Canmet/ACI International Conference on Durability of Concrete*," Barcelona, June 2000.

16. Mangat, P.S., and Limbachaya, M.K., "Repair Material Properties which Influence Long Term Performance of Concrete Structures," Construction and Building Material, Vol. 9, No. 2, pp. 81-90, 1995.

17. Mays, G. and Wilkinson, W., Polymer repairs to concrete: Their influence on structural performance. *ACI Special Publication SP-100-22,* 1987, pp. 351-375.

18. Yuan, Ying-su, and Marosszeky, M., "Restrained shrinkage in repaired reinforced concrete elements," Materials and Structures, 1994, 27, pp. 375-382.

19. Emberson, N.K., and Mays, G.C., "Significance of Property Mismatch in the Patch Repair of Structural Concrete - Part II: Axially Loaded Reinforced Concrete Members," *Magazine of Concrete Research*, Vol. 42, No. 152, 1990, pp. 161-170.

20. Vaysburd, A.M., and Emmons, P.H., "Visible and Invisible Problems of Concrete Repair," *The Indian Concrete Journal*, Technical Papers, Jan. 2001.

21. Cleland, D.J., Yeoh, K.M., and Long, A.E., "Corrosion of Reinforcement in Concrete Repair," *Construction and Building Materials*, 1997, Vol. 11, No. 4, pp. 233-238.

22. Baluch, M.H., Rahman, M.K., Al-Ghadib, A.H., "Indices for Prediction of Repair Mortar Performance," *In Symposium on Performance of Concrete Structures in the Arabian Gulf Environment*, KFUPM, Nov. 1998, pp. 317-330.

23. Chorinsky, E. G. F., "Repair of concrete floors with polymer modified cement mortars," *Proceedings of the RILEM International Symposium on Adhesion between Polymers and Concrete,* Chapman & Hall, London, 1986, pp. 230-234.

24. Austin, S., Robin, P., and Youguang, Pan, "Tensile bond testing of concrete repairs," *Materials and Structures,* U. K., 1995, No. 28, pp. 249-259.

25. Rahman, M.K., Baluch, M.H., and Al-Ghadib, A.H., "Simulation of Shrinkage distress and Creep relief in Concrete Repair," Composites: Part B 31 (2000), pp. 541-553.

26. Feldman, R.F., "CBD-119. Volume Change and Creep of Concrete," *Canadian Building Digest,* http://www.nrc.ca/irc/publications.html.

27. Shambira, M.V., Nounu, G., "On the effect of time-dependent deformations on the behavior of patch-repaired reinforced concrete short columns," *Construction and Building Materials*, 2000, Vol. 14, No. 8, pp. 425-432.

28. Ignatiev, N., Chatterji, S., "On the Mutual Compatibility of Mortar and Concrete on Composite Members," Cement and Concrete Composites, 1992, Vol. 14, pp. 179-183.

29. American Concrete Institute Committee-209, "Prediction of Creep, Shrinkage and Temperature Effects in Concrete Structures," in Designing for Effects of Creep, Shrinkage and Temperature, *ACI, Special Publication* No.27, 1971, pp. 51-93.

VITA

NAME: Mohammed Hameeduddin

ADDRESS: H. No. 4-2-24, Ramiah Bowli

Mahboobnagar – 509001, (A. P.)

INDIA

E-MAIL: md_hameed@yahoo.com

EDUCATIONAL QUALIFICATION

M.S. (Civil Engineering – Structures)

Sept. 1999 – May 2002

King Fahd University of Petroleum and Minerals, Dhahran, Saudi Arabia

GPA – 3.65/4.00

B.E. (Civil Engineering)

Aug. 1994 – May 1998

Osmania University, Hyderabad, India

First Class with Distinction